NASA
Technical
Paper
2917

February 1990

Evaluation of Two Transport Aircraft and Several Ground Test Vehicle Friction Measurements Obtained for Various Runway Surface Types and Conditions

A Summary of Test Results From Joint FAA/NASA Runway Friction Program

Thomas J. Yager,
William A. Vogler,
and Paul Baldasare

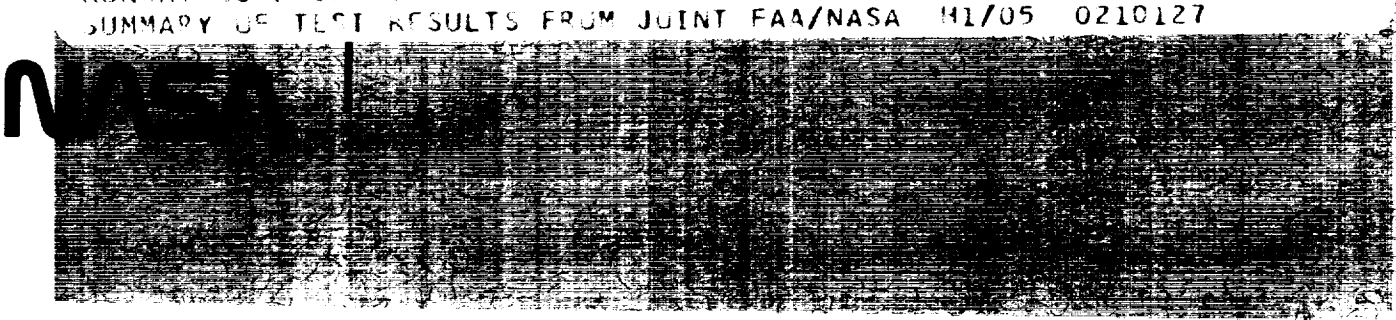

NASA Technical Paper 2917

1990

Evaluation of Two Transport Aircraft and Several Ground Test Vehicle Friction Measurements Obtained for Various Runway Surface Types and Conditions

A Summary of Test Results From Joint FAA/NASA Runway Friction Program

Thomas J. Yager
Langley Research Center
Hampton, Virginia

William A. Vogler
PRC Kentron, Inc.
Aerospace Technologies Division
Hampton, Virginia

Paul Baldasare
Langley Research Center
Hampton, Virginia

NASA
National Aeronautics and Space Administration
Office of Management
Scientific and Technical Information Division

Contents

Summary

A substantial number of tests with specially instrumented Boeing 737 and 727 aircraft together with several different ground friction measuring devices have been conducted for a variety of runway surface types and conditions. These tests are part of a Joint FAA/NASA Aircraft/Ground-Vehicle Runway Friction Program aimed at obtaining a better understanding of aircraft handling performance under adverse weather conditions and defining relationships between aircraft and ground-vehicle tire friction measurements. Aircraft braking performance for dry, wet, and snow- and ice-covered runway conditions is evaluated as well as ground-vehicle friction data obtained under similar runway conditions. A limited number of tests were conducted to evaluate aircraft engine reverser performance, snow-impingement drag on the aircraft, and the influence of runway chemical treatments on control of snow and ice contaminants. All the friction measurements taken during this program from aircraft and ground-vehicle test runs have been tabulated by major discriminators such as test site, runway condition, and vehicle type. Appendixes contain the aircraft/ground-vehicle friction data collected during tests with the two aircraft.

Results from this test program have made it possible to identify the relationship between ground-vehicle and aircraft friction data for a given contaminated runway condition. A better definition of both aircraft ground handling performance and ground-vehicle operational limits under adverse weather conditions has been obtained. The influence of major test parameters on tire-runway friction measurements such as speed, type and amount of surface contaminant, tire characteristics, and ambient temperature has been evaluated, and a substantial friction data base for further analysis and development has been established. Several recommendations are given, including the need for additional tests under winter runway conditions to further define the influence of several factors on aircraft and ground-vehicle friction measurements.

Introduction

There is an imperative operational need for information on runways which may become slippery because of various forms and types of contaminants. Since the beginning of "all weather" aircraft operations, there have been landing and aborted-takeoff incidents and/or accidents each year in which aircraft have either run off the end or veered off the shoulder of low-friction runways. These incidents/accidents have provided the motivation for various government agencies and aviation industries to conduct extensive research to examine the factors involved in the problem of less-than-acceptable runway friction.

Research conducted by the National Aeronautics and Space Administration (NASA), the Federal Aviation Administration (FAA), the U.S. Air Force (USAF), the Army Cold Regions Laboratory (CREL), the United Kingdom Ministry of Transportation, the Canadian Ministry of Transport, and others has established that tire braking friction does diminish on contaminated runway surfaces. The degree of friction reduction is related to many factors, including depth of contaminant (water, snow, mixture) on the surface, pavement surface texture, tire inflation pressure, and brake application speed. Much of this research effort has been directed towards obtaining a better understanding of the runway slipperiness problem exemplified in the commercial-transport-aircraft, landing-overrun accidents at Erie, Pennsylvania, in February 1986 and at Charlotte, North Carolina, in October 1986.

In early 1983, shortly after the Air Florida accident at Washington National Airport and the World Airways accident at Boston Logan International Airport, congressional recommendations on aviation safety by the Glickman/Gore subcommittee led to an appropriations bill for FAA research and development programs in the area of runway friction measurements. This bill recommended a funding level of $400 000 and directed that "the FAA, in conjunction with NASA, study the correlation between aircraft stopping performance and runway friction measurements on wet and contaminated surfaces. This research will be aimed at determining if it is possible to predict aircraft stopping performance based on runway friction measurements using new technology friction measuring devices." The recommendation was supported by the Air Line Pilots Association (ALPA). Should the correlation between ground-vehicle and aircraft friction measurements be validated, the Glickman/Gore subcommittee further recommended that runway friction measurement devices be made available to airport operators through the Airport and Airway Trust Fund.

The FAA and NASA, working together in response to the congressional directive, have conducted extensive runway friction evaluation tests with two instrumented aircraft and several ground friction-measuring vehicles for a wide variety of runway surface types and conditions. Six different test sites were used during this 5-yr program, and 12 grooved and ungrooved concrete and asphalt runway surfaces were evaluated under dry, truck-wet and rain-wet, and snow-, slush-, and ice-covered conditions. Over 200 test runs were conducted with two specially instrumented aircraft, a NASA Boeing 737 and an FAA

Boeing 727, and over 1100 test runs were conducted with six different ground test vehicles. The ground friction-measuring devices used in this program were the Mu-Meter and BV-11 skiddometer trailers, the surface friction tester, the diagonal-braked vehicle, the runway friction tester, and the runway condition reading vehicle. The primary goals of this Joint FAA/NASA Aircraft/Ground-Vehicle Runway Friction Program were to obtain a better understanding of aircraft ground handling performance under adverse weather conditions and to define relationships between aircraft and ground-vehicle tire friction measurements. The following secondary objectives were also identified: obtain aircraft ground handling data which will enhance simulation software modeling; evaluate aircraft engine thrust reverser performance; investigate influence of runway chemical treatments on control of snow and ice runway contaminants; obtain aircraft and ground-vehicle tire friction measurements to further develop and validate computational methodology used to estimate tire friction performance for different surface conditions; and identify the best tools and test procedures to provide airport operators and users with an accurate assessment of runway friction capability under all weather conditions.

Symbols

B_0	intercept value of dependent variable
B_1	slope of linear regression equation
g	acceleration due to gravity, g units ($1g = 32.2$ ft/sec^2)
p	tire inflation pressure, psi
V_G	ground speed, knots
W	aircraft gross weight, lb
μ	tire-pavement friction coefficient
μ_{eff}	aircraft effective braking friction coefficient
σ	standard deviation

Abbreviations:

A/C	aircraft
AFB	Air Force Base
ALPA	Air Line Pilots Association
ARINC	Aeronautical Radio, Inc.
ASTM	American Society for Testing and Materials
BNAS	Brunswick Naval Air Station
BOW	Bowmonk brakemeter
BV-11	BV-11 skiddometer
CAL	calibration
c.g.	center of gravity
CPT	controlled position transducer
CREL	Army Cold Regions Laboratory
DBV	diagonal-braked vehicle
DECOM	decommutating equipment
EPR	engine pressure ratio
FAA	Federal Aviation Administration
FAATC	Federal Aviation Administration Technical Center
flt	flight
G	grooved
GMT	Greenwich mean time
INS	inertial navigation system
IRIG	Inter-Range Instrumentation Group
M.A.C.	mean aerodynamic chord
Mu-M	Mu-Meter
N/A	not applicable
NASA 36	time-code system developed by NASA
NG	nongrooved
NTSB	National Transportation Safety Board
PCC	Portland cement concrete
PCM	pulse-code modulation
PFC	porous-friction-course overlay
P.R.	ply rating
RC filter	resistor capacitor filter
RCR	runway condition reading
RFT	runway friction tester (Model 6800 van)
R/W	runway
SFT	surface friction tester
SSA	slurry-seal asphalt
Sta.	station
TAP	Tapley meter
UCAR	liquid chemical used as a pavement deicing and anti-icing agent

Test Sites

General

Selection of the different test sites used in this study was based on their proximity to Langley Research Center in Hampton, Virginia, and the FAA Technical Center near Atlantic City, New Jersey; the variety of runway surface treatments available for both aircraft and ground-vehicle friction tests; necessary support equipment and personnel; and weather conditions. The primary test sites were NASA Wallops Flight Facility, the FAA Technical Center, and Brunswick Naval Air Station (BNAS). The Wallops Flight Facility, located on the eastern shore of Virginia approximately midway between Langley and the FAA Technical Center, has 15 different test surfaces, and substantial aircraft and ground-vehicle friction data have been collected on these surfaces during previous investigations. (See refs. 1 to 10.) The FAA Technical Center airport runway was used because the asphalt runway has groove configurations which differ in spacing from those at Wallops. The winter runway test conditions were evaluated at BNAS, located approximately 40 miles northeast of Portland, Maine. Some limited aircraft and ground-vehicle test runs were conducted at three other test sites—Langley AFB, Virginia, Portland International Jetport, Maine, and Pease AFB, New Hampshire. The runway at Langley AFB has a Portland cement concrete (PCC) surface. Tests under rain-wet conditions were conducted with only the 727 aircraft on the porous-friction-course (PFC) runway surface treatments installed at Portland International Jetport and Pease AFB. Table I gives the test-runway designation at each of these test sites and a description of the test-surface treatment and average macrotexture depth values. Additional information on the runway test surfaces evaluated at the different test sites is contained in the following sections.

Wallops Flight Facility

The three-runway layout at Wallops Flight Facility is shown in figure 1. Runway 17/35 was not used in this study. Runway 10/28 is 200 ft wide and 8000 ft long with a uniform, medium-macrotexture, slurry-seal asphalt surface that is 6000 ft long in the middle with 1000-ft-long PCC sections at each end. The average runway crown or cross slope is 1 percent. Dry, truck-wet, and rain-wet test conditions were evaluated on the slurry-seal asphalt surface shown in figure 2. Runway 4/22, also referred to as the landing research runway, is 150 ft wide and 8750 ft long. The specially constructed level (no crown) test section, 50 ft by 4140 ft, consists of four grooved and four nongrooved sections, each 350 ft long, one nongrooved transition section that is 650 ft long, and two new asphalt sections that are each 345 ft long. The groove configuration, transversely cut into the pavement, is 1/4 in. wide and 1/4 in. deep and is spaced 1 in. apart. Figure 3 shows schematically the test-surface arrangement on runway 4/22. Close-up views of test surface A, which has the lowest macrotexture depth (0.006 in.), and test surface B, which is grooved and has a higher macrotexture, are given in figure 4. The relatively new asphalt test surfaces, labeled J-1 and J-2, are shown in figure 5. Surface J-2 was obtained by using a grinding technique on a portion of surface J-1; this technique resulted in longitudinal ridges and valleys that resembled corduroy. The equipment used for grinding is similar to that used for surface grooving, but the cutting (diamond edged) blades are thinner and are spaced much closer together on the high-speed, rotating drum. The level test section constructed in the center of the runway provides a safety overrun at each end and along both sides. A channel cut 1/4 in. wide and 1 in. deep surrounds each test section and supports the rubber-belt dams used to control the water depth. Additional details and information concerning Wallops Flight Facility runway test surfaces are given in references 1 and 8 to 10.

FAA Technical Center

The FAA Technical Center airport is similar to the one at Wallops, with a three-runway layout as shown in figure 6. Figure 7 is a schematic of the test-surface arrangement on runway 13/31. The overall runway is 10 000 ft long and 200 ft wide and has a 1.5-percent crown. The saw-cut, transverse grooving installed in the new asphalt overlay is 1/4 in. wide and 1/4 in. deep. Grooved surface C at the north end of the runway has a groove spacing of 1.5 in., whereas grooved surface D at the south end of the runway has a groove spacing of 3.0 in. Close-up photographs of these two grooved-surface configurations are shown in figure 8. A small portion of the new asphalt overlay was left ungrooved and was labeled surface B. (See fig. 7.)

Brunswick Naval Air Station

The Brunswick Naval Air Station (BNAS) was selected as the winter test site because of its northern location in Maine and because of the parallel runway layout shown in figure 9. The nongrooved asphalt surface has a good macrotexture, as indicated in the close-up surface photograph inset in figure 9. Naval aircraft use the inboard runway, which is kept clear of snow and ice during the winter months. The

outboard runway (1L/19R), which is not normally cleared of winter weather contaminants, was used as the test runway for most runs. The runway dimensions are 200 ft by 8000 ft, and there is a 1-percent crown.

Langley Air Force Base

Langley Air Force Base, Hampton, Virginia, was selected as a test site because it is located adjacent to Langley Research Center. The main runway (7/25) is constructed of nongrooved Portland cement concrete, is 10 000 ft long by 150 ft wide, and has a 1-percent crown.

Pease Air Force Base

The runway at Pease Air Force Base, Portsmouth, New Hampshire, was selected as a test site because of its proximity to BNAS, Maine, and because the PFC surface was relatively new (installed July 1985). This overlay surface treatment, approximately 3/4 in. thick, has a very open texture and is designed to permit internal water drainage to help minimize the potential for tire hydroplaning. As indicated by the overview photograph in figure 10(a), the PFC treatment was installed in the middle 150 ft of the 300-ft-wide runway and extended to within 1500 ft of the runway thresholds. Runway 16/34 at Pease AFB is 11 320 ft long and has a 1.5-percent crown and a 1000-ft-long overrun area at both ends. The PFC installation met both FAA and USAF specifications. A close-up view of the joint between the PFC and conventional asphalt surfaces under rain-wet conditions is shown in figure 10(b).

Portland International Jetport

Runway 11/29 at Portland International Jetport, Maine, was also selected as a test site because of its proximity to BNAS and because the PFC surface had been in use for 11 years. The water drainage capability and the uniformity of the overlay surface matrix remain excellent; most of the changes in the touchdown areas are the result of traffic loading and rubber buildup. This runway has a 1-percent crown and is 6800 ft long and 150 ft wide.

Test Apparatus

Test Aircraft

NASA Boeing 737 aircraft. The instrumented Boeing 737-100 jet transport test aircraft was operated by NASA Langley flight crews. Figure 11 shows the NASA 737 aircraft during a flooded-runway test at Wallops, and figure 12 depicts the external configuration and dimensions of this aircraft. The dual-wheel nose gear was equipped with 24 × 7.7, 16 P.R., type VII aircraft tires, and the dual-wheel main gear used 40 × 14, 24 P.R., type VII aircraft tires. The maximum authorized landing weight W for this aircraft is 89 700 lb with 40° landing flaps. Maximum brake application ground speed V_G varied with weight and with test-section length and conditions from 110 knots down to 25 knots. The test landing brake energy ranged from 1.039×10^9 lb-kt^2 down to 0.849×10^9 lb-kt^2. The brake-energy values were computed in these units to correspond to aircraft flight-manual plots.

Prior to the test program, the antiskid-brake-system components were removed and sent to the manufacturer for inspection, checkout, and refurbishment as needed. This check was made to insure that the aircraft braking system was within tolerance and at peak performance for the subsequent testing. The aircraft brake system has two operational, full-antiskid, braking modes. The first one is called "manual" because it relies on pilot brake-pedal deflection. For manual braking, the pilot used full brake-pedal deflection, which permitted the antiskid brake system to modulate pressure to a value commensurate with the friction level available. The manual braking mode was used for most of the test runs in this program. The other brake-system mode is "automatic"; braking automatically commences immediately after touchdown without pilot brake-pedal deflection. If the automatic mode is used, the pilot can select one of three levels of deceleration—minimum, medium, or maximum. The automatic system controls brake pressure to achieve the constant deceleration level selected. The few braking test runs conducted during this program in the automatic, full-antiskid, braking mode were all conducted at the maximum deceleration level.

New wheel brake units and new (unworn) tires were installed on the main gear prior to testing. The dual-wheel nose gear was also equipped with new tires prior to testing. The tire inflation pressures, maintained within ±5 lb/in^2 throughout the course of the test program, were 155 lb/in^2 for the main-gear tires and 135 lb/in^2 for the nose-gear tires. When tread wear reached 50 percent on a given tire, both tires on the landing gear were replaced with new ones.

An extensive instrumentation package was used aboard the aircraft to monitor the position of flight control surfaces, brake-system performance, engine speed and throttle settings, and aircraft acceleration, heading, attitude, and forward speed. The primary aircraft instrumentation pallet is shown in figure 13(a), and figure 13(b) is a data-acquisition flow

chart. All instrumentation sensors and transducers were properly calibrated prior to conducting test runs and after completion of the program to document any change. The range and accuracy of all the aircraft parameters measured during the test runs are listed in table II(a). Although the NASA 737 aircraft system can provide a maximum data sample rate of 100 samples/sec, most parameter data were evaluated at a rate of 40 samples/sec. Additional details on the instrumentation features and equipment onboard the test aircraft are contained in reference 11.

FAA Boeing 727 aircraft. The instrumented Boeing 727-100QC jet transport was equipped with a wide, side-opening, cargo door and served as a cargo airplane prior to FAA acquisition. Figure 14 shows the FAA 727 test aircraft during a wet-runway test at Wallops Flight Facility. The dual-wheel nose gear was equipped with 32×11.5–15, 12 P.R., type VII aircraft tires and the dual-wheel main gear used 49×17, 26 P.R., type VII aircraft tires. The external configuration and dimensions of this aircraft are depicted in figure 15. The maximum authorized landing weight W for this aircraft is 142 500 lb with 30° landing flaps. Maximum brake application speed V_G varied with aircraft weight and with test-section length and conditions. For the braking test runs conducted with the 727 aircraft in this program, ground speeds ranged from 105 knots to 5 knots. The brake energy ranged from 1.418×10^9 lb-kt^2 to 0.0033×10^9 lb-kt^2.

Prior to the test program, the antiskid-brake-system components were removed and sent to the manufacturer for inspection, checkout, and refurbishment as needed. This check was made to insure that the aircraft braking was within tolerance and at peak performance for the subsequent testing. The 727 test aircraft had a manually armed (switch in cockpit) nose-wheel braking feature in addition to the conventional main-wheel braking system. Most braking test runs were conducted with only main-wheel braking, but some runs were performed with nose-wheel braking active.

New wheel brake units and new (unworn) tires were installed on the main gear prior to testing. The dual-wheel nose gear was also equipped with new brakes and tires prior to testing. The tire inflation pressures, maintained within ± 5 lb/in^2 throughout the course of the test program, were 145 lb/in^2 for the main-gear tires and 100 lb/in^2 for the nose-gear tires. When tread wear reached 50 percent on a given tire, both tires on the landing gear were replaced with new ones.

An extensive instrumentation package was used aboard the aircraft to monitor the position of flight control surfaces, brake-system performance, engine speed and throttle settings, and aircraft acceleration, heading, attitude, and forward speed. The primary aircraft instrumentation pallet is shown in figure 16(a). A three-axis accelerometer package is shown in figure 16(b), the inertial navigation system hookup is shown in figure 16(c), and figure 16(d) is a data-acquisition flow chart. All instrumentation sensors and transducers were properly calibrated prior to and after completion of program test runs. The range and accuracy of all the aircraft parameters measured during the test runs are listed in table II(b). This system is similar to the one used on the NASA 737 test aircraft, in that the maximum data sample rate is 100 samples/sec, but most parameter data were evaluated at a rate of 40 samples/sec.

Ground Test Vehicles

General. In the overall planning and implementation of this extensive test program, an effort was made to include as many of the different ground friction-measuring vehicles as possible. The diagonal-braked vehicle (DBV) was not available for tests at BNAS. The runway friction tester and the electronic Tapley meter were not available until after the 737 aircraft tests were completed. Except for the DBV and the Tapley meter/Bowmonk brakemeter/runway condition reading (RCR) vehicles, the ground test vehicles were equipped with self-wetting systems. These systems were not used during the program, however, since the test aircraft had to rely on truck- or rain-wetting of the test surfaces. The friction-measuring system on each ground test vehicle was carefully inspected and calibrated each day before conducting the scheduled test runs. If a vehicle was found to be out of calibration or in need of equipment repair, it was excluded from testing until the problem was corrected. Table III summarizes the test tire conditions for each friction-measuring vehicle. Photographs showing the tread pattern on the principal ground-vehicle test tires are presented in figure 17. Typical examples of the records produced by the different ground vehicles (except the RCR vehicle) during test runs on the slurry-seal asphalt surface at Wallops under truck-wet conditions are given in figure 18. Except for the DBV, which measured locked-wheel friction from 60 mph to a complete stop, the ground-vehicle, runway friction tests were normally conducted at 20, 40, and 60 mph. The following sections provide additional information on the equipment and instrumentation used on each of the ground test vehicles.

Diagonal-braked vehicle. The diagonal-braked vehicle (DBV) is equipped with a high-performance engine for rapid acceleration to the normal test speed of 60 mph. This vehicle, shown in figure 19(a), has a specially modified braking system to provide locked-wheel braking on the diagonal wheel pair. With the remaining two freely rotating wheels, this braking configuration permits adequate vehicle stability and directional control when the diagonal wheels are locked at high speed. Figure 19(b) is a schematic of the diagonal-braked system. The diagonal-braked wheels are fitted with American Society for Testing and Materials (ASTM) smooth-tread test tires (specification E-524) inflated to 24 psi. (See fig. 17.) The unbraked wheels are equipped with standard road tires that have a good tread design and are inflated to 32 psi.

The key test parameters monitored by the instrumentation system onboard the DBV are speed, acceleration, and stopping distance from the point of braked-wheel lockup. The longitudinal accelerometer is mounted on the floor inside the vehicle near the center of gravity. Vehicle speed and distance sensors are mounted on the fifth wheel (bicycle wheel attached to rear bumper). Vehicle speed and stopping distance are displayed to the operator by digital counters mounted on the vehicle dashboard. These values of brake application speed and stopping distance are manually recorded by a test observer positioned in the back seat of the vehicle. Magnetic pickups on each wheel provide information on exactly when wheel lockup occurs. The vehicle speed, longitudinal acceleration, and braked-wheel revolutions are recorded on an analog tape recorder mounted inside the vehicle and within reach of the operator. Upon completion of a test-run series, the analog tape data are transferred to a strip chart for review and evaluation. An example of a typical DBV test-run time history is shown in figure 18(a). The upper plot shows the drop in vehicle speed from brake application down to a complete stop in approximately 7.5 sec. The variation in vehicle longitudinal deceleration from diagonal braking only during the test run is determined using the datum line that accounts for vehicle air-drag and rolling-resistance values. In other words, the datum line represents DBV deceleration on the given test surface and conditions in a free-rolling, nonbraking mode. The DBV test records also verify that the diagonal-braked wheels stop rotating and remain locked throughout the test run to the vehicle stop position. The DBV test runs conducted without complete lockup of the diagonal wheels were not accepted, and a repeat test run was conducted. Additional information on the DBV capabilities is given in references 12 and 13.

Mu-Meter. The Mu-Meter is a side-force-measuring trailer pulled with an appropriate tow vehicle. Both the Mark III and the newer Mark IV model Mu-Meters shown in figure 20 were used in this program; these trailers each weigh approximately 540 lb. The older Mark III unit, with limited data readout capability in the tow vehicle cab, was used during tests with the 737 aircraft. The Mark IV unit, with a data computer readout display in the cab of the tow vehicle, was used during most of the 727 aircraft tests. The Mark IV unit works on the same principle as the Mark III unit, but uses solid-state electronic sensors instead of the hydraulic-load cell and the mechanical chart drive of the Mark III recorder. For similar test conditions and speeds, no significant difference was found in measurements collected with the two units. Figures 21(a) to (c) show the basic trailer configuration with two friction-measuring wheels positioned at 7.5°; this positioning produces an apparent wheel-slip ratio of 13.5 percent. A rear wheel is used for distance-traveled measurements and for trailer stability. A vertical load of 171 lb is produced by ballast from a shock absorber on each friction wheel. Smooth-tread tires, size 16 × 4, 6 ply, RL 2 (see fig. 17), are used on the friction-measuring wheels, and the rear wheel is a similar size but has a conventional tread design. The friction-wheel tires are maintained at an inflation pressure of 10 psi, and the rear-wheel tire is kept at 30 psi.

The main components of the Mu-Meter instrumentation system are the load cell and the distance sensor. When combined with real-time increments, trailer speed is determined from the distance sensor. The load cell reads minute tension variations from the friction-measuring wheels. The Mark III Mu-Meter recorder features are shown in figure 21(d). The newer, Mark IV Mu-Meter computer data display to the tow vehicle operator is shown in figure 21(e). An example of a Mu-Meter test-run record that shows the variation in friction coefficient with runway distance is given in figure 18(b). Additional information on the Mu-Meter trailer capability can be obtained from references 14 and 15.

Surface friction tester. The surface friction tester (SFT) is equipped with front-wheel drive and a hydraulically retractable friction-measuring wheel installed behind the rear axle. (See fig. 22.) The measuring wheel is positioned at zero yaw in respect to rear vehicle wheels. Schematic views of the major SFT components are shown in figure 23. The friction-measuring-wheel arm (figs. 23(c) and (d)). consists of a chain-drive connection with the vehicle's rear axle and contains the torque gauge used to compute braking friction values. With this drive

arrangement, the measuring wheel will operate at a slower speed than the vehicle and at a fixed braking slip ratio between 10 and 12 percent, depending on the tire configuration. The braking torque on the measuring wheel is fed back to the vehicle rear wheels by the chain drive, and consequently, little energy is required from the vehicle's drive train during test runs. A vertical load of 310 lb is applied on the friction-measuring wheel with a spring and shock absorber. For dry- and wet-runway friction surveys, a smooth-tread tire (16 × 4, 6 ply, RL 2) is used for the test wheel with an inflation pressure of 30 psi. For winter runway snow and ice conditions, a special high-pressure (100 psi), grooved-tread, 16 × 4, aero tire is used. (See fig. 17.)

The torque acting on the friction-measuring wheel during a test run at constant vehicle speed is input to a digital computer, where the information is converted into friction-coefficient form. These friction values, together with distance-traveled measurements, are continuously stored in the computer for strip-chart printout (fig. 18(c)) upon completion of a friction survey. The computer is programmed to calculate the average friction value of a preselected distance and the average vehicle speed over that distance. References 16 and 17 give additional information concerning the SFT equipment and test capabilities.

BV-11 skiddometer. The BV-11 skiddometer trailer, pictured with the tow vehicle in figure 24, is equipped with a friction-measuring wheel designed to operate at a fixed slip ratio between 15 and 17 percent, depending on test-tire configuration. The trailer weighs approximately 795 lb and consists of a welded frame supported by three in-line wheels, of which two are independently sprung wheels. (See fig. 25(a).) The two trailer wheels and the middle (measuring) wheel are coupled together by roller chains and sprocket wheels with a gear ratio selected to force the center friction-measuring wheel to operate at the desired fixed braking slip ratio. A vertical load of 220 lb is applied to the friction-measuring wheel with a spring and shock absorber. A smooth-tread tire (16 × 4, 6 ply, RL 2) is used for the test with an inflation pressure of 30 psi for dry- and wet-pavement friction surveys. For winter pavement conditions with snow and ice, the special high-pressure (100 psi), grooved-tread, 16 × 4 aero tire is used. (See fig. 17.)

Trailer speed and torque applied to the test wheel by braking friction forces are data inputs to the skiddometer computer shown in figure 25(b). The trailer speed is measured by a tachometer generator driven by one of the roller chains. A special torque transducer continuously measures the torque applied to the middle braked wheel. The data obtained during a test run are processed by the computer and recorded on a strip chart as a continuous plot of friction values over the distance traveled. (See fig. 18(d).) Also printed on the chart are average friction values and trailer speed for each 500-ft segment surveyed during a given run. References 18 and 19 provide additional information on the test capabilities of the BV-11 skiddometer trailer.

Runway friction tester. The runway friction tester (RFT) (Model 6800) was recently developed by an American company located in Michigan. A minivan with front-wheel drive was modified as shown in figure 26 with a friction-measuring wheel connected to the rear axle by a gear drive that produced a constant 13-percent braking slip ratio on the measuring wheel. The test-tire instrumentation includes a two-axis force transducer which measures both vertical and drag loads. Tire friction values can be computed directly without having to consider effects from vehicle oscillations and tire wear. A smooth-tread tire (16 × 4, 6 ply, RL 2, figs. 17 and 27(a)) is used on the friction-measuring wheel with an inflation pressure of 30 psi. A test-tire vertical load of 300 lb is applied by weights mounted on a double-shock-absorber spring assembly.

Measurement signals of test-tire drag and vertical loads are transmitted, together with vehicle speed, into a computer mounted near the vehicle operator's front seat. The computer calculates friction-coefficient values for each foot of runway traveled and can be programmed to compute average friction and speed values for a preselected distance. A digital printer can provide a tabulated listing of friction coefficient versus speed, and a plot of these two parameters can be generated for the distance traveled. (See fig. 18(e).) Figure 27(b) shows the computer keyboard installation inside the runway friction tester vehicle. The operator can use the keyboard to enter test-run information and conditions. Reference 20 provides additional information on the test capabilities and features of the runway friction tester.

Runway condition reading vehicle. The Navy runway condition reading (RCR) vehicle is shown in figure 28. This conventional, rear-axle-drive, pickup truck is equipped with mud- and snow-grip tread, bias-ply tires on the rear wheels, and conventional, grooved and siped, bias-ply tires on the front wheels; all tires are inflated to 32 psi. The RCR vehicle operator accelerates the vehicle up to the desired test speed and applies hard braking to momentarily lock all four wheels. A decelerometer reading from either

the Tapley meters shown in figure 29 or the Bowmonk brakemeter unit shown in figure 30 is manually recorded for the locked-wheel braking portion of the test run. There are two types of Tapley meters available—the original mechanical meter shown in figure 29(a) and the newer electronic airfield friction meter shown in figure 29(b). The mechanical meter is a small pendulum-based decelerometer that consists of a dynamically calibrated oil-damped pendulum in a sealed housing. The pendulum is magnetically linked to a lightweight gear mechanism to which is attached a circumferential scale that shows values as a percentage of g, $1g = 32.2$ ft/sec^2. A lightweight ratchet retains the maximum scale deflection reached upon completion of a test. The mechanism is enclosed in an aluminum case and the scale is covered with a glass face. The whole assembly is mounted in a cast base plate by means of a fork assembly. Each meter is statically tested and dynamically calibrated before being issued a calibration certificate. When the meter is used in a friction survey, it is placed on the floor of the vehicle. The data have to be visually read and recorded by the operator. The electronic Tapley airfield friction meter (fig. 29(b)) provides a recording of the data taken during a friction survey, including averages for each segment (one third) of the runway. The meter is a pendulum-activated, semiautomatic, recording decelerometer, and it operates on the same principles as the original Tapley mechanical decelerometer. When preparing to conduct a friction survey, the operator places the meter on the floor of the test vehicle. The actuating pad is fitted to the brake pedal, and the command module is attached to the vehicle window by a suction pad in front of the driver's side at another suitable location that is readily visible to the operator. The power leads are connected either to the vehicle battery or to a separate battery. The equipment is now ready for testing the runway. These devices should only be used on runway surfaces covered with ice and/or compacted snow, because, under dry and most wet-runway conditions, RCR vehicle wheel lockup becomes inconsistent and vehicle stability is degraded. Additional information on the operation and test capability of the Tapley meter can be obtained from references 19 and 21.

The Bowmonk brakemeter-dynometer used in the RCR vehicle is shown in figure 30. The unit consists of a finely balanced pendulum that is free to respond to any changes in speed and angle. The pendulum movement is coupled with a quadrant gear train to rotate the dial needle. The dial is calibrated as a percentage of g. The meter should always be installed in the vehicle with a floor-mounting stand, and, to damp out excessive vehicle vibrations, the instrument is cushioned with a fluid that is insensitive to temperature changes. Like the Tapley meter, the manufacturer of the Bowmonk meter recommends use only on runway surfaces covered with ice and/or compacted snow where vehicle wheel lockups are more consistent and controllable. Reference 22 contains additional details on the test capabilities and operation of the Bowmonk brakemeter.

Supplemental Instrumentation and Data Measurements

Portable three-axis accelerometer. The main components of this accelerometer package used onboard the test aircraft are shown in figure 31. The unit consists of a four-channel analog tape recorder and a three-axis (longitudinal, vertical, and lateral) linear-accelerometer package that can be operated from battery power or a 110-V ac power source. An audio recorder channel and microphone are available to annotate conditions and events of each aircraft test run. The nominal range of the three-axis accelerometer is $\pm 1g$ with a frequency response of 6 cycles/sec and an accuracy of $\pm 0.1g$. The RC filter is used in the cable that connects the accelerometer package to the tape-recorder input channels. Acceleration measurements with this portable unit were found to closely agree with readings obtained from the primary data-acquisition system of the test aircraft for a given run.

Surface temperature gauge. For noncontact surface temperature measurements such as test-tire treads, wheel brake units, and runway pavement surfaces, an infrared pyrometer device was used during the test program. The unit used by ground test personnel (fig. 32) is a self-contained, battery-operated device that includes a sensing head and a display unit. The power source is a single 9-V alkaline battery or a 110-V ac power source for long-term monitoring. The sensing head contains a passive sensor that receives and measures heat radiation from an object. The display unit can indicate temperature values in either degrees Fahrenheit or Centigrade. The temperature range is 0° to 500°F or 0° to 260°C with a 1° resolution and an accuracy of $\pm 1\% + 1$ digit. Temperature measurements can be taken from a distance of about 1/4 in. to 6 in. from the source.

Portable wind anemometer. Prior to each aircraft test run, ground personnel located near the runway test section took a wind reading with the handheld, portable wind anemometer shown in figure 33. The unit has a trigger-actuated, wind-speed dial gauge and, when the built-in compass rose is aligned

with the runway heading, the wind direction can also be determined. These wind readings, together with the runway elevation, ambient temperature, and pressure altitude, were used in computing the aircraft ground handling performance. Additional environmental parameters were obtained for each aircraft test run using airport tower gauges and instrumentation.

Water-depth gauge. Runway surface water depth was measured with a gauge designed by NASA (ref. 23) and shown in figure 34. The gauge works on the principle of reflectivity. Polished Plexiglas rods with adjustable protrusions through a black plastic disk are positioned in a circular arrangement. The disk is mounted on a small metal tripod. The base height of each rod above the plane of the tripod feet (corresponding to the surface on which the water depth is to be measured) is numerically indicated on the top of the disk. When the lower countersunk end of the clear Plexiglas rod contacts the water surface, a capillary effect is initiated. The effect is instantly visible by light refraction at the polished upper end of the rod. Water depth is indicated by the highest immersed rod. In figure 34, for example, the gauge indicates a water depth of 0.06 in.

Texture-depth kit. A pavement surface texture-depth measuring kit, developed by NASA (refs. 24 and 25) and shown in figure 35, was used to measure the average depth of the surface macrotexture on the different test runways. For this measurement, a known volume of grease (usually 0.5 in^3) was spread on the surface with a rubber squeegee in an area between two strips of masking tape positioned at a known distance apart. After the grease was evenly spread as far as possible, the covered area was measured. The average surface macrotexture depth was computed by dividing the volume of grease that was spread by the area covered. The macrotexture-depth values recorded for the test surfaces evaluated during this program are listed in table I.

Snow density data. During the snow- and slush-covered runway tests at BNAS, samples of the winter contaminant were obtained to determine density values. Known volumes of the snow or slush material were collected (fig. 36), weighed, and compared with the weight of an equivalent volume of water. In previous tests (refs. 26 and 27), snow and slush density values were shown to affect impingement drag levels on the aircraft.

Rain gauge. Some tests were conducted under wet-runway conditions that resulted from light to moderate rainfall. The portable rain gauge, labeled in figure 33 and shown in figure 37, was used to measure the rain accumulation with time near the runway test section. Readings were normally taken at 15-min intervals during periods of steady rain. If the rainfall intensity changed noticeably, readings were taken more frequently.

Support Equipment

Runway markers. Aluminum tripods with painted nylon markers were set up as shown in figure 38 along the left side (as viewed by the pilot) of the runway at 500-ft intervals. These markers were used as visual aids to the pilot in entering the runway test section at the desired speed. These markers also served as reference points to the flight-test engineer for actuating the event marker on the airborne recorder and to the ground crew for locating the point of brake application and release.

Snow removal equipment. The different types of snow removal equipment and the 737 test aircraft used during the tests at BNAS are shown in figure 39(a). Snow blowers were used to remove most of the snow from either end and both sides of the test runway (figs. 39(b) and (c)). Plows (fig. 39(d)) were used to reach bare pavement and to adjust the depth of snow in the test section. These plows were equipped with a secondary leveling bar located behind the front wheel. The person shown in figure 39(d) is pointing to this leveling bar.

Runway water tankers. A variety of tanker trucks were used in obtaining both wet-surface conditions and solid-ice conditions. The large (6000-gal) tanker truck used at Wallops was equipped with a 30-ft spreader bar in the rear to help distribute the water. Figure 40(a) is a photograph of this tanker truck in operation. The water truck used at the FAA Technical Center airport had a spray nozzle located on the left side of the vehicle which permitted wetting an area as much as 50 ft in width. Figure 40(b) shows this tanker truck in operation. Two smaller (2000-gal) tanker trucks were used at BNAS to obtain wet-surface conditions and, when the temperature was below freezing, a solid-ice-covered surface condition. Figure 40(c) shows these two tanker trucks in operation.

Photographic coverage. Extensive photographic coverage was used during the course of this program to help document test conditions, run sequence, aircraft and ground-vehicle performance, and support personnel. A motion-picture camera and television camera, each equipped with a zoom lens, were

mounted on tripods and were operated adjacent to the runway test section near the midpoint. The tests at Wallops Flight Facility were covered with two additional, 16-mm color motion-picture cameras. A hydraulically operated camera mount (converted gun mount) with azimuth and elevation control was placed about 800 ft from the side of the runway near the test-section midpoint. This camera mount held two cameras. One, with a 4-in. lens that took 128 frames per second, was focused on the overall aircraft; the other, with a 10-in. lens that took 200 frames per second, was focused on the aircraft wheels. These cameras tracked the aircraft from just prior to touchdown to test-section exit. Numerous color still photographs were also taken to help document the test operations, conditions, and data measurements.

Miscellaneous. Portable, battery-powered, handheld, two-way radios (fig. 32) were used by ground test personnel to help coordinate testing activities and the proper sequence of aircraft and ground-vehicle test runs. A tire tread depth gauge, marked in 1/32-in. increments, was used to monitor aircraft tire tread wear as shown in figure 41. When the aircraft tire tread groove depth reached 50-percent worn, the two tires on a given landing gear were replaced with new tires. A portable, battery-powered, optical pyrometer was used by aircraft ground crews to check tire and brake temperatures after braking test runs. Tire inflation pressure gauges were used daily to check both aircraft and ground-vehicle test-tire pressures. Appropriate tools, replacement parts, and repair kits were also available to accomplish on-site repair and maintenance of the test aircraft and ground vehicles. A plastic, 1-pint measuring cup with handle was used to collect runway snow samples for weight measurements and density computations. A 1/16-in. graduated folding ruler was used to determine average snow depth on the runway test surface at BNAS.

Test Procedures

General

All personnel were assigned duties and data collection tasks to help complete the required tests. For each test run conducted by the aircraft and ground vehicles, a run number, time of day, test-run heading, speed, and runway surface condition were recorded along with appropriate environmental measurements such as temperature, wind speed and direction, and rain rate.

Dry Runways

Aircraft and ground-vehicle tests under dry conditions were not performed on every test surface because of tire wear considerations, weather restrictions, and the small effect of variation in surface type on dry friction performance. (See refs. 28 and 29.) Aircraft maximum-braking test runs were performed either from a start point at the end of the runway with the aircraft accelerating up to the desired speed prior to the test section, or from a landing on and rollout into the test section. When aircraft speed reached approximately 15 knots, the pilot was instructed to release the brake pedals, because the antiskid protection cuts off at that speed. For dry conditions, the aircraft tests were performed separately from the ground-vehicle test runs, because the friction data were not time dependent. Some nonbraking, baseline aircraft data runs were performed on runway 10/28 at Wallops Flight Facility and on the test runways at Langley AFB, the FAA Technical Center, and the BNAS. Upon aircraft arrival at a given test site, the initial landing was treated as a baseline data run with full reversers and no brakes. Also, some tare test runs were performed to determine aircraft aerodynamic drag and tire rolling resistance for each test configuration. Dry friction measurements were obtained at 20, 40, and 60 mph for all the vehicles except the DBV, which provided friction data from 60 mph down to a complete stop.

Wet Runways

For runways under truck-wet test conditions, the following sequence of events and procedures were followed:

1. The test aircraft was positioned for beginning of a run, either at the end of runway or in the air.
2. Water trucks made two passes over the marked runway test section.
3. Surface water-depth measurements were collected. Depths of approximately 0.02 to 0.03 in. were used for most wet runway tests. For flooded runway tests, water depths between 0.1 and 0.2 in. were maintained.
4. One or more ground test vehicles made test runs at selected speeds.
5. Surface water-depth measurements were collected.
6. The aircraft made a test run with maximum wheel braking after entering the marked test section. The test ended when the aircraft exited the marked section or slowed to approximately 15 knots, whichever came first.
7. After exiting the test section, the aircraft (a) continued to a stop by using reverse thrust and/or brakes as required and awaited the next run;

(b) stopped, made a 180° turn, and took off for brake cooling if required; or (c) accelerated and took off for brake cooling. The action taken depended on the runway geometry, winds, and brake cooling requirements of a particular run.

8. Surface water-depth measurements were collected.
9. One or more ground test vehicles made test runs at selected speeds.
10. Surface water-depth measurements were collected.

The above test sequence generally took between 5 and 10 min to complete.

For rain-wet runway conditions, step 2 above is not necessary, and rain-gauge readings versus time are collected in addition to surface water-depth measurements. Tests performed with both aircraft on the nongrooved slurry-seal asphalt surface at Wallops with a rainfall rate of 0.03 in/hr produced an average surface water depth of 0.01 to 0.02 in. During rain-wet tests with the 727 aircraft on the nongrooved asphalt surface at BNAS, the average surface water depth was 0.05 to 0.06 in. for a rainfall rate of 0.16 in/hr. Flooded test runs were performed only on surfaces A and B (nongrooved and grooved concrete) of runway 4/22 at Wallops. For a given aircraft run on runway 4/22, braking data were collected on two adjacent test surfaces because of their relatively short length (700 ft). Also, multiple aircraft runs in different directions on the same two surfaces of runway 4/22 are required at different brake application speeds to obtain sufficient friction-speed gradient data for both surfaces. This multiple-aircraft-run procedure was also used for the short (200-ft) nongrooved asphalt surface B at the FAA Technical Center. For all wet-runway braking test runs, ground-vehicle test runs were conducted before and after each aircraft test. Figures 42(a) and (b) show truck-wet and rain-wet runway surface conditions at Wallops.

Snow- and Slush-Covered Runways

The winter runway test conditions were all evaluated at BNAS. The initial aircraft landing was made on the cleared inboard runway (1R/19L) using normal reversers and braking techniques as required. The outboard test runway (1L/19R) was cleared of snow and slush contaminants at both ends for 2000 ft and along the shoulder to provide a contaminated test section approximately 150 ft wide by 4000 ft long near the middle of the 8000-ft runway. (See fig. 9.) The cleared runway end sections provided adequate conditions for aircraft and ground-vehicle acceleration and stopping. Aircraft testing commenced after the contaminated runway characteristics were measured and documented by ground test team members. Figures 42(c) and (d) show typical compacted snow-covered and slush-covered runway surfaces at BNAS. An accelerate-stop procedure was used for the aircraft test runs, with the initial run of each test series conducted at low (approximately 60 knots) brake application speed. Subsequent test runs were conducted at gradually increasing brake application speeds up to a desired maximum ground speed of 100 knots. Ground-vehicle test runs at 20, 40, and 60 mph in both directions for a given winter runway condition were generally conducted after the aircraft test run series was completed. Several nonbraking aircraft test runs were performed to determine the magnitude of the drag produced on the aircraft from the winter runway conditions. The standard aircraft landing configuration was used for these nonbraking tests, and the aircraft engine thrust was set at idle throughout the contaminated test section. A landing on and rollout into the test section was required to collect sufficient aircraft test data at the higher operating speeds.

Ice-Covered Runways

The procedure used to obtain an appropriate ice-covered runway test surface involved water application from the tanker trucks at BNAS. During nighttime hours, when ambient temperatures were well below freezing and the runway surface was bare (clear of contaminants), water was sprayed over an area approximately 60 ft wide and 2000 ft long near the middle of the runway. After several passes, the water that had collected on the surface froze and formed a solid ice-covered condition similar to that shown in figure 42(e). Aircraft braking test runs, starting at low speeds, were scheduled right after daybreak when the winds were nearly calm. Ground-vehicle test runs at 20, 40, and 60 mph were performed immediately after completion of the aircraft runs.

A limited number of 727 aircraft and ground-vehicle test runs were conducted to evaluate chemical treatments to remove compacted snow and ice or to act as an anti-icing treatment applied to bare pavement. Figure 43(a) shows the truck that was used to apply dry urea on compacted snow and ice at a rate of 0.008 lb/ft^2. The chemical distribution equipment shown in figure 43(b) was used to evaluate liquid UCAR as a pavement deicing and anti-icing agent. As a deicing treatment, the liquid UCAR was applied at a rate of 0.00146 gal/ft^2, but the application rate was 0.0005 gal/ft^2 as an anti-icing treatment.

Compilation of Test Data

General

The overall chronology of aircraft and ground-vehicle test runs is given in table IV. The NASA Boeing 737 aircraft with the DBV, the Mu-Meter (Mu-M), the SFT, and the BV-11 skiddometer were tested first followed by the FAA Boeing 727 aircraft with the same ground test vehicles. The runway friction tester and the Navy RCR vehicle equipped with both a Tapley meter and a Bowmonk brakemeter were also used during tests with the 727 aircraft. Appendix A contains tables that list the 737 aircraft and ground-vehicle friction data, and appendix B contains tables that list the 727 aircraft and ground-vehicle friction data. The first table in each of the appendixes (tables AI and BI) contains aircraft and ground-vehicle test-run sequence data obtained at each test site.

Aircraft Braking Friction Data

Tables AII and BII contain compilations of 737 and 727 aircraft braking friction data by test-surface type and wetness condition. Run numbers and flight numbers are identified with the aircraft gross weight, center-of-gravity (c.g.) station, type of braking (either manual or automatic for 737 aircraft; main wheel only or main and nose wheel for 727 aircraft), and the effective braking friction coefficients at 5-knot ground speed increments. These aircraft effective braking friction coefficients, derived from aircraft test-run time-history performance data that was sampled at the rate of 40 samples per second, are average values and are determined from linear-regression-analysis procedures. These data are listed in tables AII and BII by test site, starting with Wallops.

Ground-Vehicle Friction Data

All the ground-vehicle friction data were tabulated by test aircraft and test-surface condition. Tables AIII and BIII contain the dry-runway test-surface data obtained during 737 and 727 aircraft tests. Tables AIV and BIV list the wet-runway friction data that were obtained before and after the 737 and 727 aircraft braking test runs at each site. The ground-vehicle, wet-surface, friction data are grouped by test-vehicle type and test-run time relative to the time of the aircraft test run. Average friction-coefficient values are listed in 10-mph increments up to 60 mph. Supplemental ground-vehicle friction data obtained on wet-runway test surfaces without the test aircraft are contained in tables AV and BV. These friction data are given in 10-mph increments up to 60 mph and are arranged by ground test vehicle type and runway test site. Date of test and test run number are also given. Ground-vehicle friction data obtained during 737 aircraft tests at BNAS in March 1985 are given in table AVI by winter-runway surface condition. The diagonal-braking vehicle was not used during the tests at BNAS. Similar data collected during 727 aircraft tests at BNAS and Pease AFB are listed in table BVI. A total of 495 test runs by the different ground friction-measuring vehicles were included for analysis and evaluation with respect to 737 aircraft tire friction performance compared with 634 ground-vehicle test runs with the 727 aircraft. Friction data obtained only with the runway friction tester used during the 727 aircraft tests are included for analysis with the 737 aircraft and the other ground test vehicle friction data for similar surface type and wetness conditions.

Data Reduction and Analysis

Aircraft Data

Aircraft test-run parameter data (see table II) recorded on analog magnetic tape filtered at 100 Hz were transcribed into a digital format and processed into engineering unit (EU) tapes. From these EU tapes, time histories of all instrumented aircraft system parameters required for data analysis were generated. Uniformity in pilot brake application and proper aircraft configuration for a given series of test runs was determined from careful review of these time-history plots. A maximum sample rate of 40/sec was used in digitizing the aircraft parameter data. For a given runway surface condition, longitudinal acceleration data from nonbraking tare runs were analyzed to identify incremental components attributable to aerodynamic drag, tire rolling resistance, engine idle thrust, and a change in the zero value of the accelerometer as the result of runway contaminant displacement drag. These tare run values of aircraft longitudinal acceleration were then used to correct the measured values recorded during maximum-braking test runs. Tabulations of the empirical factors assigned to the various test conditions are given in tables AVII and BVII. The aircraft effective braking friction coefficients for a given run were derived by using an average percentage of the aircraft gross weight supported on the main-gear braking wheel; this percentage varied as a function of the nominal center-of-gravity position. A least-squares curve was fitted to the effective friction coefficient μ_{eff} data variation with ground speed V_G, and a statistical measure (standard deviation σ) of the dispersion of the measured μ_{eff} values about the

least-squares curve fit was calculated. Figure 44 is a flow chart of this overall aircraft tire friction, data-reduction process. Tables AVIII and BVIII give the 737 and 727 aerodynamic and geometric data useful in determining the aircraft theoretical braking performance.

Examples of several 737 aircraft test-run parameter time histories and cross plots are provided in figures 45(a) to (r) for dry, snow-covered, and ice-covered runway conditions. Figures 45(a) to (l) present the data taken during nonbraking free-rolling tare runs of the 737 on the small aggregate asphalt runway at BNAS. The ground speed and longitudinal acceleration time histories and the cross plots of acceleration versus speed all display the steadily reducing speed and the low, steadily reducing deceleration values indicative of predominately aerodynamic-drag-induced velocity decay. The low, relatively steady values of brake-pedal position, brake valve control voltage, and brake pressure displayed on the time-history plots (figs. 45(a), (c), (e), (g), (i), and (k)) are indicative of a nonbraking test run, as is the fact that the wheel speed is synchronous with the ground speed. The cross plots of figures 45(f) and (h) show that the longitudinal deceleration during free-rolling tare runs on the 4-in. wet-snow-covered runway is slightly higher (≈ 0.05) than the dry runs shown in figures 45(b) and (d). The cross plots of figures 45(j) and (l) show that the longitudinal deceleration during free-rolling tare runs on the 6-in. loose-snow-covered runway, with a snow density less than that of the 4-in. wet snow, is lower than on the wet-snow case but higher (≈ 0.03) than the dry runs shown in figures 45(b) and (d). Figures 45(m) to (r) present the data taken during maximum anti-skid braking runs on the small aggregate asphalt runway at BNAS under dry, 6-in. loose-snow-covered and ice-covered conditions. By examining the time slice on these three runs, during which the brake-pedal position indicates a call for maximum brake application, several observations can be made. The deceleration values displayed during these three runs, taken over a speed range of 60 to 80 knots for ease of comparison, show a decrease from a range of 0.46 to 0.50 in the dry case to a range of 0.30 to 0.35 in the snow-covered case to a low for the ice-covered case of 0.10 to 0.12. The deceleration values in the ice-covered case are not significantly different from the dry nonbraking run values. As the friction level decreases, the reduced effective braking action can be seen by the increase in the average level and activity of the anti-skid brake valve control voltage (figs. 45(m), (o), and (q)), in the reduced average brake pressure, and in the depressed wheel speed compared with the ground speed that is indicative of an increased slip ratio.

Similar examples of test-run-parameter time histories and cross plots for the 727 aircraft are given in figures 46(a) to (r) for dry, truck-wet, loose-snow-covered, and ice-covered conditions. Figures 46(a) to (h) present the data taken during nonbraking, free-rolling tare runs of the 727 on the small aggregate asphalt runway at BNAS. The ground speed and longitudinal acceleration time histories and the cross plots of acceleration versus speed all display the steadily reducing speed and the low, steadily reducing deceleration values indicative of predominately aerodynamic-drag-induced velocity decay. The run data shown in figure 46(a) are indicative of one of two test procedures used whereby the aircraft was accelerated from a stop to the desired test speed and then proceeded under idle thrust for the remainder of the free-rolling or maximum-braking portion of the run. The longitudinal acceleration at the beginning of the test portion displayed is just finishing transitioning from the acceleration portion of the run to the free-rolling portion of the run. The run data shown in figure 46(c) are indicative of the second test procedure used, in which the test was conducted from a landing-on condition and then proceeded through the test section under idle thrust. The beginning data presented are at the end of the landing, and touchdown occurs at about 2.5 sec. The touchdown of the left outboard occurs at about 3 sec. The engines have spooled down and are at idle thrust about 9 sec into the run time history. The low, relatively steady values of brake-pedal position, brake-valve control voltage, and brake pressure displayed in figures 46(a), (c), (e), and (g) are indicative of a nonbraking test run, as is the fact that the wheel speed is synchronous with the ground speed. The cross plots of figures 46(f) and (h) show that the longitudinal deceleration during free-rolling tare runs on the 4.5-in. loose-snow-covered runway is slightly higher (≈ 0.06) than during the dry runs shown in figures 46(b) and (d). Figures 46(i) to (r) present the data taken during maximum anti-skid braking runs on the small aggregate asphalt runway at BNAS under dry, truck-wet, 4.5-in. loose-snow-covered, and UCAR on ice-covered conditions. By examining the time slice on these five runs, during which the brake-pedal position indicates maximum brake application, several observations can be made. The deceleration values displayed during these five runs, taken over a speed range of 40 to 80 knots for ease of comparison, show a decrease from a range of 0.4 to 0.5 in the dry case to 0.35 to 0.42 in the truck-wet case, to a range of 0.25 to 0.28 in the snow-covered case, to a low for the ice-covered case of 0.20 to 0.25. These values for the UCAR on ice-covered conditions are significantly higher than the values for the dry

nonbraking free-rolling values. As a comparison is made between figures 46(i), (k), (m), and (o) to (q) and the previous two sets, going to an increasingly reduced-friction surface of dry to truck-wet to snow- and ice-covered, several observations should be made. As the friction level decreases, the reduced effective braking action can be seen in the increase in the average level and activity of the antiskid brake-valve control voltage, in the reduced average brake pressure, and in the depressed wheel speed compared with the ground speed and the increased frequency and depth of wheel spin-down.

Ground-Vehicle Data

Each ground test vehicle operator was responsible for checking and tabulating the tire friction readings obtained during each test run. These values were further validated at NASA Langley during reexamination of the ground-vehicle test records. For the Tapley and Bowmonk brakemeter devices used on the RCR vehicle during winter runway tests, readings were taken and recorded manually by the test observer. These values were recorded on log sheets and were accepted as written. Values of RCR were determined by multiplying the decelerometer meter reading (percentage G) by 100 and dividing by 3.2. In analyzing the ground-vehicle snow- and ice-covered runway data, similar friction data reported in references 3, 7, 12 to 14, and 20 were also considered. For wet-runway data, test-tire inflation pressure and dynamic hydroplaning speed were considered together with the test-tire operational mode. Table V is a summary of the important test-tire characteristics for the two aircraft and the different ground test vehicles. The equations shown for computing the critical hydroplaning spin-down speeds together with the characteristic dry friction-coefficient values were defined in references 7, 28, 30, and 31.

Correlation Methodology

A considerable amount of tire friction performance data has been collected by researchers at NASA Langley. (See refs. 1 to 10 and 24 to 36.) The test results from these studies have identified several major factors that influence tire friction behavior on dry, wet, flooded, snow-covered, and ice-covered surfaces. In analyzing the wet- and flooded-surface data, several empirical relationships have been derived to define the friction performance, either braking or cornering, of a generic pneumatic tire. A methodology to estimate the tire friction performance of a particular vehicle, whether for an aircraft or a ground vehicle, has been developed from this tire friction data-base analysis. This methodology to estimate the tire friction performance of one vehicle from the tire friction measurement of another vehicle through a speed range on a wet surface continues to be developed and modified, but the current data reduction and computational procedures are outlined below. For this report, the ground-vehicle measurements are used to calculate the estimated variation of 737 and 727 aircraft tire effective braking friction coefficient with ground speed.

Step 1. Determine the best-fit curve for the measured, ground-vehicle tire, friction-speed gradient data for a given test-surface type and condition.

Step 2. For each vehicle, calculate the minimum tire dynamic hydroplaning spin-down speed in knots by using the following equation (see table V and refs. 28, 31, and 32):

$$V_p = 9\sqrt{p} \tag{1}$$

where p is the tire inflation pressure in psi. Experimental values obtained with the Mu-Meter tire indicate that instead of 28.5 knots of tire spin-down velocity calculated using equation (1), 39.1 knots is a better value. This higher value was used in estimating aircraft tire friction performance from Mu-Meter data.

Step 3. Determine experimentally from low-speed (<3 mph) braked rolling, yawed rolling, or locked-wheel sliding, the values of ground-vehicle tire maximum friction coefficient on a dry pavement. These values are identified as the characteristic dry friction coefficient μ_{cd} for a given tire. For aircraft tires, μ_{cd} may be calculated from the following equation (ref. 36):

$$\mu_{cd} = 0.93 - C_1 \times p \tag{2}$$

where $C_1 = 0.0011$ with p expressed in psi.

Step 4. Determine the ratio of ground speed to hydroplaning speed V_G/V_p associated with each ground-vehicle tire friction-speed gradient data set.

Step 5 Determine ground-vehicle tire hydroplaning parameter values using the following general relationship:

$$\overline{Y} = \frac{\mu_{\text{exp}}}{\mu_{cd}} \tag{3}$$

where

$\overline{Y}$ = Tire hydroplaning parameter

and

μ_{exp} = Experimental or estimated wet-pavement friction coefficient

In determining the tire hydroplaning parameter, a distinction is made between two types of tire operating modes—nonrotating and rotating. For locked-wheel, sliding (nonrotating) tire friction data (e.g., DBV), the tire hydroplaning parameter is labeled $\overline{Y}_L$. For braked or yawed rolling (rotating) tire friction data (e.g., BV-11, SFT, RFT, and Mu-Meter), the tire hydroplaning parameter is labeled $\overline{Y}_R$. The relationship between $\overline{Y}_L$ and $\overline{Y}_R$, which was empirically derived from NASA track aircraft tire test data, is given in reference 32. Hence, knowing one tire hydroplaning parameter allows the determination of the other.

Step 6. Calculate aircraft tire maximum braking friction coefficient μ_{max} by simply multiplying the $\overline{Y}_R$ values determined in step 5 by the aircraft tire characteristic dry friction coefficient determined from equation (2) in step 3 (see table V).

Step 7. Determine estimated aircraft tire effective braking coefficient μ_{eff} by using the following equations:

$$\mu_{eff} = 0.2\mu_{max} + 0.7143\mu_{max}^2 \quad (\text{for } \mu_{max} \leq 0.7) \quad (4a)$$

$$\mu_{eff} = 0.7\mu_{max} \quad (\text{for } \mu_{max} > 0.7) \quad (4b)$$

These relationships between aircraft tire maximum braking and effective braking friction coefficient are based on the assumption that the total aircraft braking-system (tires, brakes, hydraulics, gear, and antiskid) efficiency can be generated by a single curve defined by equations 4(a) and (b).

Step 8. Calculate an equivalent aircraft ground speed associated with each value of μ_{eff} by multiplying the computed aircraft dynamic hydroplaning spin-down speed value (see step 2) by the appropriate ground-vehicle speed ratio obtained in step 4.

Step 9. The values derived from steps 7 and 8 can define the estimated friction-speed gradient of the aircraft tire from a particular set of ground-vehicle tire friction measurements through a speed range for a given wet-surface condition.

Tables VI and VII provide generalized listings of estimated μ_{eff} variation with ground-vehicle friction measurements from 1.10 to 0 and for aircraft tire inflation pressures from 100 to 400 psi in 20-psi increments. For the ground vehicles which measure a rolling-tire friction coefficient ($\overline{Y}_R$ parameter), e.g., the RFT, SFT, BV-11, and Mu-Meter, equivalent aircraft ground speed values for each aircraft tire inflation pressure and ground-vehicle speed are listed in table VI. For the diagonal-braked vehicle, which measures locked-wheel tire friction coefficient ($\overline{Y}_L$ parameter), table VII lists equivalent aircraft ground speed values for each aircraft tire inflation pressure and DBV speed.

For winter runway conditions of compacted snow- or ice-covered surfaces, a more simple and direct aircraft tire friction estimation procedure appears reasonable from ground-vehicle friction data collected for the same surface condition. Available data suggest that, with the low shear strength of snow and ice, the tire friction-speed characteristics are determined by the physical properties of the snow and ice contaminant. It is assumed that friction variations from speed, tire size, vertical load, and inflation pressure are insignificant for compacted snow- and ice-covered surfaces. Hence, estimated aircraft tire effective braking friction coefficients can be determined directly from the following equation:

$$\mu_{eff} = 0.2\mu_{GV} + 0.7143(\mu_{GV})^2 \quad (5)$$

where

μ_{GV} = Ground-vehicle tire friction coefficient

For DBV locked-wheel, sliding friction-coefficient values, the computed values of $\overline{Y}_R$ should be used in equation (5) for μ_{GV}.

Statistical Analysis

Data presented in this report have been analyzed in various ways as an aid to a clearer presentation

and as a tool to further analysis in support of conclusions. On data presentation plots such as figure 47, a curve is shown which represents the least-squares linear regression of the data. This first-order, least-squares, linear regression of the form $y = B_0 + B_1 x$ has been used to represent the trends in the data sets throughout this report. The primary relationship used in the correlation methodology between aircraft and ground-vehicle friction data is the relationship between the experimental wet-pavement friction coefficient and the characteristic dry friction coefficient. Because μ_{exp} is more sensitive to runway wetness conditions than to speed (within the speed range tested), and because the constant term in the regression analysis is also more sensitive to runway wetness conditions, the term chosen to indicate the appropriateness of the fit of this regression curve to the fitted data is the square root of the variance about the regression σ. The coefficients B_0 and B_1 for the regression curves and associated values of σ appear in table VIII.

Results and Discussion

General

With the exception of the ground-vehicle, dry-surface friction data, the 737 aircraft and ground-vehicle friction data are discussed first, followed by the 727 aircraft and ground-vehicle friction data. Most of the plots (e.g., fig. 47) show the variation in tire friction coefficient with ground speed for a given test vehicle and surface condition. Some data comparisons are given to indicate the effect of one or more parameters on tire friction performance. For wet, snow-covered, and ice-covered runway conditions, four-graph, composite figures that show the test aircraft and one ground-test vehicle, tire friction performance are combined with the estimated aircraft braking friction performance based on the ground-vehicle friction data. An assessment of the agreement between the estimated and actual aircraft braking performance is given in the fourth graph in these composite figures. Aircraft ground performance parameters of snow impingement drag, engine thrust-reverser performance, and braking configuration are discussed separately for each test aircraft. Some supplemental data analysis plots are also presented that concern ground-vehicle and aircraft friction correlation on compacted snow- and ice-covered runways, 727 aircraft braking performance on porous friction course surfaces, and effects of runway chemical treatments and temperature on winter runway tire friction measurements. Some limited data are described which indicate surface water drainage and accumulation characteristics for a particular runway surface. Plots of aircraft stopping distance versus brake energy are not included in this report, because other factors, such as aircraft configuration, wind speed and direction, and runway slope gradients influence aircraft ground handling performance and stopping capability.

Boeing 737 Aircraft and Ground-Vehicle Data Evaluation

Dry runways. The variation of the 737 effective friction coefficient with ground speed on different dry-runway surfaces is given in figure 47. For dry-surface conditions, ground speed has a small effect on tire friction performance. The friction value varies from approximately 0.44 at 100 knots to approximately 0.47 at 20 knots. Surface type or macrotexture characteristics also appear to have little effect on dry-runway tire friction performance with both nongrooved and grooved asphalt and concrete surfaces included in the data shown in figure 47. The linear-regression equation of the best-fit data curve and the calculated standard deviation σ are given in the figure. All the 737 aircraft dry-surface friction data shown in figure 47 were derived from only manual-braking test runs.

All the ground-vehicle friction measurements obtained on dry-runway surfaces during the course of the entire test program (both airplanes) are given in figure 48 as functions of speed and test-vehicle type. The linear-regression equation and standard-deviation values for each of these ground-vehicle, friction-versus-speed curves are listed in table VIII, starting with the Mu-Meter and followed, in order, by the BV-11 skiddometer, the surface friction tester, the runway friction tester, and the diagonal-braked vehicle. These ground-vehicle, tire friction measurements are similar to the 737 friction data, in that speed and surface type (macrotexture) appear to have little effect. The fixed-slip braking devices (BV-11, SFT, and RFT) produced the highest dry-surface friction values, and the Mu-Meter (side force) and diagonal-braked vehicle (locked wheel) produced the lowest values. For a given dry test surface, tire temperature effects were most noticeable on the DBV data that were collected during a continuous test run from 60 mph down to a complete stop. The test method and mode of test-tire operation on the other ground vehicles helped minimize the effect of tire temperature on the friction data.

A comparison of the 737 aircraft and ground-vehicle data collected at various runway surface conditions is given in figure 49, with the dry runway surface data shown in figure 49(a). Because of differences in tire characteristics (tables III and V),

test operational mode, and brake-system control, the ground-vehicle friction-coefficient variations with speed were all well above the 737 friction-speed curve. The slightly negative slopes of the ground-vehicle and friction-speed data are similar, except for the Mu-Meter, which indicated a slightly positive slope (increasing friction with increasing speed).

Wet runways. The range of wet-runway friction data for the ground vehicles and for the 737 is shown in figure 49(b) for rain-wet, slurry-seal asphalt, in figure 49(c) for truck-wet, nongrooved and grooved surfaces, and in figure 49(d) for flooded, nongrooved surface A and grooved surfaces B and C. For these wet surfaces, the data indicate that both speed and surface macrotexture significantly affect the tire friction performance. Decreasing macrotexture and increasing speed decrease the friction level. The grooved surfaces provided much higher friction levels than similar nongrooved surfaces. In general, the ground vehicles measured higher friction than the 737 for rain-wet and truck-wet conditions, but the 737 tire friction was higher for flooded conditions at high (>60 knots) speed. This latter result was probably attained because the inflation pressure used in the aircraft tire was much higher than that used in the ground-vehicle test tires. (See table V.)

Figures 50 to 52 are composite plots that show tire friction performance comparison between one ground-test vehicle and the 737 on wet-runway surfaces that are grouped as follows: truck-wet, nongrooved surfaces (fig. 50); truck-wet, grooved surfaces (fig. 51); and rain-wet, nongrooved slurry-seal asphalt surfaces (fig. 52). A data point and curved-line code are used to distinguish between friction data collected on the different surfaces. For the data in figures 50 and 51, an average of all the nongrooved surface values (fig. 50) and all the grooved surface values (fig. 51) is also plotted for each aircraft and ground-vehicle data set. In these composite figures, the upper left plots show the variation of 737 effective friction coefficient with speed, and the upper right plots show the variation of comparable ground-vehicle average friction coefficient with speed. The lower left plots give the variation of estimated aircraft effective friction coefficient with speed derived from the ground-vehicle friction measurements by using the tire friction methodology discussed previously. The lower right plots show the agreement between the estimated and actual aircraft effective friction coefficient for speeds between 10 and 110 knots. A ±0.1 effective coefficient band is indicated by dashed lines on this plot, and a solid line indicates perfect agreement. For most of the truck- and rain-wet surface data, the plots in figures 50 to 52 indicate that the agreement between estimated and actual aircraft tire friction performance is within this ±0.1 friction-coefficient bandwidth.

Snow- and ice-covered runways. The range of 737 aircraft and ground-vehicle data collected on snow- and ice-covered runway surfaces at BNAS is indicated in figures 49(e) and (f). For tests with the 737 aircraft, only the BV-11 skiddometer and the Mu-Meter were available to collect comparable friction measurements. An increase in 737 tire friction coefficient as speed increases is shown in figure 49(e), but the opposite tire friction performance is indicated on glare ice. (See fig. 49(f).) The BV-11 skiddometer data are similar for both the snow- and ice-covered surfaces, but the 737 data show a significant decrease on the glare ice when compared with the 1.5-in. new-wet-snow condition. These test results are also indicated in the upper plots of the composite figure 53, which also gives the estimated 737 tire friction performance from a given ground-vehicle data set. The agreement between estimated and actual 737 tire friction performance is well within the ±0.1 friction-coefficient band for the glare-ice condition and mostly within the bandwidth for the snow-covered condition, based on both ground-vehicle friction measurements.

Boeing 737 Aircraft Snow-Impingement Drag

A series of free-rolling, idle-thrust, landing-configuration test runs were conducted with the 737 in a 6-in-deep, loose-snow-covered runway condition at BNAS to determine the magnitude of impingement drag (ref. 37) developed on the aircraft. The variation of 737 deceleration with ground speed for this snow-covered condition is shown in figure 54. The deceleration varies from nearly $0.3g$ at 80 knots down to $0.08g$ at 40 knots. Based on 737 aircraft engine thrust data, the aircraft could not achieve the required rotational speed for takeoff under these conditions. The specific gravity of the loose snow was relatively low (0.32), and additional test runs are recommended to determine the effect of this factor and snow depth on aircraft impingement drag.

Boeing 737 Aircraft Engine Thrust-Reverser Performance

Several test runs were made with the 737 in a landing configuration and using engine reverse thrust combined with aerodynamic drag and tire rolling resistance to slow the aircraft down to taxi speeds. These tests were performed on dry-runway surfaces at NASA Wallops Flight Facility and at the FAA Technical Center. The head-wind component during these runs varied from 0 to 17 knots. The variation

of 737 aircraft deceleration with ground speed using only engine reverse thrust (no wheel braking) is shown in figure 55 for 18 different runs. These test runs vary in engine-pressure-ratio (EPR) settings from 1.9 to 1.12; the higher EPR settings produce the higher aircraft deceleration values. An approximate variation of 0.15g longitudinal aircraft deceleration was measured for this range of EPR settings. Four different, best-fit, linear-regression curves, distinguished by line codes, were used for the following EPR ranges: 1.79 to 1.9; 1.6 to 1.65; 1.39 to 1.55; and 1.12 to 1.28. The magnitude of the aircraft deceleration performance caused by engine reverse thrust, aerodynamic drag, and tire rolling resistance becomes extremely significant on low-friction surfaces, where wheel braking produces little drag force, particularly at high speeds. Hence, the pilot procedure recommended for landing on slippery runways is to first deploy the spoilers, then apply full engine thrust reversers, and then apply maximum wheel braking.

Comparison of Boeing 737 Aircraft Braking Techniques

During most of the braking test runs with the 737 aircraft, the full manual antiskid braking control mode was used. Some runs were made using a special, automatic, full antiskid braking, control mode onboard the aircraft with the pilot selecting the maximum deceleration level of approximately 10 ft/sec^2. For the nongrooved slurry-seal asphalt under truck-wet conditions, a comparison of 737 manual and automatic braking modes is shown in figure 56. The variation of effective friction-coefficient data with ground speed measured for each braking mode indicates that the manual mode produces approximately 25 percent higher tire friction performance than the automatic braking mode. Although the automatic braking mode relieves some of the pilot work load after touchdown, the manual braking mode is recommended, particularly on critical-balanced-field-length runways.

Boeing 727 Aircraft and Ground-Vehicle Data Evaluation

Dry runways. Variation of effective friction coefficient with ground speed for seven nongrooved and grooved runway test surfaces under dry conditions is shown in figure 57 for the 727 aircraft. These dry-surface aircraft tire friction data are similar to the 737 data, in that speed and surface macrotexture appear to have little effect. All the 727 data in figure 57 were obtained with only main-wheel braking and with the aircraft in the standard braking configuration. The standard deviation and the equation for the best-fit, linear-regression curve are given. For dry-runway conditions, the two test aircraft are nearly identical in effective friction-coefficient variation with ground speed. For comparison, the 727 dry-runway friction data are replotted in figure 58(a), along with the ground-vehicle friction measurements. (See fig. 48.) All the ground-vehicle, dry-surface friction measurements are about twice as much as those measured by the instrumented 727 aircraft. Figure 58 contains 727 aircraft and ground-vehicle friction data comparisons for each runway test-surface condition.

Wet runways. The range of 727 aircraft and ground-vehicle friction data for rain- and truck-wet surface conditions is shown in figures 58(b) to (e). For rain-damp conditions on the porous-friction-course (PFC) surface at Pease AFB, the variation of friction coefficient with speed shown in figure 58(b) does not differ much from that indicated for dry-surface conditions (fig. 58(a)). The PFC surface provides excellent internal water drainage and, as a consequence, both aircraft and ground-vehicle tire friction measurements are relatively high. Similar 727 tire friction performance was obtained on a rain-damp, slurry-seal asphalt surface. (See fig. 58(c).) The DBV data, however, show a much greater influence of speed, which is attributed to the low (24 psi) tire pressure, smooth test-tire tread, and locked-wheel braking mode. For rain-wet conditions with a water depth between 0.04 and 0.06 in. on the nongrooved small aggregate asphalt runway at BNAS, 727 aircraft tire friction performance was lower than for rain-damp conditions. (See fig. 58(d).) The ground-vehicle friction data on this rain-wet asphalt remained higher than that for the 727 aircraft, but the friction-speed gradient is higher than that for the rain-damp PFC surface. (See fig. 58(b).) All the truck-wet, nongrooved- and grooved-surface friction data collected with the 727 aircraft and the five different ground vehicles are shown in figure 58(e). In general, the grooved-surface friction data are higher than those measured on the nongrooved surfaces for all vehicles, and the influence of speed is less.

All the rain- and truck-wet data are replotted in figures 59 to 62 to show the 727 aircraft and individual ground-vehicle friction variations with speed (upper two plots). The estimated 727 aircraft tire friction performance based on a given ground-vehicle friction measurement is shown in the lower left plot. The lower right plot indicates the agreement between estimated and actual 727 aircraft tire friction performance. Dashed lines indicate a ± 0.1 friction-coefficient band, and a solid line indicates

perfect agreement. Most of the 727 aircraft estimated tire friction performance for rain- and truck-wet conditions is within this friction-coefficient band for data between speeds of 10 and 110 knots, except for the rain-wet small aggregate asphalt surface at BNAS. (See fig. 61.) For this particular wet-surface condition, the estimated 727 aircraft tire friction performance from SFT, BV-11, RFT friction measurements is considerably higher than the actual 727 measurements.

Snow- and ice-covered runways. The range of 727 aircraft and ground-vehicle friction data collected for a variety of winter runway conditions is shown in figures 58(f) to (m). For most of these winter runway conditions, the ground-vehicle friction measurements are higher than for the 727 aircraft except on loose dry snow (fig. 58(f)) and 0.25 in. of slush (fig. 58(m)). The higher pressure aircraft tires, apparently pushed through these two types of winter contaminants and regained contact with the relatively high-macrotexture, small-aggregate asphalt surface. Consequently, the 727 tire friction values are higher than most of the ground-vehicle data. For these winter runway conditions, the highest 727 tire friction performance was measured on the 0.25-in-deep slush condition, and the lowest values were obtained on the solid-ice condition. (See fig. 58(e).) The urea dry-chemical treatment on ice resulted in less improvement in 727 friction performance (fig. 58(i)) than that measured for the UCAR liquid chemical treatment on ice (fig. 58(k)). Other factors that influenced these measurements besides the type of chemical treatment were the ambient temperature, solar heating, and elapsed time after chemical application. These winter runway test results for the 727 aircraft and a given ground test vehicle are also indicated in the upper two plots of figure 63 for five different snow- and ice-covered runway conditions. The derived estimated 727 tire friction performance from each of the ground test vehicles is shown to be in good agreement with the actual 727 tire friction performance. (See lower right plots in figs. 63(a) to (d).)

Boeing 727 Aircraft Snow-Impingement Drag

A series of free-rolling, idle-thrust, landing-configuration test runs were conducted for the 4.5-in. loose snow-covered runway condition at BNAS to determine the magnitude of impingement drag developed on the 727 aircraft. The variation of aircraft deceleration with ground speed for the snow-covered condition is shown in figure 64. The deceleration varies from nearly $0.2g$ at 80 knots down to 0.05 at 40 knots. These 727 deceleration values are slightly less, as expected, than the measured values for the 737 traveling through 6 in. of loose snow. (See fig. 54.) The specific gravity of the loose snow was measured at 0.27 for the 727 aircraft tests, which is less than the 0.32 measured during the 737 impingement drag tests.

Boeing 727 Aircraft Engine Thrust-Reverser Performance

Several test runs were performed with the 727 in a landing configuration using engine thrust reversers combined with aerodynamic drag and tire rolling resistance to slow the aircraft down to taxi speeds. These tests were made on dry-runway surfaces with a range of engine pressure ratios from 2.0 down to 1.5. The variation of 727 deceleration with ground speed using only engine thrust reversers (no wheel braking) is shown in figure 65 for 10 different runs. The head-wind components during these runs varied from 2.6 to 24.6 knots. Two best-fit, linear-regression curves, distinguished by line codes, were determined for a range of EPR from 1.75 to 2.0 (solid line) and 1.5 to 1.7 (dashed line). Like the data collected with the 737 aircraft (fig. 55), higher values of EPR and higher ground speed produced higher 727 aircraft deceleration. For equivalent EPR settings, the two-engine (wing mounted) 737 thrust reversers were slightly more effective than the three-engine (fuselage mounted) 727 thrust reversers.

Comparison of Boeing 727 Aircraft Braking Techniques

The majority of the 727 braking test runs were performed with conventional braking with the main wheel only. Since the test aircraft was also equipped with on-command, nose-wheel braking, several main and nose-wheel-braking test runs were made for comparison. This comparison of the 727 aircraft tire friction-coefficient variation with speed for both braking test modes is given in figure 66. These data were collected on the nongrooved, slurry-seal asphalt surface under truck-wet conditions, and the difference between the two braking techniques is not considered significant.

Supplemental Data Analysis

The variation of 737 and 727 effective friction coefficient with ground speed for different runway conditions is shown in figure 67. The values for both aircraft range from near 0.5 for dry surfaces down to 0.01 on glare ice. Friction measurements with both aircraft indicated that, for the snow-covered-runway condition, the friction level increased with

increasing speed; this trend was opposite from data trends collected on other surface conditions. Under wet-runway conditions, different surface water depths produce different aircraft tire friction performance, as indicated by the wet (0.02-in. to 0.03-in. water depth) and the flooded (0.1-in. to 0.2-in. water depth) data shown in figure 67(a) for the 737 aircraft. As a consequence of this effect of surface water depth on tire friction performance, the correlation between ground-vehicle and aircraft friction measurements is affected. Significant changes in rainfall rates at an airport, such as 1 in/hr, would merit additional ground-vehicle friction measurements to document the effect of increased surface water depth on tire friction performance.

During the tests at NASA Wallops Flight Facility on the nongrooved slurry-seal asphalt surface, a number of surface water-depth measurements were taken after truck wetting or during natural rainfall. These surface water-depth values are presented in figure 68 to indicate the water drainage rate after truck wetting and the water accumulation rate with rainfall rate. The winds were calm during these measurements, and the runway surface has a 1-percent crown and an average texture depth of 0.0263 in. For these test conditions, the data indicate a water drainage rate of 0.0043 in/min, and the surface water depth increases with increasing rainfall at a rate of 0.041 in/in/hr. These data indicate that runway-surface water depth can vary rapidly not only under artificial (truck) wetting conditions, but also under natural rain conditions.

Test results from several previous aircraft and ground-vehicle runway friction programs (refs. 1 to 3, 7, and 38) have indicated the porous-friction-course (PFC) pavements offer wet friction performance comparable to grooved surfaces and dry conditions. During testing with the 727 aircraft, an opportunity to collect comparable braking performance data on two PFC surfaces was available. The variation of 727 tire friction with ground speed on these two rain-damp runways is shown in figure 69. The Pease AFB runway had just been resurfaced within a year of testing, and the Portland International Airport runway PFC surfaces had been installed and used for 11 years. Evidently, traffic and weathering have had a smoothing effect on the PFC surface at Portland—the 727 tire friction measurements were somewhat lower than those measured on the newly installed PFC surface at Pease AFB. At Pease AFB, the 727 aircraft braking performance on the rain-damp PFC surface was almost equal to dry-surface performance, as indicated by the solid line in figure 69.

The effectiveness of dry urea and UCAR liquid chemical treatments on compacted snow- and ice-covered runways is difficult to evaluate, because factors such as ambient temperature, wind, solar heating, and elapsed time after chemical application influence the performance of the chemical treatment. Some limited data were collected with the 727 aircraft at BNAS, and a data comparison is shown in figure 70. Both chemical types increased the 737 tire friction performance, and the magnitude of the increase was directly related to the elapsed time from chemical application. Additional tests are needed to better define the effects of these factors and others on using chemicals both as deicing and anti-icing runway treatments.

Some limited ground-vehicle friction data, collected using the Tapley meter, have been evaluated in an effort to better define the effects of ambient temperature and solar heating on tire friction performance. These data are given in figure 71; the solid line indicates the variation in friction readings with temperature during overcast conditions or at night (minimum solar heating). The dashed curve indicates tire friction variation with temperature measured during daylight hours with bright sunlight (maximum solar heating). These comparable data indicate that solar heating has a significant effect on tire friction performance and that only temperature is significant near (±5°F) the freezing point.

The friction measurements obtained with the different ground vehicles operating on compacted snow- and ice-covered conditions at BNAS indicated that speed had little effect on the magnitude of the friction values. (See figs. 49(e) and (f), 53(a) and (b), 58(h) to (l), and 63(a) to (d).) For these two winter conditions, the ground-vehicle friction measurements showed little difference. Table IX is a listing of the range of friction readings for four braking-action classifications derived from the tests conducted at BNAS and other similar winter runway test results (refs. 2, 9, 16, 18, 19, and 22) obtained at other locations. The vehicle test-tire conditions, range of ambient temperatures, and test speeds are included in table IX. Qualitative verbal braking-action terms—namely, excellent, good, marginal, and poor—were used to identify four distinct levels or ranges in friction readings for each device. The correlations between each of the ground-vehicle friction measurements and the Tapley meter readings (TAP) are as follows:

Regression equation	σ	Correlation coefficient
Mu-M = −0.08 + 1.26TAP	0.024	0.976
BOW = −0.01 + 0.96TAP	.021	.984
BV-11/SFT = −0.024 + 1.19TAP	.028	.964
RFT = −0.05 + 1.13TAP	.012	.989
RCR = 100/3.2(TAP)	0	1.000

In general, the excellent friction readings were close to some wet-surface values (e.g., 0.5 and above), but the poor friction readings were normally below 0.25 and were found on the solid glare ice. The data contained in table IX are plotted in figure 72 to illustrate the friction relationship between the different ground-vehicle devices. The format for this figure was derived from a chart contained in reference 18 and used by European countries. The Mu-Meter and the runway friction tester, which measured similar friction values, are plotted together. The four lines represent sample derivations of the vehicle friction measurements that are comparable or equivalent to RCR values of 5, 10, 15, and 20. The range of friction values at each of these four levels is nearly the same for the Mu-Meter, runway friction tester, Tapley meter, and Bowmonk meter. Slightly higher values of friction for each level were obtained with the surface friction tester and the BV-11 skiddometer mainly because a higher test-tire inflation pressure was used (100 psi versus 30 psi or less) combined with a grooved tread pattern on the tire instead of a smooth (blank) tread.

The variation of both the 727 and 737 aircraft effective friction-coefficient values with ground speed for compacted snow- and ice-covered runway conditions is shown in figure 73. The data symbols and line codes distinguish between the different test runs and surface conditions. The best-fit linear curve for the compacted snow-covered surface friction data (solid line) is nearly four times greater than that measured on the solid ice-covered surface. With increasing speed, the level of aircraft braking performance decreased on the ice-covered surface but slightly increased on the compacted snow-covered runway. These slight variations in μ_{eff} with speed, however, are not considered significant.

Since both aircraft indicated a significant tire friction performance difference between the compacted snow-covered and ice-covered surface conditions, two ranges of aircraft friction data were selected to define the relationship with the ground-vehicle friction measurements. The resulting aircraft and ground-vehicle friction-correlation chart is shown in figure 74, where the compacted snow-covered and ice-covered surface conditions are delineated for the two aircraft. For the compacted snow-covered surface condition, an aircraft effective friction coefficient of 0.21 was selected for the excellent-braking-action level and 0.12 was used for the poor-braking-action level. For the ice-covered surface condition, an effective friction-coefficient range from 0.055 to 0.010 was selected for comparable aircraft braking-action levels. Again, the four lines represent sample derivations of vehicle friction measurements comparable or equivalent to RCR values of 5, 10, 15, and 20. The relationships shown in figure 74 between the various ground-vehicle and aircraft friction measurements were derived from the range of values collected from a variety of tests that were conducted under compacted snow- and ice-covered conditions. Not all the winter runway test conditions were evaluated with either or both aircraft. Consequently, a distinct regression equation and correlation coefficient values between the two test aircraft and six ground-vehicle friction values cannot be determined.

From the viewpoint of an aircraft operator, these values of friction for a snow- or ice-covered runway must be considered with respect to the actual runway geometry and several environmental conditions, such as pressure and altitude, winds, and ambient temperature at the time of a particular aircraft operation. It is also recognized that aircraft operations can occur on runways which have a nonuniform mixture of compacted snow-covered area and exposed solid ice-covered surfaces. In such circumstances, additional ground-vehicle friction measurements need to be taken to adequately determine average friction numbers for each portion (surface condition change) of the runway. How well this established relationship between aircraft and ground-vehicle friction values holds for other aircraft types is somewhat questionable, although the available data tend to suggest a similar correlation (refs. 16 and 19). The use of actual friction numbers in place of qualitative braking-action terms is strongly recommended, because, with experience, these runway friction values measured by a ground vehicle provide the pilot a more precise and accurate gauge on the safety margins available for landing on a given runway. Proper and timely use of snow removal equipment and runway chemical treatments to minimize and/or remove snow and ice contaminants is still recognized as a necessity to return, as soon as possible, runway friction levels back up to near dry surface performance.

Concluding Remarks

A substantial number of tests with specially instrumented Boeing 737 and 727 aircraft, together with several different ground friction-measuring devices, have been conducted on a variety of runway surface types and conditions. These tests were identified as part of a Joint FAA/NASA Aircraft/Ground-Vehicle Runway Friction Program to obtain a better understanding of aircraft ground handling performance under adverse weather conditions and to define relationships between aircraft and ground-vehicle tire friction measurements. Aircraft braking performance on dry, rain-damp and rain-wet, truck-wet, and flooded, snow-, slush-, and ice-covered

runway conditions has been discussed, together with ground-vehicle friction data obtained under similar runway conditions. Additional tests were conducted to evaluate aircraft engine reverser performance, snow-impingement drag on the aircraft, and the influence of runway chemical treatments on control of snow and ice contaminants. The major test findings, conclusions, and recommendations are summarized in the following sections.

Major Test Findings

1. For wet-runway conditions, the estimated aircraft braking performance from the ground-vehicle friction measurements was within ±0.1 friction-coefficient value of the measured values, except for some rain-wet data.
2. For snow- and ice-covered runway conditions, the estimated aircraft braking performance from the ground-vehicle friction measurements was within ±0.1 friction-coefficient value of the measured values.
3. A reasonable method of estimating aircraft tire wet, snow-covered, and ice-covered runway braking performance from different ground-vehicle friction measurements has been established, and available data show good agreement.
4. Speed, water depth, surface type and texture, tire tread design, inflation pressure, and test operating mode were identified as major factors that influence wet-runway tire friction performance.
5. The grooved and porous friction course surfaces provided the highest tire friction levels and the nongrooved concrete surface with the lowest macrotexture value gave the lowest tire friction level for wet conditions.
6. The ground-vehicle and aircraft tire friction correlations derived from the available wet-runway data suggest that the friction relationships change with surface water depth.
7. Solar heating appears to affect tire friction performance on snow- and ice-covered surfaces as well as at ambient temperatures near (±5°F) the freezing point.
8. Runway-surface snow depth ≥2 in. prevented towed-trailer friction measuring devices from maintaining constant speed, and trailer instability was observed.
9. Impingement drag from tire-displaced snow and slush can significantly degrade aircraft takeoff performance.
10. The two-engine, wing-mounted Boeing 737 thrust-reverser performance was slightly more effective than the three-engine, rear-fuselage-mounted Boeing 727.
11. The liquid chemical deicing treatment appeared to be more effective than the dry chemical treatment, but additional tests are required.
12. Aircraft and ground-vehicle friction measurements showed little influence of speed and type of surface for dry-runway condition.

Conclusions

1. With proper maintenance, equipment checkout, and instrument calibration performed on a regular schedule, each ground friction measuring device operated satisfactorily and produced consistent, repeatable, and accurate friction data.
2. Water ponding, effect of surface winds, and elapsed time after water application from tanker trucks are factors which greatly influence scatter and repeatability of tire friction-measurement data.
3. Tire friction measurements should be obtained for a range of rainfall rates on a given runway to identify the influence of surface water depth.
4. The range of friction values measured by the different ground vehicles under compacted snow- and ice-covered runway conditions could reasonably be divided into four distinct levels of braking action- excellent, good, marginal, and poor.
5. Ground-vehicle friction measurements have been shown to correlate with aircraft tire friction data; consequently, vehicle friction data collected under adverse weather conditions should be routinely reported to all air traffic using the airport facility.

Recommendations

1. Proper and timely use by airport operators of snow and ice removal equipment and chemical treatments is essential to restore runway friction levels to near-dry surface performance as soon as possible.
2. Additional tests are recommended to better evaluate the various runway chemical treatments used for anti-icing and deicing the runway surfaces.
3. Widespread usage of ground-vehicle friction measurements is strongly recommended for runway surface maintenance and is a valuable tool for monitoring current runway friction conditions.
4. Additional tests under winter runway conditions are recommended so as to further define the influence of temperature, aircraft type, chemical treatments, and type of surface contamination on the friction correlation between aircraft and ground vehicles.

NASA Langley Research Center
Hampton, VA 23665-5225
August 28, 1989

References

1. *Pavement Grooving and Traction Studies.* NASA SP-5073, 1969.
2. Yager, Thomas J.; Phillips, W. Pelham; Horne, Walter B.; and Sparks, Howard C. (appendix D by R. W. Sugg): *A Comparison of Aircraft and Ground Vehicle Stopping Performance on Dry, Wet, Flooded, Slush-, Snow-, and Ice-Covered Runways.* NASA TN D-6098, 1970.
3. Joyner, Upshur T.; Phillips, W. Pelham; and Yager, Thomas J.: Recent Studies on Effects of Runway Grooving on Airplane Operations. AIAA Paper No. 69-773, July 1969.
4. Yager, Thomas J.; Phillips, W. Pelham; and Deal, Perry L.: *Evaluation of Braking Performance of a Light, Twin-Engine Airplane on Grooved and Ungrooved Pavements.* NASA TN D-6444, 1971.
5. Merritt, Leslie R.: Impact of Runway Traction on Possible Approaches to Certification and Operation of Jet Transport Aircraft. Preprint 740497, Soc. of Automotive Engineers, Apr.–May 1974.
6. Horne, Walter B.: *Wet Runways.* NASA TM X-72650, 1975.
7. Horne, Walter B.: Status of Runway Slipperiness Research. *Aircraft Safety and Operating Problems*, NASA SP-416, 1976, pp. 191–245.
8. Horne, Walter B.; Yager, Thomas J.; Sleeper, Robert K.; and Merritt, Leslie R.: *Preliminary Test Results of the Joint FAA-USAF-NASA Runway Research Program, Part I—Traction Measurements of Several Runways Under Wet and Dry Conditions With a Boeing 727, a Diagonal-Braked Vehicle, and a Mu-Meter.* NASA TM X-73909, 1977.
9. Horne, Walter B.; Yager, Thomas J.; Sleeper, Robert K.; Smith, Eunice G.; and Merritt, Leslie R.: *Preliminary Test Results of the Joint FAA-USAF-NASA Runway Research Program, Part II—Traction Measurements of Several Runways Under Wet, Snow Covered, and Dry Conditions With a Douglas DC-9, a Diagonal-Braked Vehicle, and a Mu-Meter.* NASA TM X-73910, 1977.
10. Yager, Thomas J.; and White, Ellis J.: *Recent Progress Towards Predicting Aircraft Ground Handling Performance.* NASA TM-81952, 1981.
11. Staff of NASA Langley Research Center and Boeing Commercial Airplane Co.: *Terminal Configured Vehicle Program—Test Facilities Guide.* NASA SP-435, 1980.
12. Yager, Thomas J.: Progress in Airport Pavement Slipperiness Control. Paper presented at the Air Line Pilots Association 18th Air Safety Forum (Dallas, Texas), July 20–22, 1971.
13. Horne, Walter B.; and Joyner, Upshur T.: Determining Causation of Aircraft Skidding Accidents or Incidents. Paper presented at the 23rd Annual International Air Safety Seminar, Flight Safety Foundation, Inc. (Washington, D.C.), Oct. 1970.
14. Standard Test Method for Side Force Friction on Paved Surfaces Using the Mu-Meter. ASTM Designation: E 670-87. *Volume 04.03 of 1988 Annual Book of ASTM Standards*, 1987, pp. 599–604.
15. Sugg, R. W.: *The Development and Testing of the Runway Friction Meter MK 1 (Mu-Meter).* AF/542/043, British Ministry of Defence, June 1972.
16. Fristedt, Knut; and Norrbom, Bo: *Studies of Contaminated Runways.* FFA Memo. 121, Aeronautical Research Inst. of Sweden, 1980. (Available from DTIC as AD A140 918.)
17. Yager, Thomas J.: A Summary of Recent Aircraft/Ground Vehicle Friction Measurement Tests. SAE Tech. Paper Ser. 881403, Oct. 1988.
18. *Airport Services Manual. Part 2—Pavement Surface Conditions*, Second ed. Doc. 9137-AN/898 Pt. 2, International Civil Aviation Organization, 1984.
19. Fristedt, Knut; and Norrbom, Bo: *Studies Concerning Snow, Ice and Slush on Runways.* FFA Memo. 106, Aeronautical Research Inst. of Sweden, 1975.
20. Yager, Thomas J.: Aircraft and Ground Vehicle Friction Measurements Obtained Under Winter Runway Conditions. SAE Tech. Paper Ser. 891070, Apr. 1989.
21. *Manual of Snow Removal and Ice Control.* AK-72-40-000, Airports and Construction Services Directorate, Transport Canada, Apr. 1983. (Supersedes AK-72-40 to 47.)
22. *Bowmonk Brakemeter—Dynometer, Technical Evaluation.* AK-71-09-211, Mobile Equipment Div., Transport Canada, May 1986.
23. Davis, Quinton C., IV: *Water Surface Depth Instrument.* NASA Tech Brief 70-10103, Apr. 1970.
24. Leland, Trafford J. W.; Yager, Thomas J.; and Joyner, Upshur T.: *Effects of Pavement Texture on Wet-Runway Braking Performance.* NASA TN D-4323, 1968.
25. Yager, T. J.; and Bühlmann, F.: Macrotexture and Drainage Measurements on a Variety of Concrete and Asphalt Surfaces. *Pavement Surface Characteristics and Materials*, C. M. Hayden, ed., ASTM Spec. Tech. Publ. 763, c.1982, pp. 16–30.
26. Joyner, Upshur T.; Horne, Walter B.; and Leland, Trafford J. W.: *Investigations on the Ground Performance of Aircraft Relating to Wet Runway Braking and Slush Drag.* AGARD Rep. 429, Jan. 1963.
27. *Joint Technical Conference on Slush Drag and Braking Problems.* FAA and NASA, Dec. 1961.
28. Horne, Walter B.; Yager, Thomas J.; and Taylor, Glenn R.: *Review of Causes and Alleviation of Low Tire Traction on Wet Runways.* NASA TN D-4406, 1968.
29. Horne, Walter B.; and Leland, Trafford J. W.: *Influence of Tire Tread Pattern and Runway Surface Condition on Braking Friction and Rolling Resistance of a Modern Aircraft Tire.* NASA TN D-1376, 1962.
30. Yager, Thomas J.: *Factors Influencing Aircraft Ground Handling Performance.* NASA TM-85652, 1983.
31. Horne, Walter B.; and Dreher, Robert C.: *Phenomena of Pneumatic Tire Hydroplaning.* NASA TN D-2056, 1963.
32. Horne, W. B.; and Buhlmann, F.: A Method for Rating the Skid Resistance and Micro/Macrotexture Characteristics of Wet Pavements. *Frictional Interaction of Tire and Pavement*, W. E. Meyer and J. D. Walter, eds., ASTM Spec. Tech. Publ. 793, c.1983, pp. 191–218.

33. Byrdsong, Thomas A.; and Yager, Thomas J.: *Some Effects of Grooved Runway Configurations on Aircraft Tire Braking Traction Under Flooded Runway Conditions.* NASA TN D-7215, 1973.

34. Yager, Thomas J.; and Dreher, Robert C.: *Traction Characteristics of a 30 × 11.5-14.5, Type VIII, Aircraft Tire on Dry, Wet and Flooded Surfaces.* NASA TM X-72805, 1976.

35. Leland, Trafford J. W.; and Taylor, Glenn R.: *An Investigation of the Influence of Aircraft Tire-Tread Wear on Wet-Runway Braking.* NASA TN D-2770, 1965.

36. Smiley, Robert F.; and Horne, Walter B.: *Mechanical Properties of Pneumatic Tires With Special Reference to Modern Aircraft Tires.* NASA TR R-64, 1960. (Supersedes NACA TN 4110.)

37. Herb, H. R.: *Problems Associated With the Presence of Water, Slush, Snow and Ice on Runways.* AGARD Rep. 500, 1965.

38. Agrawal, Satish K.; and Daiutolo, Hector: *Traction of an Aircraft Tire on Grooved and Porous Asphaltic Concrete.* DOT/FAA/CT-84/300-2, Jan. 1984.

Table I. Runway Test-Surface Description and Average Macrotexture-Depth Values

Test site	Test R/W	Test surface		
		Description	Groove[1] spacing, in.	Macrotexture depth, in.
NASA Wallops Flight Facility	10/28	Slurry-seal asphalt (SSA)	None	0.019
	4/22	Canvas-belt-finished concrete	None	0.006
		Canvas-belt-finished and burlap-drag-finished concrete	1	0.072
		Large-aggregate asphalt	None	0.015
		Modified (longitudinal grinding treatment) large-aggregate asphalt	None	0.162
FAA Technical Center	13/31	Dryer-drum-mix asphalt overlay, aggregate size <1 in.	None	0.008
		Dryer-drum-mix asphalt overlay, aggregate size <1 in.	1.5	0.049
		Dryer-drum-mix asphalt overlay, aggregate size <1 in.	3	0.028
BNAS	1/19	Small aggregate asphalt	None	0.017
Pease AFB	16/34	Porous friction course overlay (PFC)[2]	None	0.049
Langley AFB	7/25	Portland cement concrete (PCC)	None	0.027

[1]Transverse, saw-cut grooves of equal 0.25-in. width and depth.
[2]Evaluated similar PFC surface on runway 11/29 at Portland International Jetport, with Boeing 727 test aircraft.

Table II. Test Aircraft Instrumentation Parameter Listing, Range, and Accuracy

(a) NASA Boeing 737; maximum data sample rate, 100/sec; frequency response, 5 cps

Parameter	Range	Accuracy
Computed airspeed	20 to 150 knots	±2 knots
True airspeed	20 to 150 knots	±2 knots
Ground speed (INS)	20 to 150 knots	±2 knots
Ground speed expanded		
Nose-wheel speed	0 to 150 knots	±2 knots
Nose-wheel angle	±20°	±0.2°
Forward[1] throttle handle 1	−150 to +70°	±1.3°
Forward[1] throttle handle 2	−150 to +70°	±1.3°
Forward[1] speed brake	8 positions	±0.2%
Magnetic heading	±180°	±0.72°
Normal acceleration, c.g.	±1.0g	±0.005g
Lateral acceleration, c.g.	±0.5g	±0.002g
Longitudinal acceleration, c.g.	±1.0g	±0.005g
Nose-gear weight	0 to 25 512 lb	±128 lb
Left main-gear weight	0 to 66 744 lb	±334 lb
Right main-gear weight	0 to 66 744 lb	±334 lb
Weight c.g. voltage reference		
Left brake-pedal deflection	0 to 100%	±6.5%
Right brake-pedal deflection	0 to 100%	±6.5%
Left outboard brake temperature	0 to 200°C	±0.4°C
Right outboard brake temperature	0 to 200°C	±0.4°C
Left outboard brake antiskid command	0 to 10 V	±0.5 V
Left inboard brake antiskid command	↓	↓
Right inboard brake antiskid command		
Right outboard brake antiskid command		

[1]Reference to forward cockpit of NASA Boeing 737.

Table II. Continued

(a) Concluded

Parameter	Range	Accuracy
Left outboard brake pressure	0 to 3600 psia	±19.0 psia
Left inboard brake pressure	↓	↓
Right inboard brake pressure		
Right outboard brake pressure		
Left outboard wheel speed	0 to 150 knots	±2 knots
Left inboard wheel speed	↓	↓
Right inboard wheel speed		
Right outboard wheel speed		
Engine pressure ratio 1	0 to 3	±1.5%
Engine pressure ratio 2	0 to 3	±1.5%
Yaw rate	±28°/sec	±0.2°/sec
Roll attitude 2	±45°	±0.18°
Pitch 2	±22.5°	±0.09°
Rudder position 1	±25°	±0.15°
Stabilizer position	−8 to +9°	±0.73°
Left trailing-edge flap	0 to 63°	±0.13°
Right trailing-edge flap	0 to 63°	±0.13°
Right aileron position	±20°	±0.4°
Left aileron position	±20°	±1.8°
Left elevator position	±22°	±0.61°
Flight spoiler 2	0 to 40°	±0.6°
Flight spoiler 3	↓	↓
Flight spoiler 6		
Flight spoiler 7		
Event marker	Full scale	

Table II. Concluded

(b) FAA Boeing 727 aircraft; maximum data sample rate, 40/sec; frequency response, 5 cps

Parameter	Range	Accuracy
Rudder position	−20 to +20°	−2 to +2°
Flap position	0 to 40°	−1 to +1°
Throttle handle no. 1 position	0 to 100%	−2 to +2%
Throttle handle no. 2 position	↓	↓
Throttle handle no. 3 position		
Nose gear, brake position		
Left brake-pedal deflection		
Right brake-pedal deflection		
Left outboard wheel speed	20 to 120 knots	−2 to +2 knots
Left inboard wheel speed	↓	↓
Right inboard wheel speed		
Right outboard wheel speed		
Nose wheel speed		
Left outboard antiskid valve	0 to 10 V	−50 to 50 mV
Left inboard antiskid valve	↓	↓
Right inboard antiskid valve		
Right outboard antiskid valve		
Nose-wheel antiskid valve		
Event mark	Full scale	N/A
Roll attitude, INS	−40 to +40°	−0.5 to +0.5°
Pitch attitude, INS	−20 to +20°	−0.5 to +0.5°
Heading, INS	0 to 360°	−2 to +2°
Left outboard brake pressure	0 to 3000 psi	−30 to 30 psi
Left inboard brake pressure	↓	↓
Right inboard brake pressure		
Right outboard brake pressure		
Nose-wheel brake pressure		
Engine pressure ratio 1	1 to 3	−0.03 to +0.03
Engine pressure ratio 2	1 to 3	−0.03 to +0.03
Engine pressure ratio 3	1 to 3	−0.03 to +0.03
Longitudinal acceleration, c.g.	−1 to +1g	−0.005 to +0.005g
Lateral acceleration, c.g.	−0.5 to +0.5g	−0.002 to +0.002g
Normal acceleration, c.g.	0 to 2g	−0.005 to +0.005g
Computed ground speed, INS	20 to 120 knots	−2 to +2 knots

Table III. Test-Tire Conditions on Ground-Friction-Measuring Vehicles

Ground test vehicle	Tire test mode	Test tires			
		Type	Tread design	Inflation pressure, psi	Vertical load, lb
Mu-Meter	7.5° yawed rolling	RL 2	Smooth	10	171
Navy RCR vehicle (pick-up truck) equipped with Tapley meter and Bowmonk brakemeter[1]	Locked wheel	Light truck, bias-ply	Grooved and siped	32	1000
Surface friction tester[2]	Fixed slip, 10 to 12%	RL 2 Aero	Smooth 3-groove	30 100	310
Runway friction tester	Fixed slip, 13%	RL 2	Smooth	30	300
BV-11 skiddometer[2]	Fixed slip, 15 to 17%	RL 2 Aero	Smooth 3-groove	30 100	220
Diagonal-braked vehicle[3]	Locked wheel	ASTM E 524	Smooth	24	1300

[1]RCR vehicle data only collected at BNAS and Pease AFB.
[2]Used RL 2 smooth tire, 30 psi, for dry- and wet-runway tests; aero tire used for winter runway conditions.
[3]Diagonal-braked vehicle used only at Wallops Flight Facility and FAA Technical Center.

Table IV. Overall Chronology of Aircraft and Ground-Vehicle Test Runs

Date	Test site	Test aircraft		Aircraft flight number	Ground test vehicles
		737	727		
6-15-83	Wallops	X		409	DBV, Mu-M
6-17-83	Wallops	X		410	DBV, Mu-M
6-21-83	Wallops	X		412	DBV, Mu-M, SFT, BV-11
6-23-83	FAATC	X		413	DBV, Mu-M, SFT, BV-11
6-24-83	FAATC	X		414	DBV, Mu-M, SFT, BV-11
6-28-83	Wallops	X		415	DBV, Mu-M
11-20-84	Wallops	X		426	None
2-5-85	Langley AFB	X		429	DBV
3-6-85	BNAS	X		430	RCR
3-7-85	BNAS	X		431	RCR, Mu-M, BV-11
3-8-85	BNAS	X		432	RCR, Mu-M, BV-11
3-9-85	BNAS	X		433	RCR, Mu-M, BV-11

Table IV. Continued

Date	Test site	Test aircraft		Aircraft flight number	Ground test vehicles
		737	727		
3-22-85	Wallops	X		434	DBV
3-22-85	Wallops		X	003	DBV
3-27-85	BNAS		X	004	Mu-M, BV-11
3-27-85	BNAS		X	005	Mu-M, BV-11
3-28-85	BNAS		X	006	None (dry conditions)
4-10-85	Langley AFB		X	007	None (dry conditions)
4-18-85	Wallops		X	008	DBV, Mu-M, SFT, BV-11
8-12-85	Wallops		X	011	DBV, Mu-M, SFT, RFT, BV-11
8-13-85	Wallops		X	012	DBV, Mu-M, SFT, RFT, BV-11
8-15-85	FAATC		X	013	DBV, Mu-M
8-21-85	FAATC		X	014	Mu-M, SFT, BV-11
8-22-85	FAATC		X	015	None (dry conditions)

Table IV. Concluded

Date	Test site	Test aircraft		Aircraft flight number	Ground test vehicles
		737	727		
1-28-86	BNAS		X	019	Mu-M, SFT, RFT, BV-11, RCR
1-29-86	BNAS		X	020	Mu-M, SFT, BV-11, RCR
1-30-86	BNAS		X	021	Mu-M, SFT, BV-11, RCR
2-18-86	BNAS		X	022	Mu-M, SFT, BV-11, RCR
2-19-86	BNAS		X	023	SFT, RFT, BV-11, RCR
2-19-86	BNAS		X	024	SFT, RFT, BV-11, RCR
2-20-86	BNAS		X	025	SFT, RFT, BV-11, RCR
3-19-86	BNAS		X	026	Mu-M, SFT, RFT, BV-11, RCR
3-19-86	Portland International Jetport		X	027	None
3-19-86	Pease AFB		X	027	Mu-M, SFT, RFT, BV-11, RCR
3-21-86	BNAS		X	028	Mu-M, SFT, RFT, BV-11, RCR
3-21-86	BNAS		X	029	Mu-M, SFT, RFT, BV-11, RCR

Table V. Compilation of Test-Aircraft and Ground-Vehicle Tire Friction Parameters

Parameter	Test aircraft		Ground test vehicles			
	737	727	Diagonal braked	Mu-Meter	Friction testers, SFT and RFT	BV-11 skiddometer
Tire:	Main gear	Main gear	ASTM E 524	RL 2	RL 2	RL 2
Size	40 × 14	49 × 17	G78 × 15	4.00 8	4.00 8	4.00 8
Inflation pressure, psi	155	145	24	10	30	30
Tread design	4-groove	6-groove	Smooth	Smooth	Smooth	Smooth
Braking method	Maximum antiskid	Maximum antiskid	Locked wheel	None (7.5° yaw)	Constant slip	Constant slip
Friction reading	μ_{eff}	μ_{eff}	μ_{skid}	μ_{side}	μ_{drag}	μ_{drag}
Spin-down hydroplaning speed, V_p, knots (mph)	[a]112 (129)	[a]108.4 (124.8)	[a]44.1 (50.8)	39.1 (45)	[a]49.3 (56.7)	[a]49.3 (56.7)
Low-speed characteristic dry friction, μ_{cd}	[b]0.76	[b]0.77	1.20	1.10	1.10	1.10

[a] V_p (spin-down) in knots = $9\sqrt{p}$.
[b] $\mu_{cd} = 0.93 - 1.1 \times 10^{-3}p$.

Table VI. Estimated Aircraft Effective Braking Friction Coefficients for Range of Tire Inflation Pressures Based on Runway Friction Tester, Surface Friction Tester, BV-11 Skiddometer, and Mu-Meter Friction Measurements for Wet-Runway Surface Conditions

Ground-vehicle μ	Estimated aircraft μ_{eff}															
	100 psi	120 psi	140 psi	160 psi	180 psi	200 psi	220 psi	240 psi	260 psi	280 psi	300 psi	320 psi	340 psi	360 psi	380 psi	400 psi
1.10	0.644	0.614	0.585	0.557	0.529	0.502	0.476	0.450	0.425	0.401	0.377	0.354	0.332	0.310	0.290	0.270
1.05	0.594	0.567	0.540	0.514	0.488	0.464	0.439	0.416	0.393	0.371	0.349	0.328	0.307	0.288	0.268	0.250
1.00	0.546	0.521	0.497	0.473	0.449	0.427	0.405	0.383	0.362	0.341	0.322	0.302	0.284	0.265	0.248	0.231
0.95	0.500	0.477	0.455	0.433	0.412	0.391	0.371	0.351	0.332	0.314	0.295	0.278	0.261	0.244	0.228	0.213
0.90	0.456	0.435	0.415	0.395	0.376	0.357	0.339	0.321	0.304	0.287	0.270	0.254	0.239	0.224	0.209	0.195
0.85	0.414	0.395	0.377	0.359	0.342	0.325	0.308	0.292	0.276	0.261	0.246	0.232	0.218	0.204	0.191	0.178
0.80	0.373	0.357	0.340	0.324	0.309	0.294	0.279	0.264	0.250	0.237	0.223	0.210	0.198	0.185	0.174	0.162
0.75	0.335	0.320	0.306	0.292	0.278	0.264	0.251	0.238	0.226	0.213	0.201	0.190	0.178	0.168	0.157	0.147
0.70	0.299	0.286	0.273	0.260	0.248	0.236	0.224	0.213	0.202	0.191	0.180	0.170	0.160	0.150	0.141	0.132
0.65	0.265	0.253	0.242	0.231	0.220	0.210	0.199	0.189	0.180	0.170	0.161	0.152	0.143	0.134	0.126	0.118
0.60	0.232	0.222	0.213	0.203	0.194	0.185	0.176	0.167	0.158	0.150	0.142	0.134	0.126	0.119	0.112	0.104
0.55	0.202	0.194	0.185	0.177	0.169	0.161	0.153	0.146	0.138	0.131	0.124	0.117	0.111	0.104	0.098	0.092
0.50	0.174	0.167	0.159	0.152	0.146	0.139	0.132	0.126	0.120	0.114	0.108	0.102	0.096	0.091	0.085	0.080
0.45	0.147	0.141	0.135	0.130	0.124	0.118	0.113	0.108	0.102	0.097	0.092	0.087	0.082	0.078	0.073	0.069
0.40	0.123	0.118	0.113	0.109	0.104	0.099	0.095	0.090	0.086	0.082	0.078	0.074	0.070	0.066	0.062	0.058
0.35	0.101	0.097	0.093	0.089	0.085	0.082	0.078	0.074	0.071	0.068	0.064	0.061	0.058	0.055	0.052	0.049
0.30	0.080	0.077	0.074	0.071	0.068	0.066	0.063	0.060	0.057	0.054	0.052	0.049	0.047	0.044	0.042	0.039
0.25	0.062	0.060	0.057	0.055	0.053	0.051	0.049	0.047	0.045	0.043	0.041	0.039	0.037	0.035	0.033	0.031
0.20	0.046	0.044	0.042	0.041	0.039	0.038	0.036	0.035	0.033	0.032	0.030	0.029	0.028	0.026	0.025	0.023
0.15	0.031	0.030	0.029	0.028	0.027	0.026	0.025	0.024	0.023	0.022	0.021	0.020	0.019	0.018	0.017	0.017
0.10	0.019	0.018	0.018	0.017	0.016	0.016	0.015	0.015	0.014	0.014	0.013	0.012	0.012	0.011	0.011	0.010
0.05	0.008	0.008	0.008	0.008	0.007	0.007	0.007	0.007	0.006	0.006	0.006	0.006	0.006	0.005	0.005	0.005
0.00	0.000	0.000	0.000	0.000	0.000	0.000	0.000	0.000	0.000	0.000	0.000	0.000	0.000	0.000	0.000	0.000

Vehicle speed, mph	Equivalent aircraft ground speed, knots, based on RFT, SFT, and BV-11 skiddometer															
20	31.7	34.8	37.6	40.2	42.6	44.9	47.1	49.2	51.2	53.1	55.0	56.8	58.5	60.2	61.9	63.5
30	47.6	52.2	56.3	60.2	63.9	67.3	70.6	73.8	76.8	79.7	82.5	85.2	87.8	90.4	92.8	95.2
40	63.5	69.6	75.1	80.3	85.2	89.8	94.2	98.4	102.4	106.2	110.0	113.6	117.1	120.5	123.8	127.0
50	79.4	86.9	93.9	100.4	106.5	112.2	117.7	123.0	128.0	132.8	137.5	142.0	146.3	150.6	154.7	158.7
60	95.2	104.3	112.7	120.5	127.8	134.7	141.3	147.5	153.6	159.4	165.0	170.4	175.6	180.7	185.7	190.5

Vehicle speed, mph	Equivalent aircraft ground speed, knots, based on Mu-Meter speed															
20	40.0	43.8	47.3	50.6	53.7	56.6	59.3	62.0	64.5	66.9	69.3	71.6	73.8	75.9	78.0	80.0
30	60.0	65.7	71.0	75.9	80.5	84.9	89.0	93.0	96.7	100.4	103.9	107.3	110.6	113.8	117.0	120.0
40	80.0	87.6	94.7	101.2	107.3	113.1	118.7	123.9	129.0	133.9	138.6	143.1	147.5	151.8	155.9	160.0
50	100.0	109.5	118.3	126.5	134.2	141.4	148.3	154.9	161.2	167.3	173.2	178.9	184.4	189.7	194.9	200.0
60	120.0	131.5	142.0	151.8	161.0	169.7	178.0	185.9	193.5	200.8	207.8	214.7	221.3	227.7	233.9	240.0

Table VII. Estimated Aircraft Effective Braking Friction Coefficients for Range of Tire Inflation Pressures Based on Diagonal-Braked Vehicle Friction Measurements for Wet-Runway Surface Conditions

Ground-vehicle μ	Estimated aircraft μ_{eff}															
	100 psi	120 psi	140 psi	160 psi	180 psi	200 psi	220 psi	240 psi	260 psi	280 psi	300 psi	320 psi	340 psi	360 psi	380 psi	400 psi
1.00	0.606	0.578	0.550	0.524	0.498	0.472	0.448	0.424	0.400	0.377	0.355	0.334	0.313	0.293	0.273	0.254
0.95	0.595	0.567	0.541	0.514	0.489	0.464	0.440	0.416	0.393	0.371	0.349	0.328	0.308	0.288	0.269	0.250
0.90	0.584	0.557	0.531	0.505	0.480	0.456	0.432	0.409	0.386	0.364	0.343	0.322	0.302	0.283	0.264	0.246
0.85	0.563	0.537	0.512	0.487	0.463	0.439	0.417	0.394	0.373	0.352	0.331	0.311	0.292	0.273	0.255	0.237
0.80	0.542	0.517	0.493	0.469	0.446	0.423	0.401	0.380	0.359	0.339	0.319	0.300	0.282	0.263	0.246	0.229
0.75	0.516	0.493	0.470	0.447	0.425	0.404	0.383	0.363	0.343	0.323	0.305	0.287	0.269	0.252	0.235	0.219
0.70	0.482	0.460	0.438	0.417	0.397	0.377	0.358	0.339	0.320	0.302	0.285	0.268	0.252	0.236	0.220	0.205
0.65	0.434	0.414	0.395	0.377	0.358	0.340	0.323	0.306	0.290	0.274	0.258	0.243	0.228	0.214	0.200	0.186
0.60	0.393	0.376	0.358	0.342	0.325	0.309	0.293	0.278	0.263	0.249	0.235	0.221	0.208	0.195	0.182	0.170
0.55	0.354	0.339	0.323	0.308	0.293	0.279	0.265	0.251	0.238	0.225	0.212	0.200	0.188	0.177	0.165	0.154
0.50	0.321	0.307	0.293	0.280	0.267	0.254	0.241	0.229	0.217	0.205	0.194	0.182	0.172	0.161	0.151	0.141
0.45	0.290	0.277	0.265	0.253	0.241	0.229	0.218	0.207	0.196	0.186	0.175	0.165	0.156	0.146	0.137	0.128
0.40	0.257	0.246	0.235	0.224	0.214	0.203	0.194	0.184	0.174	0.165	0.156	0.147	0.139	0.130	0.122	0.115
0.35	0.222	0.212	0.203	0.194	0.185	0.176	0.168	0.160	0.151	0.144	0.136	0.128	0.121	0.114	0.107	0.100
0.30	0.193	0.184	0.176	0.169	0.161	0.154	0.146	0.139	0.132	0.125	0.119	0.112	0.106	0.100	0.094	0.088
0.25	0.156	0.150	0.144	0.137	0.131	0.125	0.120	0.114	0.108	0.103	0.097	0.092	0.087	0.082	0.077	0.073
0.20	0.116	0.112	0.107	0.103	0.098	0.094	0.090	0.085	0.081	0.077	0.074	0.070	0.066	0.062	0.059	0.055
0.15	0.077	0.074	0.071	0.068	0.066	0.063	0.060	0.058	0.055	0.052	0.050	0.047	0.045	0.043	0.040	0.038
0.10	0.043	0.042	0.040	0.039	0.037	0.036	0.034	0.033	0.032	0.030	0.029	0.028	0.026	0.025	0.024	0.022
0.05	0.017	0.017	0.016	0.016	0.015	0.015	0.014	0.014	0.013	0.013	0.012	0.012	0.011	0.011	0.010	0.010
0.00	0.000	0.000	0.000	0.000	0.000	0.000	0.000	0.000	0.000	0.000	0.000	0.000	0.000	0.000	0.000	0.000

Vehicle speed, mph	Equivalent aircraft ground speed, knots															
20	35.4	38.8	41.9	44.8	47.5	50.1	52.6	54.9	57.1	59.3	61.4	63.4	65.3	67.2	69.1	70.9
30	53.1	58.2	62.9	67.2	71.3	75.2	78.8	82.3	85.7	88.9	92.1	95.1	98.0	100.8	103.6	106.3
40	70.9	77.6	83.8	89.6	95.1	100.2	105.1	109.8	114.3	118.6	122.7	126.8	130.7	134.5	138.1	141.7
50	88.6	97.0	104.8	112.0	118.8	125.3	131.4	137.2	142.8	148.2	153.4	158.5	163.3	168.1	172.7	177.2
60	106.3	116.4	125.8	134.5	142.6	150.3	157.7	164.7	171.4	177.9	184.1	190.2	196.0	201.7	207.2	212.6

Table VIII. Statistical Description of Friction-Speed Data Curves in Summary Figures

[Refer to figures 3 and 7 for test-surface letter-code identification]

Figure	Runway/vehicle type	Curve label	B_0	B_1	σ
47	Nongrooved	737	0.48	−0.000438	0.0296
48	Nongrooved	Mu-M	0.847	0.000705	0.0272
		BV-11	1.083	−.00188	.0532
		SFT	.999	−.00176	.0649
		RFT	1.0068	−.00312	.0821
		DBV	.841	−.000376	.0886
49(a)	Nongrooved	737	0.48	−0.000438	0.0296
		Mu-M	.847	.000705	.0272
		BV-11	1.083	−.00188	.0532
		SFT	.999	−.00176	.0649
		RFT	1.0068	−.00312	.0821
		DBV	.841	−.000376	.0886
49(b)	Nongrooved	737	0.317	0.001896	0.0183
		Mu-M	.825	.000633	.0156
		BV-11	.996	−.00143	.0722
		SFT	1.0953	−.0056	.0592
		DBV	.961	−.00888	.0416
49(c)	Nongrooved	737	0.499	−0.00479	0.0691
		Mu-M	.954	−.00877	.192
		BV-11	1.132	−.0141	.158
		SFT	1.128	−.0131	.127
		RFT	.929	−.00688	.12
		DBV	.756	−.00987	.114
	Grooved	737	0.449	−0.00162	0.0504
		Mu-M	.851	−.000876	.0703
		BV-11	.997	−.00206	.0651
		SFT	1.011	−.00283	.0477
		RFT	.927	−.00365	.0514
		DBV	.837	−.00715	.0879
49(d)	Nongrooved	737	0.255	−0.00233	0.0107
		Mu-M	.999	−.0214	.074
		BV-11	1.05	−.018	.0671
		SFT	1.154	−.0194	.0623
		DBV	.505	−.00679	.018
	Grooved	737	0.549	−0.00396	0.0161
		DBV	.843	−.00917	.0324
49(e)	Nongrooved	737	0.0936	0.000995	0.0177
		Mu-M	.18	−.0035	0
		BV-11	.19	0	0

Table VIII. Continued

Figure	Runway/vehicle type	Curve label	B_0	B_1	σ
49(f)	Grooved	737	0.0474	−0.000542	0.0101
		Mu-M	.191	−.0006	.00316
		BV-11	.238	−.0018	.00118
50	Aircraft	SSA	0.498	−0.0028	0.0228
		A	.295	−.0029	.013
		J-1	.507	−.00516	.0206
		B, FAATC	.489	−.00356	.0208
		NG	.499	−.00479	.0691
50(a)	DBV	SSA	0.795	−0.00882	0.071
		A	.626	−.0092	.0843
		J-1	.787	−.01	.0733
		B, FAATC	.899	−.013	.11
		NG	.756	−.00987	.115
50(b)	Mu-Meter	SSA	0.93	−0.00403	0.0568
		A	.912	−.0121	.163
		J-1	1.01	−.013	.125
		B, FAATC	1.13	−.0149	.0835
		NG	.954	−.00877	.192
50(c)	SFT	SSA	1.161	−0.011	0.0663
		A	1.03	−.0159	.0742
		J-1	1.128	−.0126	.054
		B, FAATC	1.105	−.142	.0911
		NG	1.128	−.0131	.127
50(d)	BV-11	SSA	1.155	−0.0103	0.049
		A	1.124	−.0168	.0853
		J-1	1.059	−.0133	.0872
		B, FAATC	1.205	−.0189	.0913
		NG	1.132	−.0141	.159
51	Aircraft	B/C	0.488	−0.0233	0.0451
		J-2	.555	−.0039	.0371
		C, FAATC	.43	−.000714	.019
		D, FAATC	.326	.000121	.0137
		G	.449	−.00162	.0504
51(a)	DBV	B/C	0.711	−0.00429	0.0348
		J-2	1.14	−.0144	.0623
		C, FAATC	.818	−.00753	.0247
		D, FAATC	.897	−.0065	.0257
		G	.837	−.00715	.0879

Table VIII. Continued

Figure	Runway/vehicle type	Curve label	B_0	B_1	σ
51(b)	Mu-Meter	B/C	0.842	−0.00148	0.0797
		J-2	.965	−.0018	.0442
		C, FAATC	.799	.000168	.00921
		D, FAATC	.819	−.000184	.0128
		G	.85	−.000876	.0703
51(c)	SFT	B/C	1.087	−0.0057	0.0739
		J-2	1.205	−.008	.0466
		C, FAATC	.98	−.00164	.00909
		D, FAATC	.985	−.00197	.0158
		G	1.011	−.00283	.0477
51(d)	BV-11	B/C	1.256	−0.009	0.0707
		J-2	1.266	−.0087	.0448
		C, FAATC	.903	.000475	.0546
		D, FAATC	.96	−.0012	.298
		G	.997	−.00206	.0652
52	Aircraft	737	0.317	0.001896	0.0183
(a)	Ground vehicle	DBV	.961	−.00888	.0416
(b)		Mu-M	.825	.000633	.0156
(c)		SFT	1.095	−.0056	.0592
(d)		BV-11	.996	−.00143	.0722
53	Aircraft	Snow	0.0936	0.000995	0.0177
		Ice	.0474	−.000542	.0101
53(a)	Mu-Meter	Snow	0.18	−0.0035	0
		Ice	.191	−.0006	.00316
53(b)	BV-11	Snow	0.19	0	0
		Ice	.238	−.0018	.00118
55	Nongrooved	1.8	0.11	0.002	0.0166
		1.6	.059	.00239	.0109
		1.5	.07	.00167	.0236
		1.2	.022	.0016	.109
56	Nongrooved	Manual	0.507	−0.00292	0.0204
		Auto	.318	−.00169	.048
57	Nongrooved	727	0.497	−0.000604	0.0327
58(a)	Nongrooved	727	0.497	−0.000604	0.0327
		Mu-M	.847	.000705	.0272
		BV-11	1.083	−.00188	.0532
		SFT	.99869	−.001759	.0649
		RFT	1.0068	−.00312	.0821
		DBV	.841	−.000376	.0886

Table VIII. Continued

Figure	Runway/vehicle type	Curve label	B_0	B_1	σ
58(b)	Nongrooved	727	0.449	−0.000572	0.021
		Mu-M	.787	−.00125	.0204
		BV-11	1.06	−.0035	
		SFT	1.005	−.00325	0
		RFT	.933	−.00375	.0204
58(c)	Nongrooved	727	0.554	−0.00172	0.0427
		DBV	1.00117	−.00941	.026
58(d)	Nongrooved	727	0.382	−0.00114	0.0434
		Mu-M	.823	−.00225	.00408
		BV-11	.95	−.0055	.0245
		SFT	1.007	−.004	.0408
		RFT	.933	−.00375	.0204
58(e)	Nongrooved	727	0.445	−0.00141	0.104
		Mu-M	.823	−.00596	.141
		BV-11	1.019	−.00715	.209
		SFT	1.106	−.0083	.184
		RFT	.929	−.00688	.12
		DBV	.949	−.0117	.145
	Grooved	727	0.551	−0.00237	0.0446
		Mu-M	.765	−.00127	.0424
		BV-11	1.078	−.00431	.082
		SFT	1.0428	−.00396	.0778
		RFT	.927	−.00365	.0514
		DBV	.805	−.00714	.0661
58(f)	Nongrooved	727	0.0701	0.000501	0.014
		Mu-M	.26	−.00185	.0201
		BV-11	.22	.0005	.0245
		SFT	.227	.00025	.00408
		RFT	.36	−.0015	0
58(g)	Nongrooved	727	0.166	0.000313	0.0149
		Mu-M	.247	−.00175	.0204
		BV-11	.177	.0015	.0163
		SFT	.245	−.000125	.00968
		RFT	.338	−.00112	.0151
58(h)	Nongrooved	727	0.114	0.000454	0.0137
		Mu-M	.232	−.000667	.02
		BV-11	.211	.00117	.0707
		SFT	.175	.00128	.121
58(i)	Nongrooved	727	0.14	−0.000657	0.0351
		Mu-M	.18	0	
		BV-11	.102	.00221	.0134
		SFT	.0969	.000486	.00586

Table VIII. Continued

Figure	Runway/vehicle type	Curve label	B_0	B_1	σ
58(j)	Nongrooved	727	0.114	0.000454	0.0137
		Mu-M	.103	−.00075	.00408
		BV-11	.107	.00075	.00408
		SFT	.14	−.00075	.0122
58(k)	Nongrooved	727	0.203	−0.00072	0.026
		BV-11	.243	.00025	.0204
		SFT	.223	−.00025	.0204
		RFT	.287	−.00075	.00408
58(l)	Nongrooved	727	0.0397	−0.000143	0.0176
		Mu-M	.158	.000536	.0184
		BV-11	.187	−.000656	.0228
		SFT	.186	−.00047	.00619
		RFT	.128	.000264	.0158
58(m)	Nongrooved	727	0.354	−0.000286	0.0685
		Mu-M	.683	−.004	.139
		BV-11	.81	−.00775	.11
59	Aircraft	SSA	0.533	−0.00188	0.0342
		A	.381	−.00371	.0196
		B, FAATC	.32	−.00094	.0252
		NG	.445	−.00141	.104
59(a)	DBV	SSA	0.967	−0.00947	0.0385
		A	.671	−.0102	.0403
		B, FAATC	.934	−.014	.0411
		NG	.949	−.0117	.145
59(b)	Mu-Meter	SSA	0.826	−0.0046	0.0582
		A	.977	−.0153	.0618
		B, FAATC	.772	−.00275	.0525
		NG	.823	−.00596	.141
59(c)	SFT	SSA	1.096	−0.00552	0.0348
		A	1.113	−.0159	.0872
		B, FAATC	1.332	−.0122	.0925
		NG	1.106	−.0083	.184
59(d)	BV-11	SSA	1.042	−0.0036	0.0757
		A	1.197	−.0168	.0962
		B, FAATC	1.257	−.0172	.0794
		NG	1.019	−.00715	.209
59(e)	RFT	SSA	0.94	−0.00531	0.0435
		A	.477	0	
		B, FAATC	1.007	−.011	.00816
		NG	.93	−.00688	.12

Table VIII. Continued

Figure	Runway/vehicle type	Curve label	B_0	B_1	σ
60	Aircraft	B, FAATC	0.605	−0.0037	0.0159
		C, FAATC	.543	−.00185	.187
		D, FAATC	.556	−.00235	.0463
		G	.551	−.00237	.0446
60(a)	DBV	B	0.699	−0.0057	0.0519
		C, FAATC	.832	−.0069	.0415
		D, FAATC	.836	−.00589	.0186
		G	.805	−.00714	.0661
60(b)	Mu-Meter	B	0.809	−0.0025	0.0574
		C, FAATC	.706	0	.0296
		D, FAATC	−.769	−.001	.0264
		G	−.765	−.00127	.0414
60(c)	SFT	B	1.064	−0.0057	0.0718
		C, FAATC	1.036	−.0025	.0301
		D, FAATC	1.054	−.00325	.0665
		G	1.043	−.00396	.0778
60(d)	BV-11	W-B	1.237	−0.009	0.0676
		C, FAATC	1.01	−.00125	.0122
		D, FAATC	.997	−.0015	.00816
		G	1.078	−.00431	.082
60(e)	RFT	B	0.735	0	
		C, FAATC	.987	−.00375	0.00408
		D, FAATC	.9	−.0025	
		G	.927	−.00365	.0514
61	Aircraft	727	0.382	−0.00114	0.0434
(a)	Ground vehicle	SFT	1.007	−.004	.0408
(b)		BV-11	.95	−.0055	.0245
(c)		RFT	.933	−.00375	.0204
62	Aircraft	727	1.356	−0.0109	0.0973
(a)	Ground vehicle	DBV	.702	−.0047	.0237
(b)		Mu-M	.823	−.00225	.00408
63	Aircraft	1.5-in. snow	0.0701	0.000501	0.014
		2.0-in. snow	.0719	.000811	.0115
		Dry snow	.114	.000454	.0137
		Packed	.166	.000313	.0149
		Ice	.0397	−.000143	.0176
63(a)	Mu-Meter	1.5-in. snow	0.26	−0.00185	0.02
		2.0-in. snow	.103	−.00075	.00408
		Dry snow	.232	−.000667	.02
		Packed	.247	−.00175	.0204
		Ice	.158	.000536	.0184

Table VIII. Concluded

Figure	Runway/vehicle type	Curve label	B_0	B_1	σ
63(b)	SFT	1.5-in. snow	0.227	0.00025	0.00408
		2.0-in. snow	.14	−.00075	.0122
		Dry snow	.175	.00128	.121
		Packed	.245	−.000125	.00968
		Ice	.186	−.00047	.00619
63(c)	BV-11	1.5-in. snow	0.22	0.0005	0.0245
		2.0-in. snow	.107	.00075	.00408
		Dry snow	.211	.00117	.0708
		Packed	.177	.0015	.0163
		Ice	.187	−.000656	.0228
63(d)	RFT	1.5-in. snow	0.36	−0.0015	0
		Packed	.338	−.00112	.0151
		Ice	.128	.000264	.0158
65	Nongrooved	2.0	0.0385	0.00279	0.0114
		1.7	.0714	.00183	.0159
66	Nongrooved	727	0.532	−0.00188	0.0339
69	Nongrooved	Dry	0.497	−0.000604	0.0327
		Pease	.446	−.000531	.0217
		Portland	.439	−.0016	.0291
70	Nongrooved	Flt 29	0.204	−0.000718	0.025
		Flt 25	.368	−.00114	.0228
		Flt 21	.14	−.000648	.0347
74	Nongrooved	Snow	0.144	0.000268	0.0265
		Ice	.039	.000227	.016

Table IX. Ground-Vehicle Friction Correlation for Compacted Snow- and Ice-Covered Runway Conditions

[Ambient-air temperature range of 5 to 41°F; test-speed range of 20 to 60 mph]

Braking-action level	Ground-vehicle friction readings						
	Mu-Meter[1]	Tapley meter	Runway condition readings (RCR)[2]	Bowmonk meter	Surface friction tester[3]	Runway friction tester[4]	BV-11 skiddometer[3]
Excellent	0.50 and above	0.53 and above	17 and above	0.51 and above	0.53 and above	0.50 and above	0.58 and above
Good	0.47 to .35	0.50 to .38	16 to 12	0.48 to .37	0.50 to .37	0.47 to .35	0.54 to .41
Marginal	0.33 to .26	0.35 to .28	11 to 9	0.34 to .27	0.34 to .28	0.33 to .26	0.37 to .31
Poor	0.24 and below	0.26 and below	8 and below	0.25 and below	0.25 and below	0.24 and below	0.27 and below

[1]Mu-Meter equipped with smooth RL 2 tires inflated to 10 lb/in^2.
[2]RCR values equal Tapley meter reading × 32.
[3]Surface friction tester and BV-11 skiddometer equipped with grooved aero tire inflated to 100 lb/in^2.
[4]Runway friction tester equipped with smooth RL 2 tire inflated to 30 lb/in^2.

Appendix A

Compilation of Boeing 737 Aircraft and Ground-Vehicle Test Data

The chronological test-run sequence for the 737 aircraft and the different ground vehicles is given in table AI for each test site. Test-runway surface conditions, temperature, and wind readings are also listed. Table AII provides a compilation by test site and run number of the 737 aircraft braking friction data. In this table, the aircraft gross weight, c.g. station, test-surface type and wetness condition, type of braking, and ground speed are given. The ground-vehicle friction data obtained on dry-runway test surfaces are listed by test site, surface type, and vehicle type in table AIII. Table AIV contains the ground-vehicle friction data obtained during wet-runway 737 aircraft braking test runs. The data are listed by vehicle type and test-surface type, with the aircraft test-run number and the elapsed time relative to the aircraft test run given for each ground-vehicle run. The average ground-vehicle friction coefficient values are listed in 10-mph increments up to 60 mph. Some supplemental ground-vehicle test runs were conducted on wet-runway test surfaces without the test aircraft. These data are compiled in table AV by test-vehicle type, date, test site, and test-surface type and wetness condition. The ground-vehicle friction measurements obtained during 737 aircraft tests at BNAS, Maine, in March 1985 are listed in table AVI by surface condition. The appropriate aircraft flight and run numbers and the ambient temperatures are also given. The surface friction tester and the runway friction tester were not available for this test series at BNAS. The empirical runway condition factors used for 737 aircraft data reduction are given in table AVII. The aerodynamic and geometric data for the 737 test aircraft are listed in table AVIII for use with aircraft equations of balance.

Table AI. Boeing 737 Aircraft and Ground-Vehicle Test-Run Sequence Data

[Temperature and wind values indicated only at times of measurement]

(a) Wallops Flight Facility

Date	Test vehicle	Run	Time of day, GMT	Test R/W	Test surface		Temperature, °F		Wind	
					Type	Wetness	Ambient	Surface	Deg	Knots
6-15-83	Mu-M	17	1215	10	SSA	Dry	74	80		0
	DBV	11	1216							
	Mu-M	18	1219							
	DBV	12	1220							
	Mu-M	19	1230	22	A, B					
		20	1233							
		21	1236							
		22	1239							
		23	1242							
	737	1	1331	10	SSA		78	85		
		2	1444							
		3	1501							
		4	1513							
		6	1647	22	A, B		80	95	160	6
		7	1658	04	B, A					
		5	1715	10	SSA					
		8	1722	22	A, B				150	8
		9	1739	04	B, A					
6-17-83	737	10	1309	10	SSA	Dry	77	86	110	6
	Mu-M	50	1404	22	A, B	Wet		80		
	DBV	26	1405							
	737	11	1406							
	Mu-M	51	1406							
	DBV	27	1407							
	Mu-M	52	1422	04	B, A					
	DBV	28	1423		B, A					
	737	12	1424		B					
	Mu-M	53	1425		B, A					
	DBV	29	1426		B, A			84		
	Mu-M	54	1441	22	A, B					
	DBV	30	1442				77	84	110	6
	737	13	1443							
	Mu-M	55	1444							
	DBV	31	1444							
	Mu-M	56	1502	04	B, A					
	DBV	32	1502							
	737	14	1503				80	85	150	4
	Mu-M	57	1504							
	DBV	33	1505							
	737	19	1632	22	B					

Table AI. Continued

(a) Continued

Date	Test vehicle	Run	Time of day, GMT	Test R/W	Test surface		Temperature, °F		Wind	
					Type	Wetness	Ambient	Surface	Deg	Knots
6-17-83	Mu-M	58	1650	22	A, B	Wet				
	DBV	34	1650							
	737	15	1651				81		130	6
	Mu-M	59	1652							
	DBV	35	1652							
	Mu-M	60	1710	04	B, A					
	DBV	36	1710							
	737	16	1712							
	Mu-M	61	1713							
	DBV	37	1714							
	737	17	2122	10	SSA	Dry		98		
	737	18	2134	10	SSA	Dry				
6-21-83	737	20	1432	10	SSA	Dry	75	87	110	9
	SFT	17	1543			Wet				
	Mu-M	81	1543							
	BV-11	20	1543							
	DBV	44	1544							
	737	21	1547				72		112	13
	SFT	18	1548							
	Mu-M	82	1548							
	BV-11	21	1548				72	31(87)	112	13
	DBV	45	1548							
	SFT	19	1600							
	Mu-M	83	1600							
	BV-11	22	1600							
	DBV	46	1601							
	737	22	1604						110 to 122	12
	SFT	20	1604							
	Mu-M	84	1605							
	BV-11	23	1605							
	DBV	47	1605							
	SFT	21	1741	04	C-B	Damp to flooded		78		
	Mu-M	85	1741							
	BV-11	24	1741							
	DBV	48	1742							
	737	23	1743				73		110	13
	SFT	22	1746							
	Mu-M	86	1746							
	BV-11	25	1747							
	DBV	49	1747							
	SFT	23	1804						102	11

Table AI. Continued

(a) Continued

Date	Test vehicle	Run	Time of day, GMT	Test R/W	Test surface		Temperature, °F		Wind	
					Type	Wetness	Ambient	Surface	Deg	Knots
6-21-83	Mu-M	87	1804	04	C-B	Damp				
	BV-11	26	1804			to				
	DBV	50	1804			flooded				
	737	24	1806				74	80	108	16
	SFT	24	1806							
	Mu-M	88	1807							
	BV-11	27	1807							
	DBV	51	1807						098	14
	SFT	25	1835	22	J-1, J-2	Wet	75	92	091	
	Mu-M	89	1835							
	BV-11	28	1835				75	92	085	17
	DBV	52	1835							
	737	28	1837		J-1				083	17
	SFT	26	1839		J-1, J-2					
	Mu-M	90	1839							
	BV-11	29	1839							
	DBV	53	1840				74		108	16
	SFT	27	1858	04	J-2, J-1		73		104	14
	Mu-M	91	1858							
	BV-11	30	1858							
	DBV	54	1859							
	737	29	1900		J-2				102	17
	SFT	28	1901		J-2, J-1					
	Mu-M	92	1901							
	BV-11	31	1901							
	DBV	55	1902						098 (variable)	12
	SFT	29	1919	22	J-1, J-2		72	90	093	11
	Mu-M	93	1919							
	BV-11	32	1919							
	DBV	56	1919							
	737	30	1922						097	9
	SFT	30	1923							
	Mu-M	94	1923							
	BV-11	33	1923							
	DBV	57	1924						100	9
	SFT	31	1941	04	J-2, J-1		74			
	Mu-M	95	1941							
	BV-11	34	1941							
	DBV	58	1941						099 to 107	15
	737	31	1943						084	14

Table AI. Continued

(a) Continued

Date	Test vehicle	Run	Time of day, GMT	Test R/W	Test surface		Temperature, °F		Wind	
					Type	Wetness	Ambient	Surface	Deg	Knots
6-21-83	SFT	32	1944	04	J-2, J-1	Wet	74	90	084	14
↓	Mu-M	96	1944	↓	↓	↓				
	BV-11	35	1944							
	DBV	59	1944							
6-28-83	737	20R2	1030	10	SSA	Dry	70	76	220	4
↓	Mu-M	104	1044	04	B, C	Flooded		74		
	DBV	92	1045	↓	↓	↓				
	737	32	1047						250	4
	Mu-M	105	1048							
	DBV	93	1049							
	Mu-M	106	1100	22						
	DBV	94	1101	↓						
	737	33	1102						270	8
	Mu-M	107	1103							
	DBV	95	1104							
	Mu-M	108	1117							
	DBV	96	1118							
	737	34	1119						250	8
	Mu-M	109	1120							
	DBV	97	1121							
	737	35	1133						240	6
	737	36	1142	↓	↓				260	4
	Mu-M	110	1400	04	A		80	82	250	10
	DBV	98	1401	↓	↓					
	737	37	1402							
	Mu-M	111	1403							
	DBV	99	1404	↓						
	Mu-M	112	1407	22						
	DBV	100	1408	↓						
	737	38	1410						260	10
	Mu-M	113	1411							
	DBV	101	1412				80	82	260	10
	Mu-M	114	1417							
	DBV	102	1418							
	737	39	1419						230	14
	Mu-M	115	1420							
	DBV	103	1421							
	737	40	1424						250	8
	737	40R1	1428							
↓	737	41	1431	↓	↓	↓			250	10

Table AI. Continued

(a) Concluded

Date	Test vehicle	Run	Time of day, GMT	Test R/W	Test surface		Temperature, °F		Wind	
					Type	Wetness	Ambient	Surface	Deg	Knots
11-20-84	737	12	1836	10	SSA	Dry	40		350	10
		1	1845	28	↓	Dry				
		13	1849	10		Dry				
		2	1909	28		Wet				12
		3	1914	10		Wet				
[a]2-5-85	DBV	1	1542	07	PCC	Rain wet	35		360	5
	DBV	2	1928	↓	↓	↓				
	737	1	1931							
	DBV	3	1932							
3-22-85	737	1	1548	10	SAA	Rain wet	41		080	16
↓	DBV	1	1627	↓	↓	↓				
	DBV	2	1630							
	737	4A	1632				42			18
	DBV	3	1636							
	737	1A	1639							
	DBV	4	1642							
	737	4B	1644				43		070	16
	DBV	5	1646							
	DBV	6	1651							
	737	4C	1652							22
	DBV	7	1654							
	DBV	8	1705							16
	737	5	1706							
	DBV	9	1709	↓	↓					
	DBV	10	1717	22	A, B					
	DBV	11	1719	04	B, A					
	737	6	1724	22	A, B					
	DBV	12	1727	22	A, B					
	DBV	13	1730	04	B					
	737	7	1733	04	B, A					14
	DBV	14	1737	04	B					
	DBV	15	1739	22	A					
↓	737	[a]10	2025	07	PCC	↓			060	20

[a]Langley AFB, VA.

Table AI. Continued

(b) FAA Technical Center

Date	Test vehicle	Run	Time of day, GMT	Test R/W	Test surface		Temperature, °F		Wind	
					Type	Wetness	Ambient	Surface	Deg	Knots
6-23-83	DBV	8	1222	31	D, C, B	Wet	65	88	Variable	Light
	SFT	9	1234	13	B, C, D			89		
	Mu-M		1234							
	BV-11		1234							
	DBV		1234							
	SFT	10	1241	31	D, C, B			90		
	Mu-M		1241							
	BV-11		1241							
	DBV		1242							
	SFT	11	1315	13	B, C, D			98		
	Mu-M		1315							
	BV-11		1315							
	DBV		1316							
	SFT	12	1319	31	D, C, B			102		
	Mu-M		1319							
	BV-11		1320							
	DBV		1320							
	SFT	13	1323					103		
	Mu-M		1323							
	BV-11		1323							
	DBV		1323							
	737	1	1417	13	B, C, D	Dry				
	737	2	1658		C		85	128	120	2
	737	3	1708	31	D			131	100	8
	737	1R1	1718	13	B, C, D				200	3
6-24-83	SFT	14	1013	13	C	Wet	64	72	250	8
	Mu-M		1013							
	BV-11		1014							
	DBV		1015							
	737	4	1016							
6-23-83	SFT	1	1108		B, C, D		63	74	145	2
	Mu-M		1108							
	BV-11		1108							
	DBV		1109							
	SFT	2	1122	31	D, C, B			77		
	Mu-M		1122							
	BV-11		1122							
	DBV		1123						Variable	Light
	SFT	3	1128	13	B, C, D			75		
	Mu-M		1129							
	BV-11		1129							
	DBV		1129						320	3

Table AI. Continued

(b) Continued

Date	Test vehicle	Run	Time of day, GMT	Test R/W	Test surface		Temperature, °F		Wind	
					Type	Wetness	Ambient	Surface	Deg	Knots
6-23-83	SFT	4	1145	31	D, C, B	Wet		79		
	Mu-M		1145							
	BV-11		1146							
	DBV		1146						Variable	Light
	SFT	5	1151	13	B, C, D		64	80		
	Mu-M		1151							
	BV-11		1151							
	DBV		1152							
	SFT	6	1206	31	D, C, B			82		
	Mu-M		1206							
	BV-11		1206							
	DBV		1207							
	SFT	7	1212	13	B, C, D			85		
	Mu-M		1213							
	BV-11		1213							
	DBV		1213				65			
	SFT	8	1221	31	D, C, B			88		
	Mu-M	8	1221	31	D, C, B					
	BV-11	8	1221	31	D, C, B					
6-24-83	SFT	15	1017	13	C	Wet	64	72	250	8
	Mu-M		1017							
	BV-11		1017							
	DBV		1018						250	11
	SFT	16	1031	31	D					
	Mu-M		1031							
	BV-11		1032							
	DBV		1034							
	737	5	1035							
	SFT	17	1036						260	9
	Mu-M		1036							
	BV-11		1036							
	DBV		1037				67	74	250	11
	SFT	18	1104	13	B					
	Mu-M		1104							
	BV-11		1104							
	DBV		1105							
	737	6	1107							
	SFT	19	1108							
	Mu-M		1108							
	BV-11		1108							
	DBV		1110							
	SFT	20	1114	31						

Table AI. Continued

(b) Continued

Date	Test vehicle	Run	Time of day, GMT	Test R/W	Test surface		Temperature, °F		Wind	
					Type	Wetness	Ambient	Surface	Deg	Knots
6-24-83	Mu-M	20	1114	31	B	Wet				
	BV-11	20	1114							
	DBV	20	1114							
	737	7	1116							
	SFT	21	1117							
	Mu-M		1117							
	BV-11		1117							
	DBV		1118							
	SFT	22	1126	13			70	76	250	11
	Mu-M	22	1126							
	BV-11	22	1126							
	DBV	22	1127						270	10
	737	8	1131							
	SFT	23	1131							
	Mu-M	23	1131							
	BV-11	23	1132							
	DBV	23	1132							
	SFT	24	1139							
	Mu-M	24	1139							
	BV-11	24	1139							
	DBV	24	1139							
	737	9	1144							
	SFT	25	1144							
	Mu-M	25	1144							
	BV-11	25	1145				74	78		
	DBV	25	1145							
	737	10	1158	31						
	737	11	1205	31						
	737	12	1215	31			75			
	SFT	26	1232	13	B, C, D	Dry	76	90		
	Mu-M	26	1233	13	B, C, D					
	BV-11	26	1234	13	B, C, D					
	SFT	27	1238	31	D, C, B					
	Mu-M	27	1238	31	D, C, B					
	BV-11	27	1238	31	D, C, B					
	SFT	28	1240	13	B, C, D					
	Mu-M	28	1240	13	B, C, D					
	BV-11	28	1241	13	B, C, D					
	SFT	29	1242	31	D, C, B					
	Mu-M	29	1242	31	D, C, B					

Table AI. Continued

(b) Concluded

Date	Test vehicle	Run	Time of day, GMT	Test R/W	Test surface		Temperature, °F		Wind	
					Type	Wetness	Ambient	Surface	Deg	Knots
6-24-83	BV-11	29	1242	31	D, C, B	Dry	76	90	270	10
↓	SFT	30	1243	13	B, C, D	↓				
	Mu-M	30	1243	13	B, C, D					
	BV-11	30	1244	13	B, C, D					
	SFT	31	1246	31	D, C, B					
	Mu-M	31	1246	31	D, C, B					
	BV-11	31	1246	31	D, C, B					
↓	SFT	26R	1248	13	B, C, D	↓			270	13

Table AI. Continued

(c) BNAS

Date	Test vehicle	Run	Time of day, GMT	Test R/W	Test surface		Temperature, °F		Wind	
					Type	Wetness	Ambient	Surface	Deg	Knots
3-6-85	737	6	1816	01	Asphalt	Dry, loose	23		250	10
↓	↓	7	1825	19	↓	snow, 6 in.			360	
		9	1843	01		↓			360	
		2	2141	01			28		330	
		3	2154	19					360	14
		4	2204	01					330	8
	↓	5	2213	19			27		330	10
	RCR	1	2240	01						
	↓	2	2243	19						
		3	2246	01						
		4	2250	19						
↓	↓	5	2253	01	↓	↓				
3-7-85	RCR	6	1710	01	Asphalt	Dry, loose	30		240	8
↓	↓	7	1715	19	↓	snow, 3 in.				
		8	1718	01		↓				
		9	1721	19						
	↓	10	1725	01						
	737	7	1842	19						
	↓	9	1849	01					230	10
		3	1908	19			31		240	10
		4	1921	01		↓			240	8
		[a]14	1935	19		Dry			200	12
		5	1942	01		Dry, loose				14
		15	1951	19		snow, 3 in.				10
↓	↓	14R1	1954	19	↓	Dry				
3-8-85	Mu-M	10	1420	01	Asphalt	Wet snow,	37		220	
↓	BV-11	10	1421	↓	↓	1.5 in.				
	RCR	1	1422			↓				
	737	2	1425							
	Mu-M	11	1428							
	BV-11	11	1429							
↓	RCR	2	1430	↓	↓	↓				

[a]Inboard runway.

Table AI. Continued

(c) Continued

Date	Test vehicle	Run	Time of day, GMT	Test R/W	Test surface		Temperature, °F		Wind	
					Type	Wetness	Ambient	Surface	Deg	Knots
3-8-85	737	3	1439	01	Asphalt	1.5-in. snow	39		240	10
		2R1	1510			4.5 in.			240	10
		3R1	1516			4.5 in.			230	8
		[a]14	1524			Wet				
	Mu-M	12	1530							
	BV-11	12	1531							
	RCR	3	1532							
	Mu-M	13	1535	19						
	BV-11	13	1536							
	RCR	4	1537							
	Mu-M	14	1540	01						
	BV-11	14	1541							
	RCR	5	1542							
	RCR	6	1705	19		1-in. slush	41		240	
	737	2RC	1710							
	RCR	7	1712							
	737	3R2	1716							
		9	1724			Wet snow,			230	
		7	1728	01		4 in.				10
		3R3	1733	19		1-in. slush				8
		14R1	1745	19		Wet			210	12
		13	1946	19		Wet snow,	45		240	12
		11	1952	01		2 to 3 in.			240	10
		10	1956	19			47		220	8
		16	2002	01		Wet			220	10
		14R2	2017	19		Dry			240	6
3-9-85	RCR	8	1100	19	Asphalt	Icy	29		0	
	Mu-M	21	1114	19						
	BV-11	21	1115	19						
	Mu-M	22	1117	01						
	BV-11	22	1118	01						
	Mu-M	23	1119	19						
	BV-11	23	1120	19						
	Mu-M	24	1121	01						

[a]Inboard runway.

Table AI. Concluded

(c) Concluded

Date	Test vehicle	Run	Time of day, GMT	Test R/W	Test surface		Temperature, °F		Wind	
					Type	Wetness	Ambient	Surface	Deg	Knots
3-9-85	BV-11	24	1122	01	Asphalt	Icy	29		0	
↓	737	2	1127	19	↓	↓				
	Mu-M	25	1128	19						
	BV-11	25	1129	19						
	Mu-M	26	1131	01					310	2
	BV-11	26	1132	01						
	737	3	1135	01						
	Mu-M	27	1136	19						
	BV-11	27	1137	19						
	Mu-M	28	1138	01						
	BV-11	28	1139	01						
	Mu-M	29	1141	19			32	25	0	
	BV-11	29	1142	19						
	Mu-M	30	1143	01						
	BV-11	30	1144	01						
	737	4	1150	01						
	Mu-M	31	1151	19						
	BV-11	31	1152	19						
	Mu-M	32	1153	01						
	BV-11	32	1154	01						
	737	5	1156	19						
	Mu-M	33	1157	19						
	BV-11	33	1158	19						
	Mu-M	34	1159	01						
	BV-11	34	1200	01						
	Mu-M	35	1204	19						
	BV-11	35	1205	19						
	Mu-M	36	1206	01						
↓	BV-11	36	1207	01	↓	↓				

Table AII. Compilation of Boeing 737 Braking Friction Data by Test-Surface Type and Wetness Condition

(a) Wallops Flight Facility

Run	Flt	Test R/W	A/C gross weight, lb	A/C c.g. station	Test surface		Type of braking	Ground speed, knots	Effective braking friction coefficient
					Type	Wetness			
2	409	10	83.70×10^3	649.4	SSA	Dry	Manual	25	0.41
								30	.42
								35	.43
3	409	10	82.90×10^3	649.9	SSA	Dry	Manual	25	.43
								30	.42
								35	.42
								40	.42
								45	.42
								50	.42
18	410	10	77.30×10^3	650.9	SSA	Dry	Manual	30	.47
								40	.45
								50	.43
								60	.44
								70	.43
								80	.43
17	410	10	78.90×10^3	650.4	SSA	Dry	Automatic	40	.36
								50	.34
								60	.31
								70	.28
								80	.28
								90	.29
21	412	10	84.40×10^3	650.0	SSA	Truck wet	Manual	40	.38
								50	.37
								60	.34
								70	.27
								80	.29
22	412	10	83.00×10^3	649.5	SSA	Truck wet	Automatic	55	.28
								60	.16
								65	.14
								70	.25
								75	.20
								80	.17
								85	.21
								90	.18
								95	.13
7	409	4	80.60×10^3	650.1	A	Dry	Manual	30	.51
								35	.49
								40	.47
								45	.44
								50	.44

Table AII. Continued

(a) Continued

Run	Flt	Test R/W	A/C gross weight, lb	A/C c.g. station	Test surface		Type of braking	Ground speed, knots	Effective braking friction coefficient
					Type	Wetness			
9	409	4	77.00×10^3	651.2	A	Dry	Manual	50	0.48
								55	.47
								60	.45
								65	.43
								70	.42
6	409	22	81.10×10^3	650.0	A	Dry	Manual	45	.46
								50	.45
								55	.44
								60	.44
								65	.46
								70	.43
8	409	22	78.80×10^3	650.7	A	Dry	Manual	90	.40
								95	.38
16	410	4	80.20×10^3	650.1	A	Truck wet	Manual	53	.14
								56	.15
								59	.10
14	410	4	76.40×10^3	651.3	A	Truck wet	Manual	61	.12
								64	.10
								67	.09
11	410	22	90.98×10^3	650.0	A	Truck wet	Manual	50	.15
								55	.14
								60	.14
13	410	22	77.81×10^3	650.8	A	Truck wet	Manual	70	.08
								73	.08
								77	.08
15	410	22	81.98×10^3	649.8	A	Truck wet	Manual	93	.01
								95	.02
								97	.03
37	415	4	87.34×10^3	651.4	A	Flooded	Manual	48	.12
								53	.10
								58	.08
38	415	22	87.09×10^3	651.2	A	Flooded	Manual	72	.05
								75	.04
								78	.03

Table AII. Continued

(a) Continued

Run	Flt	Test R/W	A/C gross weight, lb	A/C c.g. station	Test surface		Type of braking	Ground speed, knots	Effective braking friction coefficient
					Type	Wetness			
39	415	22	85.79×10^3	650.5	A	Flooded	Manual	79	0.05
								82	.05
								85	.03
7	409	4	80.56×10^3	650.1	B	Dry	Manual	47	.45
								50	.43
								53	.45
								56	.43
								59	.44
								62	.41
9	409	4	77.00×10^3	651.2	B	Dry	Manual	75	.45
								78	.45
								81	.45
								84	.44
								87	.43
6	409	22	81.10×10^3	650.0	B	Dry	Manual	35	.52
								37	.50
								39	.49
								41	.48
								43	.48
								45	.46
8	409	22	78.80×10^3	650.6	B	Dry	Manual	65	.44
								70	.43
								75	.42
								80	.41
								85	.40
								90	.39
12	410	4	79.46×10^3	650.3	B	Truck wet	Manual	25	.45
								30	.44
								35	.42
								40	.41
								45	.39
								48	.37
16	410	4	80.23×10^3	650.1	B	Truck wet	Manual	62	.37
								64	.37
								66	.36
								68	.36
								70	.34
								72	.32
								74	.30

Table AII. Continued

(a) Continued

Run	Flt	Test R/W	A/C gross weight, lb	A/C c.g. station	Test surface		Type of braking	Ground speed, knots	Effective braking friction coefficient
					Type	Wetness			
14	410	4	76.36×10^3	651.3	B	Truck wet	Manual	70	0.37
								72	.35
								74	.34
								76	.32
								78	.32
								80	.30
								82	.30
11	410	22	80.98×10^3	650.0	B	Truck wet	Manual	18	.44
								20	.44
								25	.43
								30	.41
								35	.36
								40	.32
								45	.29
19	410	22	83.80×10^3	650.0	B	Truck wet	Manual	32	.39
								35	.40
								40	.39
								45	.39
								50	.38
								55	.34
13	410	22	77.80×10^3	650.8	B	Truck wet	Manual	57	.34
								60	.31
								63	.27
								66	.23
15	410	22	81.98×10^3	649.8	B	Truck wet	Manual	84	.21
								86	.21
								88	.19
								90	.18
32	415	4	83.06×10^3	649.6	B	Flooded	Manual	32	.40
								36	.40
								40	.39
								44	.36
								48	.35
								52	.34
								55	.31

Table AII. Continued

(a) Continued

Run	Flt	Test R/W	A/C gross weight, lb	A/C c.g. station	Test surface		Type of braking	Ground speed, knots	Effective braking friction coefficient
					Type	Wetness			
23	412	4	81.80×10^3	649.4	C	Truck wet	Manual	36	0.44
								38	.44
								40	.43
								42	.44
								44	.43
								62	.42
								64	.41
								66	.40
								68	.40
24	412	4	79.93×10^3	650.6	B	Truck wet	Manual	67	.35
								70	.32
								73	.30
24	412	4	79.93×10^3	650.6	C	Truck wet	Manual	87	.36
								89	.35
								91	.34
33	415	22	82.20×10^3	649.5	B	Flooded	Manual	62	.32
								64	.30
								66	.30
								68	.28
								70	.28
								72	.26
								74	.26
34	415	22	80.00×10^3	649.9	B	Flooded	Manual	85	.17
								90	.16
								95	.16
31	412	4	72.80×10^3	652.1	J1	Truck wet	Manual	51	.20
								54	.20
								57	.19
								60	.17
								63	.18
								66	.18
								69	.18
28	412	22	77.60×10^3	650.4	J1	Truck wet	Manual	34	.32
								37	.32
								40	.31
								43	.30
								46	.29
								49	.27
								52	.26
30	412	22	74.20×10^3	650.5	J1	Truck wet	Manual	67	.17
								69	.15
								71	.13
								73	.13

Table AII. Continued

(a) Continued

Run	Flt	Test R/W	A/C gross weight, lb	A/C c.g. station	Test surface		Type of braking	Ground speed, knots	Effective braking friction coefficient
					Type	Wetness			
29	412	4	75.98×10^3	651.0	J2	Truck wet	Manual	36	0.43
								40	.40
								44	.38
								48	.42
								52	.38
								56	.42
								60	.36
31	412	4	72.88×10^3	652.2	J2	Truck wet	Manual	70	.27
								72	.27
								74	.27
								76	.25
								78	.25
								80	.25
								82	.28
								84	.26
								86	.25
30	412	22	74.28×10^3	650.5	J2	Truck wet	Manual	40	.40
								42	.39
								44	.40
								46	.40
								48	.37
								50	.35
								52	.33
								54	.29
								56	.33
								58	.31
								60	.29
								62	.26
								64	.23
								66	.21

Table AII. Continued

(a) Concluded

Run	Flt	Test R/W	A/C gross weight, lb	A/C c.g. station	Test surface		Type of braking	Ground speed, knots	Effective braking friction coefficient
					Type	Wetness			
4A	434	10	85.60×10^3	651.9	SSA	Rain wet	Manual	10	0.37
								15	.34
								20	.33
								25	.34
								30	.35
								35	.38
								40	.40
4B	434	10	84.30×10^3	651.6	SSA	Rain wet	Manual	20	.34
								25	.37
								30	.38
								35	.40
								40	.41
								45	.42
								50	.42
								55	.42
								60	.41
4C	434	10	83.20×10^3	651.5	SSA	Rain damp	Manual	45	.50
								50	.49
								55	.48
								60	.46
								65	.44
								70	.44
								75	.43
								80	.42
								85	.43
								90	.42
5	434	10	81.70×10^3	651.7	SSA	Rain damp	Automatic	35	.34
								40	.33
								45	.32
								50	.31
								55	.30
								60	.28
								65	.27
								70	.26
								75	.26
								80	.25
								85	.24
								90	.23
								95	.21
								100	.20
6	434	22	79.80×10^3	652.3	A	Rain damp	Manual	85	.32
7	434	4	78.80×10^3	652.6	B	Rain damp	Manual	80	.41
								85	.40

Table AII. Continued

(b) FAA Technical Center

Run	Flt	Test R/W	A/C gross weight, lb	A/C c.g. station	Test surface		Type of braking	Ground speed, knots	Effective braking friction coefficient
					Type	Wetness			
6	414	13	80.48×10^3	650.2	B	Truck wet	Manual	29	0.37
								32	.38
								35	.39
								38	.40
7	414	13	79.98×10^3	650.3	B	Truck wet	Manual	37	.33
								39	.33
								41	.33
								43	.32
								45	.33
								47	.34
9	414	13	76.88×10^3	651.3	B	Truck wet	Manual	81	.21
								83	.19
								85	.19
								87	.17
2	413	13	82.40×10^3	649.8	C	Dry	Manual	35	.52
								40	.51
								45	.50
								50	.49
								55	.50
								60	.49
								65	.48
								70	.45
								75	.47
								80	.47
								85	.46
								90	.45
								95	.47
								100	.45

Table AII. Continued

(b) Concluded

Run	Flt	Test R/W	A/C gross weight, lb	A/C c.g. station	Test surface		Type of braking	Ground speed, knots	Effective braking friction coefficient
					Type	Wetness			
4	414	13	85.90×10^3	650.1	C	Truck wet	Manual	50	0.40
								55	.39
								60	.38
								65	.36
								70	.36
								75	.40
								80	.40
								85	.40
								90	.35
								95	.35
								100	.37
								105	.35
								110	.34
3	413	31	80.90×10^3	650.0	D	Dry	Manual	50	.51
								55	.50
								60	.49
								65	.48
								70	.47
								75	.46
								80	.46
								85	.47
								90	.46
								95	.46
								100	.45
5	414	31	82.90×10^3	649.9	D	Truck wet	Manual	50	.33
								55	.32
								60	.35
								65	.34
								70	.32
								75	.33
								80	.33
								85	.36
								90	.33
								95	.33
								100	.35
								105	.35
								110	.32

Table AII. Continued

(c) Brunswick Naval Air Station

Run	Flt	Test R/W	A/C gross weight, lb	A/C c.g. station	Test surface		Type of braking	Ground speed, knots	Effective braking friction coefficient
					Type	Wetness			
2	430	1	79.70×10^3	653.1	Asphalt	Dry, loose snow, 6 in.	Manual	8	0.10
								14	.11
								18	.14
								24	.16
								28	.15
3	430	19	79.10×10^3	654.1	Asphalt	Dry, loose snow, 6 in.	Manual	20	.13
								25	.14
								30	.16
								35	.18
								40	.20
4	430	1	78.70×10^3	653.5	Asphalt	Dry, loose snow, 6 in.	Manual	20	.13
								25	.15
								30	.17
								35	.19
								40	.19
								45	.18
								50	.19
								55	.19
								60	.19
5	430	19	78.40×10^3	652.0	Asphalt	Dry, loose snow, 6 in.	Manual	25	.15
								30	.17
								35	.18
								40	.19
								45	.19
								50	.19
								55	.19
								60	.20
								65	.20
								70	.20
3	431	19	77.10×10^3	652.9	Asphalt	Dry, loose snow, 3 in.	Manual	20	.11
								25	.14
								30	.16
								35	.17
								40	.18
								45	.17
4	431	1	76.50×10^3	653.0	Asphalt	Dry, loose snow, 3 in.	Manual	25	.14
								30	.14
								35	.16
								40	.17
								45	.16
								50	.15
								55	.15

Table AII. Continued

(c) Continued

Run	Flt	Test R/W	A/C gross weight, lb	A/C c.g. station	Test surface		Type of braking	Ground speed, knots	Effective braking friction coefficient
					Type	Wetness			
5	431	1	75.10×10^3	653.6	Asphalt	Dry, loose snow, 3 in.	Manual	25	0.15
								30	.16
								35	.16
								40	.17
								45	.18
								50	.18
								55	.16
								60	.15
								65	.16
								70	.16
2	432	1	78.20×10^3	652.5	Asphalt	New wet snow, 1.5 in.	Manual	10	.11
								15	.11
								20	.09
								25	.09
3	432	1	77.60×10^3	652.7	Asphalt	New wet snow, 1.5 in.	Manual	25	.14
								30	.14
								35	.14
								40	.14
								45	.14
								50	.13
2R1	432	1	75.80×10^3	653.3	Asphalt	Wet snow, 4.5 in.	Manual	15	.10
								20	.09
								25	.09
3R1	432	1	75.40×10^3	653.5	Asphalt	Wet snow, 4.5 in.	Manual	20	.09
								25	.10
								30	.12
								35	.13
								40	.13
								45	.13
								50	.12
2R2	432	19	79.70×10^3	651.8	Asphalt	1-in. slush	Manual	20	.09
								25	.09
								30	.09
3R2	432	19	79.40×10^3	652.1	Asphalt	1-in. slush	Manual	20	.12
								25	.12
								30	.14
								35	.14
								40	.13
								45	.12
								50	.10

Table AII. Continued

(c) Concluded

Run	Flt	Test R/W	A/C gross weight, lb	A/C c.g. station	Test surface		Type of braking	Ground speed, knots	Effective braking friction coefficient
					Type	Wetness			
3R3	432	19	78.50×10^3	652.4	Asphalt	1-in. slush	Manual	25	0.12
								30	.12
								35	.17
								40	.15
								45	.13
								50	.10
								55	.08
2	433	19	81.40×10^3	652.6	Asphalt	Icy	Manual	20	.03
								25	.04
								30	.04
3	433	1	80.00×10^3	653.0	Asphalt	Icy	Manual	35	.04
								40	.02
								45	.03
								50	.03
5	433	19	79.50×10^3	653.2	Asphalt	Icy	Manual	45	.01
								50	.01
								55	.00
								60	.01
								65	.01
								70	.02
								80	.01

Table AII. Concluded

(d) Langley Air Force Base

Run	Flt	Test R/W	A/C gross weight, lb	A/C c.g. station	Test surface		Type of braking	Ground speed, knots	Effective braking friction coefficient
					Type	Wetness			
10	434	7	87.00×10^3	652.9	PCC	Rain wet, 0.02 to 0.03 in.	Manual	50	0.35
								55	.34
								55	.34
								60	.33
								60	.33
								65	.29
								70	.25
								75	.23
								80	.20
								85	.19
								90	.19

Table AIII. Ground-Vehicle Friction Data Obtained on Dry-Runway Test Surfaces

(a) Wallops Flight Facility

Test surface	Test vehicle	Run	Speed, mph	Average friction coefficient
SSA	DBV	11	60	0.88
			50	.88
			40	.90
			30	.88
			20	.88
			10	.93
			2	.93
		12	60	.88
			50	.90
			40	.93
			30	.88
			20	↓
			10	↓
			2	↓
	Mu-M	17	20	.89
			30	.88
			40	.87
			50	.86
			60	↓
		18	20	↓
			30	↓
			40	↓
			50	↓
			60	↓
		79	20	.87
			30	.88
			40	.89
			50	.89
			58	.88
		80	20	.86
			30	.87
			40	.88
			50	.89
			60	.89
		78	1	.82
	BV-11	17	1	1.10
		18	20	1.13
			30	1.12
			40	1.10
			50	1.07
			60	1.00
		19	20	1.11
		19	30	1.11
↓	↓	19	40	1.10

Table AIII. Continued

(a) Continued

Test surface	Test vehicle	Run	Speed, mph	Average friction coefficient
SSA	BV-11	19	50	1.07
	BV-11	19	60	1.02
	SFT	15	20	.98
			30	.96
			40	.94
			50	.91
			60	.87
		16	20	.96
			30	.95
			40	.92
			50	.89
			60	.86
A	DBV	38	60	0.87
			50	.95
			40	.92
			30	.87
			20	.78
			10	.81
			2	1.00
	Mu-M	19	60	.91
		20	50	.89
		21	40	.89
		22	30	.88
		23	20	.87
		62	1	.81
		64	20	.89
		65	20	.89
		66	40	.91
		67	40	.91
		68	60	.90
		69	60	.90
	BV-11	1	1	1.10
		3	20	1.08
		4	20	1.07
		5	40	1.01
		6	40	1.02
		7	60	.94
		8	60	.97
	SFT	1	20	.99
		2	20	.99
		3	40	.98
		4	40	.98
		5	60	.97
		6	60	.96

Table AIII. Continued

(a) Continued

Test surface	Test vehicle	Run	Speed, mph	Average friction coefficient
B, C	DBV	39	60	0.84
			50	.86
			40	.84
			30	.77
			20	.73
			10	.80
			2	.98
	Mu-M	19	60	.89
		20	50	.88
		21	40	.88
		22	30	.87
		23	20	.86
		63	1	.79
		64	20	.89
		65	20	.88
		66	40	.91
		67	40	.90
		68	60	.92
		69	60	.90
	BV-11	2	1	1.11
		3	20	1.09
		4	20	1.08
		5	40	1.04
		6	40	1.04
		7	60	.98
		8	60	.99
	SFT	1	20	.99
		2	20	.99
		3	40	.98
		4	40	.99
		5	60	.98
		6	60	.98
J-1	Mu-M	40	20	0.85
		41	20	.84
		42	30	.85
		43	30	.85
		44	40	.87
		45	40	.86
		46	50	.87
		47	50	.86
		48	60	.88
		49	60	.87
		97	20	.86
		98	40	.87
		99	60	.89

Table AIII. Continued

(a) Concluded

Test surface	Test vehicle	Run	Speed, mph	Average friction coefficient
J-1	BV-11	36	20	1.10
↓	BV-11	37	40	
	BV-11	38	60	1.00
	SFT	33	20	.98
	SFT	34	40	.90
	SFT	35	60	.87
J-2	Mu-M	40	20	0.88
↓	↓	41	20	.88
		42	30	.89
		43	30	.89
		44	40	.90
		45	40	.88
		46	50	.91
		47	50	.89
		48	60	.91
		49	60	.90
	BV-11	36	20	1.07
	BV-11	37	40	1.01
	BV-11	38	60	.98
	SFT	33	20	.95
	SFT	34	40	.89
↓	SFT	35	60	.84

Table AIII. Continued

(b) FAA Technical Center

Test surface	Test vehicle	Run	Speed, mph	Average friction coefficient
B	DBV	77	60	0.86
			50	.86
			40	.71
			30	.65
			20	.76
			10	.96
			2	1.05
	Mu-M	26	20	.88
		27	20	.87
		28	40	.90
		29	40	.89
		30	60	.90
		31	60	.91
	BV-11	26	20	1.01
		27	20	.93
		28	40	.93
		29	40	.99
		30	60	.92
		31	60	.95
	SFT	26	20	.98
		27	20	.99
		28	40	.92
		29	40	.90
		30	60	.88
		31	60	.86
C	DBV	78	60	0.83
			50	.83
			40	.74
			30	.71
			20	.71
			10	.81
			2	.86
	Mu-M	26	20	.87
		27	20	.87
		28	40	.89
		29	40	.89
		30	60	.90
		31	60	.91
	BV-11	26	20	1.03
		27	20	.97
		28	40	1.00
		29	40	1.02
		30	60	.98
		31	60	.99

Table AIII. Concluded

(b) Concluded

Test surface	Test vehicle	Run	Speed, mph	Average friction coefficient
C	SFT	26R	20	0.99
↓	↓	27	20	.99
		28	40	.95
		29	40	.93
		30	60	.90
		31	60	.90
D	DBV	79	60	0.74
↓	↓	↓	50	.83
			40	.83
			30	.83
			20	.83
			10	.94
			2	.98
	Mu-M	26	20	.87
	↓	27	20	.88
		28	40	.89
		29	40	.89
		30	60	.90
		31	60	.91
	BV-11	26	20	.98
	↓	27	20	.98
		28	40	.98
		29	40	1.00
		30	60	.96
		31	60	.95
	SFT	26	20	.99
	↓	27	20	.99
		28	40	.93
		29	40	.93
		30	60	.88
↓	↓	31	60	.88

Table AIV. Ground-Vehicle Friction Data Obtained During Wet-Runway Aircraft Braking Test Runs

(a) Diagonal-braked vehicle

Test site	Test surface	A/C run	Vehicle run		Average friction coefficient at test speed, mph, of—					
			Number	Time from A/C run, min[a]	10	20	30	40	50	60
Wallops Flight Facility	SSA	21	44	−3	0.85	0.66	0.51	0.44	0.36	0.33
			45	+1		.73	.58	.51	.46	.39
		22	46	−3	0.85	0.64	0.49	0.39	0.34	0.29
			47	+1	.85	.66	.51	.44	.39	.34
	A	11	26	−1					0.15	0.07
	B, C			−1	0.64	0.58	0.56	0.53		
	A		27	+2					0.17	0.10
	B, C			+2	0.67	0.63	0.55	0.51		
	B, C	12	28	−1			0.51	0.47	0.41	0.39
	A			−1	0.55	0.36				
	B, C		29	+2			0.61	0.55	0.51	0.49
	A			+2	0.58	0.41				
	A	13	30	−2					0.15	0.10
	B, C			−2	0.70	0.63	0.58	0.51		
	A		31	+1					0.12	0.07
	B, C			+1	0.67	0.58	0.58	0.53		
	B, C	14	32	−1				0.51	0.49	0.46
	A			−1	0.61	0.44	0.24			
	B, C		33	+2				0.53	0.51	0.45
	A			+2	0.53	0.39	0.24			
	A	15	34	−1					0.17	0.12
	B, C			−1	0.70	0.63	0.59	0.56		
	A		35	+2					0.17	0.12
	B, C			+2	0.66	0.58	0.51	0.48		
	B, C	16	36	−2				0.51	0.49	0.51
	A			−2	0.58	0.36	0.24			
	B, C		37	+2				0.51	0.47	0.46
	A			+2	0.52	0.44	0.24			
		37	[b]98	−1					0.17	0.12
			[b]99	+2					.15	.10
		38	[b]100	−2					0.17	0.10
			[b]101	+2					.16	.12
		39	[b]102	−1					0.18	0.12
			[b]103	+2					.15	.10
	B, C	23	48	−2	0.72	0.66	0.61	0.56	0.51	0.49
			49	+2	.68	.63	.61	.53	.51	.51
		24	50	−1	0.73	0.64	0.58	0.50	0.51	0.49
			51	+2	.73	.63	.61	.55	.53	.51
		32	[b]92	−2				0.42	0.37	0.29
			[b]93	+2				.42	.33	.29

[a]Minus sign denotes time before A/C run; plus sign denotes time after A/C run.
[b]Flooded condition.

Table AIV. Continued

(a) Continued

Test site	Test surface	A/C run	Vehicle run		Average friction coefficient at test speed, mph, of—					
			Number	Time from A/C run, min[a]	10	20	30	40	50	60
Wallops Flight Facility	B, C	33	[b]94	−1				0.53	0.42	0.32
			[b]95	+2				.51	.39	.29
		34	[b]96	−1				0.49	0.37	0.29
			[b]97	+2				.50	.40	.29
	J-1	28	52	−2					0.39	0.24
	J-2			−2	1.00	0.85	0.66	0.58		
	J-1		53	+3					0.36	0.24
	J-2			+3	0.97	0.85	0.73	0.63		
	J-2	29	54	−1				0.36	0.36	0.29
	J-1			−1	0.73	0.56	0.49			
	J-2		55	+2					0.41	0.32
	J-1			+2	0.75	0.63	0.63	0.61		
	J-1	30	56	−3					0.27	0.12
	J-2			−3	1.09	0.94	0.69	0.53		
	J-1		57	+2					0.36	0.12
	J-2			+2	1.00	0.83	0.66	0.53		
	J-2	31	58	−1					0.36	0.29
	J-1			−1	0.73	0.55	0.34	0.49		
	J-2		59	+2				0.56	0.49	0.36
	J-1			+2	0.75	0.61	0.51			
FAA Technical Center	C	4	80	−1	0.73	0.68	0.63	0.53	0.45	0.38
	C		81	+2	.76	.66	.56	.48	.41	.38
	D	5	82	−2	0.89	0.76	0.68	0.63	0.58	0.51
	D		83	+2	.81	.73	.71	.66	.56	.51
	B	6	84	−2	0.80	0.61	0.48			
			85	+3	.76	.63	.51			
		7	86	−2	0.76	0.67	0.51	0.32		
			87							
		8	88							
			89	+2					0.25	
		9	90	−4						0.10
			91	+1						.17

[a]Minus sign denotes time before A/C run; plus sign denotes time after A/C run.
[b]Flooded condition.

Table AIV. Continued

(a) Concluded

Test site	Test surface	A/C run	Vehicle run		Average friction coefficient at test speed, mph, of					
			Number	Time from A/C run, min[a]	10	20	30	40	50	60
Wallops Flight Facility	[c]SSA	4A	1	−3	0.90	0.80	0.70	0.63	0.53	0.45
			3	+6	.88	.80	.70	.65	.55	.45
		4B	4	−1	0.90	0.80	0.72	0.62	0.52	0.42
			5	+3	.86	.80	.75	.63	.53	.45
		4C	6	−1	0.88	0.82	0.73	0.63	0.56	0.45
			7	+2	.88	.78	.70	.65	.55	.45
		5	8	−2	0.90	0.80	0.72	0.62	0.53	0.42
			9	+3	.92	.80	.70	.60	.53	.45
	[c]A	6	10	−7					0.25	0.15
			11	−5	0.58	0.42				
			12	+3			0.40	0.28		
		7	15	+6	0.60	0.42	0.32	0.22		
	[c]B	6	10	−7	0.65	0.60	0.55	0.50		
			11	−5			.62	.58	0.50	0.43
			12	+3	.76	.68				
		7	13	−3	0.66	0.62	0.56	0.56	0.50	
			14	+4	.66	.64	.56	.54	.50	

[a]Minus sign denotes time before A/C run; plus sign denotes time after A/C run.
[c]Rain-wet condition.

Table AIV. Continued

(b) Mu-Meter

Test site	Test surface	A/C run	Vehicle run		Average friction coefficient at test speed, mph, of					
			Number	Time from A/C run, min[a]	10	20	30	40	50	60
Wallops Flight Facility	SSA	21	81	−3		0.86	0.84	0.74	0.68	0.54
			82	+1		.86	.86	.84	.80	.70
		22	83	−4		0.86	0.78	0.73	0.75	0.60
			84	+1		.86	.85	.83	.83	
	A	11	50	−1				0.26		
	B/C			−1				.86		
	A		51	+1				0.23		
	B/C			+1				.76		
	B/C	12	52	−2				0.77		
	A			−2				.26		
	B/C		53	+2				0.77		
	A			+2				.22		
	A	13	54	−2				0.25		
	B/C			−2				.54		
	A		55	+1				0.23		
	B/C			+1				.74		
	B/C	14	56	−1				0.75		
	A			−1				.26		
	B/C		57	+2				0.75		
	A			+2				.28		
	A	15	58	−1				0.41		
	B/C			−1				.77		
	A		59	+1				0.35		
	B, C			+1				.74		
	B, C	16	60	−2				0.76		
	A			−2				.25		
	B, C		61	+1				0.74		
	A			+1				.24		
	A	37	[b]110	−2				0.07		
			[b]111	+1				.07		
		38	[b]112	−3				0.08		
			[b]113	+1				.12		
		39	[b]114	−2				0.16		
			[b]115	+1				.22		

[a]Minus sign denotes time before A/C run; plus sign denotes time after A/C run.
[b]Flooded condition.

Table AIV. Continued

(b) Concluded

Test site	Test surface	A/C run	Vehicle run		Average friction coefficient at test speed, mph, of					
			Number	Time wideheadfrom A/C run, min[a]	10	20	30	40	50	60
Wallops Flight Facility	B, C	23	85	−2				0.81		
			86	+3				.83		
		24	87	−2				0.81		
			88	+1				.81		
		32	[b]104	−2				0.60		
			[b]105	+1				.61		
		33	[b]106	−2				0.80		
			[b]107	+1				.81		
		34	[b]108	−2				0.78		
			[b]109	+1				.77		
	J-1	28	89	−3				0.65		
	J-2			−3				.94		
	J-1		90	+1				0.74		
	J-2			+1				.94		
	J-2	29	91	−2				0.91		
	J-1			−2				.32		
	J-2		92	+1				0.93		
	J-1			+1				.30		
	J-1	30	93	−3				0.50		
	J-2			−3				.95		
	J-1		94	+1				0.60		
	J-2			+1				.96		
	J-2	31	95	−2				0.89		
	J-1			−2				.30		
	J-2		96	+1				0.95		
	J-1			+1				.25		
FAA Technical Center	C	4	14	−2		0.82	0.81	0.82	0.82	0.82
			15	+1		.79	.80	.80	.81	
	D	5	16	−4		0.84	0.80	0.80	0.82	0.80
			17	+1		.84	.81	.81	.81	.80
	B	6	18	−3				0.62		
			19	+1				.64		
		7	20	−2				0.62		
			21	+1				.58		
		8	22	−5				0.60		
			23	+1				.62		
		9	24	−5				0.62		
			25	+1				.64		

[a]Minus sign denotes time before A/C run; plus sign denotes time after A/C run.
[b]Flooded condition.

Table AIV. Continued

(c) Surface friction tester

Test site	Test surface	A/C run	Vehicle run		Average friction coefficient at test speed, mph, of—					
			Number	Time from A/C run, min[a]	10	20	30	40	50	60
Wallops Flight Facility	SSA	21	17	−4		0.92	0.83	0.68	0.58	0.40
			18	+1		.94	.89	.83	.68	
		22	19	−4		0.90	0.75	0.65	0.55	0.45
			20	+1		.93	.87	.81	.71	.55
	B, C	23	21	−3				0.90		
			22	+2				.89		
		24	23	−2				0.90		
			24	+1				.88		
	J-1	28	25	−3				0.64		
	J-2			−3				.89		
	J-1		26	+1				0.75		
	J-2			+1				.93		
	J-2	29	27	−2				0.90		
	J-1			−2				.60		
	J-2		28	+1				0.93		
	J-1			+1				.60		
	J-1	30	29	−3				0.62		
	J-2			−3				.87		
	J-1		30	+1				0.65		
	J-2			+1				.90		
	J-2	31	31	−2				0.90		
	J-1			−2				.60		
	J-2		32	+1				0.92		
	J-1			+1				.60		
FAA Technical Center	C	4	14	−3			0.93	0.91	0.90	0.89
			15	+1		0.95	.91	.90	.89	.88
	D	5	16	−4		0.97	0.94	0.92	0.90	0.87
			17	+1		.95	.93	.91	.89	.84
	B	6	18a	−3				0.60		
			19	+1				.63		
		7	20	−2				0.50		
			21	+1				.68		
		8	22	−5				0.50		
			23	+1				.67		
		9	24	−5				0.45		
			25	+1				.68		

[a]Minus sign denotes time before A/C run; plus sign denotes time after A/C run.

Table AIV. Concluded

(d) BV-11 skiddometer

Test site	Test surface	A/C run	Vehicle run		Average friction coefficient at test speed, mph, of					
			Number	Time from A/C run, min[a]	10	20	30	40	50	60
Wallops Flight Facility	SSA	21	20	−3		0.97	0.81	0.78	0.66	0.49
			21	+1		.98	.81	.72	.67	.52
		22	22	−3		0.95	0.77	0.75	0.66	0.43
			23	+1		.95	.81	.78	.75	.57
	B, C	23	24	−2				0.92		
			25	+3				.94		
		24	26	−2				0.90		
			27	+1				.91		
	J-1	28	28	−2				0.66		
	J-2			−2				.95		
	J-1		29	+2				0.68		
	J-2			+2				1.00		
	J-2	29	30	−1				0.91		
	J-1			−1				.45		
	J-2		31	+2				0.90		
	J-1			+2				.43		
	J-1	30	32	−3				0.51		
	J-2			−3				.96		
	J-1		33	+1				0.57		
	J-2			+1				.95		
	J-2	31	34	−2				0.86		
	J-1			−2				.43		
	J-2		35	+1				0.94		
	J-1			+1				.46		
FAA Technical Center	C	4	14	−2		0.90	0.86	0.97	0.96	0.98
			15	+1		.80	.82	.88	.94	.93
	D	5	16	−3		0.88	0.87	0.87	0.91	0.89
			17	+1		.93	.90	.91	.91	.88
	B	6	18	−3				0.55		
			19	+1				.67		
		7	20	−2				0.40		
			21	+1				.49		
		8	22	−4				0.46		
			23	+1				.46		
		9	24	−5				0.34		
			25	+1				.41		

[a]Minus sign denotes time before A/C run; plus sign denotes time after A/C run.

Table AV. Supplemental Ground-Vehicle Friction Data Obtained on Wet-Runway Test Surfaces

(a) Diagonal-braked vehicle

Date	Test site	Run	Test surface		Average friction coefficient at test speed, mph, of—					
			Type	Wetness condition	10	20	30	40	50	60
6-14-83	Wallops	1	SSA	Wet	0.71	0.52	0.49	0.39	0.31	0.24
	Flight	2		Wet	.69	.49	.39	.31	.27	.24
	Facility	3		Wet	.71	.52	.42	.32	.29	.27
		4		Damp	.74	.62	.49	.44	.37	
		5		Damp	.74	.55	.49	.42	.39	.37
		6		Damp	.74	.59	.52	.44	.42	
6-20-83		41		Rain	.86	.70	.61	.51	.41	.29
6-20-83		42		Rain	.86	.77	.60	.56	.53	.44
6-20-83		43		Rain	.84	.70	.61	.56	.51	.44
6-14-83	Wallops	7	A	Wet	0.56	0.53	0.51			
	Flight	8	B, C					0.46	0.53	0.61
	Facility	8	A		.56	.41	.28			
		9	A				.51	.46	.41	
		9	B, C		.63	.58				
		10	B, C					.56	.53	.43
		10	A		.53	.36	.24			
6-20-83		40						.19	.15	.12
6-30-83		104						.18		
		106			.73	.34	.29			
		108				.39	.29			
		110			.69	.51	.24			
		112			.56	.46				
		113						.19		
		114							.12	
		115								.10
6-16-83		13	J-1						.36	.24
		13	J-2		1.08	.87	.70	.56		
		14	J-2					.53	.44	.36
		14	J-1		.75	.58	.53			
		15	J-1						.24	.12
		15	J-2		1.04	.87	.67	.53		
		16	J-2						.36	.30
		16	J-1		.70	.51	.41	.41		
		17	J-1					.41	.28	.18
		17	J-2		1.08	.90	.67			
		18	J-2						.36	.24
		18	J-1		.61	.49	.34	.36		
		19	J-1						.24	.15
		19	J-2		.95	.75	.61	.53		
		20	J-2						.36	.24
		20	J-1		.66	.46	.41	.36		
		21	J-1						.17	.12
		21	J-2		.92	.73	.58	.53		
		22	J-2						.49	.36
		22	J-1		.70	.57	.49	.46		

Table AV. Continued

(a) Concluded

Date	Test site	Run	Test surface		Average friction coefficient at test speed, mph, of—					
			Type	Wetness condition	10	20	30	40	50	60
6-22-83	Wallops	60	J-1	Wet						0.17
↓	Flight	61	J-2	↓						.22
	Facility	62	J-1							.15
		63	J-2	↓	0.94	0.78	0.70	0.61		
6-23-83	FAA	66	B	Wet	0.78	0.60	0.34			
↓	Technical	67	↓	↓		.55	.43	0.31		
	Center	68							0.15	
	↓	69								0.12
		70							.18	
		71						.15		
		72				.29	.39	.22		
		73				.54	.41	.31		
		74			.86	.77	.65	.39	.31	.25
		75			.88	.74	.51	.47	.39	.18
		76	↓		.96	.76	.66	.55	.25	.18
		64	C		.76	.70	.66	.61	.58	.47
↓	↓	65	D	↓	.76	.66	.61	.59	.54	.49
8-11-83	Wallops	4	A	Flooded	0.45	0.38	0.29	0.24		
	Flight	10	A	Flooded				.20	0.15	0.06
	Facility									

Table AV. Continued

(b) Mu-Meter

Date	Test site	Run	Test surface		Average friction coefficient at test speed, mph, of—					
			Type	Wetness condition	10	20	30	40	50	60
6-14-83	Wallops	1	SSA	Wet		0.80	0.78	0.74	0.74	
↓	Flight	2	↓	Wet		.82	.78	.74	.70	
	Facility	3		Wet		.83	.76	.74	.70	0.55
	↓	4		Damp		.79	.75	.80	.80	.75
		5		Damp		.83	.77	.77	.82	.74
↓		6		Damp		.81	.76	.81	.80	.76
6-21-83		75		Rain		.84	.86	.88	.83	
↓		76		Rain		.83	.84	.86	.86	
		77		Rain		.83	.83	.86	.85	
		81		Wet		.86	.84	.74	.68	.54
		82		↓		.86	.86	.84	.80	.70
		83				.86	.78	.73	.75	.60
↓	↓	84	↓	↓		.86	.85	.83	.82	
6-14-83	Wallops	12	A	Wet		0.73				
↓	Flight	12	B, C	↓		.75				
	Facility	13	A			.72				
	↓	13	B, C			.75				
		14	B, C			.82				
		14	A			.79				
		15	A				0.54			
		15	B, C				.76			
		16	B, C				.80			
↓		16	A				.68			
6-16-83		34	A					0.46		
↓		34	B, C					.75		
		35	B, C					.84		
		35	A					.54		
		36	A						0.44	
		36	B, C						.81	
		37	B, C						.80	
		37	A						.50	
		38	A							0.30
		38	B, C							.80
		39	A							.79
↓		39	B, C							.48
6-20-83		70	A			.70				
↓		70	B, C			.77				
		71	B, C				.83			
		71	A				.66			
		72	A					.25		
		72	B, C					.76		
		73	B, C						.84	
		73	A						.25	
		74	A							.07
↓	↓	74	B, C	↓						.60

Table AV. Continued

(b) Continued

Date	Test site	Run	Test surface		Average friction coefficient at test speed, mph, of—					
			Type	Wetness condition	10	20	30	40	50	60
6-30-83	Wallops	116	A	Wet		0.82				
	Flight	116	B, C			.81				
	Facility	117	B, C				0.85			
		117	A				.58			
		118	A					0.39		
		118	B, C					.83		
		119	B, C						0.83	
		119	A						.24	
		120	A							0.17
		120	B, C							.78
		[a]121	A			.88				
		[a]121	B, C			.88				
		[a]122	B, C				.89			
		[a]122	A				.66			
		[a]123	A					.48		
		[a]123	B, C					.86		
		[a]124	B, C						.89	
		[a]124	A						.30	
		[a]125	A							.28
		[a]125	B, C							.83
		[a]126	B, C							.84
		[a]126	A							.21
6-16-83		24	J-1			.75				
		24	J-2			.88				
		25	J-2			.89				
		25	J-1			.75				
		26	J-1				.66			
		26	J-2				.89			
		27	J-2				.92			
		27	J-1				.68			
		28	J-1					.52		
		28	J-2					.90		
		29	J-2					.91		
		29	J-1					.50		
		30	J-1						.34	
		30	J-2						.83	
		31	J-2						.84	
		31	J-1						.46	
		32	J-1							.30
		32	J-2							.86
		33	J-2							.86
		33	J-1							.34

[a]Tire inflation pressure = 30 lb/in^2.

Table AV. Continued

(b) Concluded

Date	Test site	Run	Test surface		Average friction coefficient at test speed, mph, of—					
			Type	Wetness condition	10	20	30	40	50	60
6-22-83	Wallops	100	J-1	Wet		0.76				
	Flight	100	J-2			.90				
	Facility	101	J-2				0.87			
		101	J-1				.64			
		102	J-1						0.32	
		102	J-2						.87	
		103	J-2							0.75
		103	J-1							.10
6-23-83	FAA	1	B	Wet		0.77				
	Technical	1	C			.80				
	Center	1	D			.80				
		2	D			.81				
		2	C			.80				
		2	B			.78				
		3	B				0.64			
		3	C				.80			
		3	D				.80			
		4	D				.81			
		4	C				.81			
		4	B				.70			
		5	B					0.40		
		5	C					.80		
		5	D					.80		
		6	D					.82		
		6	C					.80		
		6	B					.58		
		7	B						0.26	
		7	C						.80	
		7	D						.82	
		8	D						.82	
		8	C						.80	
		8	B						.30	
		9	B							0.15
		9	C							.80
		9	D							.82
		11	B			.77				
		12	B					.47		
		13	B							.24
8-11-83	Wallops	1	A	Flooded		0.65				
	Flight	2	A				0.32			
	Facility	3	A					0.13		
		4	A						0.05	

Table AV. Continued

(c) Surface friction tester

Date	Test site	Run	Test surface		Average friction coefficient at test speed, mph, of—					
			Type	Wetness condition	10	20	30	40	50	60
6-20-83	Wallops	12	SSA	Rain		0.98	0.97	0.96	0.90	0.80
	Flight	13	SSA	Rain		.98	.92	.90	.87	.70
	Facility	14	SSA	Rain		.92	.88	.86	.78	.65
		7	A	Wet		.72				
		7	B, C			.88				
		8	B, C				.94			
		8	A				.59			
		9	A					.29		
		9	B, C					.83		
		10	B, C						.89	
		10	A						.30	
		11	A							.07
		11	B, C							.62
6-22-83	Wallops	36	J-1	Wet		0.83				
	Flight	36	J-2			.97				
	Facility	37	J-2				0.95			
		37	J-1				.75			
		38	J-1						0.55	
		38	J-2						.83	
		39	J-2							0.63
		39	J-1							.30
6-23-83	FAA	1	B	Wet		0.78				
	Technical	1	C			.95				
	Center	1	D			.93				
		2	D			.93				
		2	C			.96				
		2	B			.82				
		3	B				0.60			
		3	C				.93			
		3	D				.90			
		4	D				.91			
		4	C				.93			
		4	B				.65			
		5	B					0.45		
		5	C					.92		
		5	D					.89		
		6	D					.93		
		6	C					.93		
		6	B					.50		
		7	B						0.20	

Table AV. Continued

(c) Concluded

Date	Test site	Run	Test surface		Average friction coefficient at test speed, mph, of—					
			Type	Wetness condition	10	20	30	40	50	60
6-23-83	FAA	7	C	Wet					0.90	
	Technical	7	D						.88	
	Center	8	D						.90	
		8	C						.91	
		8	B						.30	
		9	B							0.22
		9	C							.88
		9	D							.86
		10	D							.87
		10	C							.88
		10	B							.26
		11				0.85				
		12						0.55		
		13								.35
8-11-83	Wallops	1	A	Flooded		0.80				
	Flight	2					0.60			
	Facility	4						0.30		
		5							0.12	
		6								0.02
		7								.04

Table AV. Continued

(d) BV-11 skiddometer

Date	Test site	Run	Test surface		Average friction coefficient at test speed, mph, of—					
			Type	Wetness condition	10	20	30	40	50	60
6-20-83	Wallops	14	SSA	Rain		0.95	0.97	1.03	0.96	0.95
	Flight	15	SSA	Rain		.95	.93	1.04	.99	.83
	Facility	16	SSA	Rain		.90	.91	.95	.97	.75
		9	A	Wet		.83				
		9	B, C			1.01				
		10	B, C				1.00			
		10	A				.65			
		11	A					.33		
		11	B, C					.86		
		12	B, C						.92	
		12	A						.27	
		13	A							.18
		13	B, C							.60
6-22-83	FAA	39	J-1	Wet		0.82				
	Technical	39	J-2			1.05				
	Center	40	J-2				0.98			
		40	J-1				.65			
		41	J-1						0.36	
		41	J-2						.83	
		42	J-2							0.69
		42	J-1							.30
6-23-83	FAA	1	B	Wet		0.85				
	Technical	1	C			1.00				
	Center	1	D			.99				
		2	D			.97				
		2	C			.99				
		2	B			.85				
		3	B				0.58			
		3	C				.95			
		3	D				.94			
		4	D				.92			
		4	C				.95			
		4	B				.63			
		5	B					0.29		
		5	C					.93		
		5	D					.94		
		6	D					.93		
		6	C					.96		
		6	B					.36		
		7	B						0.15	
		7	C						.92	
		7	D						.90	

Table AV. Concluded

(d) Concluded

Date	Test site	Run	Test surface		Average friction coefficient at test speed, mph, of—					
			Type	Wetness condition	10	20	30	40	50	60
6-23-83	FAA	8	D	Wet					0.90	
	Technical	8	C						.91	
	Center	8	B						.17	
		9	B							0.06
		9	C							.88
		9	D							.89
		10	D							.89
		10	C							.92
		10	B							.16
		11				0.88				
		12						0.52		
		13								.16
8-11-83	Wallops	1	A	Flooded				0.34		
	Flight	2							0.07	
	Facility	3								0.01
		4						.36		

Table AVI. Ground-Vehicle Friction Data Obtained During Boeing 737 Tests at BNAS, March 1985

Surface condition	Run	Flt	Ambient temperature, °F	Speed, mph	Average friction coefficient for—					
					Mu-Meter	RCR	Tapley	BV-11	SFT	RFT
Loose, dry snow, 6 in.	2 to 5	430	23	20	Not	18	0.57	Not	Not	Not
				30	usable	10	.33	usable	available	available
				40	↓	7	.21	↓	↓	↓
				50		2	.06			
				60		0	0			
Loose, dry snow, 3 in.	3 to 5	431	30	20	Not	16	0.51	Not	Not	Not
				30	usable	23	.72	usable	available	available
				40	↓	14	.45	↓	↓	↓
				50		26	.84			
				60		30	.96			
New, wet snow, 1.5 in.	2, 3	432	38	20	0.11	16	0.51	0.19	Not	Not
				40	.04	23	.75	.19	available	available
Wet	None	None	41	20	0.80			0.82	Not	Not
				25		22	0.69		available	available
				40	.75			.84	↓	↓
				60	.65			.84		
1-in. slush	2R2, 3R2, 3R3	432	41	20		28	0.90		Not	Not
				40		22	.69		available	available
Glare ice	2 to 5	433	30	20	0.18	0	0	0.21	Not	Not
				30	.17	↓	↓	.17	available	available
				40	.17			.17	↓	↓
				50	.16			.15		

Table AVII. Empirical Runway Condition Factors for Boeing 737 Data

Wetness condition	Type or amount of wetness	Factor
Dry	None	0
Ice	0.25 in.	0.05
Wet Wet	Rain Truck	0.05 .05
Slush	≤1 in.	1.2
Snow ↓	1.5 in., wet 1 to 3 in., wet 1 to 3 in., dry 4 in., wet 4.5 in., wet 6 in., loose	1.5 2.5 3.0 4.5 5.0 3.5

C-2

Table AVIII. Aerodynamic and Geometric Data for Boeing 737 Brake Performance Data Reduction

Symbol	Description	Value
S	Aerodynamic reference area	980 ft^2
C_L	Lift coefficient, flaps 40°, spoilers up	0.242
C_D	Drag coefficient, flaps 40°, spoilers up	0.285
T_o	Idle thrust at Velocity = 0	2800 lb
DT/DV	Gradient of thrust versus velocity	−8 lb/knot
MUR	Rolling resistance coefficient	0.015
$CBAR$	Reference mean aerodynamic chord	134.46 in.
$(WL)_{cg}$	Center-of-gravity water line	206 in.
$(WL)_g$	Ground water line	106 in.
$(WL)_t$	Thrust-application water line	156 in.
$(BS)_{ng}$	Nose-gear balance station	286 in.
$(BS)_{mg}$	Main-gear balance station	698 in.
C_m	Pitching-moment coefficient	0.305
W	Weight (varies with condition)	≈80 000 lb
$(BS)_{cg}$	Center-of-gravity balance station (varies)	≈650 lb
$(BS)_{0.25c}$	Quarter-chord balance station	659.22 in.
K	Average percent of gross weight carried by main gear	89

Appendix B

Compilation of Boeing 727 Aircraft and Ground-Vehicle Test Data

The chronological test-run sequence for the 727 aircraft and the different ground vehicles is given in table BI for each test site. Test-runway surface conditions, temperature, and wind readings are also listed. Table BII provides a compilation by test site and run number of the 727 aircraft braking friction data. In this table, the aircraft gross weight, c.g. station, test-surface type and wetness condition, type of braking, and ground speed are given. The ground-vehicle friction data obtained on dry-runway test surfaces is listed by test site, surface type, and vehicle type in table BIII. Table BIV contains the ground-vehicle friction data obtained during wet-runway 727 aircraft braking test runs. The data are listed by vehicle type and test-surface type, with the aircraft test-run number and the elapsed time relative to the aircraft test run given for each ground-vehicle run. The average ground-vehicle friction coefficient values are listed in 10-mph increments up to 60 mph. Some supplemental ground-vehicle test runs were conducted on wet runway test surfaces without the test aircraft. These data are compiled in table BV by test-vehicle type, date, test site, and test-surface type and wetness condition. The ground-vehicle friction measurements obtained during 727 aircraft tests at BNAS and Pease AFB in March 1985 and January to March 1986 are listed in table BVI by surface condition. The appropriate aircraft flight and run numbers and the ambient temperatures are also given. The empirical runway condition factors used for 727 aircraft data reduction are given in table BVII. The aerodynamic and geometric data for the 727 test aircraft are listed in table BVIII for use with aircraft equations of balance.

Table BI. Boeing 727 Aircraft and Ground-Vehicle Test-Run Sequence Data

(a) Wallops Flight Facility

Date	Test vehicle	Run	Time of day, GMT	Test R/W	Test surface		Temperature, °F		Wind	
					Type	Wetness	Ambient	Surface	Deg	Knots
3-22-85	DBV	16	1825	10	SSA	Rain wet	42		070	20
	727	4A	1828							
	DBV	17	1831							
	DBV	18	1834							
	727	4B	1835						060	18
	DBV	19	1838	10	SSA	Rain wet				
	727	1	1844						070	74
	DBV	20	1848							
	727	4C	1850						060	18
	DBV	21	1853							
	DBV	22	1857	10	SSA	Rain wet				
	727	5	1902	10	SSA	Rain wet	43			20
	DBV	23	1904	10	SSA	Rain wet				
	DBV	24	1910	22	A, B	Rain wet				
	DBV	25	1913	04	A					
	DBV	26	1916	04	B, A					
	727	6	1917	22	A, B					16
	DBV	27	1919	22	A, B					
	DBV	28	1923	04	B, A	Rain wet				
	727	7	1926		B, A				070	18
	DBV	29	1930		A					
	DBV	30	1932		B					
4-18-85	Mu-M	1	2040	10	SSA	Wet	60		270	25
	BV-11	1	2041							
	SFT	1	2042							
	DBV	1	2044							
	727	1	2048							
	Mu-M	2	2049							
	BV-11	2	2050							
	SFT	2	2051							
	DBV	2	2052							
8-12-85	727	9	1434	10	SSA	Dry	87		050	8
	727	10	1445			Dry	83		070	6
	727	11	1459			Dry			090	10
	Mu-M	1	1533			Wet			080	
	BV-11		1533							
	SFT		1534							
	RFT		1534							
	DBV		1534							
	727	12	1536							

Table BI. Continued

(a) Continued

Date	Test vehicle	Run	Time of day, GMT	Test R/W	Test surface		Temperature, °F		Wind	
					Type	Wetness	Ambient	Surface	Deg	Knots
8-12-85	Mu-M	2	1538	10	SSA	Wet			080	
	BV-11		1538							
	SFT		1538							
	RFT		1538							
	DBV		1539							
	Mu-M	3	1551	10	SSA	Wet	81		110	8
	BV-11		1551							
	SFT		1552							
	RFT		1552							
	DBV		1552							
	727	13	1555							
	Mu-M	4	1557							
	BV-11		1557							
	SFT		1558							
	RFT		1558							
	DBV		1558							
8-13-85	727	1	0930	22	A	Dry	76		150	6
		2	0949	04	I		79		150	4
		3	1003	22	B, C		81		140	4
		R3	1026	22	B, C		81		150	6
		4	1039	04	H		80		190	8
		5	1052	22	A, B		80		170	8
		6	1100	04	B, A		81		180	6
		7	1107	22	A, B				190	6
		8	1118	04	B, A				170	8
		20	1128	22	A, B					4
	Mu-M	8	1313	04	B, A	Wet	82			10
	BV-11		1313							
	SFT		1313							
	RFT		1313							
	DBV	5	1315							
	727	15	1316							
	Mu-M	9	1317							
	BV-11		1317							
	SFT		1318							
	RFT		1318							
	Mu-M	10	1330	04	B, A	Wet	82		180	8
	BV-11	10	1330	04	B, A	Wet				
	SFT	10	1330	04	B, A	Wet				

Table BI. Continued

(a) Concluded

Date	Test vehicle	Run	Time of day, GMT	Test R/W	Test surface		Temperature, °F		Wind	
					Type	Wetness	Ambient	Surface	Deg	Knots
8-13-85	RFT	10	1330	04	B, A	Wet	82		180	8
↓	DBV	7	1331	↓	↓	↓				
	727	17	1332							
	Mu-M	11	1333							
	BV-11	↓	1333							
	SFT		1334							
	RFT		1334							
	DBV	8	1134							
	Mu-M	12	1343	22	A	Wet				12
	BV-11	↓	1343	↓	↓	↓				
	SFT		1343							
	RFT		1343							
	DBV	9	1343							
	727	18	1345							
	Mu-M	13	1347							
	BV-11	↓	1347							
	SFT		1347							
	RFT		1347							
↓	DBV	10	1347	↓	↓	↓				

Table BI. Continued

(b) FAA Technical Center

Date	Test vehicle	Run	Time of day, GMT	Test R/W	Test surface		Temperature, °F		Wind	
					Type	Wetness	Ambient	Surface	Deg	Knots
8-15-85	Mu-M	14	0738	13	C	Wet	80		240	6
↓	DBV	11	0738	↓	↓	↓				
	727	27	0740							
	Mu-M	15	0742							
	DBV	12	0742							
8-21-85	Mu-M	31	0723	13	C	Wet				
↓	SFT	31	0724	↓	↓	↓				
	727	R27	0725							
	Mu-M	32	0726							
	SFT	32	0728							
	Mu-M	33	0735	31	D	Wet				8
	SFT	33	0737	↓	↓	↓				
	727	28	0738							
	Mu-M	34	0739							
	SFT	34	0740							
	Mu-M	35	0743	31	D	Wet			040	6
	SFT	35	0746	↓	↓	↓				
	727	R28	0751							
	Mu-M	36	0752							
	SFT	36	0752							
	Mu-M	37	0800	31	B	Wet				9
	BV-11	37	0800	↓	↓	↓				
	SFT	37	0801							
	727	33	0809							
	Mu-M	38	0810				70		040	9
	BV-11	38	0810							
	SFT	38	0811							
	Mu-M	39	0829	13	B	Wet			020	6
	SFT	39	0830	↓	↓	↓				
	727	32	0831							
	Mu-M	40	0833							
↓	SFT	40	0834	↓	↓	↓				

Table BI. Continued

(b) Concluded

Date	Test vehicle	Run	Time of day, GMT	Test R/W	Test surface		Temperature, °F		Wind	
					Type	Wetness	Ambient	Surface	Deg	Knots
8-21-85	Mu-M	41	0840	13	B	Wet			030	5
	BV-11	41	0840							
	SFT	41	0840							
	727	31	0842							
	Mu-M	42	0843							
	BV-11	42	0843							
	SFT	42	0844							
	Mu-M	43	0844	31	B	Wet			010	8
	BV-11	43	0846							
	SFT	43	0846							
	727	30	0847							
	BV-11	44	0848							
	SFT	44	0848							
	Mu-M	44	0849							
	BV-11	45	0854	13			68		040	8
	Mu-M	45	0855							
	SFT	45	0857							
	727	29	0858							
	BV-11	46	0859							
	Mu-M	46	0859							
	SFT	46	0901							
8-22-85	727	21, 26	0858	13	C	Dry	64		350	7
		22, 26	0919	31	D				330	9
		23	0943	13	C				020	10
		24	0954	31	D				360	7
		25	1010	31	D				360	10

Table BI. Continued

(c) Brunswick Naval Air Station

Date	Test vehicle	Run	Time of day, GMT	Test R/W	Test surface		Temperature, °F		Wind	
					Type	Wetness	Ambient	Surface	Deg	Knots
3-27-85	Mu-M	1	1052	190	Asphalt	Slush	33		0	
	Mu-M	2	1054	010						
	Mu-M	2A	1057	010						
	BV-11	1	1059	190						
	BV-11	2	1101	010						
	727	[a]1	1102	190						
	Mu-M	3	1104	190						
	BV-11	3	1105	190						
	Mu-M	[a]4	1106	010						
	BV-11	4	1107	010						
	727	2	1109	010	Asphalt	Slush				
	Mu-M	5	1111	190						
	BV-11	5	1112	190						
	Mu-M	6	1116	010						
	BV-11	6	1118	010						
	Mu-M	4A	1120	010						
	727	[b]3	1121	010	Asphalt	Dry	34			
	727	4	1126	190		Damp				
	Mu-M	7	1128	190						
	BV-11	7	1129	190						
	Mu-M	8	1131	010						
	BV-11	8	1132	010						
	Mu-M	9	1134	190						
	BV-11	9	1135	190						
	727	[b]5	1136	010						
	Mu-M	10	1137	010	Asphalt	Damp				
	BV-11	10	1138	010						
	727	6	1146	190						
	Mu-M	11	1147	190						
	BV-11	11	1148	190						
	Mu-M	12	1149	010						
	BV-11	12	1150	010						
	727	7	1154	190						

[a]No data recorded.
[b]Inboard runway.

Table BI. Continued

(c) Continued

Date	Test vehicle	Run	Time of day, GMT	Test R/W	Test surface		Temperature, °F		Wind	
					Type	Wetness	Ambient	Surface	Deg	Knots
3-27-85	Mu-M	13	1535	010	Asphalt	Wet,	44		240	4
	BV-11	13	1536	010		0.01 in.				
	Mu-M	14	1538	190						
	BV-11	14	1539							
	B-727	8	1542							
	Mu-M	15	1543							
	BV-11	15	1544							
	Mu-M	16	1545	010						
	BV-11	16	1546	010						
	Mu-M	17	1604	010	Asphalt	Wet,			230	
	BV-11	17	1605	010		0.01 in.				
	727	9	1613	190						
	Mu-M	18	1614	190						
	BV-11	18	1615	190						
	Mu-M	19	1617	010						
	BV-11	19	1618	010						
	Mu-M	20	1632	010	Asphalt	Wet,	48		240	8
	BV-11	20	1633	010		0.01 in.				
	727	8R1	1638	190						
	Mu-M	21	1639	190						
	BV-11	21	1640	190						
	Mu-M	22	1641	010						
	BV-11	22	1642	010						
	727	10	1655	190	Asphalt	Damp			250	6
3-28-85	727	11	1540	190	Asphalt	Dry	55		310	6
	727	12	1554	010	Asphalt	Dry	58		300	12
	727	13	1604	010	Asphalt	Dry	62		310	7
4-10-85	[c]727	1	1602	070	PCC	Dry	40		270	6
	727	2	1613	070	PCC	Dry	40		270	6
1-28-86	727	1	1523	010	Asphalt	Wet snow,	31	16	340	4
	727	2	1536			1.5 in.			020	4
	BV-11	1	1543							
	RFT	1	1544							

[c]Langley Air Force Base.

Table BI. Continued

(c) Continued

Date	Test vehicle	Run	Time of day, GMT	Test R/W	Test surface		Temperature, °F		Wind	
					Type	Wetness	Ambient	Surface	Deg	Knots
1-28-86	SFT	1	1545	010	Asphalt	Wet snow,	31	14	020	4
	RCR	1	1546			1.5 in.				
	727	3	1549							
	BV-11	2	1552							
	RFT	2	1553							
	SFT	2	1555							
	RCR	2	1556							
	BV-11	3	1557	190	Asphalt	Wet snow,				
	RFT	3	1558			1.5 in.				
	SFT	3	1601							
	727	4	1604				28	12	340	8
	BV-11	4	1606							
	RFT	4	1608							
	SFT	4	1610							
	RCR	3	1610							
	BV-11	5	1611	010	Asphalt	Wet snow,				
	RFT	5	1612			1.5 in.				
	SFT	5	1613							
	RCR	4	1613							
	RCR	5	1615	190						
	RCR	6	1617	010						
	Mu-M	1	1621	190						
	RCR	7	1629	010						
	Mu-M	2	1630							
	BV-11	6	1630							
	RFT	6	1631							
	SFT	6	1632							
	RCR	8	1633							
	727	3A	1638	010	Asphalt	Wet snow,	28	12	330	8
	Mu-M	3	1639			1.5 in.				
	BV-11	7	1640							
	RFT	7	1641							
	SFT	7	1644							
	Mu-M	4	1645	190						
	SFT	8	1957	190	Asphalt	Packed	15			
	RFT	8	2000	190		snow				
	RCR	9	2001	190						
	SFT	9	2003	010						
	RCR	10	2004	010						
	RCR	11	2013	010						
	Mu-M	5	2014	190						
	SFT	10	2015	190						

Table BI. Continued

(c) Continued

Date	Test vehicle	Run	Time of day, GMT	Test R/W	Test surface		Temperature, °F		Wind	
					Type	Wetness	Ambient	Surface	Deg	Knots
1-28-86	Mu-M	6	2018	010	Asphalt	Packed				
	RCR	12	2019	010		snow				
	SFT	11	2019	010						
	Mu-M	7	2022	190						
	SFT	12	2023	190						
	RCR	13	2023	190						
	Mu-M	8	2026	010						
	SFT	13	2027	010						
	RCR	14	2027	010						
	Mu-M	9	2033	190	Asphalt	Packed				
	Mu-M	10	2037	010		snow				
	RFT	9	2043	010						
	RFT	10	2045	190						
	RFT	11	2051	190						
	RFT	12	2053	010						
1-29-86	BV-11	9	1415	190	Asphalt	Dry snow	13	10	270	8
	Mu-M	11	1419			on ice				
	SFT	14	1420							
	RCR	11	1424							
	RCR	12	1426	010						
	727	3	1430	190						
	BV-11	10	1436							
	Mu-M	12	1437							
	SFT	15	1437							
	RCR	13	1437							
	BV-11	11	1439	010	Asphalt	Dry snow			260	4
	Mu-M	13	1441			on ice				
	SFT	16	1442							
	RCR	14	1443							
	727	4	1444							
	BV-11	12	1450							
	Mu-M	14	1451							
	SFT	17	1452							
	RCR	15	1452							

Table BI. Continued

(c) Continued

Date	Test vehicle	Run	Time of day, GMT	Test R/W	Test surface		Temperature, °F		Wind	
					Type	Wetness	Ambient	Surface	Deg	Knots
1-29-86	Mu-M	15	1454	190	Asphalt	Dry snow			250	
	BV-11	13	1455			on ice				
	RCR	16	1455							
	SFT	18	1456							
	727	5	1500							
	BV-11	14	1503							
	Mu-M	16	1505							
	RCR	17	1506							
	SFT	19	1509							
	727	6	1513	190	Asphalt	Dry snow			260	5
	BV-11	15	1515			on ice			260	5
	Mu-M	17	1519				13	10	260	5
	RCR	18	1519							
	SFT	20	1520							
	BV-11	16	1521	010	Asphalt	Dry snow			0	
	Mu-M	18	1522			on ice				
	RCR	19	1522							
	SFT	21	1522							
	727	6R1	1523	190						
	BV-11	17	1526							
	Mu-M	19	1527							
	RCR	20	1527							
	SFT	22	1528							
	BV-11	18	1529	010	Asphalt	Dry snow				
	Mu-M	20	1530			on ice				
	RCR	21	1531							
	SFT	23	1532							
	727	6R2	1533							
	RCR	22	1538	190	Asphalt	Dry snow				
	727	5R	1540	190	Asphalt	on ice				
	727	7	1554	190	Asphalt				300	5
1-30-86	BV-11	19	1412	190	Asphalt	Dry snow	19	12	020	8
	Mu-M	21	1413			on ice				
	RCR	23	1415							
	SFT	24	1416							
	RCR	24	1420	010						
	SFT	25	1420							
	Mu-M	22	1422							
	BV-11	20	1424							
	BV-11	21	1425	190						
	Mu-M	23	1425	190						
	RCR	25	1426	196						

Table BI. Continued

(c) Continued

Date	Test vehicle	Run	Time of day, GMT	Test R/W	Test surface		Temperature, °F		Wind	
					Type	Wetness	Ambient	Surface	Deg	Knots
1-30-86	SFT	26	1426	190	Asphalt	Dry snow	19	12	020	8
	BV-11	22	1458	010	Asphalt	Urea on				
	Mu-M	24	1500			snow				
	SFT	27	1501							
	RCR	26	1502							
	BV-11	23	1503	190	Asphalt	Urea on				
	Mu-M	25	1504			snow				
	SFT	23	1506							
	RCR	27	1508							
	BV-11	24	1509	010	Asphalt	Urea on				
	Mu-M	26	1511			snow				
	SFT	29	1513							
	RCR	28	1513							
	727	1	1517							
	727	2	1532	010	Asphalt	Urea on			060	10
	727	2R	1545	010	Asphalt	snow			030	8
	727	2R2	1557	010	Asphalt				060	10
	727	4	1608	010	Asphalt	Urea on			020	8
	BV-11	25	1610	190		snow				
	Mu-M	27	1612							
	SFT	30	1614							
	RCR	29	1615							
	BV-11	26	1616	010	Asphalt	Urea on				
	Mu-M	28	1618			snow				
	SFT	31	1620							
	RCR	30	1620							
	BV-11	27	1621	190	Asphalt	Urea on				
	Mu-M	29	1622			snow				
	SFT	32	1624							
	RCR	31	1624							
2-18-86	727	1	1935	010	Asphalt	Loose snow,	27		050	6
		1R	1939	190		4.5 in.			050	6
		2	1943	010					040	6
		3	1948	190						5
		4	1955	010						5
		5	2020							5
		6	2054				28		050	6
		7	2105				28		040	5

Table BI. Continued

(c) Continued

Date	Test vehicle	Run	Time of day, GMT	Test R/W	Test surface		Temperature, °F		Wind	
					Type	Wetness	Ambient	Surface	Deg	Knots
2-18-86	BV-11	1	2058	010	Asphalt	Loose snow,				
	Mu-M		2102			4.5 in.				
	SFT		2103							
	RCR		2104							
	BV-11	2	2105	190	Asphalt	Loose snow,				
	Mu-M		2108			4.5 in.				
	SFT		2112							
	RCR		2113							
	Mu-M	3	2115	010	Asphalt	Loose snow,				
	SFT	3	2118	010	Asphalt	4.5 in.				
	RCR	3	2119	010	Asphalt					
	Mu-M	4	2121	190	Asphalt	Loose snow,				
	SFT	4	2124	190	Asphalt	4.5 in.				
	RCR	4	2125	190	Asphalt					
	Mu-M	5	2126	010	Asphalt	Loose snow,				
	SFT	5	2129	010	Asphalt	4.5 in.				
	RCR	5	2130	010	Asphalt					
	SFT	6	2133	190	Asphalt	Loose snow,				
	RCR	6	2134	190	Asphalt	4.5 in.				
2-19-86	BV-11	4	1519	190	Asphalt	Loose snow,		17	020	8
	SFT	7	1523			1.0 to 3.0 in.				
	RCR	7	1524							
	BV-11	5	1539							
	SFT	8	1543				28	17	020	8
	RCR	8	1544							
	BV-11	6	1546	010						
	SFT	9	1549							
	RCR	9	1550							
	727	3	1554							
	727	4	1600	190	Asphalt	Loose snow,			030	
		5	1614	010		1.0 to 3.0 in.			020	
		2	1620	190					030	
		1	1625	010					030	
		1R1	1629	190					030	
		1R2	1632	010					020	
	SFT	10	1641	190	Asphalt	Loose snow,	30			
	BV-11	7	1642	190		1.0 to 3.0 in.				
	RCR	10	1643	190						
	SFT	11	1645	010						
	BV-11	8	1646	010						
	RCR	11	1647	010						

Table BI. Continued

(c) Continued

Date	Test vehicle	Run	Time of day, GMT	Test R/W	Test surface		Temperature, °F		Wind	
					Type	Wetness	Ambient	Surface	Deg	Knots
2-19-86	SFT	12	1648	190	Asphalt	Loose snow,				
	BV-11	9	1651	190		1.0 to 3.0 in.				
	SFT	13	1652	010						
	BV-11	10	1653	010						
	SFT	14	1915	190	Asphalt	Loose snow,	33		360	6
	BV-11	11	1917	190		1 in.				
	RCR	12	1919	190						
	SFT	15	1920	010						
	BV-11	12	1921	010						
	RCR	13	1922	010						
	SFT	16	1924	190						
	BV-11	13	1925	190						
	RCR	14	1927	190						
	SFT	17	1928	010						
	BV-11	14	1929							
	RCR	15	1930							
	SFT	17R	1930				33		360	6
	SFT	18	1934	190						
	BV-11	15	1935	190						
	RCR	16	1936	190						
	SFT	19	1939	010						
	BV-11	16	1940	010						
	RCR	17	1941	010						
	SFT	20	2053	190						
	BV-11	17	2054	190						
	RCR	18	2055	190						
	SFT	21	2057	010	Asphalt	Loose snow,				
	BV-11	18	2058	010		1 in.				
	RCR	19	2059	010						
	SFT	22	2100	190						
	BV-11	19	2101	190						
	RCR	20	2102	190						
	SFT	23	1603	010						
	BV-11	20	1605	010						
	RCR	21	1606	010						
	SFT	24	1607	190						
	BV-11	21	1608	190						
	RCR	22	1609	190						
	SFT	25	1610	010						
	BV-11	22	1611	010						
	RCR	23	1613	010						

Table BI. Continued

(c) Continued

Date	Test vehicle	Run	Time of day, GMT	Test R/W	Test surface		Temperature, °F		Wind	
					Type	Wetness	Ambient	Surface	Deg	Knots
2-20-86	RFT	1	1340	190	Asphalt	Packed	28		050	4
	RCR	24	1341	190		snow on ice				
	RFT	2	1344	010						
	RCR	25	1345	010						
	727	3	1357	010						
	727	4	1402	190						
	727	5	1413	010					060	5
	BF-11	23	1420	190			30		060	5
	RFT	1R	1421							
	SFT	24	1422							
	RCR	26	1423							
	BV-11	24	1424	010						
	RFT	2R	1425							
	SFT	25	1426							
	RCR	27	1427							
	BV-11	25	1428	190	Asphalt	Packed				
	RFT	3	1429			snow on ice				
	SFT	26	1430							
	RCR	28	1431							
	BV-11	26	1432	010						
	RFT	4	1433							
	SFT	27	1434							
	RCR	29	1435							
	BV-11	27	1436	190	Asphalt	Packed	33			
	RFT	5	1437			snow on ice				
	SFT	28	1438							
	RCR	30	1439							
	BV-11	28	1440	010						
	RFT	6	1441							
	SFT	29	1442							
	RCR	31	1443							
	BV-11	29	1543	190	Asphalt	UCAR	40		120	6
	RFT	7	1544			applied				
	SFT	30	1545							
	RCR	32	1546							
	BV-11	30	1547	010						
	RFT	8	1548							
	SFT	31	1549							
	RCR	33	1550							

Table BI. Continued

(c) Continued

Date	Test vehicle	Run	Time of day, GMT	Test R/W	Test surface		Temperature, °F		Wind	
					Type	Wetness	Ambient	Surface	Deg	Knots
2-20-86	BV-11	31	1601	190	Asphalt	UCAR	40		120	6
	RFT	9	1602			applied				
	SFT	32	1603							
	RCR	34	1604				40		120	6
	BV-11	32	1605	010						
	RFT	10	1605							
	SFT	33	1606							
	RCR	35	1606							
	BV-11	33	1617	190	Asphalt	2nd UCAR				
	RFT	11	1617			application				
	SFT	34	1618							
	RCR	36	1618							
	BV-11	34	1620	010						
	RFT	12	1621							
	SFT	35	1623							
	RCR	37	1624							
	727	5R	1632	190	Asphalt	2nd UCAR				
	727	5R2	1649	010		application			160	5
	BV-11	35	1653	190						
	RFT	13	1654							
	SFT	36	1655							
	RCR	38	1655							
	BV-11	36	1656	010						
	RFT	14	1657							
	SFT	37	1658							
	RCR	39	1658							
	BV-11	37	1700	190	Asphalt	2nd UCAR				
	RFT	15	1701			application				
	SFT	38	1702							
	RCR	40	1702							
	BV-11	38	1703	010						
	RFT	16	1704							
	SFT	39	1705							
	RCR	41	1705							
	BV-11	39	1708	190	Asphalt	2nd UCAR				
	RFT	17	1709			application				
	SFT	40	1710							
	RCR	42	1710							

Table BI. Continued

(c) Continued

Date	Test vehicle	Run	Time of day, GMT	Test R/W	Test surface		Temperature, °F		Wind	
					Type	Wetness	Ambient	Surface	Deg	Knots
2-20-86	BV-11	40	1711	010	Asphalt	2nd UCAR application	40		160	5
	RFT	18	1712							
	SFT	41	1713							
	RCR	43	1715							
	BV-11	41	1910	010	Asphalt	UCAR on bare asphalt	42			
	RFT	19	1911							
	SFT	42	1912							
	RCR	44	1913							
	BV-11	42	1914							
	RFT	20	1915							
	SFT	43	1916							
	RCR	45	1917							
	BV-11	43	1918	010	Asphalt	UCAR on bare asphalt				
	RFT	21	1918							
	SFT	44	1919							
	RCR	46	1919							
	BV-11	44	1925							
	RFT	22	1925							
	SFT	45	1926							
	RCR	47	1926							
	RFT	23	1928	010	Asphalt	UCAR on bare asphalt				
	SFT	46	1929							
	RCR	48	1929							
	SFT	47	1932							
	RCR	49	1933							
3-19-86	SFT	1	1411	190	Asphalt	Rain wet			180	16
	[d]RFT	1	1411							
	Mu-M	1	1412							
	RCR	1	1412							
	SFT	2	1415	010						
	[d]RFT	2	1415							
	Mu-M	2	1416							
	RCR	2	1416							
	SFT	3	1420	190			42		180	16
	RFT		1420							
	Mu-M		1421							
	[d]RCR		1421							

[d]Tapley and Bowmonk meter readings.

Table BI. Continued

(c) Continued

Date	Test vehicle	Run	Time of day, GMT	Test R/W	Test surface		Temperature, °F		Wind	
					Type	Wetness	Ambient	Surface	Deg	Knots
3-19-86	SFT	4	1423	010	Asphalt	Rain	42		180	16
	RFT		1423			wet				
	Mu-M		1424							
	[d]RCR		1424							
	SFT	5	1427	190	Asphalt	Rain				
	RFT		1427			wet				
	Mu-M		1428							
	[d]RCR		1428							
	SFT	6	1431	010						
	RFT		1431							
	Mu-M		1432							
	[d]RCR		1432							
	727	1	1440	190	Asphalt	Rain	43			
	SFT	7	1449			wet				
	RFT	7	1449							
	Mu-M	7	1450							
	BV-11	1	1450							
	[d]RCR	7	1450							
	SFT	8	1452	010						
	RFT	8	1452							
	Mu-M	8	1453							
	BV-11	2	1453							
	[d]RCR	8	1454							
	727	2	1458	190	Asphalt	Rain	44			20
	SFT	9	1512			wet				
	RFT	9	1512							
	Mu-M	9	1513							
	BV-11	3	1513							
	[d]RCR	9	1514							
	SFT	10	1515	010						
	RFT	10	1515							
	Mu-M	10	1516				44		180	20
	BV-11	4	1516							
	[d]RCR	10	1517							
	BV-11	5	1518	190						
	BV-11	6	1519	010						

[d]Tapley and Bowmonk meter readings.

Table BI. Continued

(c) Continued

Date	Test vehicle	Run	Time of day, GMT	Test R/W	Test surface		Temperature, °F		Wind	
					Type	Wetness	Ambient	Surface	Deg	Knots
3-19-86	727	3	1520	190	Asphalt	Rain			190	16
↓	727	3R	1530	190	↓	wet				20
	BV-11	7	1531	190		↓				
	BV-11	8	1532	010	↓					
	727	[b]L1	2245	190	Asphalt	Damp	46			16
3-21-86	Mu-M	11	1100	190	Asphalt	Ice	4	10	350	10
↓	BV-11	↓	1100	↓	↓	↓				
	SFT		1101							
	RFT		1101							
	[d]RCR	↓	1101	↓						
	Mu-M	12	1104	010						
	BV-11	↓	1104	↓						
	SFT		1105							
	RFT		1105							
	[d]RCR	↓	1106	↓	↓	↓				
	Mu-M	13	1107	190	Asphalt	Ice				
	BV-11	↓	1107	↓	↓	↓				
	SFT		1107							
	RFT		1108							
	[d]RCR	↓	1108	↓						
	Mu-M	14	1109	010						
	BV-11	↓	1109	↓						
	SFT		1110							
	RFT		1110							
	[d]RCR	↓	1111	↓	↓	↓				
	Mu-M	15	1112	190	Asphalt	Ice				
	BV-11	↓	1112	↓	↓	↓				
	SFT		1113							
	RFT		1113							
	[d]RCR	↓	1114	↓						
	Mu-M	16	1115	010			4	10	350	10
	BV-11	↓	1115	↓						
	SFT		1116							
	RFT		1116							
↓	[d]RCR	↓	1116	↓	↓	↓				

[b]Inboard runway.
[d]Tapley and Bowmonk meter readings.

Table BI. Continued

(c) Continued

Date	Test vehicle	Run	Time of day, GMT	Test R/W	Test surface		Temperature, °F		Wind	
					Type	Wetness	Ambient	Surface	Deg	Knots
3-21-86	Mu-M	17	1119	190	Asphalt	Ice				
	BV-11		1119							
	SFT		1120							
	RFT		1120							
	[d]RCR		1121							
	Mu-M	18	1122	010						
	BV-11		1122							
	SFT		1123							
	RFT		1123							
	[d]RCR		1123							
	727	1	1127	010	Asphalt	Ice	5	15		
	727	2	1133	190					360	12
	727	3	1136	010					350	10
	727	4	1143	010						8
	Mu-M	19	1149	190	Asphalt	Ice	6			
	BV-11		1149							
	SFT		1150							
	RFT		1150							
	[d]RCR		1151							
	Mu-M	20	1152	010						
	BV-11		1152							
	SFT		1153							
	RFT		1153							
	[d]RCR		1153							
	Mu-M	21	1154	190	Asphalt	Ice	7	20	340	10
	BV-11		1154							
	SFT		1155							
	RFT		1155							
	[d]RCR		1156							
	727	5	1200	010						
	Mu-M	22	1202				7	20	340	10
	BV-11		1202							
	SFT		1203							
	RFT		1203							
	[d]RCR		1204							

[d]Tapley and Bowmonk meter readings.

Table BI. Continued

(c) Continued

Date	Test vehicle	Run	Time of day, GMT	Test R/W	Test surface		Temperature, °F		Wind	
					Type	Wetness	Ambient	Surface	Deg	Knots
3-21-86	Mu-M	23	1207	190	Asphalt	Ice				
	BV-11		1207							
	SFT		1208							
	RFT		1208							
	[d]RCR		1209							
	Mu-M	24	1214	010						
	BV-11		1214							
	SFT		1215							
	RFT		1215							
	[d]RCR		1216							
	Mu-M	25	1503	190	Asphalt	Slush	12	42		8
	BV-11		1503							
	SFT		1504							
	RFT		1504							
	[d]RCR		1505							
	Mu-M	26	1506	010						
	BV-11		1506							
	SFT		1507							
	RFT		1507							
	[d]RCR		1508							
	Mu-M	27	1520	190	Asphalt	UCAR application	15	48		
	BV-11		1520							
	SFT		1521							
	RFT		1521							
	[d]RCR		1522							
	Mu-M	28	1523	010						
	BV-11		1523							
	SFT		1524							
	RFT		1524							
	[d]RCR		1525							

[d]Tapley and Bowmonk meter readings.

Table BI. Continued

(c) Concluded

Date	Test vehicle	Run	Time of day, GMT	Test R/W	Test surface		Temperature, °F		Wind	
					Type	Wetness	Ambient	Surface	Deg	Knots
3-21-86	Mu-M	29	1534	190	Asphalt	UCAR				
	BV-11		1534			application				
	SFT		1535				15	48	340	8
	RFT		1535							
	[d]RCR		1536							
	Mu-M	30	1537	010						
	BV-11		1537							
	SFT		1538							
	RFT		1538							
	[d]RCR		1534							
	727	4	1546						010	6
	BV-11	31	1549	190	Asphalt	UCAR	19	59		
	SFT		1549			application				
	RFT		1550							
	[d]RCR		1550							
	BV-11	32	1552	010						
	SFT		1553							
	RFT		1553							
	[d]RCR		1554							

[d]Tapley and Bowmonk meter readings.

Table BI. Continued

(d) Pease Air Force Base

Date	Test vehicle	Run	Time of day, GMT	Test R/W	Test surface		Temperature, °F		Wind	
					Type	Wetness	Ambient	Surface	Deg	Knots
3-19-86	727	[e]P1	1719	110	PFC	Rain	44		190	16
	727	2	1753	160	PFC	wet	57		230	19
	Mu-M	1	2007	160	PFC	Rain	58		240	18
	BV-11		2007			wet				
	SFT		2008							
	RFT		2008							
	[d]RCR		2008							
	Mu-M	2	2009	340	PFC	Rain				
	BV-11		2009			wet				
	SFT		2010							
	RFT		2010							
	[d]RCR		2010							
	727	1	2011	160						
	Mu-M	3	2016							
	BV-11		2016							
	SFT		2017							
	RFT		2017							
	[d]RCR		2018							
	Mu-M	4	2019	340	PFC	Rain				12
	BV-11		2019			wet				
	SFT		2020							
	RFT		2021							
	[d]RCR		2022							
	727	2R	2033	160						
	Mu-M	5	2039							
	BV-11		2039							
	SFT		2040							
	RFT		2040							
	[d]RCR		2041							
	Mu-M	6	2043	340	PFC	Rain				15
	BV-11		2043			wet				
	RFT		2044							
	[d]RCR		2045							
	727	3	2057	160						
	Mu-M	7	2107				58		240	12
	BV-11		2107							
	RFT		2108							
	[d]RCR		2109							

[d]Tapley and Bowmonk meter readings.
[e]Portland International Jetport.

Table BI. Concluded

(d) Concluded

Date	Test vehicle	Run	Time of day, GMT	Test R/W	Test surface		Temperature, °F		Wind	
					Type	Wetness	Ambient	Surface	Deg	Knots
3-19-86	Mu-M	8	2110	340	PFC	Rain				
	BV-11		2110			wet				
	RFT		2111							
	[d]RCR		2112							
	Mu-M	9	2113	160	Asphalt	Rain				
	BV-11		2113		shoulder	wet				
	RFT		2114							
	[d]RCR		2114							
	Mu-M	10	2116	340						
	BV-11		2116							
	RFT		2117							
	[d]RCR		2117							
	SFT	6	2117	160	PFC	Rain				
	SFT	7	2125	340		wet				
	SFT	8	2126	160						
	SFT	9	2129	340						
	SFT	10	2130	160	Asphalt					
	SFT	11	2132	340	shoulder					

[d]Tapley and Bowmonk meter readings.

Table BII. Compilation of Boeing 727 Braking Friction Data by Test-Surface Type and Wetness Condition

(a) Wallops Flight Facility

Run	Flt	Test R/W	A/C gross weight, lb	A/C c.g. station	Test surface		Type of braking	Ground speed, knots	Effective braking friction coefficient
					Type	Wetness			
4A	3	10	132.5×10^3	892.0	SSA	Rain damp	Main	5	0.55
								10	.56
								15	.57
								20	.51
								25	.52
								30	.52
								35	.53
								40	.52
								45	.47
4B	3	10	131.6×10^3	891.6	SSA	Rain damp	Main	20	.44
								25	.52
								30	.48
								35	.44
								40	.44
								45	.53
								50	.49
								55	.45
								60	.48
								65	.49
								70	.39
								75	.35
4C	3	10	129.5×10^3	891.4	SSA	Rain damp	Main	20	.51
								25	.47
								30	.41
								35	.55
								40	.54
								45	.51
								50	.46
								55	.41
								60	.39
								65	.44
								70	.46
								75	.44
								80	.46

Table BII. Continued

(a) Continued

Run	Flt	Test R/W	A/C gross weight, lb	A/C c.g. station	Test surface		Type of braking	Ground speed, knots	Effective braking friction coefficient
					Type	Wetness			
5	3	10	126.5×10^3	892.8	SSA	Rain damp	Main	15	0.52
							and	20	.51
							nose	25	.50
								30	.48
								35	.45
								40	.42
								45	.45
								50	.49
								55	.49
								60	.49
								65	.49
								70	.47
								75	.44
1	8	10	128.4×10^3	891.4	SSA	Truck wet	Main	15	.45
								20	.53
								25	.46
								30	.46
								35	.41
								40	.48
								45	.40
								50	.39
								55	.42
								60	.41
								65	.37
								70	.34
								75	.36
								80	.38
								85	.33
								90	.33

Table BII. Continued

(a) Continued

Run	Flt	Test R/W	A/C gross weight, lb	A/C c.g. station	Test surface		Type of braking	Ground speed, knots	Effective braking friction coefficient
					Type	Wetness			
12	11	10	130.5×10^3	891.1	SSA	Truck wet	Main	25	0.44
								30	.44
								35	.53
								40	.50
								45	.49
								50	.45
								55	.44
								60	.43
								65	.40
								70	.42
								75	.41
								80	.44
								85	.43
								90	.36
								95	.35
13	11	10	127.1×10^3	891.7	SSA	Truck wet	Main	25	.48
							and	30	.47
							nose	35	.49
								40	.49
								45	.47
								50	.48
								55	.48
								60	.45
								65	.44
								70	.38
								75	.35
								80	.37
								85	.39
								90	.35

Table BII. Continued

(a) Continued

Run	Flt	Test R/W	A/C gross weight, lb	A/C c.g. station	Test surface		Type of braking	Ground speed, knots	Effective braking friction coefficient
					Type	Wetness			
9	11	10	139.3×10^3	890.6	SSA	Dry	Main	25	0.41
								30	.47
								35	.48
								40	.45
								45	.48
								50	.46
								55	.41
								60	.38
								65	.48
								70	.47
								75	.48
								80	.46
								85	.42
								90	.42
								95	.36
								100	.35
10	11	10	136.2×10^3	891.5	SSA	Dry	Main	30	.43
							and	35	.46
							nose	40	.45
								45	.42
								50	.44
								55	.47
								60	.46
								65	.45
								70	.43
								75	.43
								80	.42
								85	.39
								90	.38
								95	.40
								100	.36

Table BII. Continued

(a) Continued

Run	Flt	Test R/W	A/C gross weight, lb	A/C c.g. station	Test surface		Type of braking	Ground speed, knots	Effective braking friction coefficient
					Type	Wetness			
5	12	22	113.5×10^3	895.6	A	Dry	Main	45	0.53
								50	.52
								55	.55
								60	.55
								65	.54
6	12	4	113.3×10^3	895.7	A	Dry	Main	30	.49
								35	.50
								40	.47
								45	.49
7	12	22	111.8×10^3	895.9	A	Dry	Main	75	.51
							and	80	.50
							nose	85	.52
								90	.45
								95	.50
8	12	4	109.8×10^3	896.0	A	Dry	Main	25	.45
							and	30	.47
							nose	35	.47
								40	.43
								45	.44
								50	.42
								55	.41
								60	.39
7	3	4	122.9×10^3	892.2	A	Rain damp	Main	70	.45
								75	.42
6	3	22	124.7×10^3	891.8	A	Rain damp	Main	95	.19
								100	.21
								105	.17
17	12	4	131.9×10^3	891.2	A	Truck wet	Main	30	.25
								35	.24
								40	.23
								45	.23
								50	.22
								55	.21
								60	.15
								65	.12
								70	.11
								75	.10

Table BII. Continued

(a) Concluded

Run	Flt	Test R/W	A/C gross weight, lb	A/C c.g. station	Test surface		Type of braking	Ground speed, knots	Effective braking friction coefficient
					Type	Wetness			
5	12	22	113.5×10^3	895.5	B	Dry	Main	25	0.60
								30	.57
								35	.56
								40	.57
6	12	4	113.3×10^3	895.6	B	Dry	Main	50	.45
								55	.44
								60	.46
								65	.42
7	12	22	111.8×10^3	895.9	B	Dry	Main	50	.43
							and	55	.45
							nose	60	.47
								65	.46
								70	.48
8	12	4	109.8×10^3	896.0	B	Dry	Main	65	.53
							and	70	.53
							nose	75	.52
								80	.47
								85	.47
7	3	4	122.7×10^3	892.2	B	Rain wet	Main	80	.50
								85	.49
								90	.48
6	3	22	124.9×10^3	891.8	B	Rain wet	Main	85	.35
								90	.29
15	12	4	134.8×10^3	891.8	B	Truck wet	Main	25	.43
								30	.46
								35	.40
								40	.43
								45	.41
								50	.38
								55	.34
18	12	22	129.5×10^3	891.4	B	Truck wet	Main	50	.41
								55	.40
								60	.39
								65	.38
								70	.36
								75	.30
								80	.30
								85	.30
								90	.29
								95	.24

Table BII. Continued

(b) FAA Technical Center

Run	Flt	Test R/W	A/C gross weight, lb	A/C c.g. station	Test surface		Type of braking	Ground speed, knots	Effective braking friction coefficient
					Type	Wetness			
29	14	13	118.9×10^3	892.9	B	Truck wet	Main	26	0.30
								31	.29
								36	.29
								41	.28
30	14	31	118.9×10^3	892.9	B	Truck wet	Main	45	.27
								50	.27
31	14	13	119.9×10^3	892.7	B	Truck wet	Main	70	.27
								75	.20
32	14	13	122.0×10^3	892.3	B	Truck wet	Main	75	.29
31	14	13	119.9×10^3	892.7	C	Dry	Main	80	.42
32	14	13	122.0×10^3	892.3	C	Dry	Main	80	.45
23	15	13	124.1×10^3	893.2	C	Dry	Main	20	.41
								25	.45
								30	.44
								35	.50
								40	.51
								45	.48
								50	.49
								55	.47
								60	.47
								65	.47
								70	.46
								75	.50
								80	.49
								85	.46
								90	.45
27R	14	13	130.9×10^3	892.2	C	Truck wet	Main	55	.43
								60	.42
								65	.43
								70	.41
								75	.44
								80	.41
								85	.37
								90	.36
								95	.35
								100	.37

Table BII. Continued

(b) Concluded

Run	Flt	Test R/W	A/C gross weight, lb	A/C c.g. station	Test surface		Type of braking	Ground speed, knots	Effective braking friction coefficient
					Type	Wetness			
24R	15	31	122.3×10^3	893.4	D	Dry	Main	30	0.49
								35	.50
								40	.48
								45	.45
								50	.43
								55	.41
								60	.48
								65	.47
								70	.46
								75	.45
								80	.44
								85	.43
25	15	31	120.6×10^3	897.2	D	Dry	Main	20	.49
							and	25	.53
							nose	30	.56
								35	.53
								40	.51
								45	.50
								50	.49
								55	.49
								60	.48
								65	.46
								70	.46
								75	.46
								80	.45
								85	.44
								90	.41
28	14	31	128.6×10^3	891.4	D	Truck wet	Main	95	.27
								100	.26
								105	.25
28R	14	31	126.3×10^3	892.8	D	Truck wet	Main	35	.43
								40	.42
								45	.46
								50	.43
								55	.41
								60	.42
								65	.47
								70	.40
								75	.42
								80	.41
								85	.43
								90	.37
								95	.36

Table BII. Continued

(c) Brunswick Naval Air Station

Run	Flt	Test R/W	A/C gross weight, lb	A/C c.g. station	Test surface		Type of braking	Ground speed, knots	Effective braking friction coefficient
					Type	Wetness			
2	4	1	126.3×10^3	892.8	Asphalt	Slush	Main	25	0.37
								30	.25
								35	.35
								40	.45
								45	.36
								50	.30
								55	.32
4	4	19	123.0×10^3	892.0	Asphalt	Damp	Main	35	.38
								40	.31
								45	.16
								50	.22
								55	.22
								60	.26
6	4	19	122.3×10^3	893.4	Asphalt	Damp	Main	30	.42
								35	.38
								40	.41
								45	.40
								50	.36
								55	.34
								60	.31
								65	.36
								70	.34
								75	.29
								80	.24
								85	.29
8	5	19	129.5×10^3	891.7	Asphalt	Truck wet	Main	35	.36
								40	.36
								45	.35
								50	.34
								55	.33
								60	.35
								65	.35
								70	.30
								75	.31
								80	.29
								85	.32
								90	.31
								95	.26

Table BII. Continued

(c) Continued

Run	Flt	Test R/W	A/C gross weight, lb	A/C c.g. station	Test surface		Type of braking	Ground speed, knots	Effective braking friction coefficient
					Type	Wetness			
9	5	19	124.8×10^3	892.0	Asphalt	Truck wet	Main	25	0.38
							and	30	.38
							nose	35	.36
								40	.37
								45	.35
								50	.32
								55	.34
								60	.42
								65	.41
								70	.39
								75	.36
								80	.35
								85	.29
								90	.41
								95	.40
8R1	5	19	121.1×10^3	892.6	Asphalt	Truck wet	Main	20	.40
								25	.42
								30	.40
								35	.43
								40	.41
								45	.38
								50	.36
								55	.39
								60	.36
								65	.42
								70	.38
								75	.34
								80	.32
								85	.32
11	6	19	134.9×10^3	891.9	Asphalt	Dry	Main	20	.45
								25	.42
								30	.40
								35	.49
								40	.48
								45	.44
								50	.40
								55	.36
								60	.47
								65	.43
								70	.42
								75	.52
								80	.51
								85	.43
								90	.42

Table BII. Continued

(c) Continued

Run	Flt	Test R/W	A/C gross weight, lb	A/C c.g. station	Test surface		Type of braking	Ground speed, knots	Effective braking friction coefficient
					Type	Wetness			
12	6	1	131.6×10^3	892.2	Asphalt	Dry	Main	35	0.51
							and	40	.49
							nose	45	.45
								50	.42
								55	.43
								60	.52
								65	.50
								70	.47
								75	.47
								80	.44
								85	.41
								90	.38
3	19	1	128.2×10^3	891.5	Asphalt	Wet snow,	Main	25	.07
						1.5 in.		30	.07
								35	.07
								40	.07
								45	.08
								50	.09
								55	.09
								60	.09
4	19	19	127.7×10^3	891.6	Asphalt	Wet snow,	Main	30	.11
						1.5 in.		35	.11
								40	.12
								45	.10
								50	.10
								55	.10
								60	.10
								65	.10
3R1	19	1	123.6×10^3	892.2	Asphalt	Wet snow,	Main	30	.08
						1.5 in.		35	.08
								40	.09
								45	.10
								50	.11
								55	.10
3	20	19	129.1×10^3	891.5	Asphalt	Dry snow on ice	Main	28	.14
								33	.14
								38	.13
								43	.15

Table BII. Continued

(c) Continued

Run	Flt	Test R/W	A/C gross weight, lb	A/C c.g. station	Test surface		Type of braking	Ground speed, knots	Effective braking friction coefficient
					Type	Wetness			
4	20	1	128.2×10^3	891.4	Asphalt	Dry snow on ice	Main	27	0.13
								32	.12
								37	.13
								42	.14
								47	.14
								52	.14
								57	.13
								62	.14
5	20	19	125.2×10^3	891.8	Asphalt	Dry snow on ice	Main	30	.13
								35	.13
								40	.15
								45	.14
								50	.15
								55	.11
								60	.14
								65	.15
								70	.16
								75	.18
								80	.16
								85	.12
								90	.16
5R1	20	19	121.9×10^3	892.3	Asphalt	Dry snow on ice	Main	30	.12
								35	.14
								40	.13
								45	.13
								50	.13
								55	.12
								60	.12
								65	.13
								70	.16
								75	.14
								80	.17
								85	.15
								90	.15
1	21	1	129.3×10^3	891.7	Asphalt	Urea on ice	Main	30	.06
								35	.07
								40	.07
								45	.08
								50	.11
								55	.13
								60	.10

Table BII. Continued

(c) Continued

Run	Flt	Test R/W	A/C gross weight, lb	A/C c.g. station	Test surface		Type of braking	Ground speed, knots	Effective braking friction coefficient
					Type	Wetness			
2	21	1	127.1×10^3	892.1	Asphalt	Urea on ice	Main	55	0.15
								60	.12
								65	.10
								70	.07
								75	.03
								80	.04
								85	.03
								90	.01
								95	.01
2R2	21	1	123.4×10^3	892.0	Asphalt	Urea on ice	Main	35	.10
								40	.11
								45	.13
								50	.13
								55	.12
								60	.11
								65	.12
								70	.13
								75	.12
								80	.09
								85	.09
								90	.12
4	21	1	121.5×10^3	892.6	Asphalt	Urea on ice	Main	40	.14
								45	.12
								50	.11
								55	.10
								60	.12
								65	.14
								70	.13
								75	.12
								80	.13
								85	.11
3	22	19	121.9×10^3	983.5	Asphalt	Loose snow, 4.5 in.	Main	30	.11
								35	.11
								40	.10
								45	.11
								50	.12
								55	.11

Table BII. Continued

(c) Continued

Run	Flt	Test R/W	A/C gross weight, lb	A/C c.g. station	Test surface		Type of braking	Ground speed, knots	Effective braking friction coefficient
					Type	Wetness			
4	22	1	121.6×10^3	984.1	Asphalt	Loose snow, 4.5 in.	Main	25	0.11
								30	.12
								35	.13
								40	.14
								45	.15
								50	.15
								55	.14
								60	.13
5	22	1	117.5×10^3	894.9	Asphalt	Loose snow, 4.5 in.	Main	25	.12
								30	.14
								35	.15
								40	.15
								45	.15
								50	.15
								55	.15
								60	.16
								65	.16
								70	.16
								75	.16
								80	.15
								85	.15
3	23	1	133.7×10^3	891.8	Asphalt	Loose snow, 1.0 to 3.0 in.	Main	25	.08
								30	.09
								35	.10
								40	.12
								45	.13
								50	.12
								55	.11
4	23	19	133.0×10^3	892.1	Asphalt	Loose snow, 1.0 to 3.0 in.	Main	30	.10
								35	.10
								40	.11
								45	.11
								50	.11
								55	.11
								60	.11
								65	.10

Table BII. Continued

(c) Continued

Run	Flt	Test R/W	A/C gross weight, lb	A/C c.g. station	Test surface		Type of braking	Ground speed, knots	Effective braking friction coefficient
					Type	Wetness			
5	23	1	130.5×10^3	891.9	Asphalt	Loose snow, 1.0 to 3.0 in.	Main	35	0.08
								40	.11
								45	.13
								50	.12
								55	.11
								60	.11
								65	.12
								70	.13
								75	.14
								80	.15
								85	.14
3	24	1	127.2×10^3	892.3	Asphalt	Loose snow, 1 in.	Main	30	.14
								35	.15
								40	.15
								45	.16
								50	.16
4	24	19	126.8×10^3	892.7	Asphalt	Loose snow, 1 in.	Main	25	.13
								30	.14
								35	.14
								40	.14
								45	.14
								50	.13
								55	.14
								60	.14
5	24	1	124.9×10^3	893.6	Asphalt	Loose snow, 1 in.	Main	50	.18
								55	.16
								60	.16
								65	.13
								70	.18
								75	.20
								80	.18
3	25	1	135.3×10^3	891.1	Asphalt	Packed snow on ice	Main	30	.14
								35	.15
								40	.18
								45	.20
								50	.21
								55	.19

Table BII. Continued

(c) Continued

Run	Flt	Test R/W	A/C gross weight, lb	A/C c.g. station	Test surface		Type of braking	Ground speed, knots	Effective braking friction coefficient
					Type	Wetness			
4	25	19	134.8×10^3	891.9	Asphalt	Packed snow on ice	Main	25	0.16
								30	.17
								35	.19
								40	.19
								45	.19
								50	.18
								55	.18
								60	.18
5	25	1	133.2×10^3	891.8	Asphalt	Packed snow on ice	Main	30	.16
								35	.17
								40	.19
								45	.19
								50	.19
								55	.19
								60	.19
								65	.20
								70	.20
								75	.19
								80	.19
								85	.19
								90	.18
								95	.17
5R1	25	19	131.3×10^3	892.2	Asphalt	UCAR on snow/ice	Main	25	.14
								30	.16
								35	.18
								40	.18
								45	.19
								50	.19
								55	.19
								60	.18
								65	.18
								70	.17
5R2	25	1	128.3×10^3	892.0	Asphalt	UCAR on snow/ice	Main	50	.17
								55	.14
								60	.19
								65	.18
								70	.15
								75	.12
								80	.10
								85	.12

Table BII. Continued

(c) Continued

Run	Flt	Test R/W	A/C gross weight, lb	A/C c.g. station	Test surface		Type of braking	Ground speed, knots	Effective braking friction coefficient
					Type				
1	26	19	132.7×10^3	893.6	Asphalt	Rain wet	Main	40	0.42
								45	.39
								50	.34
								55	.32
								60	.33
								65	.34
								70	.31
								75	.28
								80	.29
2	26	19	129.4×10^3	984.7	Asphalt	Rain wet	Main	40	.26
								45	.28
								50	.29
								55	.30
								60	.30
L1	27	19	115.0×10^3	895.1	Asphalt	Rain wet	Main and nose with reverse	25	.04
								30	.04
								35	.04
								40	.04
								45	.05
								50	.08
								55	.10
								60	.12
								65	.13
								70	.14
								75	.10
								80	.06
								85	.03
								90	.00
								95	.01
								100	.04
								105	.09
1	28	1	131.6×10^3	895.2	Asphalt	Ice	Main and nose	15	.06

Table BII. Continued

(c) Concluded

Run	Flt	Test R/W	A/C gross weight, lb	A/C c.g. station	Test surface		Type of braking	Ground speed, knots	Effective braking friction coefficient
					Type	Wetness			
2	28	19	131.2×10^3	895.3	Asphalt	Ice	Main	40	0.06
								45	.05
								50	.04
								55	.03
								60	.00
3	28	1	130.7×10^3	894.4	Asphalt	Ice	Main	55	.02
								60	.01
								65	.02
								70	.04
								75	.02
4	28	1	130.1×10^3	895.5	Asphalt	Ice	Main	65	.02
								70	.02
								75	.03
								80	.05
								85	.05
1	29	19	126.4×10^3	896.0	Asphalt	UCAR on ice	Main	15	.07
							and	20	.07
							nose		
4	29	1	125.9×10^3	896.0	Asphalt	UCAR on ice	Main	25	.33
								30	.32
								35	.32
								40	.36
								45	.32
								50	.34
								55	.27
								60	.33
								65	.29
								70	.26
								75	.27
								80	.29
								85	.27

Table BII. Continued

(d) Langley Air Force Base

Run	Flt	Test R/W	A/C gross weight, lb	A/C c.g. station	Test surface		Type of braking	Ground speed, knots	Effective braking friction coefficient
					Type	Wetness			
1	7	7	125.6×10^3	896.0	PCC	Dry	Main	20	0.47
								25	.46
								30	.15
								35	.44
								40	.55
								45	.48
								50	.50
								55	.46
								60	.48
								65	.45
								70	.46
								75	.43
								80	.42

(e) Portland International Jetport

Run	Flt	Test R/W	A/C gross weight, lb	A/C c.g. station	Test surface		Type of braking	Ground speed, knots	Effective braking friction coefficient
					Type	Wetness			
P1	27	11	135.3×10^3	896.2	PFC	Rain wet	Main	35	0.36
								40	.40
								45	.39
								50	.33
								55	.33
								60	.33
								65	.36
								70	.32
								75	.33
								80	.32
								85	.29
								90	.34
								95	.31
								100	.22

Table BII. Concluded

(f) Pease Air Force Base

Run	Flt	Test R/W	A/C gross weight, lb	A/C c.g. station	Test surface		Type of braking	Ground speed, knots	Effective braking friction coefficient
					Type	Wetness			
2	27	16	130.0×10^3	894.0	PFC	Rain wet	Main	40	0.45
								45	.42
								50	.43
								55	.43
								60	.39
								65	.41
								70	.44
								75	.42
								80	.41
								85	.42
								90	.41
								95	.40
								100	.39
1	27	16	128.6×10^3	894.4	PFC	Rain wet	Main	25	.43
								30	.43
								35	.42
								40	.46
								45	.41
								50	.41
								55	.37
								60	.40
								65	.43
								70	.40
								75	.40
								80	.37
								85	.34
2R1	27	16	125.4×10^3	895.9	PFC	Rain wet	Main	40	.43
								45	.43
								50	.43
								55	.41
								60	.38
								65	.42
								70	.44
								75	.43
								80	.42
								85	.41
								90	.40
								95	.39

Table BIII. Ground-Vehicle Dry-Surface Friction Data Obtained at Wallops Flight Facility and FAA Technical Center

[Includes friction data obtained during previous tests]

Test site	Test surface	Speed, mph	Average friction coefficient				
			Mu-Meter	BV-11	SFT	RFT	DBV
Wallops	SSA	10					0.67
		20				0.87	.54
		30					.59
		40	0.81	0.90		.78	.72
		50					.76
		60	.81			.74	.76
Wallops	A	10	0.81				0.81
		20	.88	1.08	0.99	0.90	.78
		30	.88				.87
		40	.90	1.01	.98	.83	.92
		50	.89				.95
		60	.90	.96	.96	.80	.87
Wallops	B	10					0.80
		20	0.87	1.08	0.99	0.96	.73
		30	.87				.77
		40	.89	1.04	.98	.87	.84
		50	.88				.86
		60	.91	.98	.98	.83	.84
FAATC	B	10					0.78
		20	0.78	0.98	0.98	0.85	.60
		30					.60
		40	.78	.99	.88	.78	.66
		50					.76
		60	.77	.98	.82	.73	.78
FAATC	C	10					0.80
		20	0.84	0.99	0.99	0.97	.74
		30					.74
		40	.85	.98	.99	.90	.72
		50					.83
		60	.86	.97	.96	.86	.83
FAATC	D	10					0.94
		20	0.88	0.98	0.99		.83
		30					.83
		40	.89	.99	.93		.83
		50					.83
		60	.90	.96	.88		.74

Table BIV. Ground-Vehicle Friction Data Obtained During Wet-Surface Boeing 727 Test Runs at Wallops Flight Facility and FAA Technical Center

(a) Diagonal-braked vehicle

A/C run	Vehicle run	Time from A/C run, min[a]	Test speed, mph	Average friction coefficient					
				Wallops			FAA Technical Center		
				SSA[b]	A[b]	B[b]	B	C	D
4A	16	−3	10	0.90					
↓	↓	↓	20	.80					
			30	.76					
			40	.68					
			50	.58					
	↓	↓	60	.46					
	17	+3	10	.92					
	↓	↓	20	.82					
			30	.70					
			40	.58					
			50	.48					
↓	↓	↓	60	.44					
4B	18	−1	10	.94					
↓	↓	↓	20	.82					
			30	.72					
			40	.62					
			50	.54					
	↓	↓	60	.42					
	19	+3	10	.86					
	↓	↓	20	.78					
			30	.70					
			40	.60					
			50	.48					
↓	↓	↓	60	.42					
4C	20	−2	10	.90					
↓	↓	↓	20	.80					
			30	.72					
			40	.64					
			50	.58					
	↓	↓	60	.44					
	21	+3	10	.92					
	↓	↓	20	.84					
			30	.76					
			40	.60					
			50	.52					
↓	↓	↓	60	.44					

[a]Minus sign denotes time before A/C run; plus sign denotes time after A/C run.
[b]Rain-damp data.

Table BIV. Continued

(a) Continued

A/C run	Vehicle run	Time from A/C run, min[a]	Test speed, mph	Average friction coefficient					
				Wallops			FAA Technical Center		
				SSA[b]	A[b]	B[b]	B	C	D
5	22	−3	10	0.92					
↓	↓	↓	20	.84					
			30	.72					
			40	.60					
			50	.52					
			60	.44					
	23	+2	10	.90					
	↓	↓	20	.80					
			30	.70					
			40	.62					
			50	.56					
↓	↓	↓	60	.44					
6	24	−7	10			0.68			
↓	↓	↓	20			.60			
			30			.54			
			40		0.24				
			50		.20				
	26	−1	10		.54				
	↓	↓	20		.38				
			30		.30				
			40			.48			
			50			.44			
			60			.44			
	27	+2	10			.68			
	↓	↓	20			.58			
			30		.38				
			40		.30				
↓	↓	↓	50		.20				
7	28	−3	10			.64			
↓	↓	↓	20			.60			
			30			.58			
			40			.54			
↓	↓	↓	50			.48			

[a]Minus sign denotes time before A/C run; plus sign denotes time after A/C run.
[b]Rain-damp data.

Table BIV. Continued

(a) Continued

A/C run	Vehicle run	Time from A/C run, min[a]	Test speed, mph	Average friction coefficient					
				Wallops			FAA Technical Center		
				SSA	A	B	B	C	D
7	29	+4	10		[b]0.58				
			20		.40				
			30		.34				
			40		.30				
	30	+6	10			[b]0.68			
			20			.58			
			30			.56			
			40			.54			
18	9	−2	50		.10				
	9	−2	55		.08				
	9	−2	60		.10				
	10	+2	55		.10				
	10	+2	50		.12				
27	11	−2	10					0.76	
			20					.66	
			30					.58	
			40					.46	
			50					.46	
			60					.42	
	12	+2	10					.76	
			20					.68	
			30					.62	
			40					.56	
			50					.50	
			60					.48	
12	1	−2	10	0.84					
			20	.78					
			30	.66					
			40	.58					
			50	.50					
			60	.34					
	2	+3	10	.84					
			20	.76					
			30	.70					
			40	.60					
			50	.50					
			60	.44					

[a]Minus sign denotes time before A/C run; plus sign denotes time after A/C run.
[b]Rain-damp data.

Table BIV. Continued

(a) Concluded

A/C run	Vehicle run	Time from A/C run, min[a]	Test speed, mph	Average friction coefficient					
				Wallops			FAA Technical Center		
				SSA	A	B	B	C	D
13	3	−3	10	0.88					
			20	.80					
			30	.72					
			40	.56					
			50	.42					
			60	.36					
	4	+3	10	.90					
			20	.80					
			30	.72					
			40	.64					
			50	.54					
			60	.50					
15	5	−1	30			0.48			
			35			.46			
			40			.42			
			45			.40			
			50			.42			
			55			.40			
			60			.38			
17	7	−1	40			.40			
			45			.38			
			50			.36			
			55			.40			
			60			.40			
	8	+2	30			.52			
			35			.46			
			40			.42			
			45			.40			
			50			.38			
			55			.40			
			60			.36			

[a]Minus sign denotes time before A/C run; plus sign denotes time after A/C run.

Table BIV. Continued

(b) Mu-Meter

A/C run	Vehicle run	Time from A/C run, min[a]	Test speed, mph	Average friction coefficient					
				Wallops			FAA Technical Center		
				SSA	A	B	B	C	D
12	1	−3	20	0.72					
↓	↓	↓	30	.71					
			40	.63					
			50	.57					
	↓	↓	60	.42					
	2	+2	20	.70					
	↓	↓	30	.70					
			40	.68					
			50	.65					
↓	↓	↓	60	.60					
13	3	−4	20	.73					
↓	↓	↓	30	.71					
			40	.65					
			50	.56					
	↓	↓	60	.38					
	4	+2	20	.68					
	↓	↓	30	.69					
			40	.66					
			50	.68					
↓	↓	↓	60	.63					
15	8	−3	40		0.35	0.65			
15	9	+1			.38	.65			
17	10	−2			.35	.65			
17	11	+1			.35	.66			
18	12	−2			.29				
18	13	+2			.33				
27	14	−2						0.69	
27	15	+2						.69	
R27	31	−2						.75	
R27	32	+1						.74	
28	33	−3							0.75
28	34	+1							.75
R28	35	−8							.74
R28	36	+1							.75

[a]Minus sign denotes time before A/C run; plus sign denotes time after A/C run.

Table BIV. Continued

(b) Concluded

A/C run	Vehicle run	Time from A/C run, min[a]	Test speed, mph	Average friction coefficient					
				Wallops			FAA Technical Center		
				SSA	A	B	B	C	D
33	37	−9					0.68		
33	38	+1					.73		
32	39	−2					.65		
32	40	+2					.63		
31	41	−2					.63		
31	42	+1					.61		
30	43	−3					.70		
30	44	+2					.74		
29	45	−3					.61		
29	46	+1					.57		

[a]Minus sign denotes time before A/C run; plus sign denotes time after A/C run.

Table BIV. Continued

(c) Surface friction tester

A/C run	Vehicle run	Time from A/C run, min[a]	Test speed, mph	Average friction coefficient					
				Wallops			FAA Technical Center		
				SSA	A	B	B	C	D
12	1	−2	20	0.98					
			30	.93					
			40	.86					
			50	.78					
			60	.73					
	2	+2	20	.98					
			30	.94					
			40	.88					
			50	.85					
			60	.83					
13	3	−3	20	.98					
			30	.92					
			40	.88					
			50	.82					
			60	.72					
	4	+3	20	.97					
			30	.94					
			40	.94					
			50	.90					
15	8	−3	40		0.42	0.76			
15	9	+2			.47	.81			
17	10	−2			.52	.83			
17	11	+2			.42	.80			
18	12	−2			.63	.90			
18	13	+2			.62	.86			
R27	31	−1						0.95	
R27	32	+3						.97	
28	33	−1							0.98
28	34	+2							.96
R28	35	−5							.97
R28	36	+1							.98
33	37	−8					0.85		
33	38	+2					.93		
32	39	−1					.86		
32	40	+3					.88		

[a]Minus sign denotes time before A/C run; plus sign denotes time after A/C run.

Table BIV. Continued

(c) Concluded

A/C run	Vehicle run	Time from A/C run, min[a]	Test speed, mph	Average friction coefficient					
				Wallops			FAA Technical Center		
				SSA	A	B	B	C	D
31	41	−2					0.83		
31	42	+2					.88		
30	43	−1					.90		
30	44	+1					.93		
29	45	−1					.87		
29	46	+3					.93		

[a]Minus sign denotes time before A/C run; plus sign denotes time after A/C run.

Table BIV. Continued

(d) BV-11 skiddometer

A/C run	Vehicle run	Time from A/C run, min[a]	Test speed, mph	Average friction coefficient					
				Wallops			FAA Technical Center		
				SSA	A	B	B	C	D
12	1	−3	20	0.98					
↓	↓	↓	30	.97					
			40	.95					
			50	.84					
	↓	↓	60	.83					
	2	+2	20	.98					
	↓	↓	30	.97					
			40	.97					
			50	.95					
↓	↓	↓	60	.95					
13	3	−4	20	.98					
↓	↓	↓	30	.95					
			40	.86					
			50	.83					
	↓	↓	60	.86					
	4	+2	20	.98					
	↓	↓	30	.97					
			40	.94					
			50	.92					
↓	↓	↓	60	.88					
15	8	−3	40		0.57	0.88			
15	9	+1			.62	.84			
17	10	−2			.55	.87			
17	11	+1			.65	.88			
18	12	−2			.51				
18	13	+2			.61				
33	37	−9					0.62		
33	38	+1					.75		
31	41	−2					.52		
31	42	+1					.58		
30	43	−1					.57		
30	44	+1					.61		
29	45	−4					.53		
29	46	+1					.50		

[a]Minus sign denotes time before A/C run; plus sign denotes time after A/C run.

Table BIV. Concluded

(e) Runway friction tester

A/C run	Vehicle run	Time from A/C run, min[a]	Test speed, mph	Average friction coefficient					
				Wallops			FAA Technical Center		
				SSA	A	B	B	C	D
12	1	−2	20	0.83					
↓	↓	↓	30	.76					
			40	.70					
			50	.67					
	↓	↓	60	.55					
	2	+2	20	.84					
	↓	↓	30	.82					
			40	.78					
			50	.74					
↓	↓	↓	60	.62					
13	3	−3	20	.79					
↓	3	−3	30	.74					
	3	−3	40	.68					
	4	+3	20	.83					
	↓	↓	30	.82					
			40	.77					
↓	↓	↓	50	.75					
15	8	−3	40		0.48	0.72			
15	9	+2			.49	.74			
17	10	−2			.57	.74			
17	11	+2			.48	.74			
18	12	−2			.42				
18	13	+2			.42				

[a]Minus sign denotes time before A/C run; plus sign denotes time after A/C run.

Table BV. Supplemental Ground-Vehicle Friction Data Obtained on Different Test Surfaces Under Truck-Wet Conditions

Test vehicle	Test speed, mph	Average friction coefficient					
		Wallops			FAA Technical Center		
		SSA	A	B	B	C	D
Mu-Meter	10						
↓	20	0.72	0.72	0.80	0.73	0.69	0.72
	30	.70	.60	.78			
	40	.68	.26	.76	.70	.69	.71
	50	.63	.25	.73			
	60	.58	.13	.70	.62	.69	.68
BV-11	10						
↓	20	0.94	0.83	1.01	0.89	0.98	0.97
	30	.82	.65	1.00			
	40	.76	.33	.89	.47	.97	.93
	50	.72	.27	.92			
	60	.65	.18	.60	.20	.93	.91
SFT	10						
↓	20	0.96	0.72	0.88	0.94	0.98	0.93
	30	.93	.59	.94			
	40	.88	.49	.90	.70	.90	.85
	50	.80	.30	.89			
	60	.70	.07	.62	.45	.88	.80
RFT	20				0.79	0.91	0.85
RFT	40	0.69			.56	.84	.80
RFT	60	.59			.35	.76	
DBV	10	0.84	0.56	0.72	0.78	0.81	0.80
↓	20	.77	.47	.64	.70	.78	.70
	30	.69	.40	.60	.52	.63	.65
	40	.58	.30	.52	.32	.54	.60
	50	.45	.15	.48	.22	.50	.53
	60	.35	.12	.46	.13	.43	.50

Table BVI. Ground-Vehicle Friction Data Obtained During Boeing 727 Tests at BNAS and Pease AFB, March 1985 and January to March 1986

Surface condition	Run	Flt	Ambient temperature, °F	Speed, mph	Average friction coefficient for —					
					Mu-Meter	RCR	Tapley	BV-11	SFT	RFT
Wet snow, 1.5 in.	3, 4	19	31	20	0.23	10	0.33	0.24	0.23	0.33
				40	.17	11	.36	.22	.24	.30
				54	.17	12	.39			
				60		14	.45	.26	.24	.27
Packed snow on ice	None	None	28	20	0.22	7	0.21	Not	0.25	0.33
				40	.16	7	.22	available	.24	.28
				60	.15	8	.24		.24	.29
Dry snow on ice	3, 4, 5, 5R1	20	13	20	0.23	8	0.24	0.29	0.31	Not
				30	.23	8	.24	.31	.29	available
				40	.22	8	.24	.30	.32	
				50	.21	9	.30	.30	.30	
				60	.19	11	.36	.32	.31	
Dry snow on ice	None	None	18	20	0.20	6	0.18	0.14	0.04	Not
				40	.17	5	.15	.18	.09	available
				60	.19	5	.15	.22	.15	
Urea on ice, 15 min	None	None	19	20	0.18	8	0.27	0.15	0.11	Not
				40	.18	8	.24	.18	.11	available
				50				.22	.12	
				60	.18	7	.21		.13	
Urea on ice, 90 min	1, 2, 2R2, 4	21	19	20	0.27	9	0.30	0.21	0.17	Not
				40	.22	7	.21	.25	.21	available
				50	.26			.35		
				60		8	.24		.18	
Urea on ice, 60 min	None	None	28	20	Not	22	0.36	0.29	0.13	Not
				40	available	15	.48	.09	.10	available
				60		18	.57		.10	

Table BVI. Continued

Surface condition	Run	Flt	Ambient temperature, °F	Speed, mph	Average friction coefficient for --					
					Mu-Meter	RCR	Tapley	BV-11	SFT	RFT
Loose dry, snow, 2 in.	3, 4, 5	23	33	20	0.09	13	0.39	0.12	0.13	Not available
				40	.07	16	.48	.14	.10	
				60	.06	19	.57	.15	.10	
Packed snow on ice	3, 4, 5	25	28	20	Not available	15	0.45	0.20	0.23	0.31
				40		16	.48	.25	.25	.29
				60		17	.51	.26	.23	.26
UCAR on ice, 60 min	5R1, 5R2	25	41	20	Not available	14	0.42	0.24	0.21	0.27
				40		16	.48	.27	.23	.26
				60		17	.51	.25	.20	.24
UCAR on asphalt	None	None	42	20	Not available	21	0.63	Not available	0.20	0.65
				30		28	.84		.30	.66
				40		29	.87		.25	.69
				50		30	.90		.62	.69
				60					.60	.64
Dry asphalt	11, 12	6	42	20	Not available	28	0.84	Not available	0.70	1.08
				30		29	.87		.75	1.03
				40		32	.96		.75	.98
				50		32	.96		.78	.95
				60					.75	.93
Rain wet, 0.04 to 0.06 in., Rate = 0.06 in/hr	1, 2, L1	26	42	20	0.78	23	0.69	0.83	0.91	0.85
				40	.73	20	.60	.75	.88	.80
				60	.69	25	.75	.61	.75	.70
Rain damp PFC at Peace AFB	1, 2, 2R1	27	58	20	0.77	29	0.87	0.99	0.94	0.85
				40	.72	25	.75	.92		.80
				60	.72	25	.75	.85	.81	.70
Rain damp shoulder at Pease AFB	None	None	58	40	0.65	31	0.93	0.88	0.88	0.68

Table BVI. Concluded

Surface condition	Run	Flt	Ambient temperature, °F	Speed, mph	Average friction coefficient for—					
					Mu-Meter	RCR	Tapley	BV-11	SFT	RFT
Solid ice	1 to 4	28	5	5	0.14	4	0.12	0.16	0.18	0.11
				20	.19	4	.12	.20	.18	.15
				30	.19	5	.15	.18	.17	.15
				40	.17	6	.18	.15	.17	.14
				50	.19	7	.21	.17	.17	.13
				60	.18	8	.24	.13	.15	.14
UCAR on ice, 30 min	1, 4	29	15	40	0.29	13	0.42	0.34	0.42	0.39
0.25-in. slush	1, 2	4	33	20	0.66	Not available	Not available	0.70	Not available	Not available
				40	.41			.41		
				60	.50			.39		
Truck wet	8, 9	5	44	40	0.80	Not available	Not available	0.83	Not available	Not available
Dry asphalt	11, 12	6	60	20	0.84	Not available	Not available	0.95	Not available	Not available
				40	.85			.89		
				60	.84			.84		

Table BVII. Empirical Runway Condition Factors for Boeing 727 Data

Wetness condition	Type or amount of wetness	Factor
Dry	None	0
Ice	0.25 in.	0
Ice	UCAR	0
Ice	Urea	0
Wet	Rain	0.05
Wet	Truck	.05
Damp	≤0.01 in.	0.1
Slush	≤1 in.	0.5
Snow	Packed/ice	0.5
↓	1 in., loose	3.0
	1.5 in., wet	1.0
	1.5 in., loose	2.0
	1 to 3 in., dry	4.5
	4.5 in., dry	4.0

Table BVIII. Aerodynamic and Geometric Data for Boeing 727 Brake Performance Data Reduction

Symbol	Description	Value
S	Aerodynamic reference area	1560 ft^2
C_L	Lift coefficient, flaps 30°, spoilers up	0.140
C_D	Drag coefficient, flaps 30°, spoilers up	0.253
T_o	Idle thrust at Velocity = 0	2400 lb
DT/DV	Gradient of thrust versus velocity	−10.5 lb/knot
MUR	Rolling resistance coefficient	0.015
$CBAR$	Reference mean aerodynamic chord	180 in.
$(WL)_{cg}$	Center-of-gravity water line	209 in.
$(WL)_g$	Ground water line	89 in.
$(WL)_t$	Thrust-application water line	237 in.
$(BS)_{ng}$	Nose-gear balance station	311 in.
$(BS)_{mg}$	Main-gear balance station	951 in.
C_m	Pitching-moment coefficient	Assume 0
W	Weight (varies with condition)	≈130 000 lb
$(BS)_{cg}$	Center-of-gravity balance station (varies)	≈893 in.
$(BS)_{0.25c}$	Quarter-chord balance station	905.20 in.
C_L	Lift coefficient, flaps 15°, spoilers down	0.440
C_D	Drag coefficient, flaps 15°, spoilers down	0.109
K	Average percent of gross weight carried by main gear	91

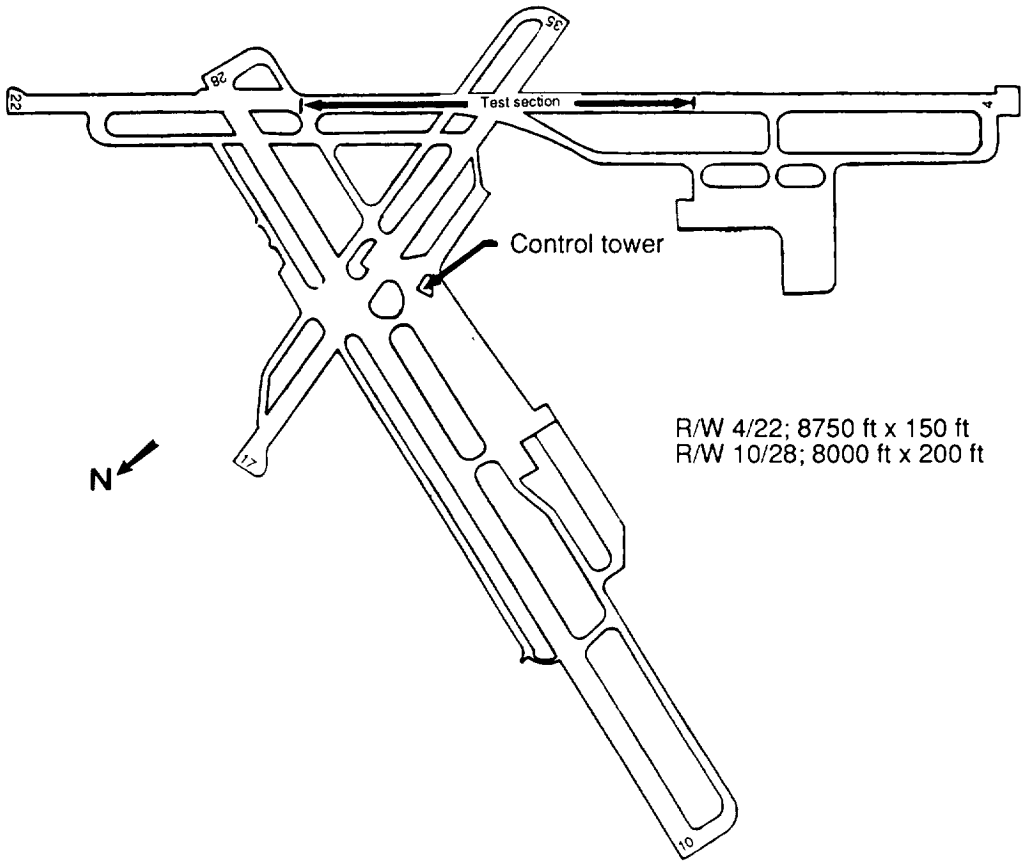

Figure 1. Schematic of runways at Wallops Flight Facility.

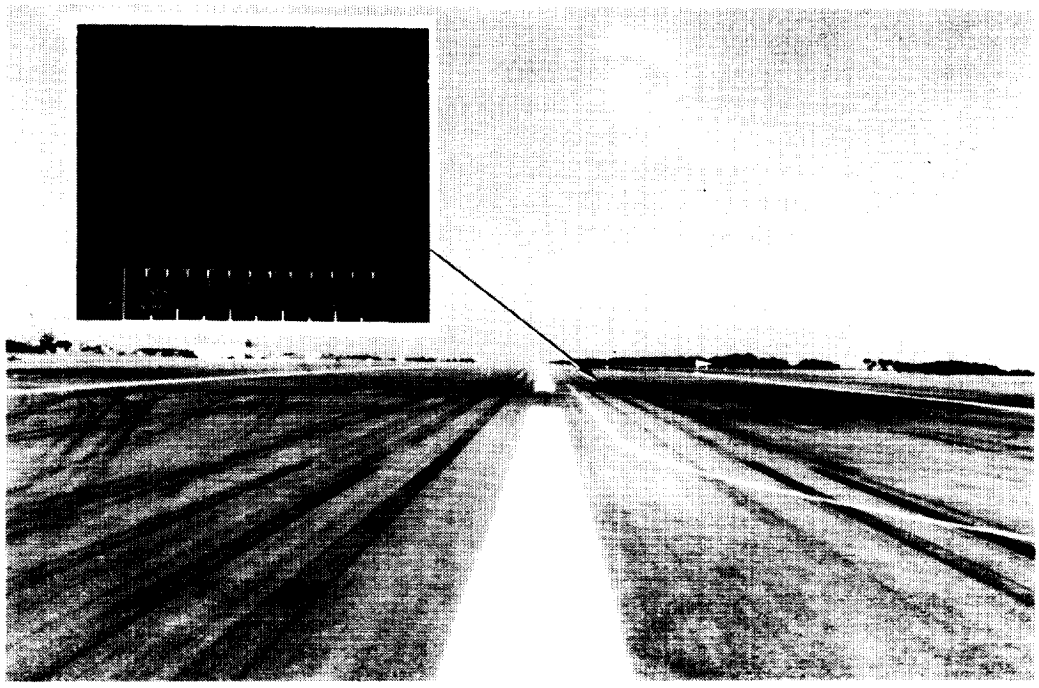

L-89-57

Figure 2. Runway 10/28 at Wallops Flight Facility.

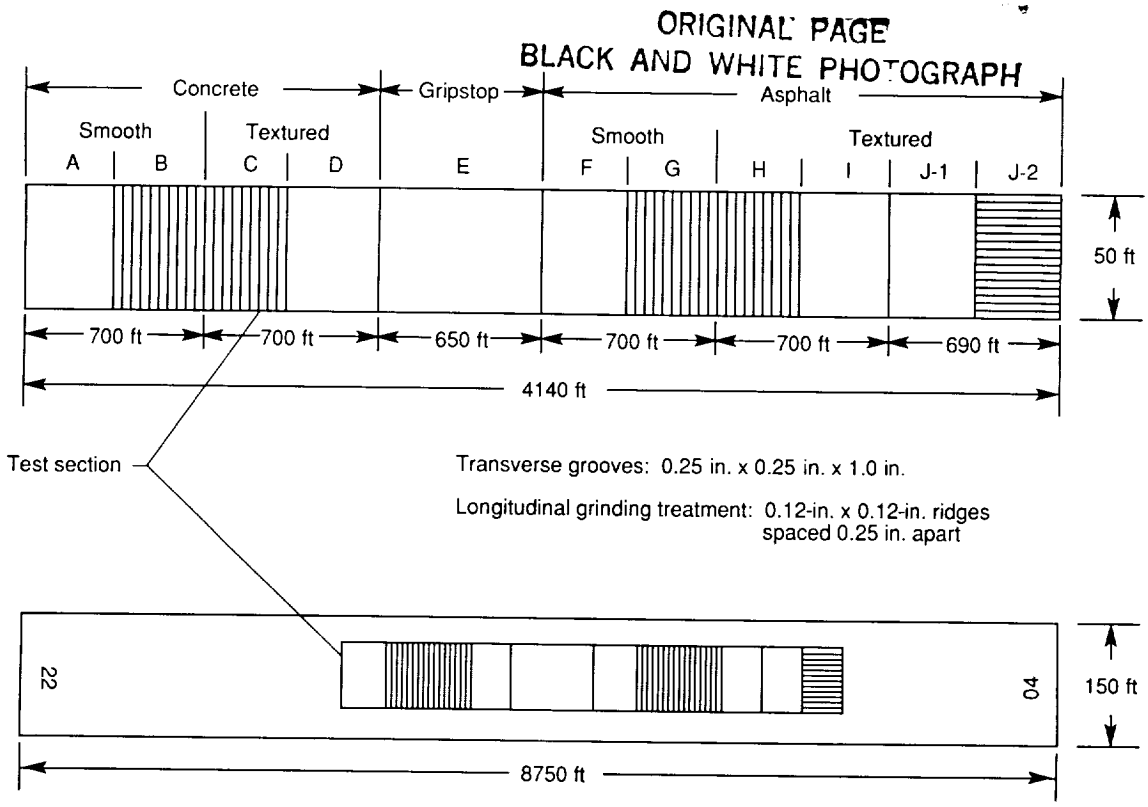

Figure 3. Schematic of runway 4/22 test surfaces at Wallops Flight Facility.

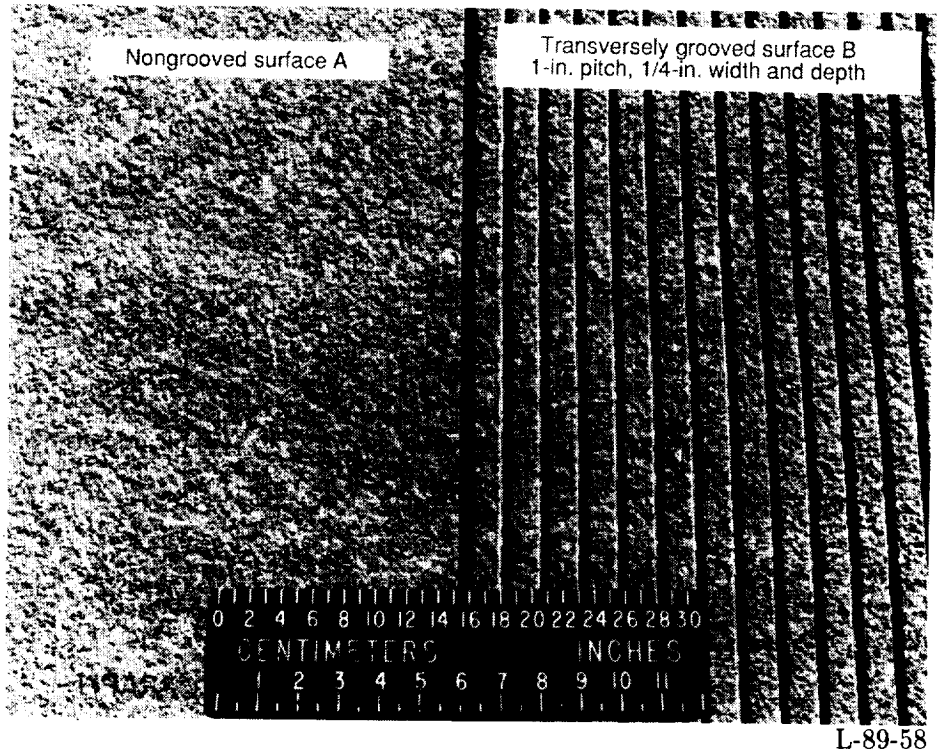

Figure 4. Close-up photographs of concrete test surfaces A (nongrooved) and B (transversely grooved, 1 in. × 0.25 in. × 0.25 in.) on runway 4/22 at Wallops Flight Facility.

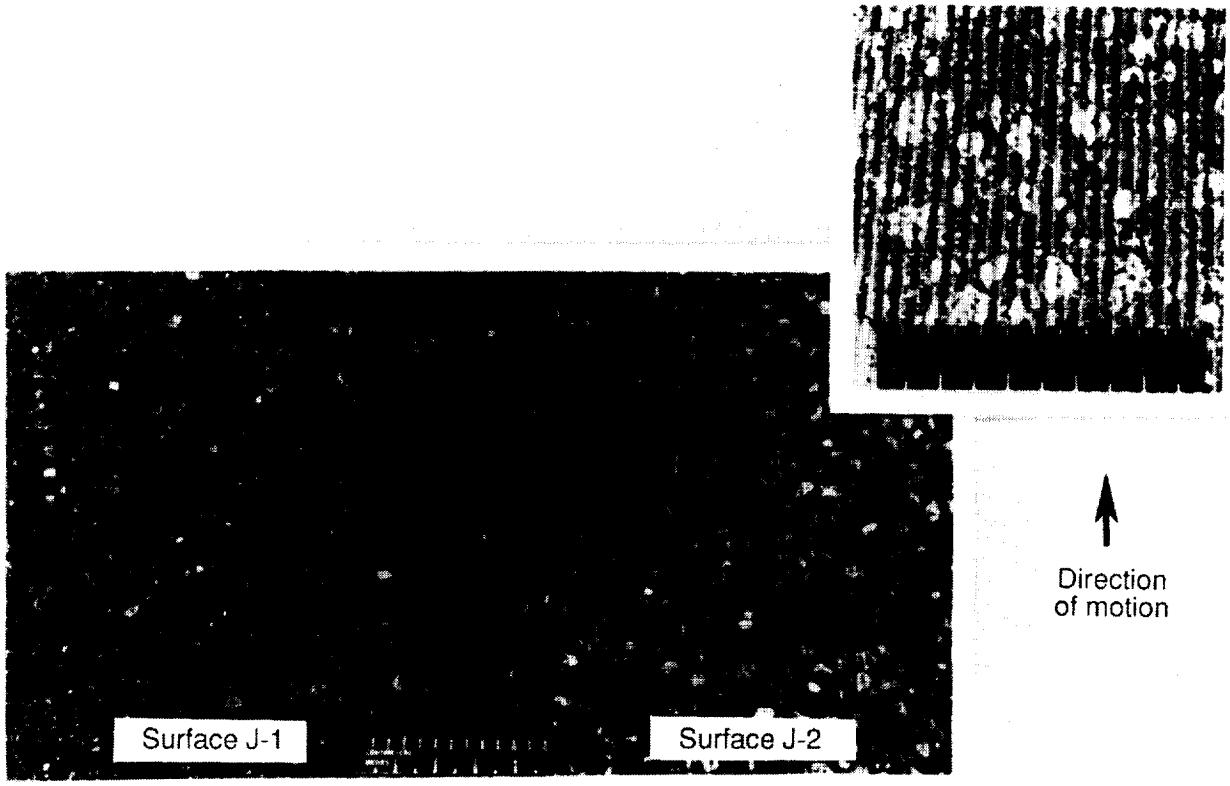

L-89-59

Figure 5. New asphalt test surfaces J-1 and J-2 on runway 4/22.

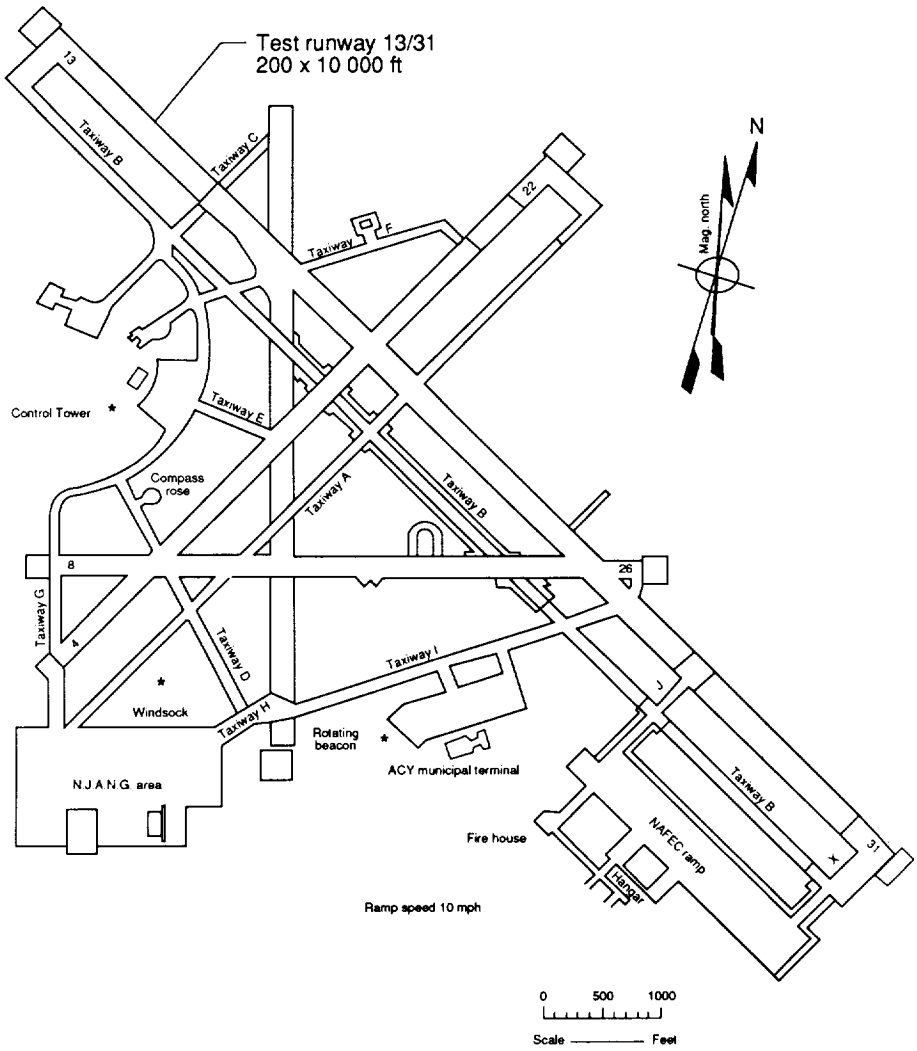

Figure 6. Runway layout at FAA Technical Center airport.

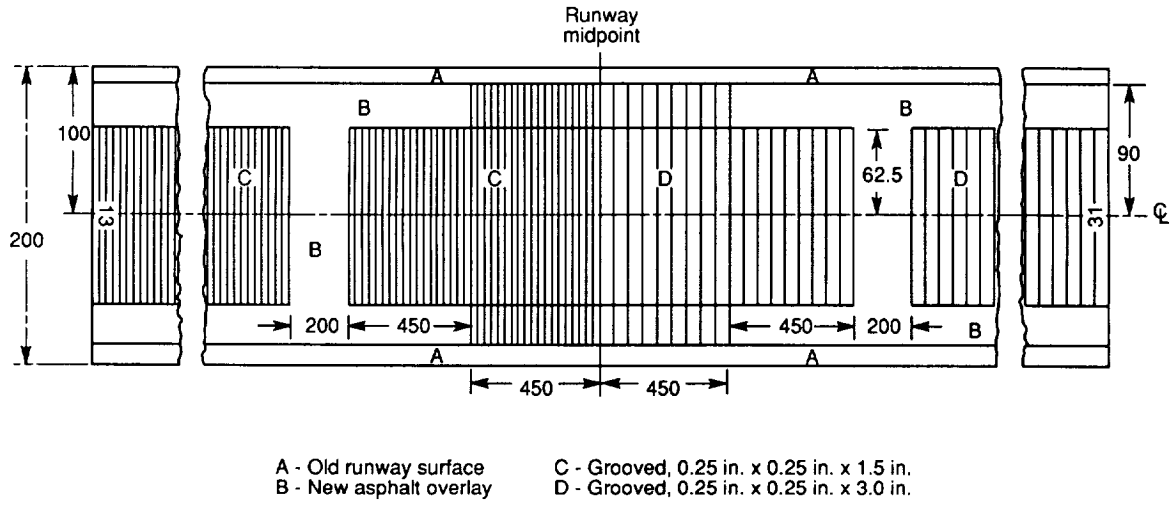

Figure 7. FAA Technical Center airport runway 13/31 test surfaces. All dimensions are in ft; drawing not to scale; surfaces C and D extend approximately 3900 ft to each end of runway.

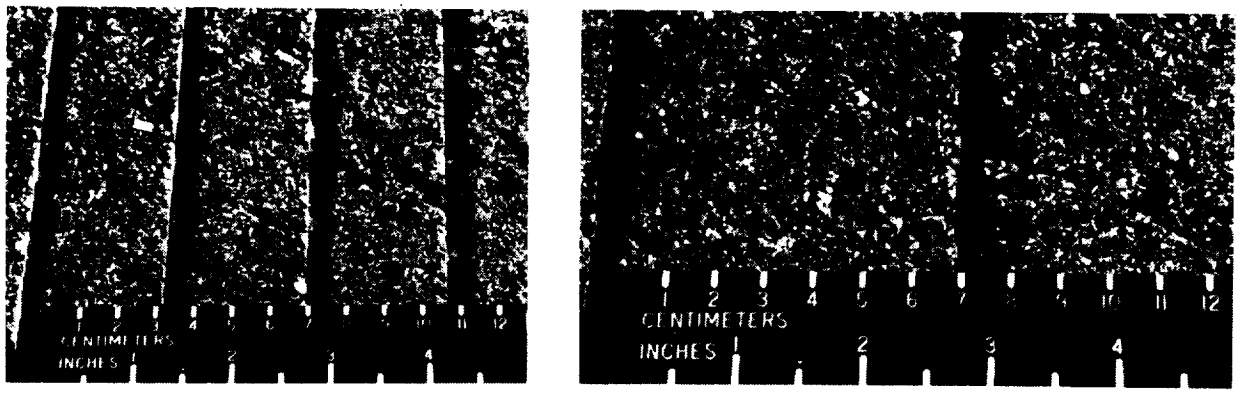

TEST SURFACE C

TEST SURFACE D

L-89-60

Figure 8. Close-up photographs of grooved test surfaces C and D on runway 13/31 at FAA Technical Center airport.

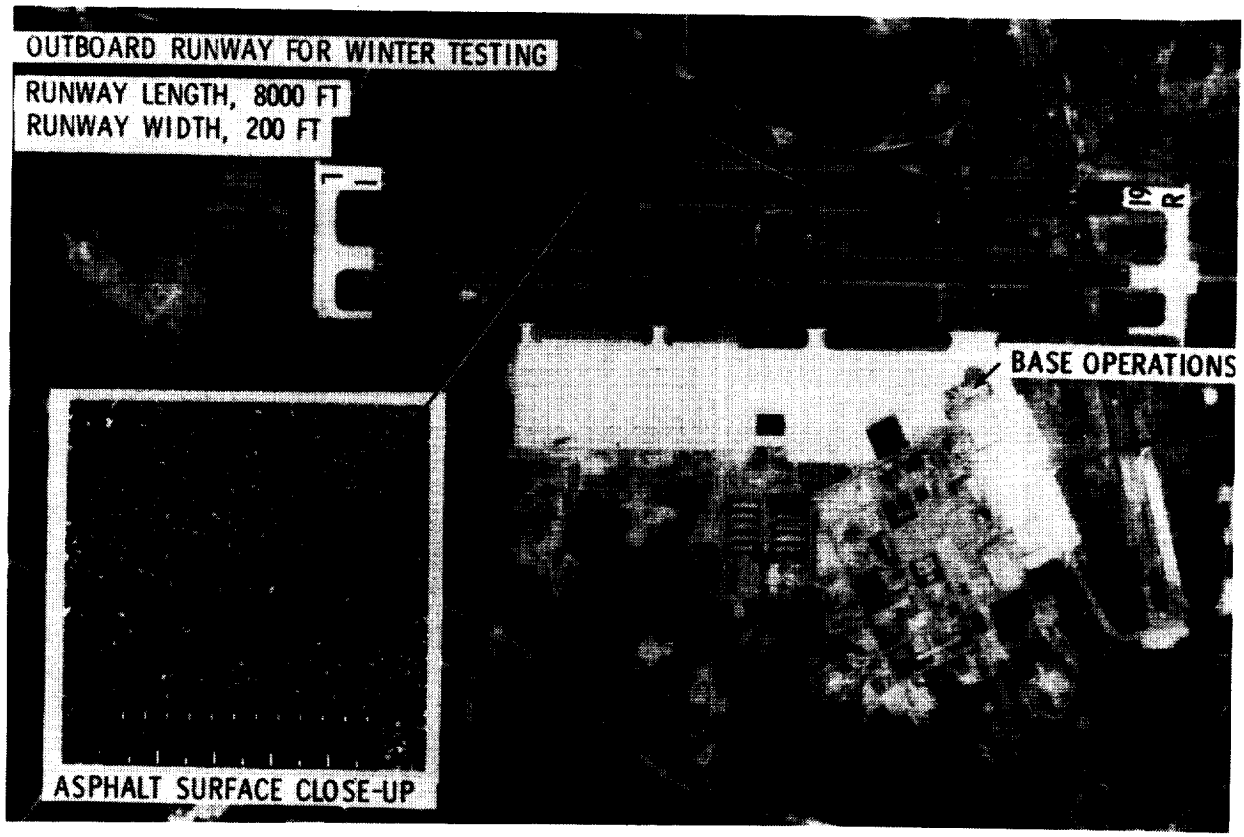

L-89-61

Figure 9. Aerial view of Brunswick Naval Air Station. Test runway 19R/11.

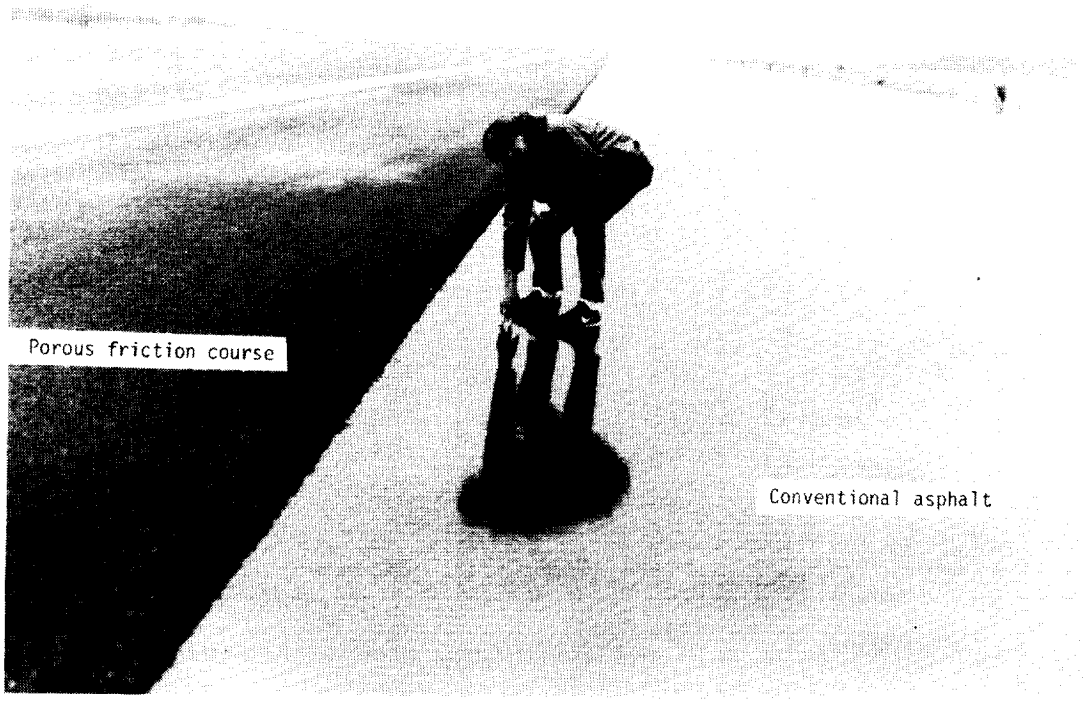

L-89-62

(a) Overview.

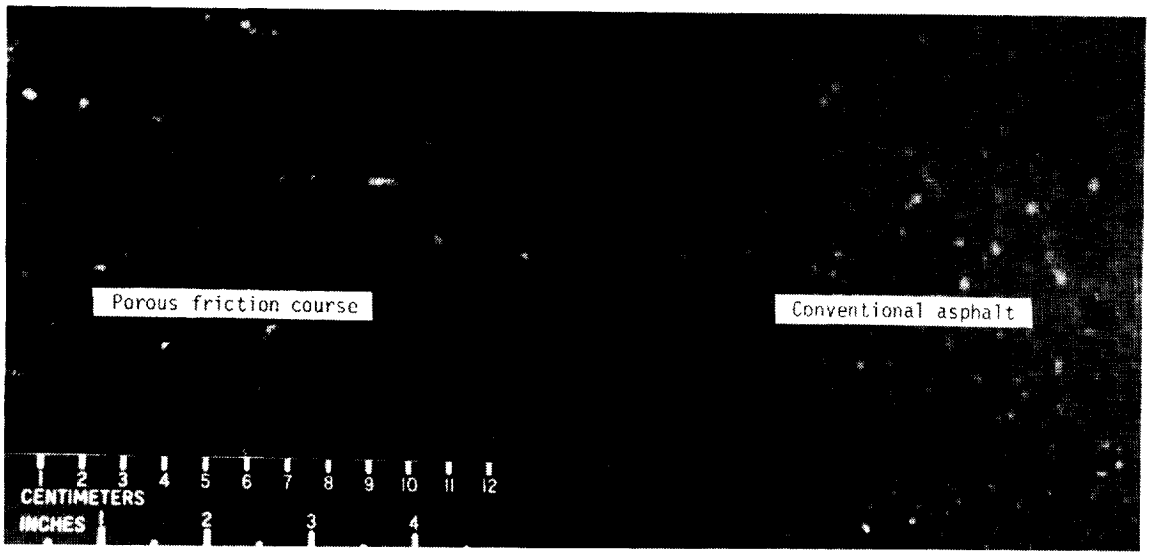

L-89-63

(b) Close-up view.

Figure 10. Porous friction course runway surface at Pease AFB under rain-wet conditions.

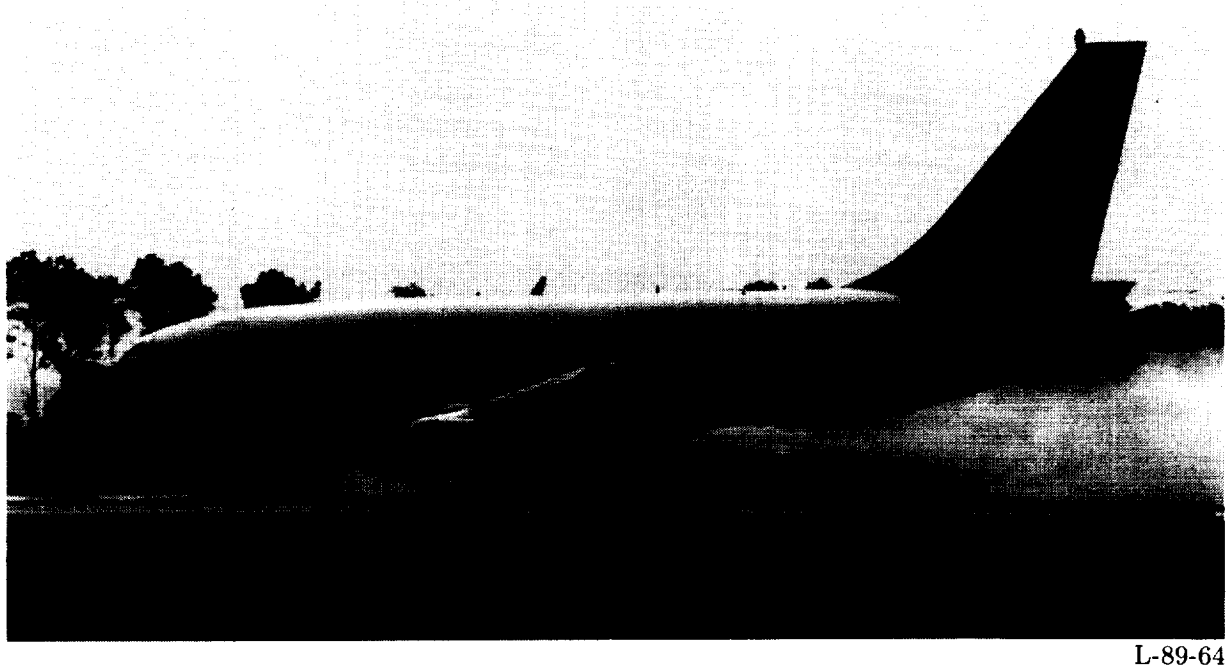

L-89-64

Figure 11. NASA Boeing 737 test aircraft during flooded-runway test.

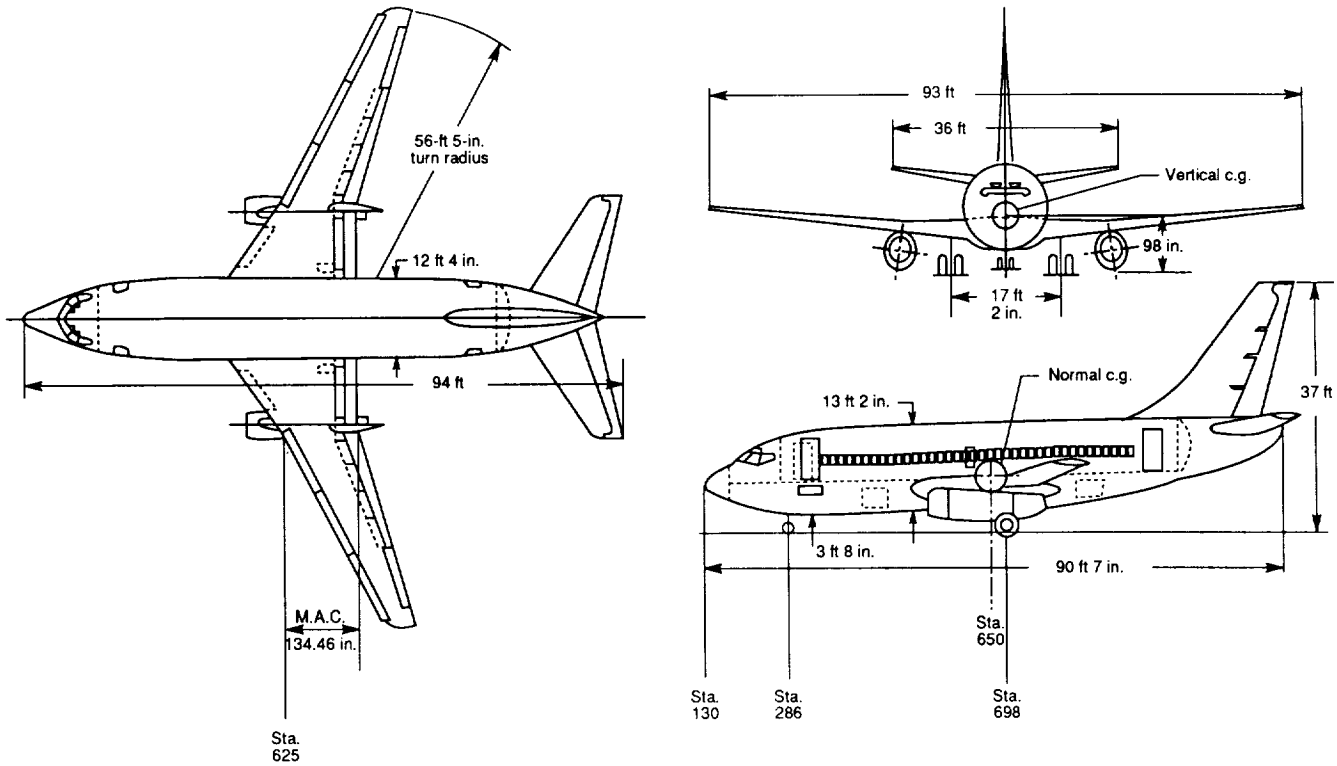

Figure 12. Schematics of NASA Boeing 737 aircraft geometry.

ORIGINAL PAGE
BLACK AND WHITE PHOTOGRAPH

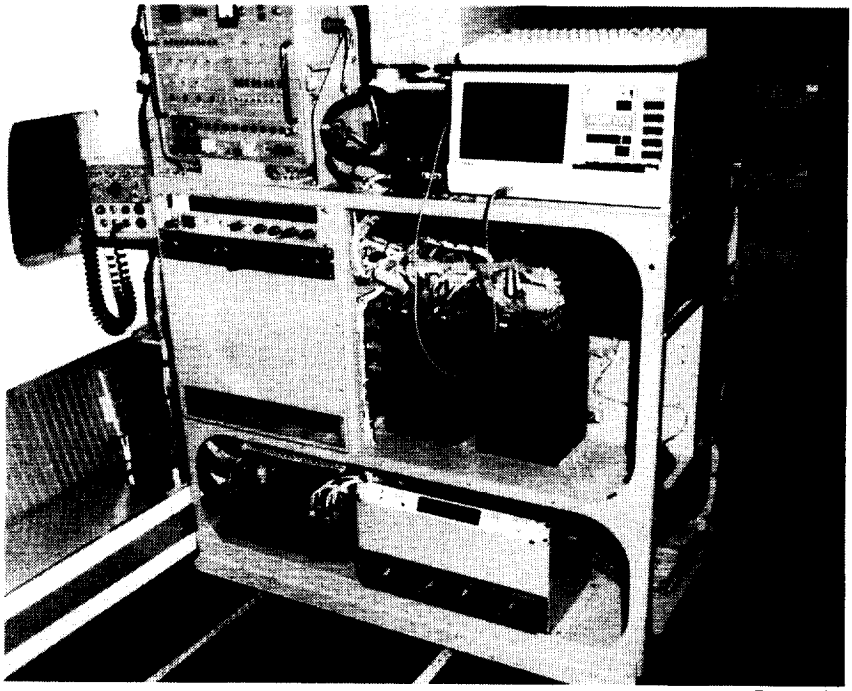

L-89-65

(a) Primary instrumentation pallet.

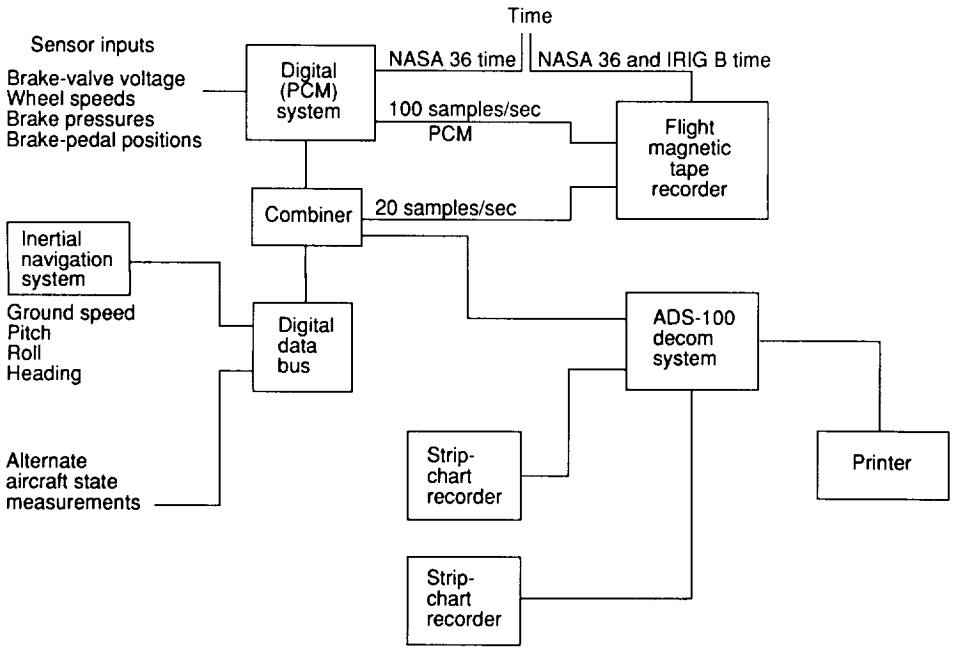

(b) Data-acquisition flow chart.

Figure 13. NASA Boeing 737 data-acquisition system.

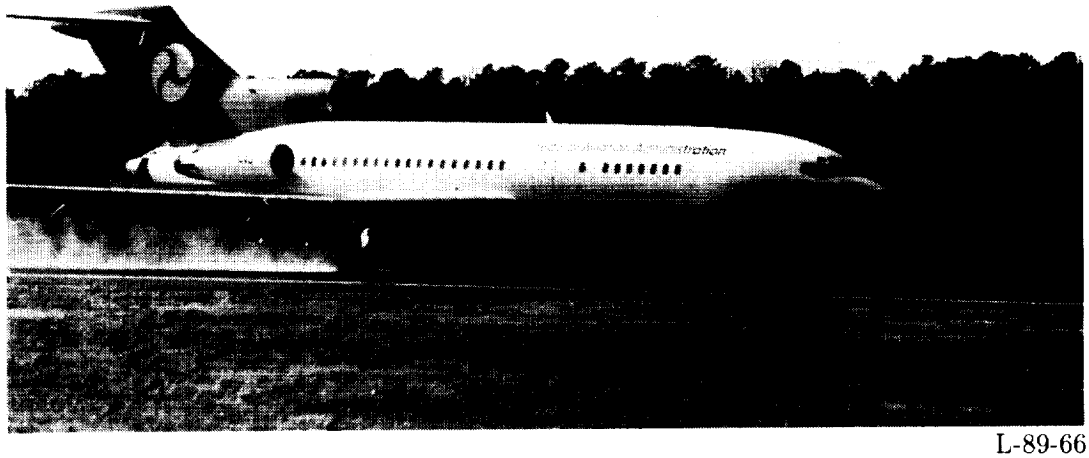

L-89-66

Figure 14. FAA Boeing 727 test aircraft during wet-runway test.

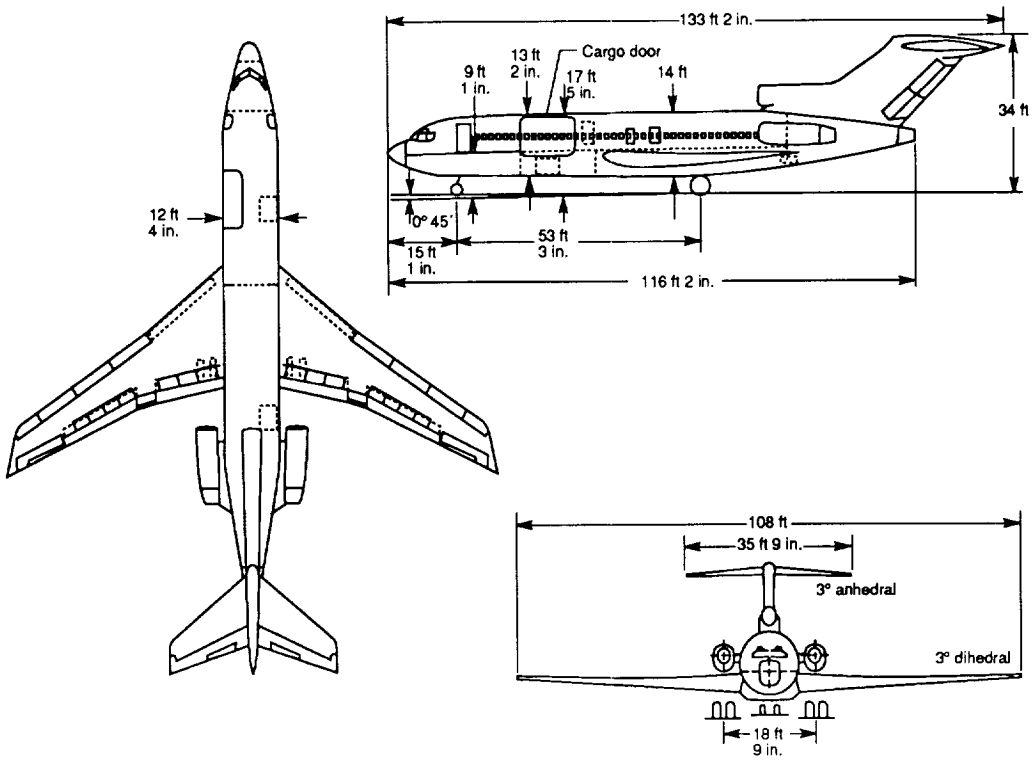

Figure 15. Schematics of FAA Boeing 727 aircraft geometry.

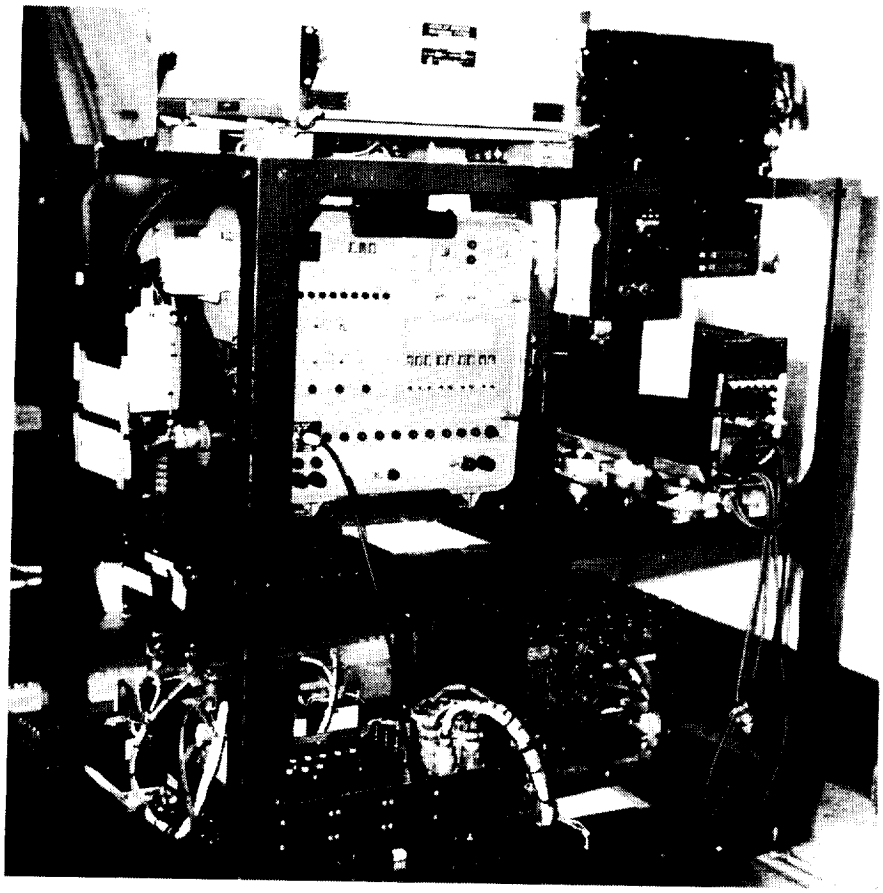

L-89-67

(a) Primary instrumentation pallet.

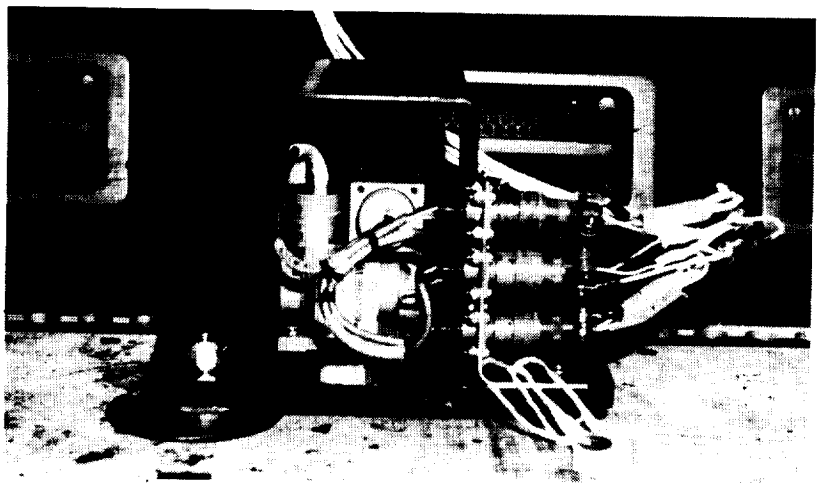

L-89-68

(b) Primary three-axis accelerometer package.

Figure 16. FAA Boeing 727 aircraft data-acquisition system.

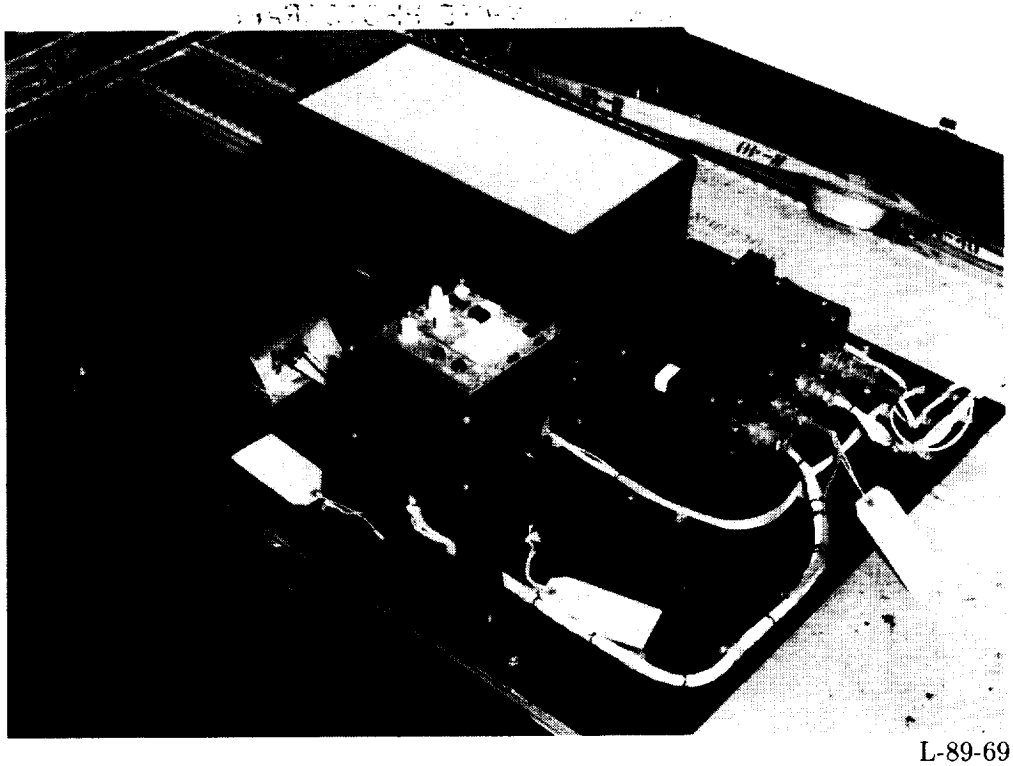

L-89-69

(c) Inertial navigation system hookup with data-acquisition system.

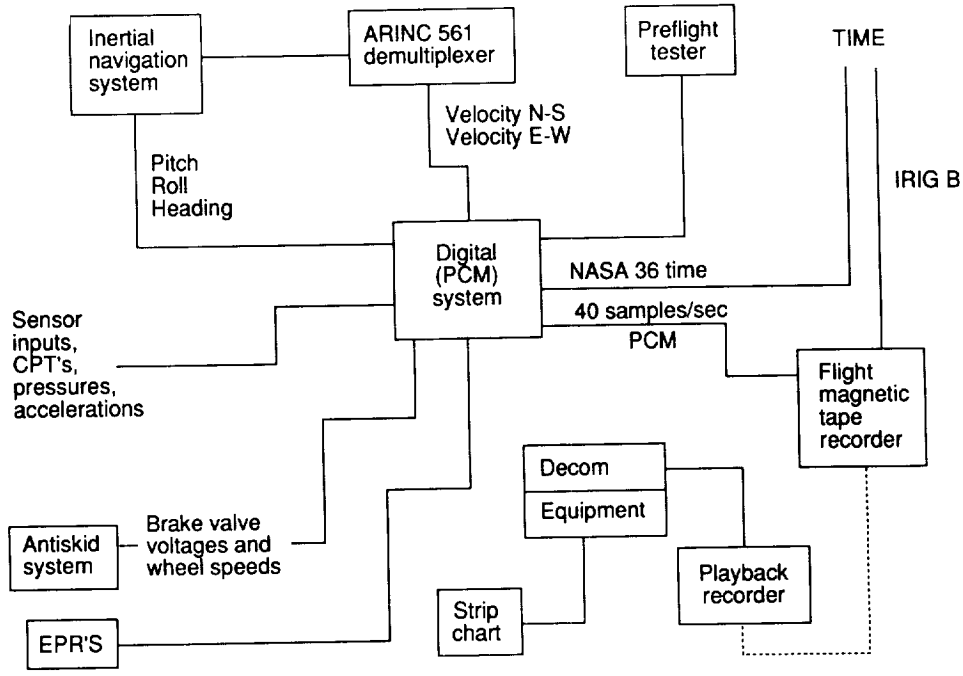

(d) Data-acquisition flow chart.

Figure 16. Concluded.

L-89-70

Figure 17. Test tires on friction-measuring vehicle.

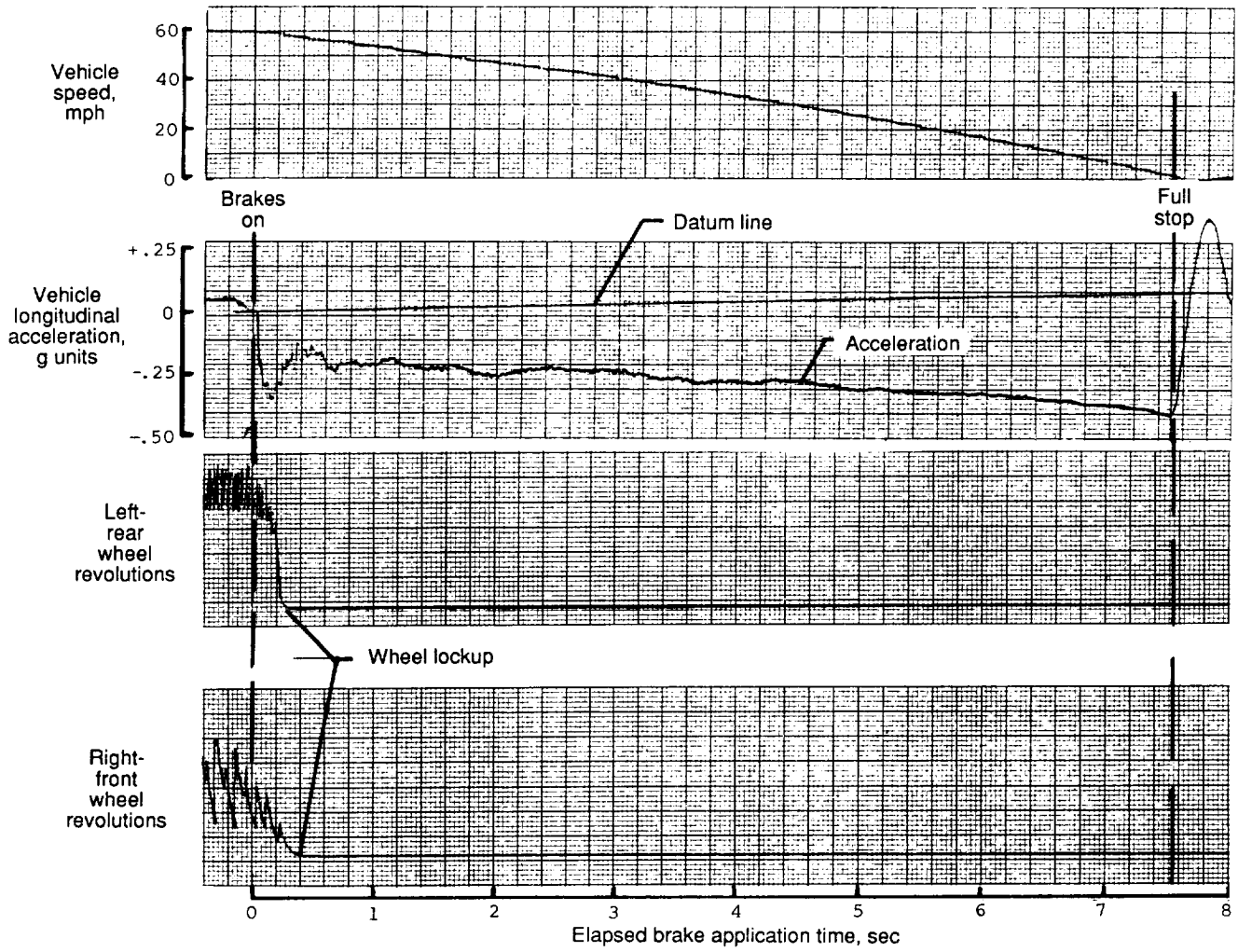

(a) Diagonal-braked vehicle.

Figure 18. Samples of ground-vehicle test-run records.

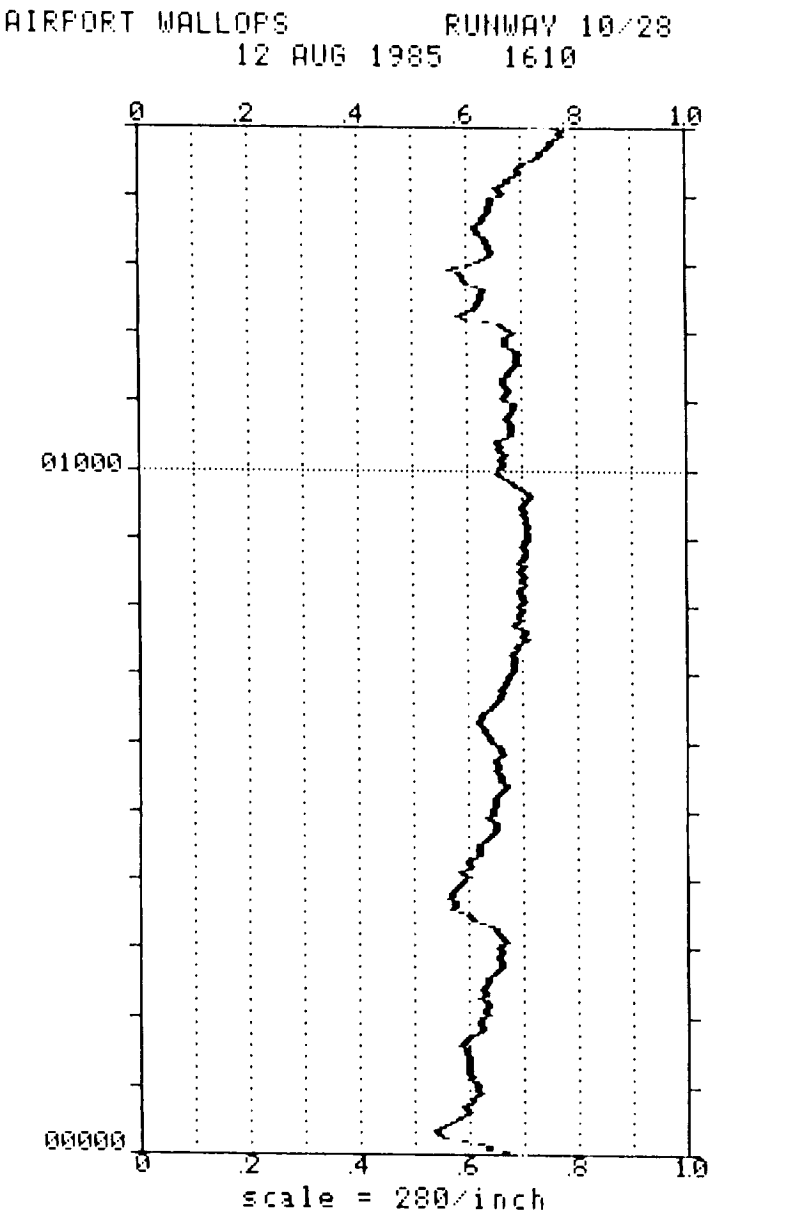

(b) Mu-Meter.

Figure 18. Continued.

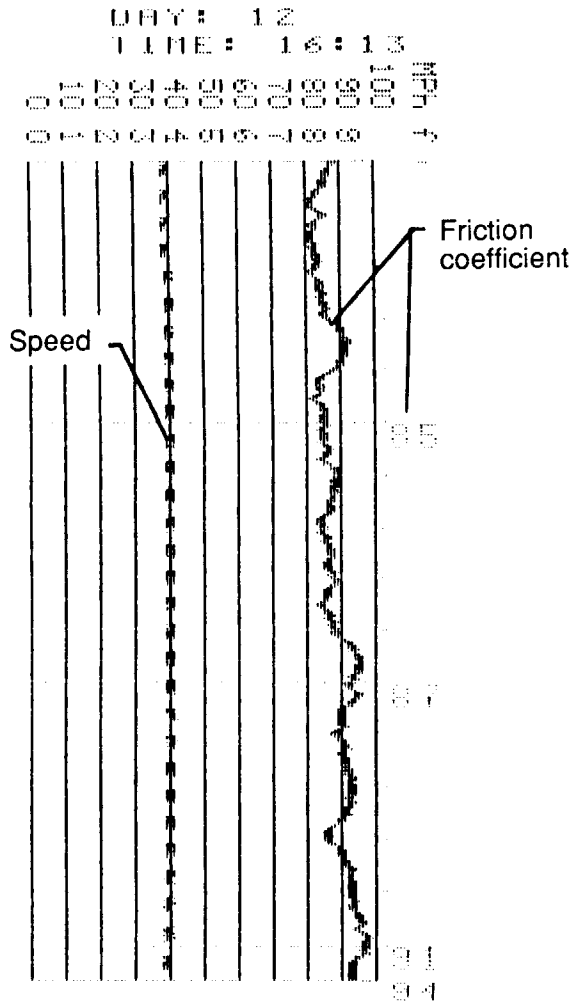

(c) Surface friction tester.

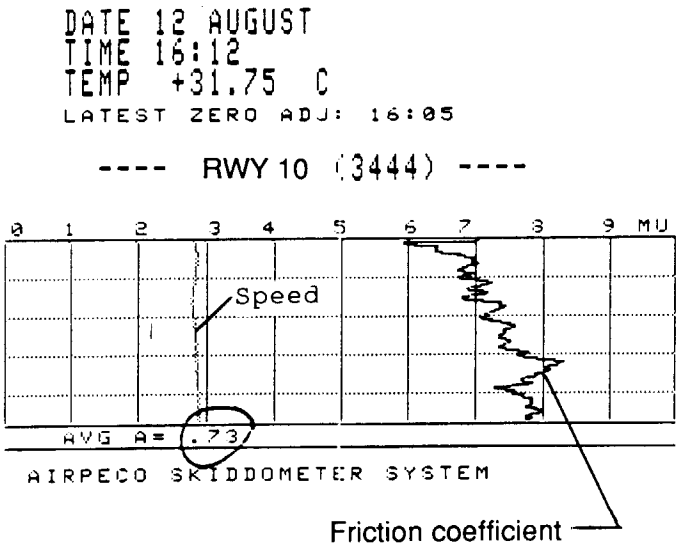

(d) BV-11 skiddometer.

Figure 18. Continued.

TIME: 16:11:54
DATE: 8/12/85

M6800 RUNWAY FRICTION TESTER

RUN NUMBER = 5
AIRPORT NAME: WALLOPS RUNWAY #10 OPERATOR: DJH

SCALE- 1 in = 300 ft

COEFF.	SPEED (MPH)	FLOW (GPM)	LENGTH (FT)	V
0.590	40.4 (MPH)	0.0 (GPM)	500. (FT)	
0.690	41.1 (MPH)	0.0 (GPM)	1000. (FT)	
0.730	41.1 (MPH)	0.0 (GPM)	1500. (FT)	

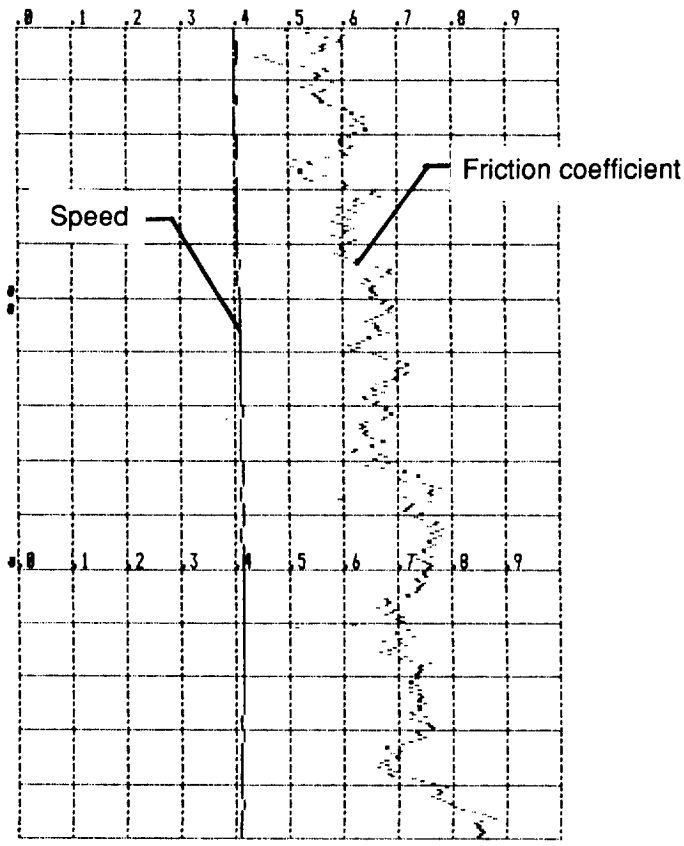

AVERAGE FRICTION (mu) 0.675
AVERAGE SPEED (mph) 40.9
AVERAGE FLOW RATE (gpm) 0.0

COMMENTS

END OF RUN

(e) Runway friction tester.

Figure 18. Concluded.

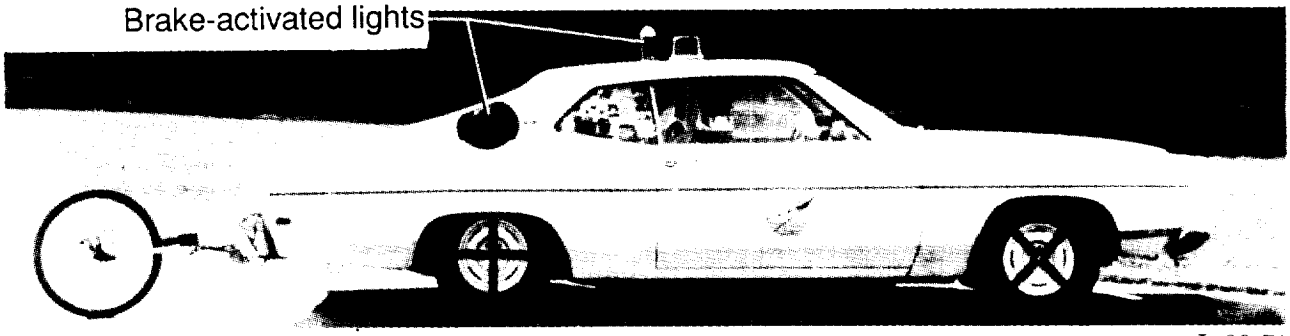

L-89-71

(a) NASA diagonal-braked vehicle.

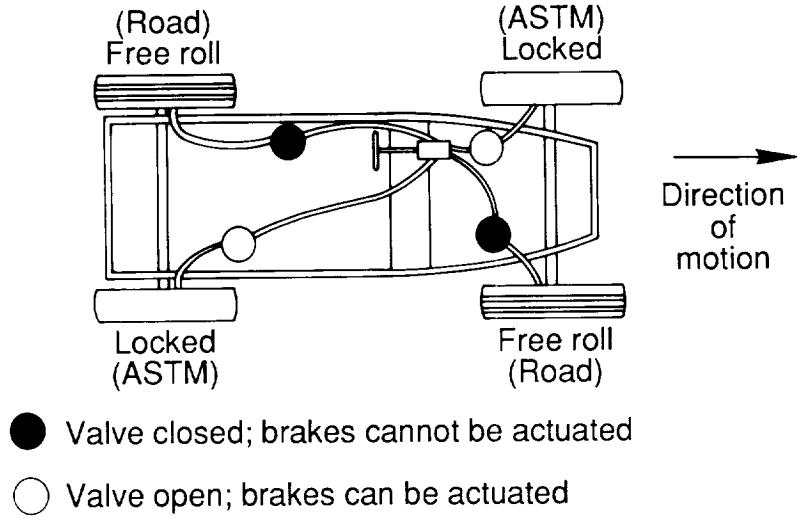

(b) Schematic of diagonal-braked system.

Figure 19. NASA diagonal-braked vehicle system.

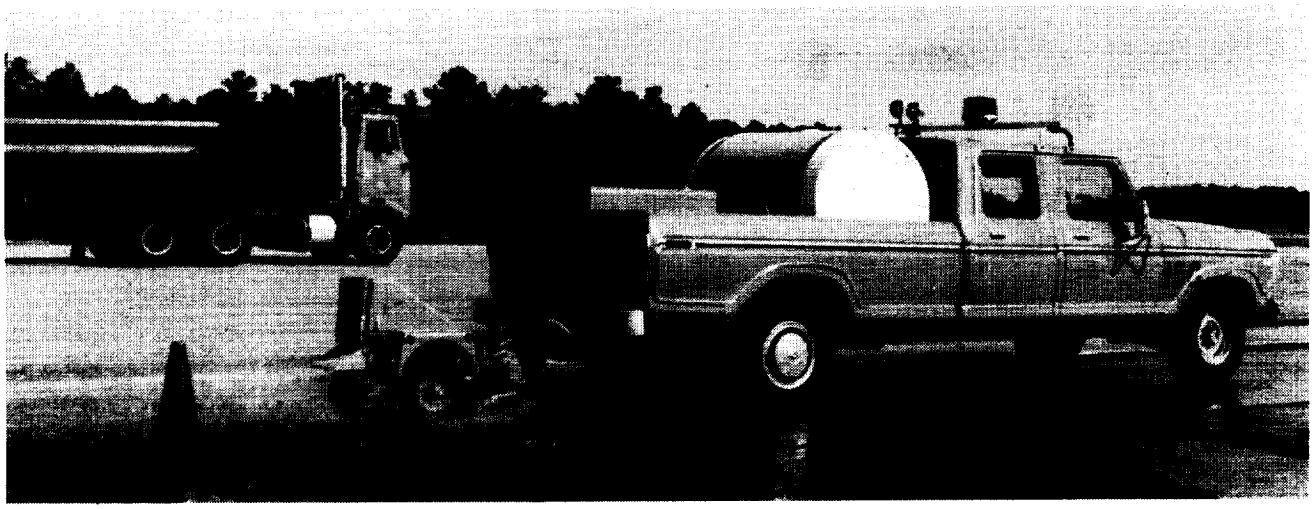

(a) Mark III unit at Wallops Flight Facility.

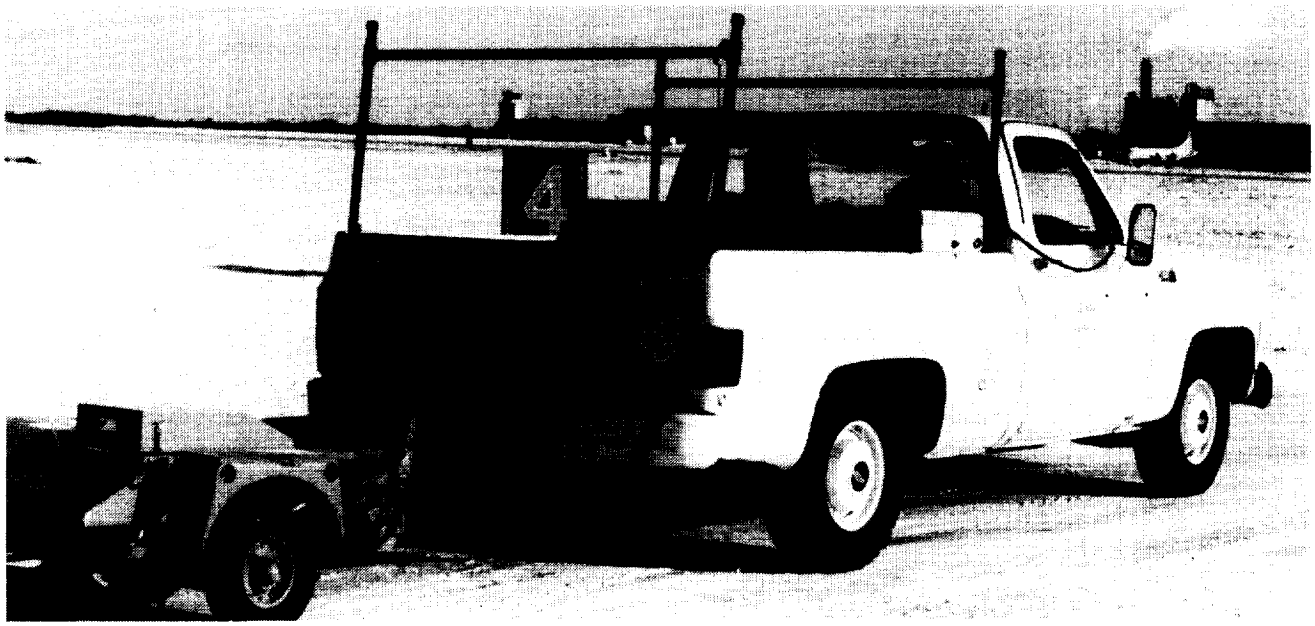

(b) Mark IV unit at BNAS.

L-89-72

Figure 20. Mu-Meter trailers with towing vehicle.

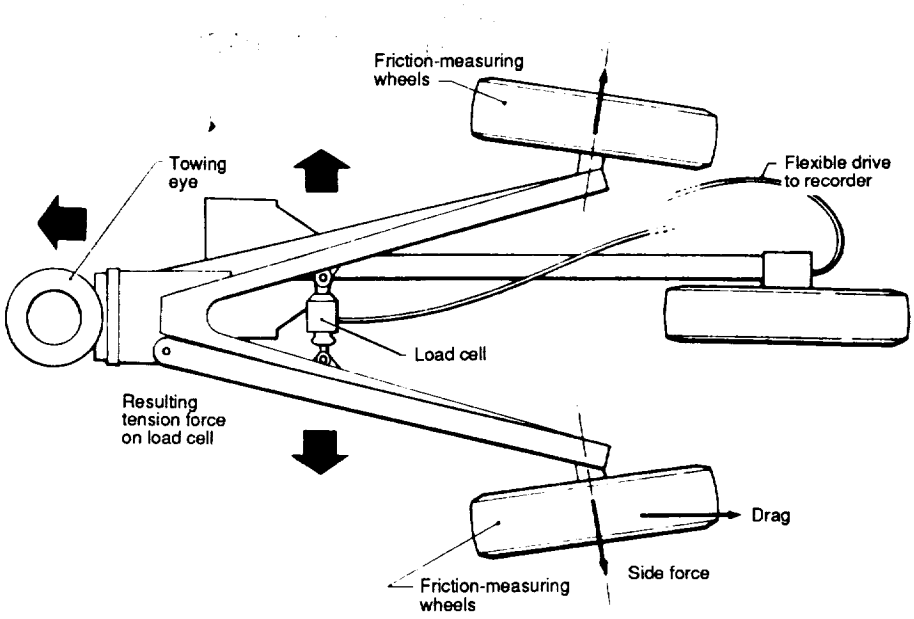

(a) Plan view without top frame.

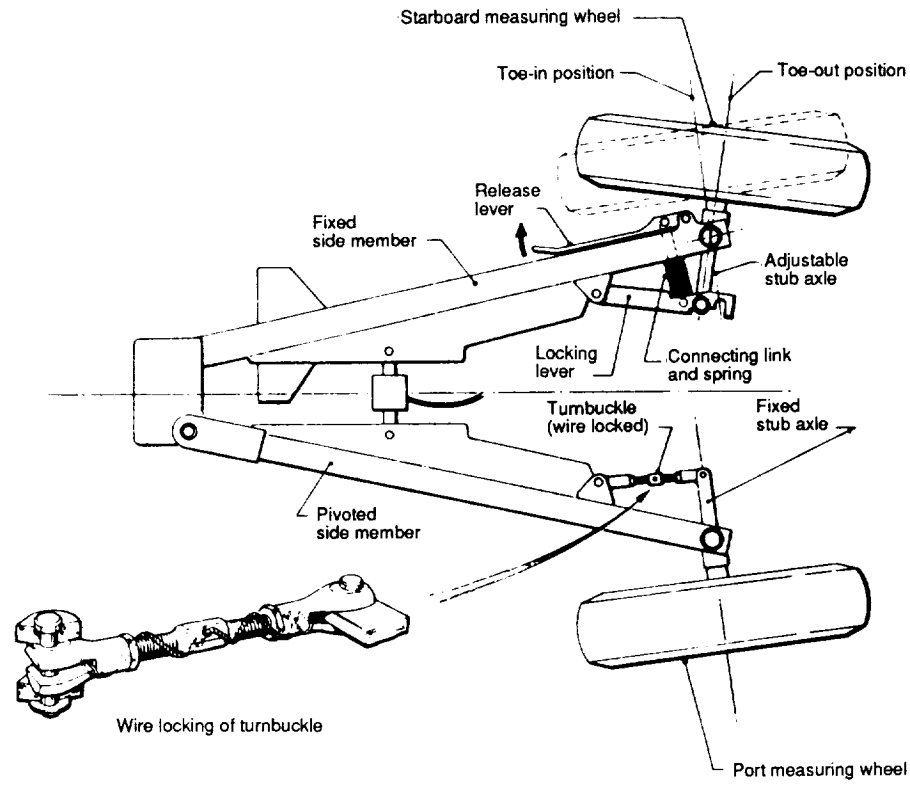

(b) Measuring-wheel settings.

Figure 21. Features of Mu-Meter measurement system.

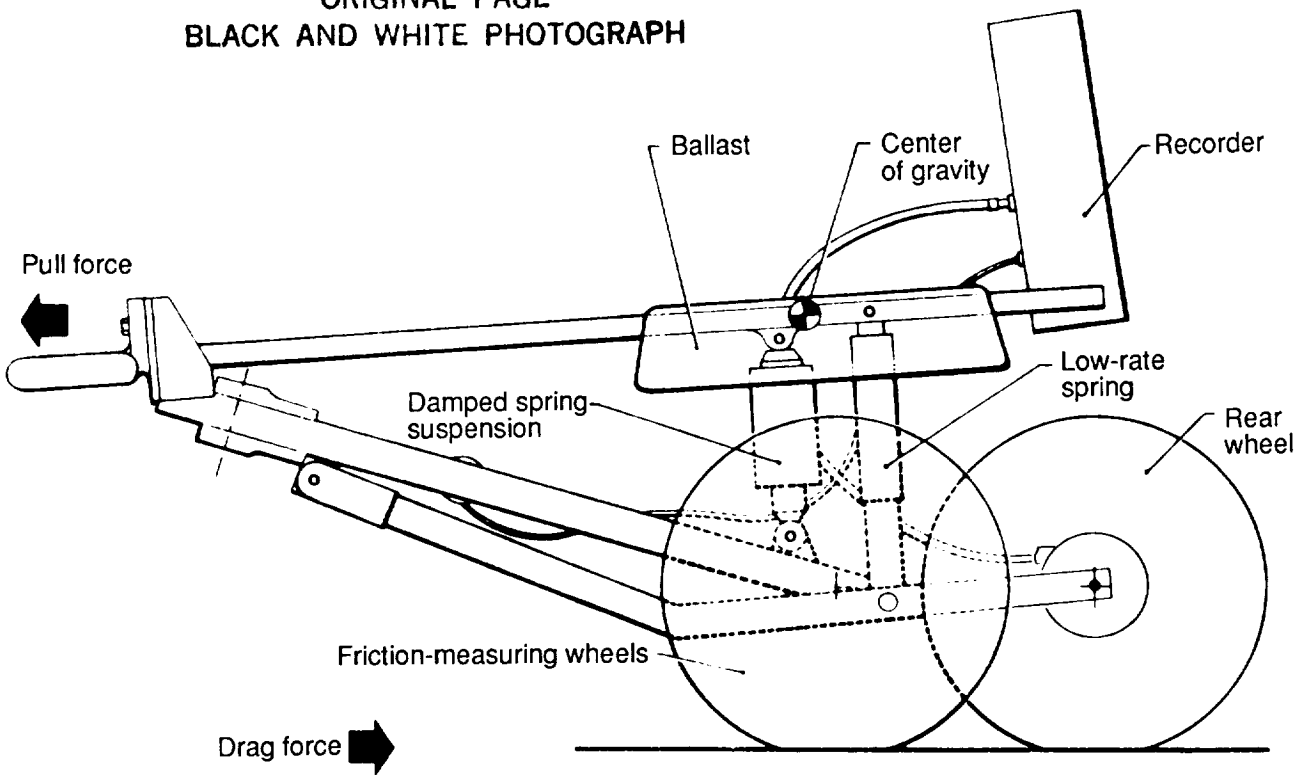

(c) Side view without top frame.

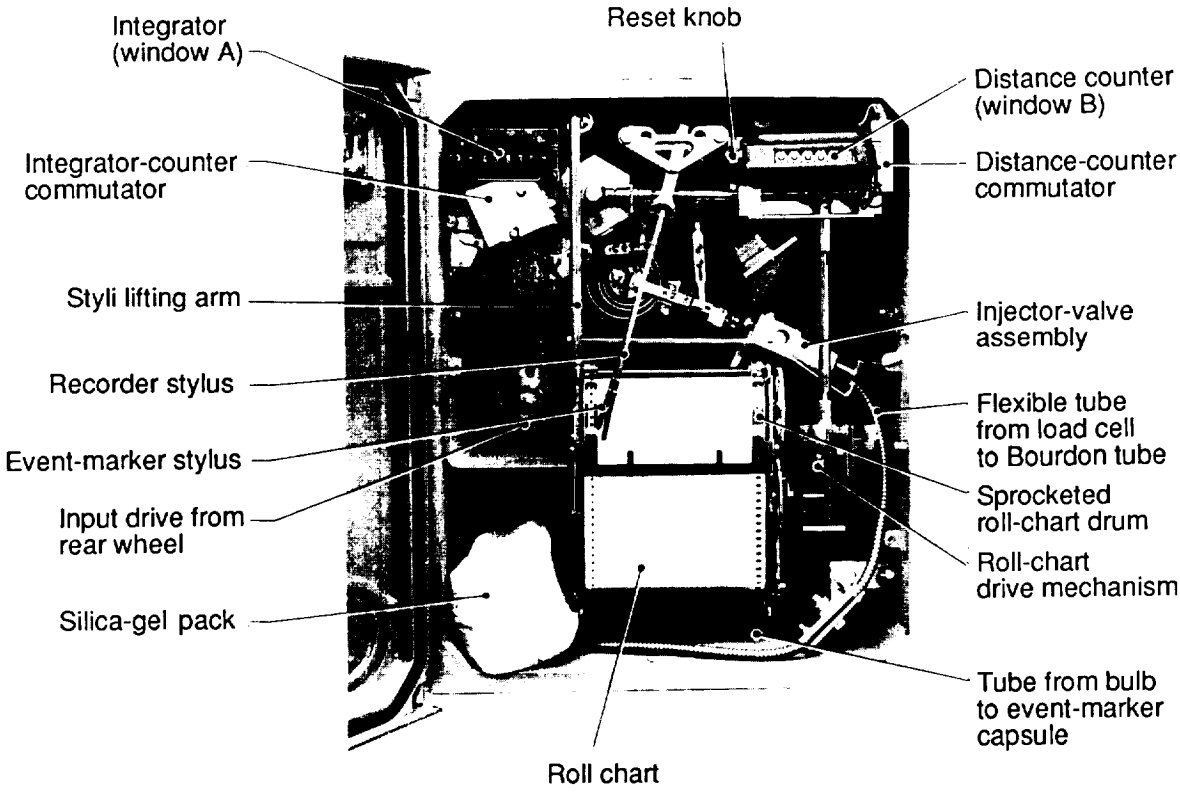

(d) Mark III recorder features.

Figure 21. Continued.

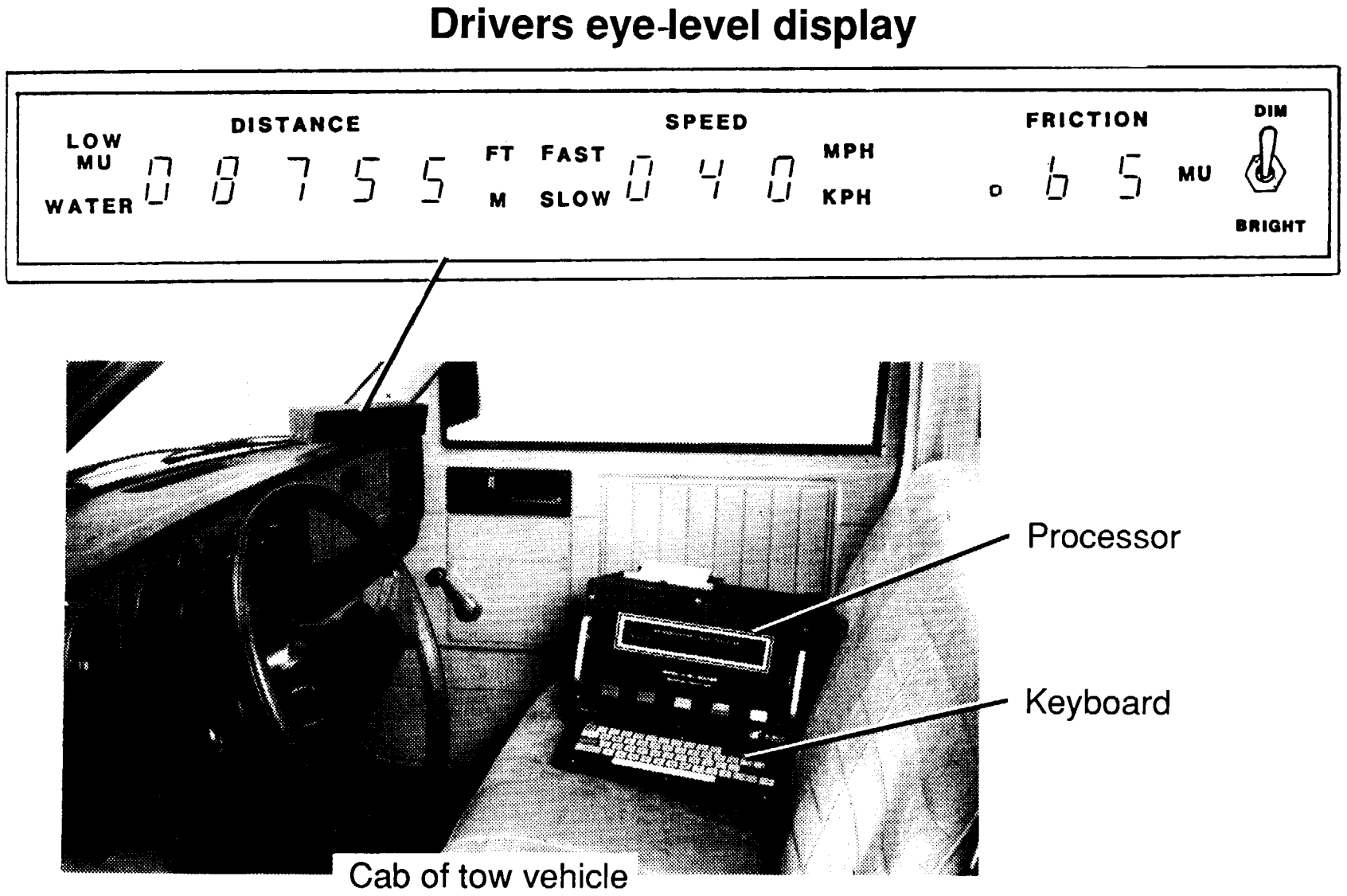

L-89-74

(e) Features of new Mark IV Mu-Meter unit.

Figure 21. Concluded.

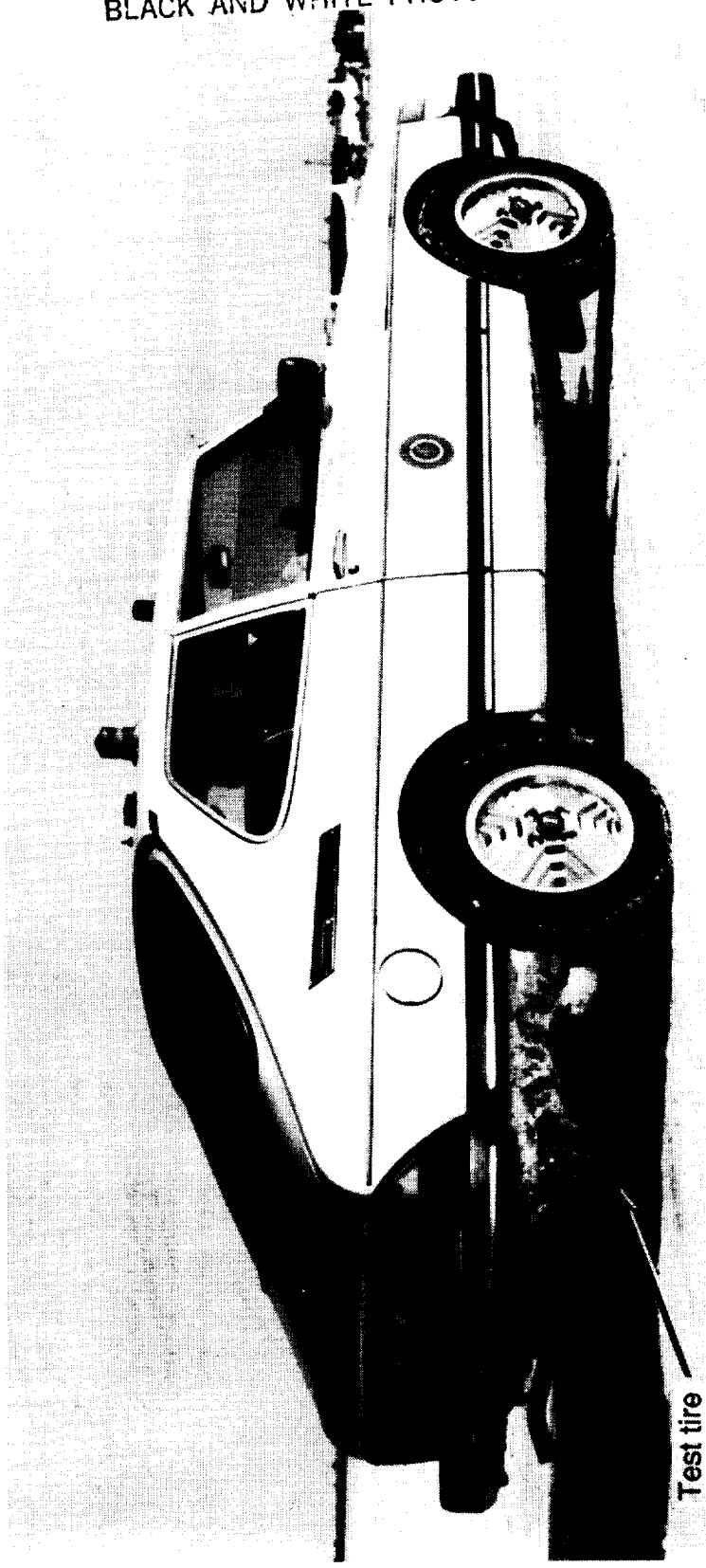

L-89-75

Figure 22. Surface friction tester.

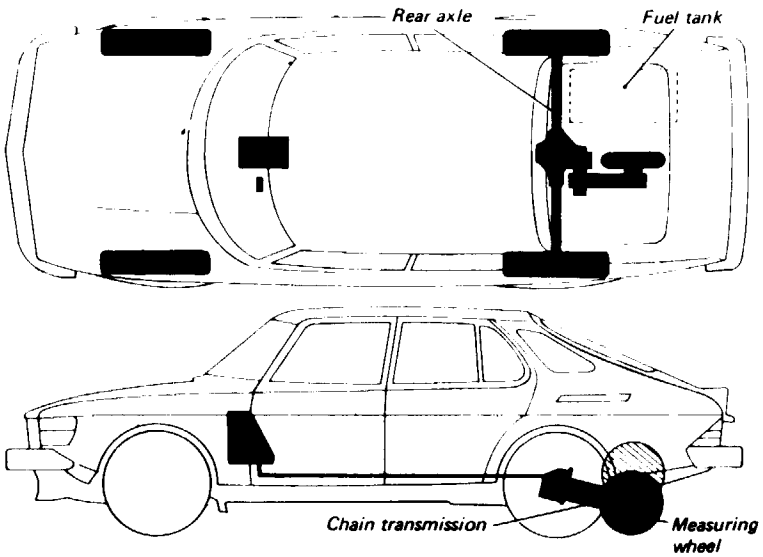

(a) Overall vehicle configuration.

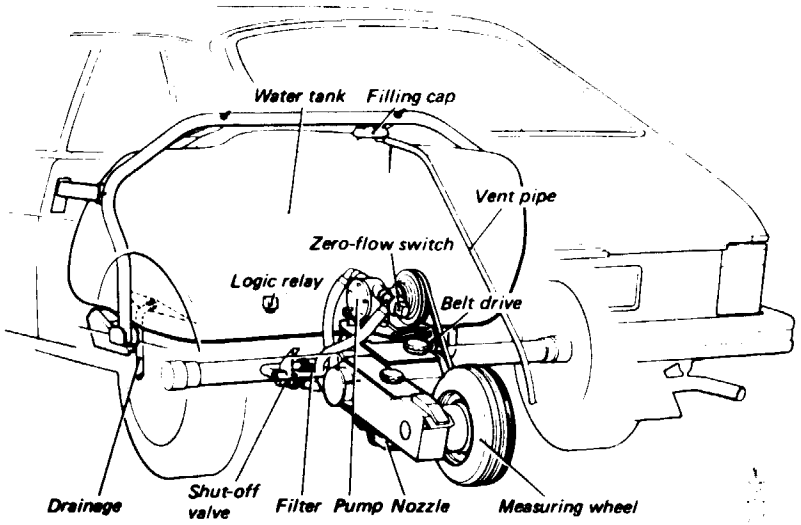

(b) Self-wetting system.

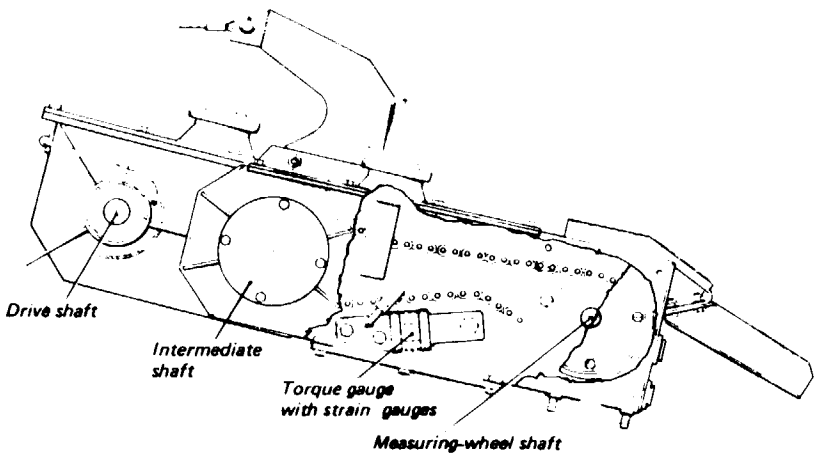

(c) Cutaway side view of measuring-wheel arm with chain drive.

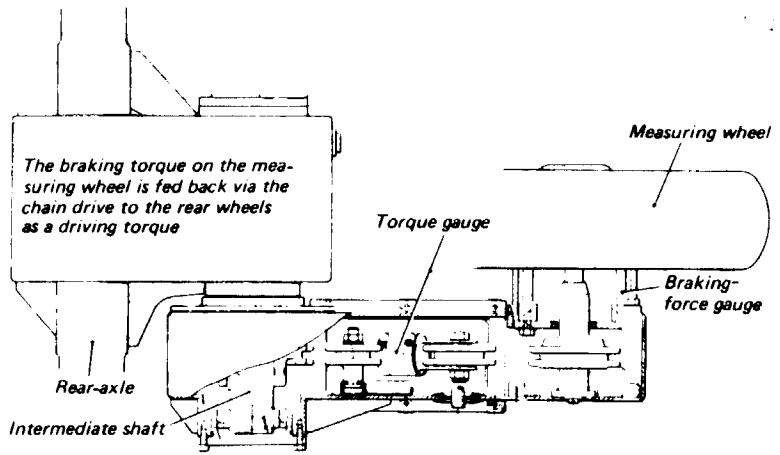

(d) Cutaway plan view of measuring-wheel arm.

Figure 23. Schematics of surface friction tester vehicle with details on self-wetting system and measuring-wheel arm.

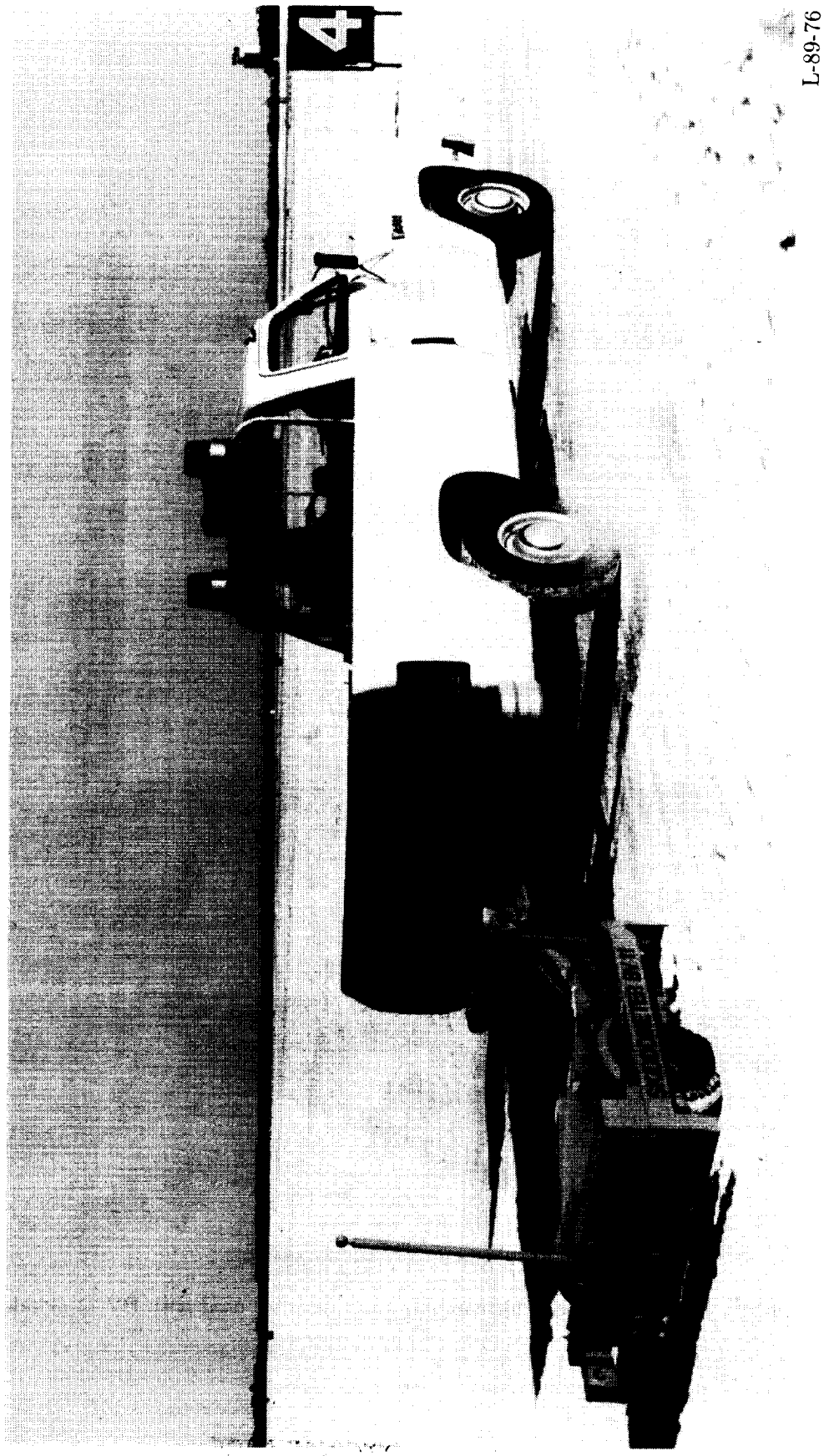

L-89-76

Figure 24. BV-11 skiddometer trailer and tow vehicle.

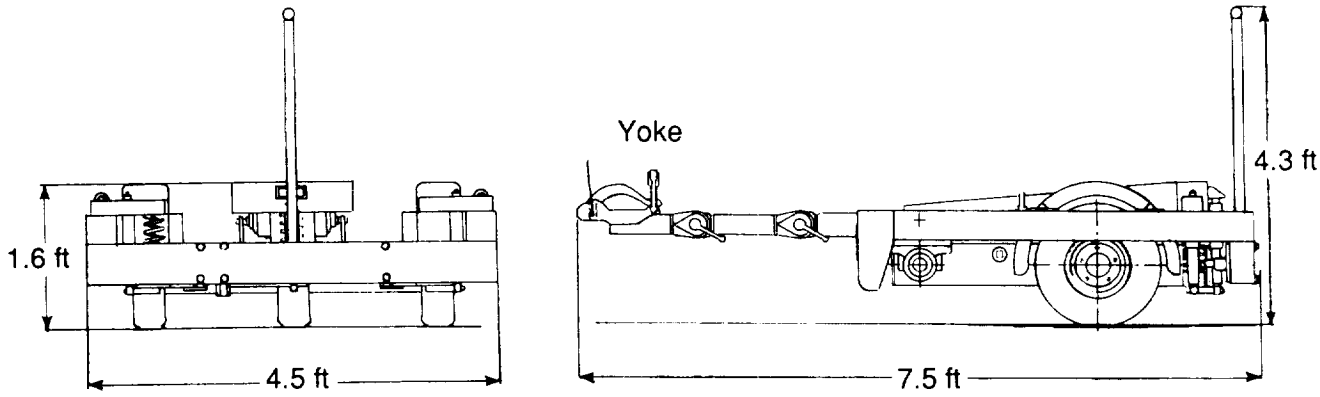

(a) Schematic.

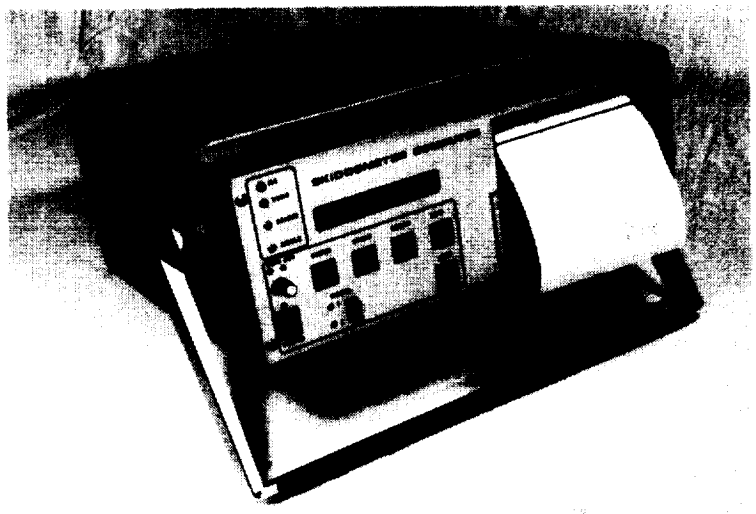

L-89-77

(b) Portable computer and recorder.

Figure 25. Trailer schematic and portable computer and recorder used with BV-11 skiddometer.

ORIGINAL PAGE
BLACK AND WHITE PHOTOGRAPH

L-89-78

Figure 26. Runway friction tester during test run on compacted snow.

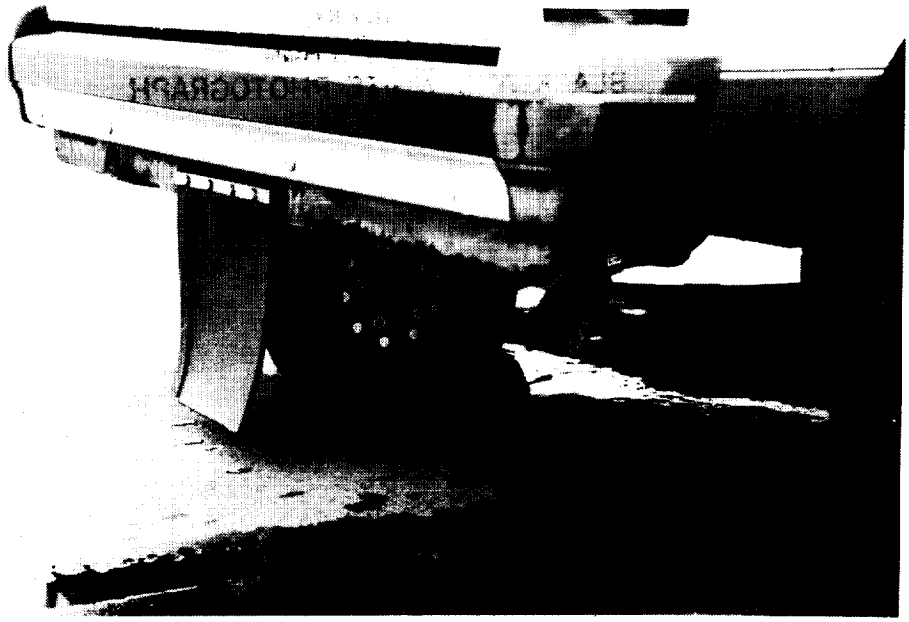

L-89-79

(a) Close-up view of test tire.

L-89-80

(b) Operator cab compartment.

Figure 27. Test tire and operator cab compartment on runway friction tester.

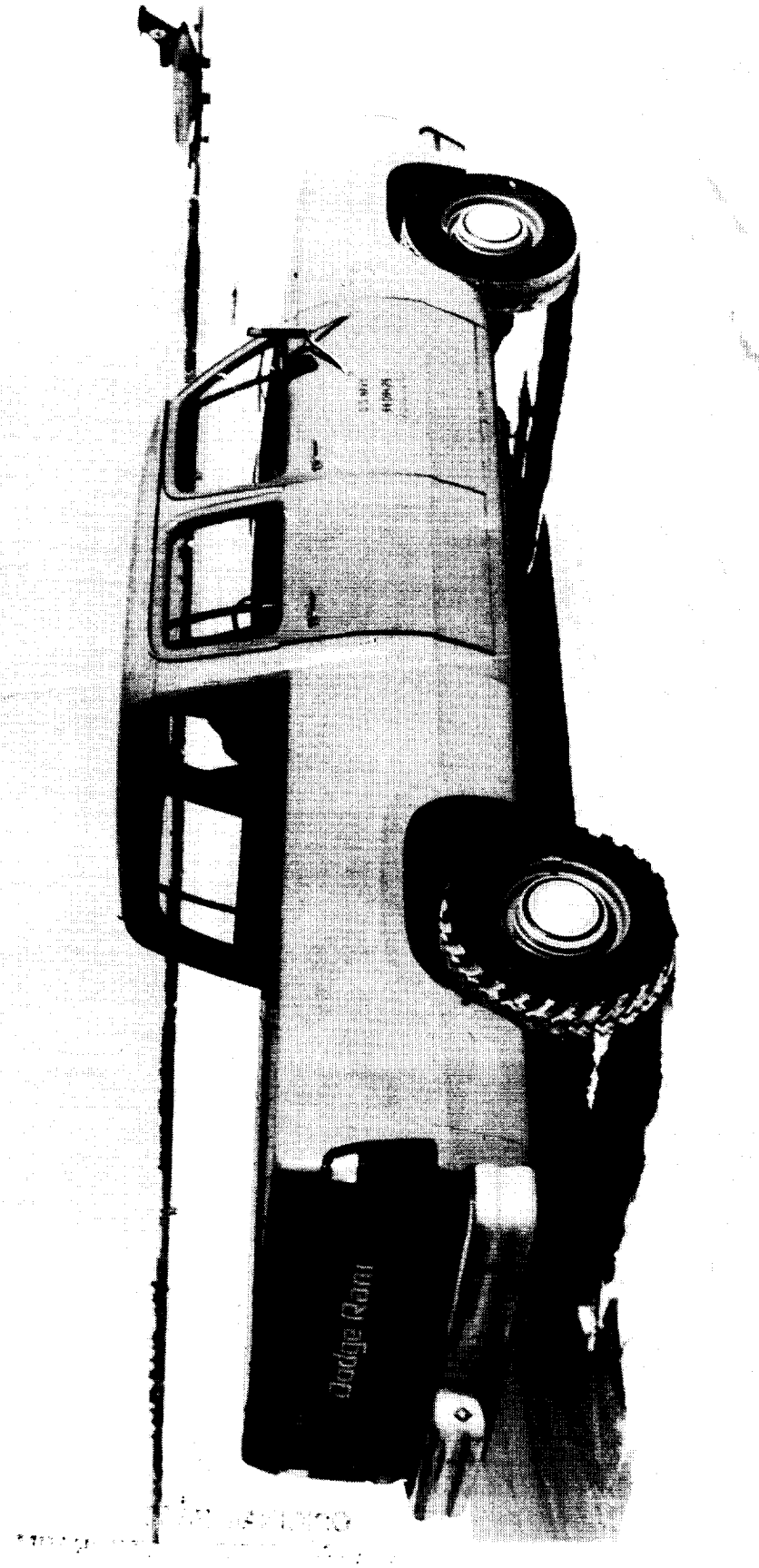

L-89-81

Figure 28. Navy runway condition reading (RCR) test vehicle.

L-89-82

(a) Mechanical Tapley meter used in runway condition reading vehicle.

Figure 29. Portable Tapley meter units.

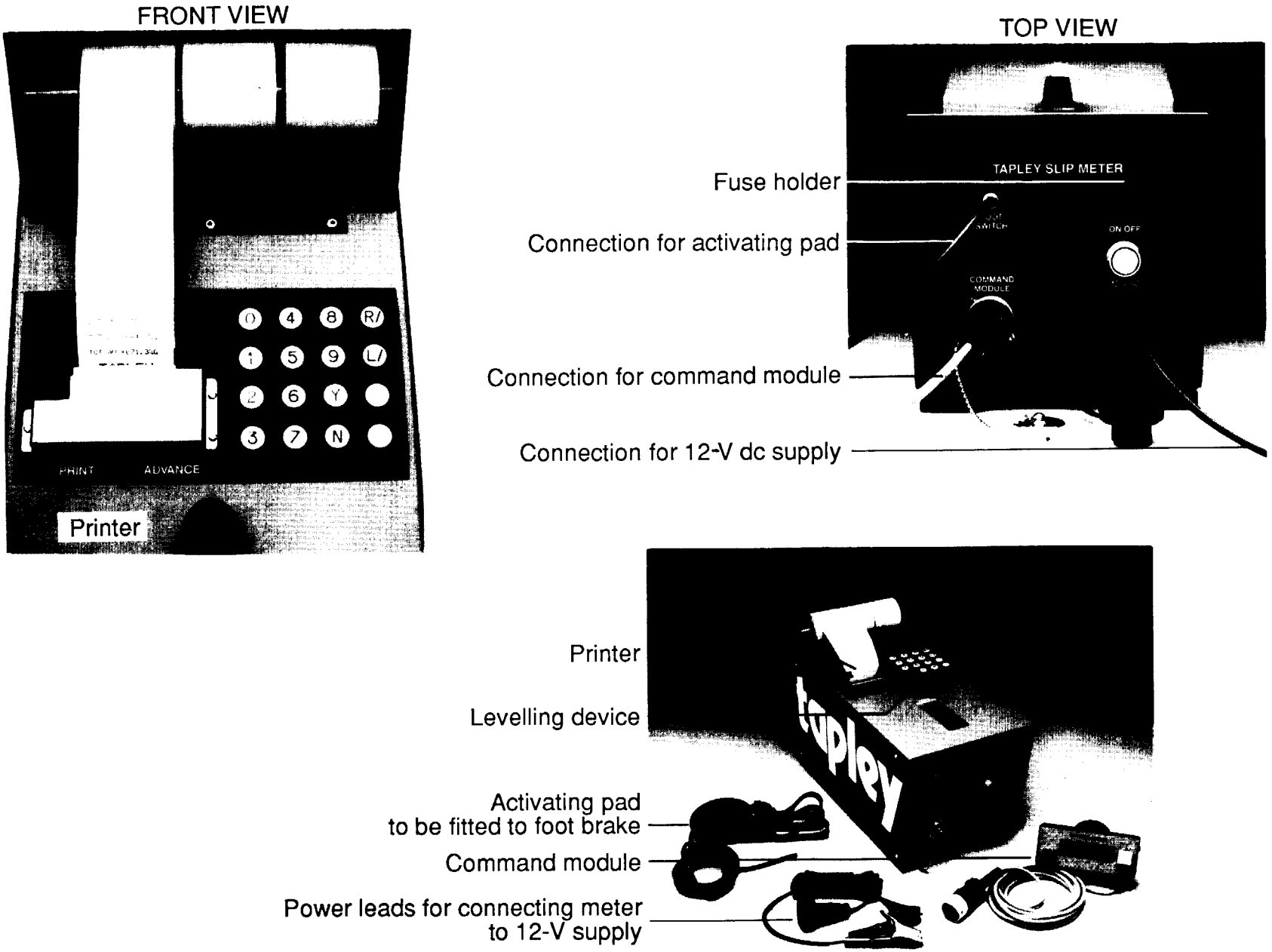

(b) Electronic Tapley meter.

L-89-83

Figure 29. Concluded.

ORIGINAL PAGE
BLACK AND WHITE PHOTOGRAPH

L-89-84

Figure 30. Bowmonk brakemeter unit used in runway condition reading test vehicle.

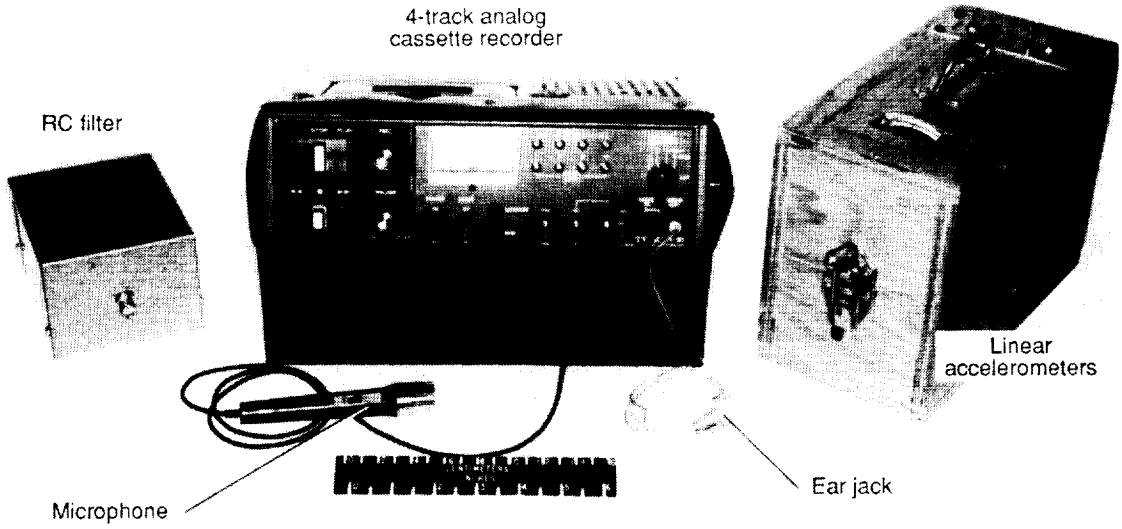

L-89-85

Figure 31. Portable three-axis accelerometer packaged used on test aircraft as backup instrumentation system.

L-89-86

Figure 32. Surface temperature gauge.

L-89-87

Figure 33. Portable wind anemometer used for measurements at runway test-section site.

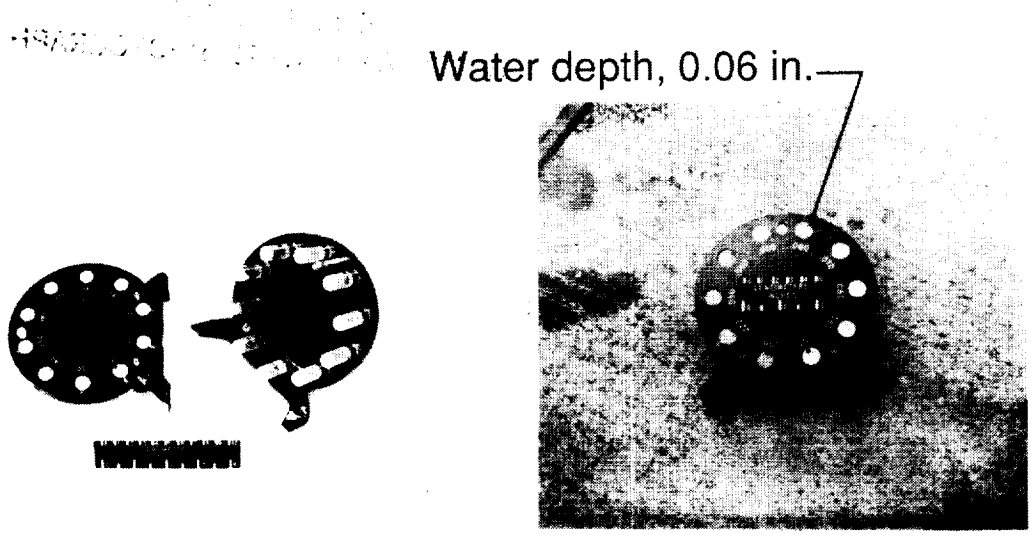

L-89-88

Figure 34. Different views of NASA portable water-depth gauge.

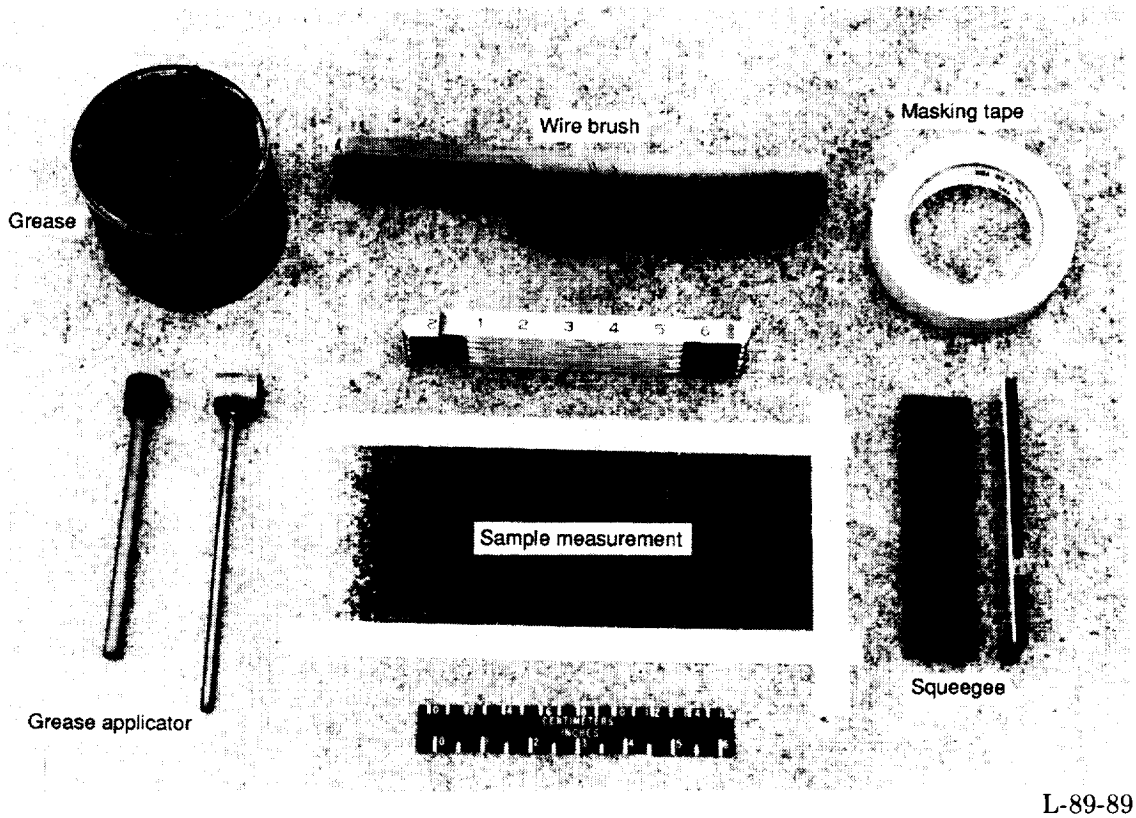

L-89-89

Figure 35. Equipment for taking surface macrotexture-depth measurement using NASA grease-sample method.

L-89-90

Figure 36. Collection of snow sample for density measurement.

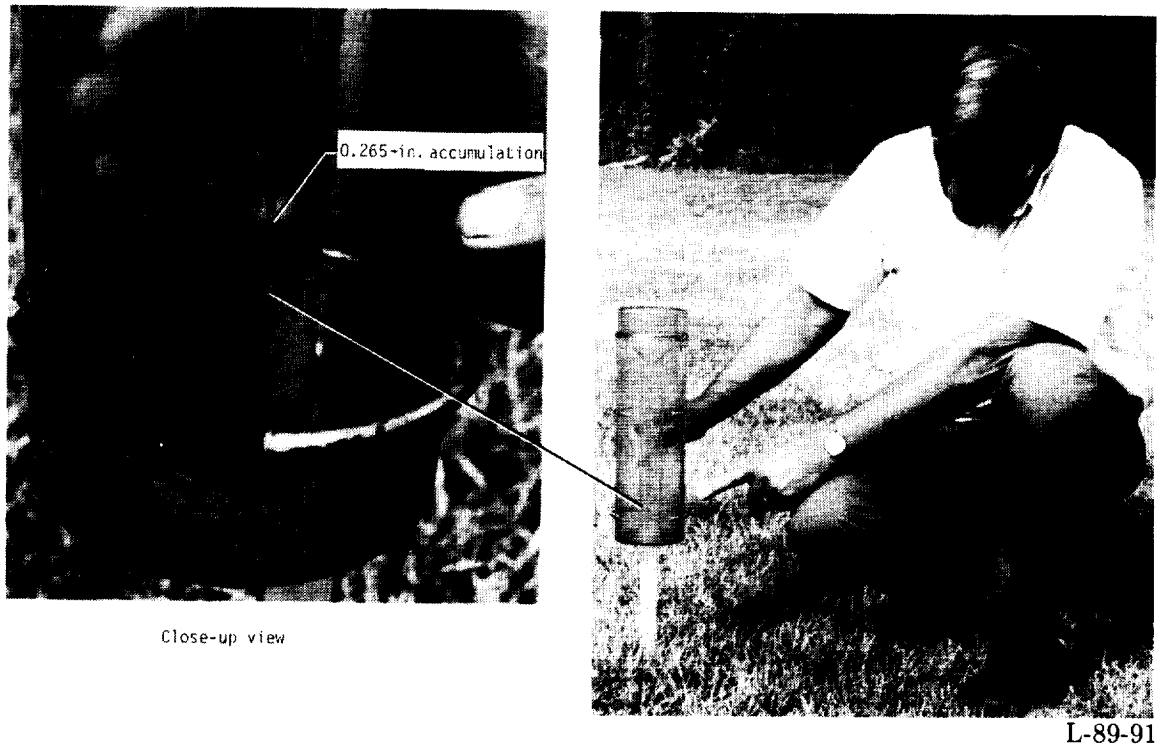

L-89-91

Figure 37. Portable rain gauge.

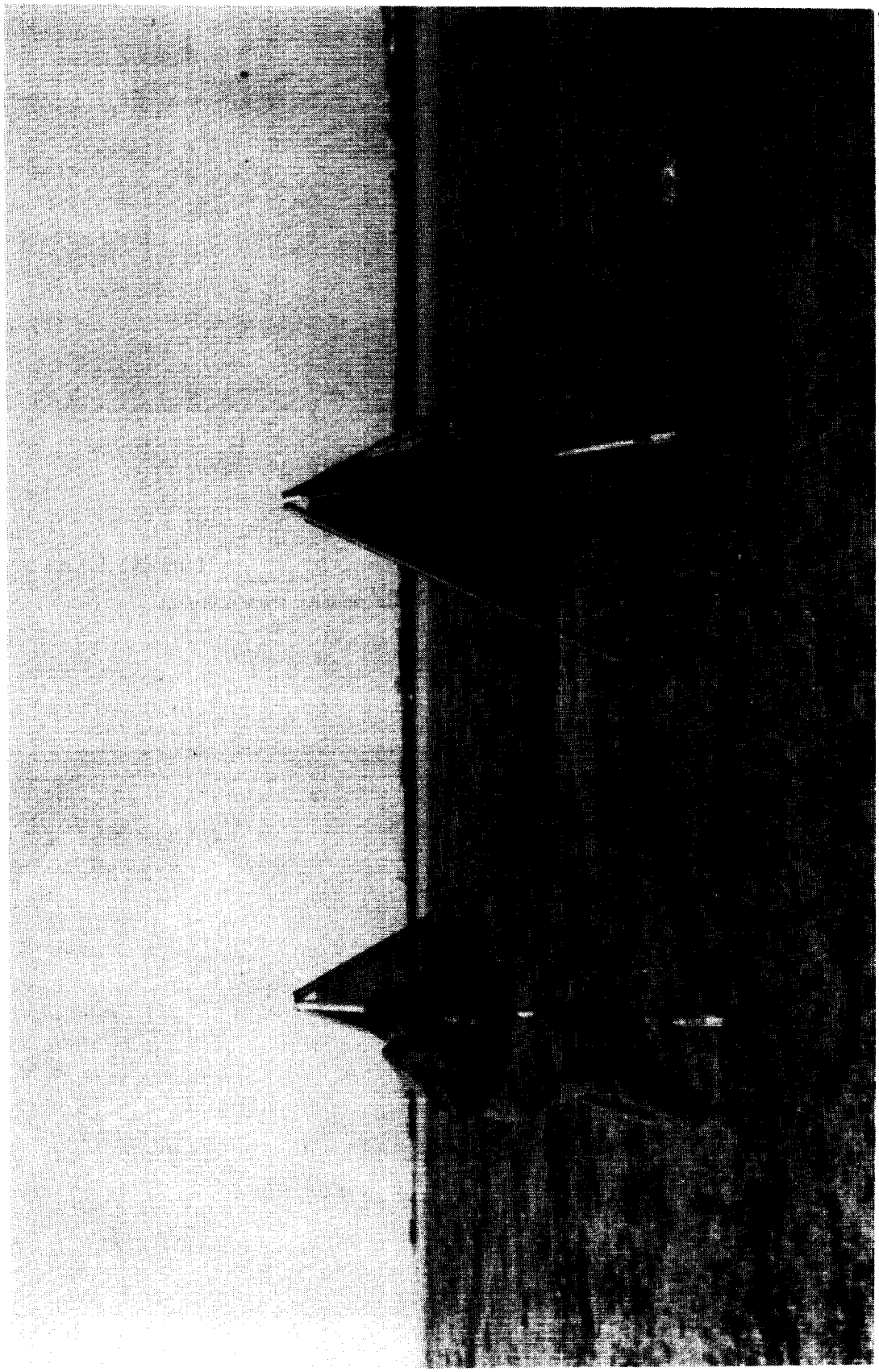

L-89-92

Figure 38. Portable tripod runway markers.

C-3

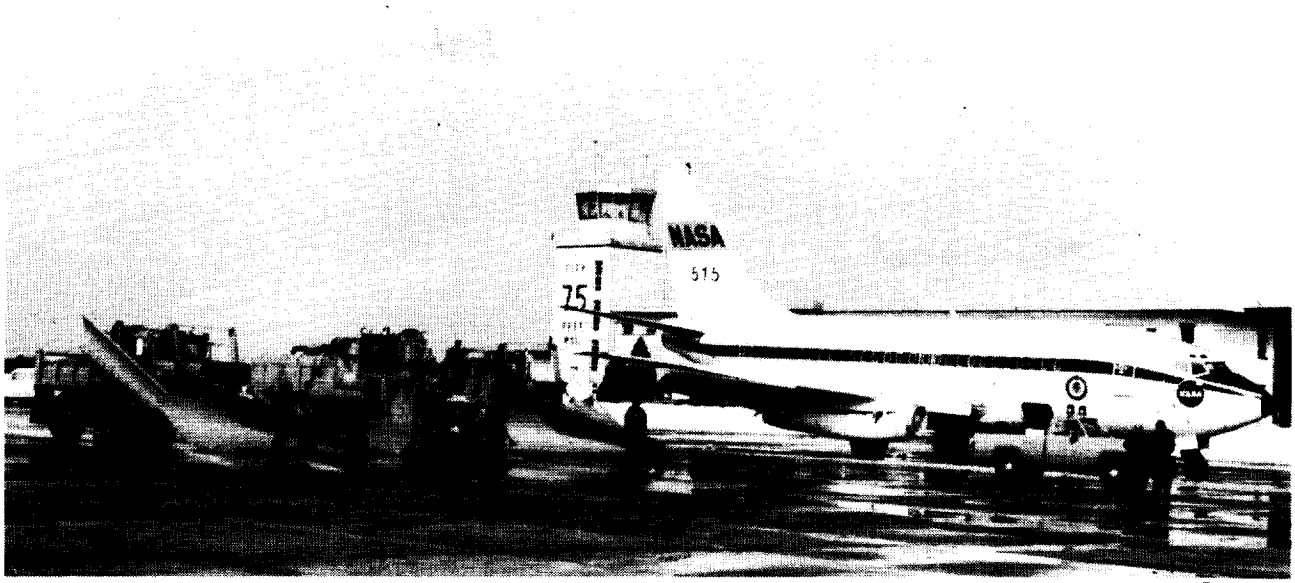

L-89-93

(a) Runway snow removal equipment with Boeing 737 test aircraft.

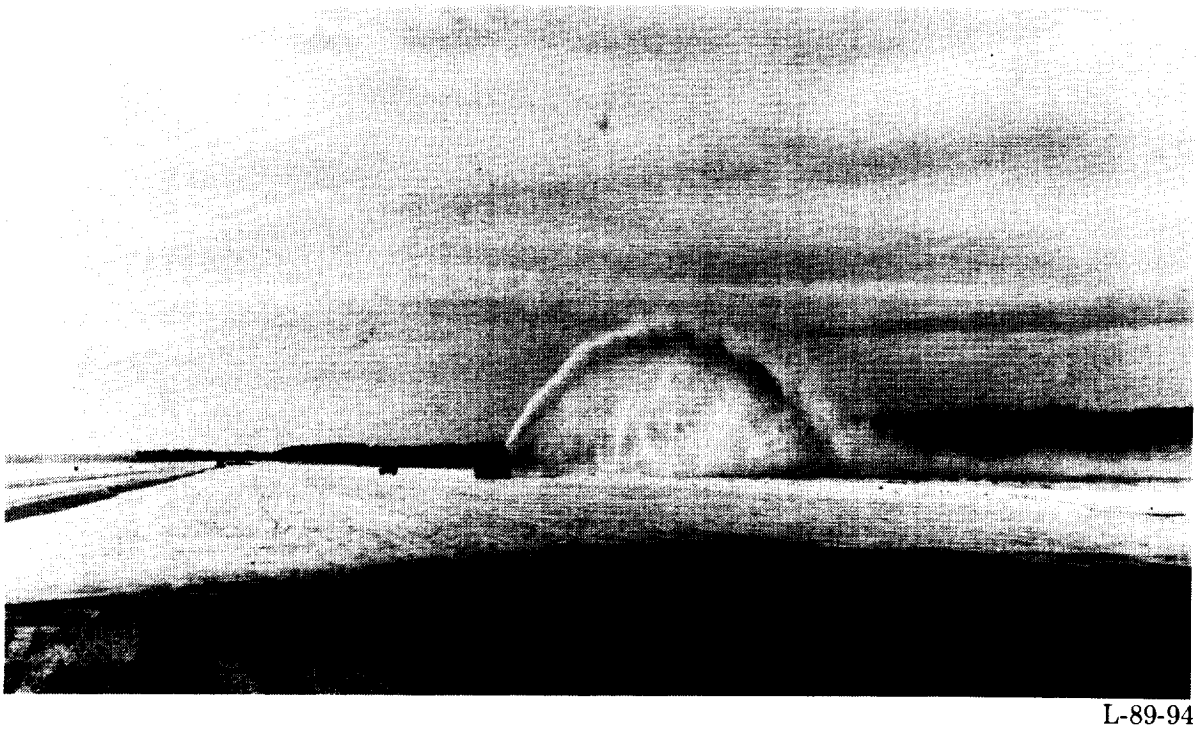

L-89-94

(b) Overview of snow blower in operation.

Figure 39. Snow removal equipment used at BNAS.

L-89-95

(c) Close-up view of snow blower in operation.

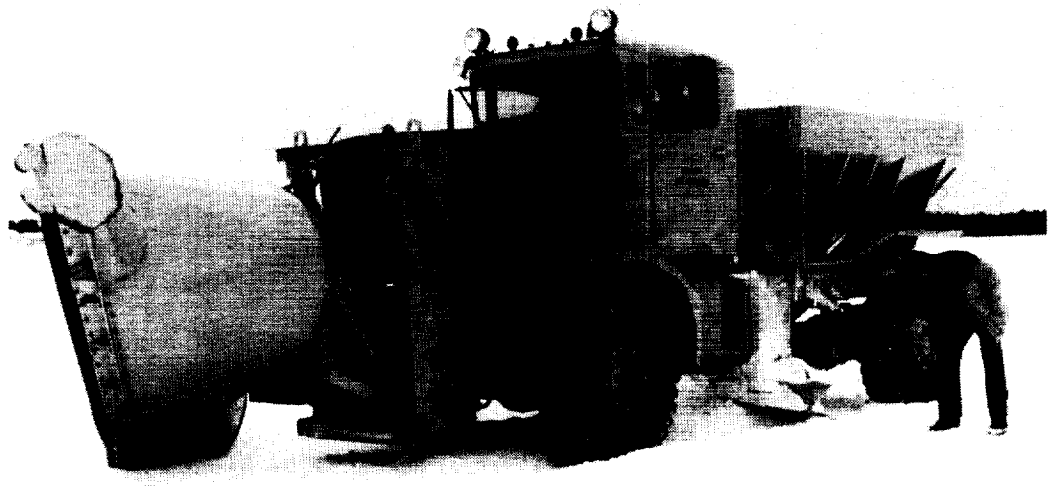

L-89-96

(d) Snow plow.

Figure 39. Concluded.

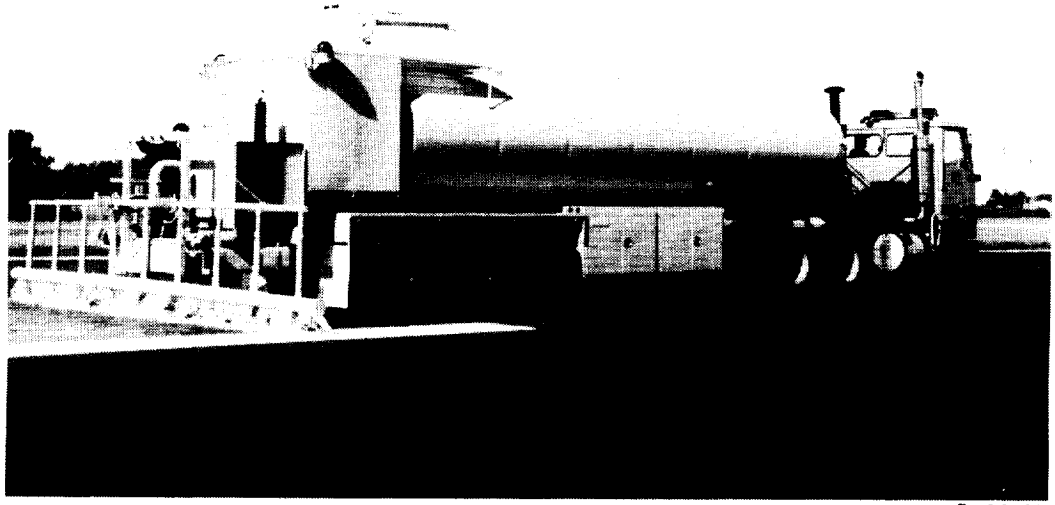

L-89-97

(a) Truck used at Wallops Flight Facility.

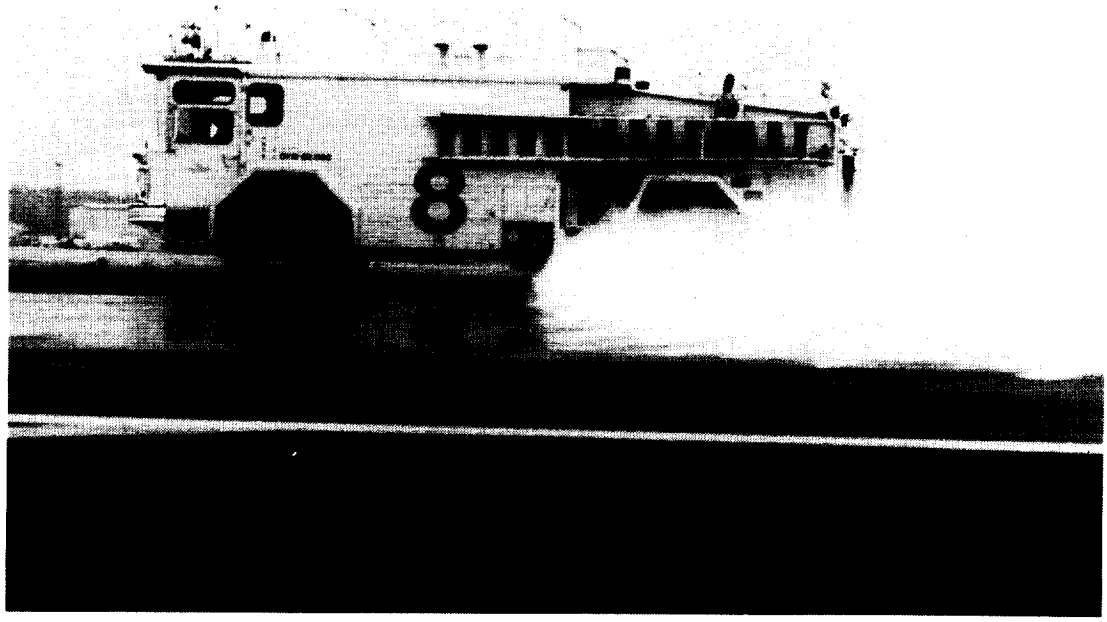

L-89-98

(b) Truck used at FAA Technical Center.

Figure 40. Trucks used to wet test surfaces.

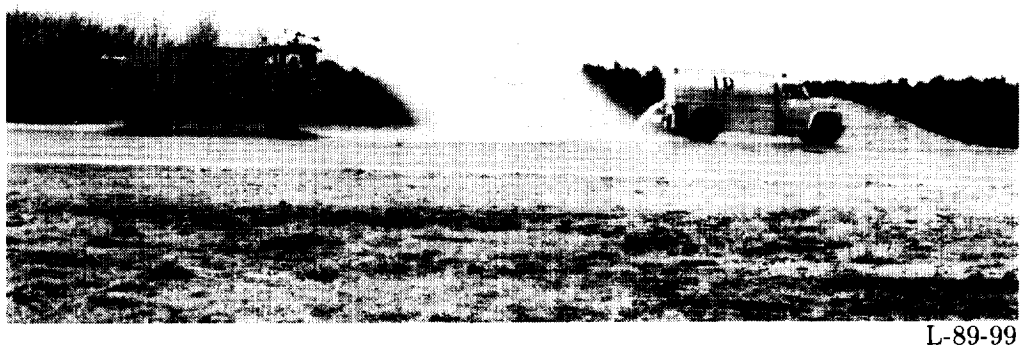

L-89-99

(c) Trucks used at BNAS.

Figure 40. Concluded.

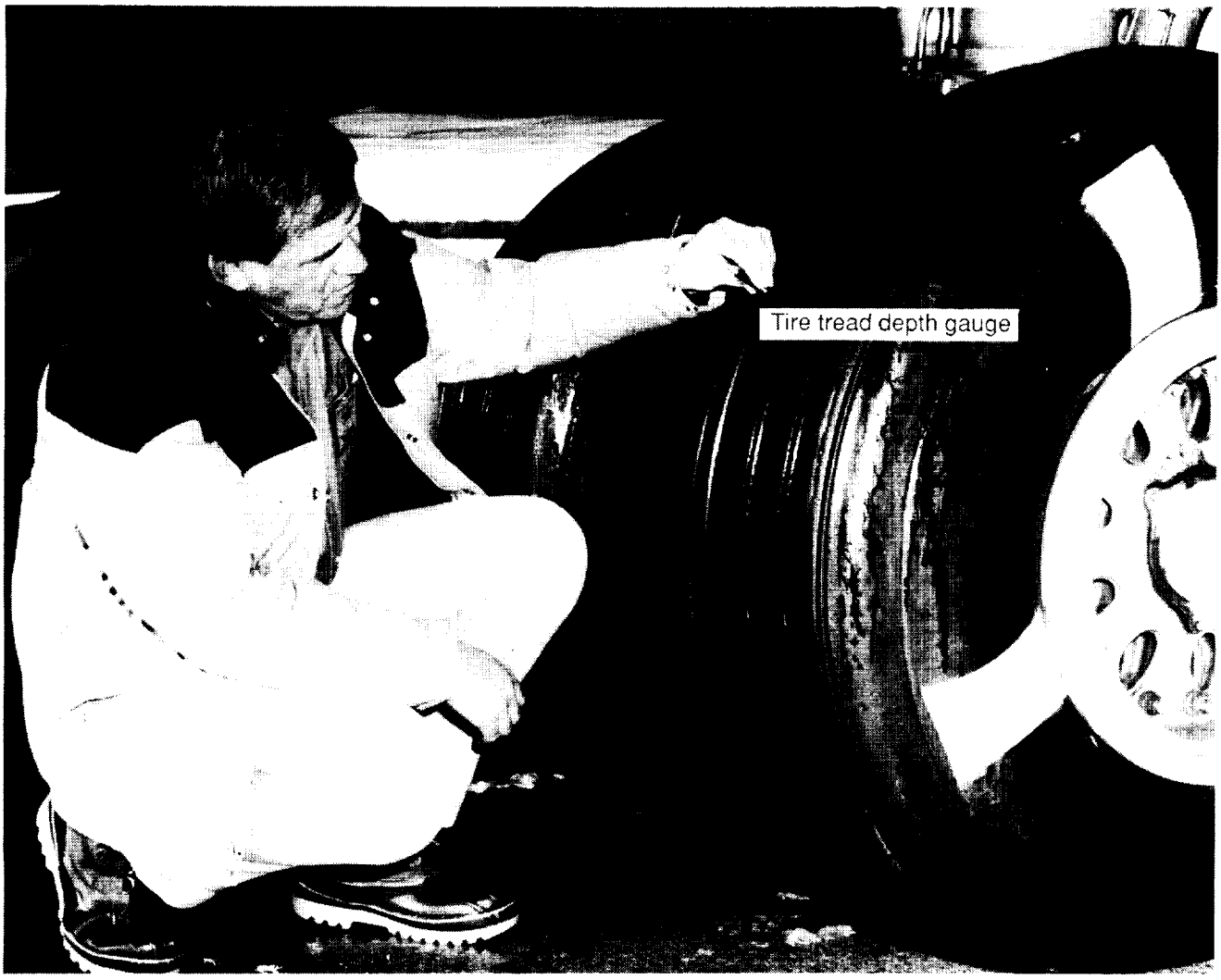

L-89-100

Figure 41. Measurement of aircraft tire tread groove depth.

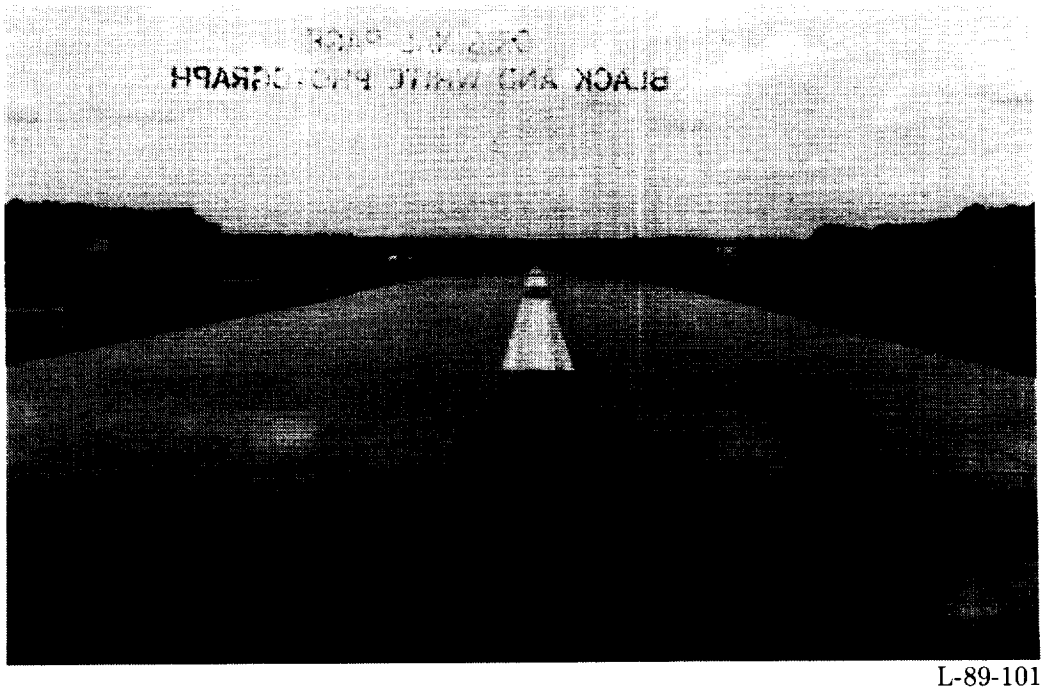

L-89-101

(a) Truck-wet runway surface.

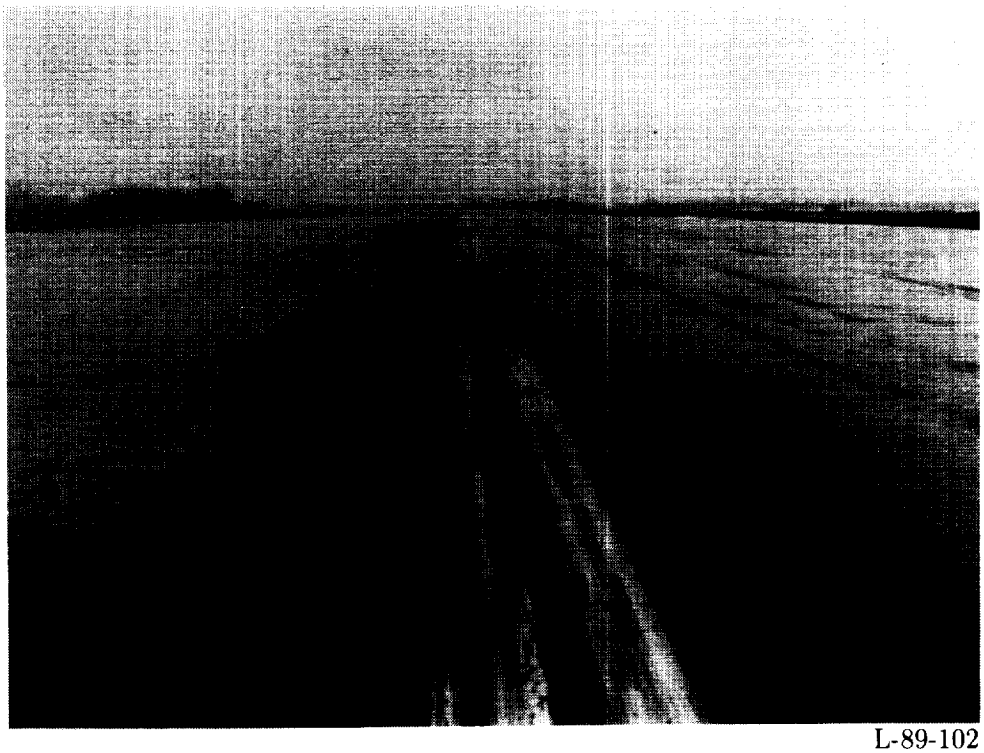

L-89-102

(b) Rain-wet runway surface.

Figure 42. Contaminated runway test-surface conditions.

L-89-103

(c) Compacted snow-covered runway surface.

L-89-104

(d) Slush-covered runway surface.

Figure 42. Continued.

L-89-105

(e) Ice-covered runway surface.

Figure 42. Concluded.

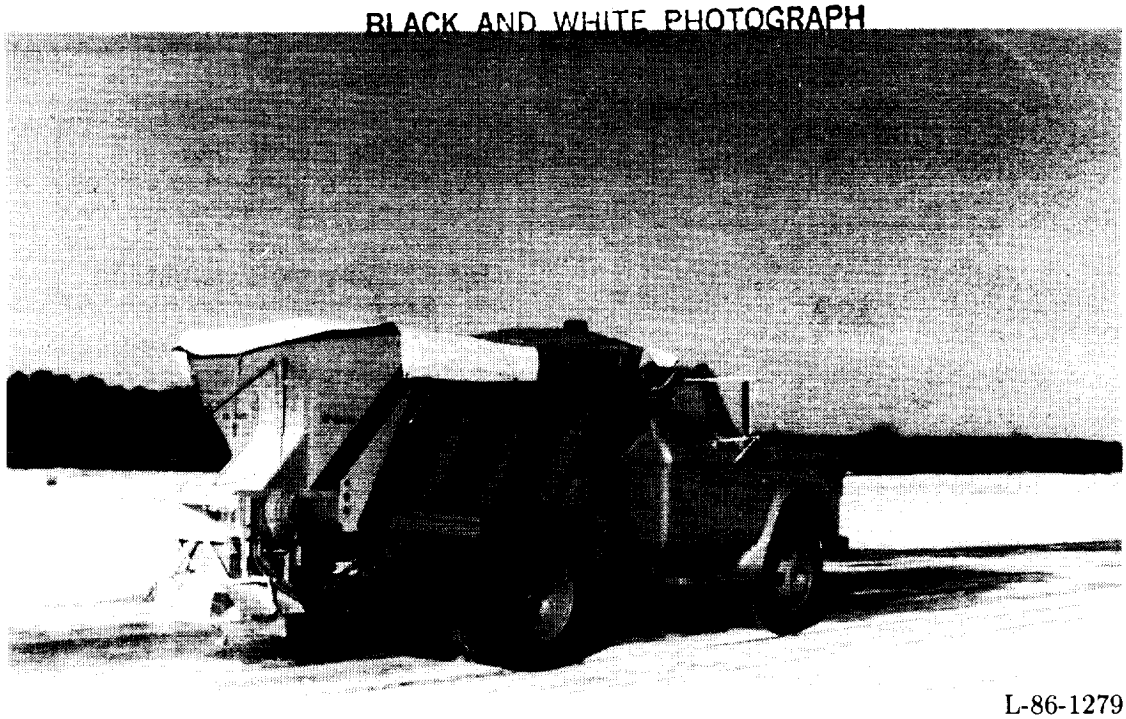

L-86-1279

(a) Dry urea.

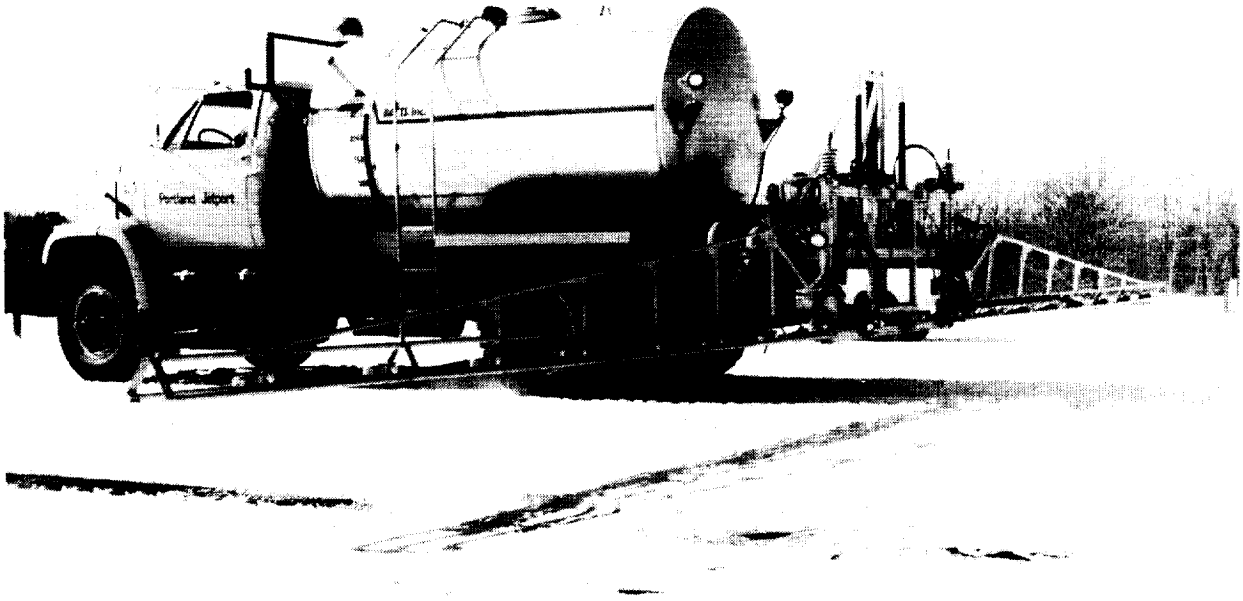

L-86-2503

(b) Liquid UCAR.

Figure 43. Chemical distribution trucks used at BNAS.

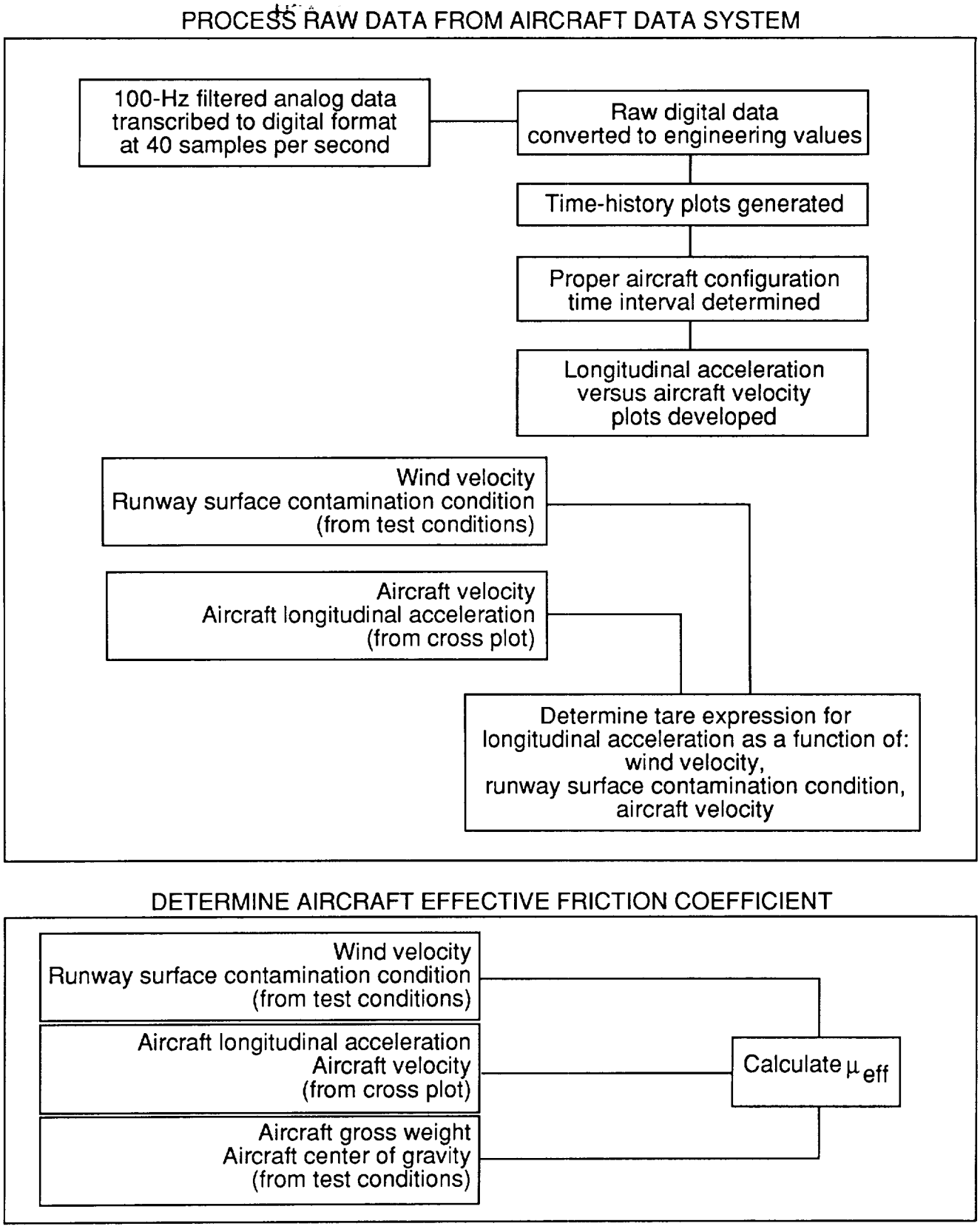

Figure 44. Flow chart of aircraft tire friction data-reduction process.

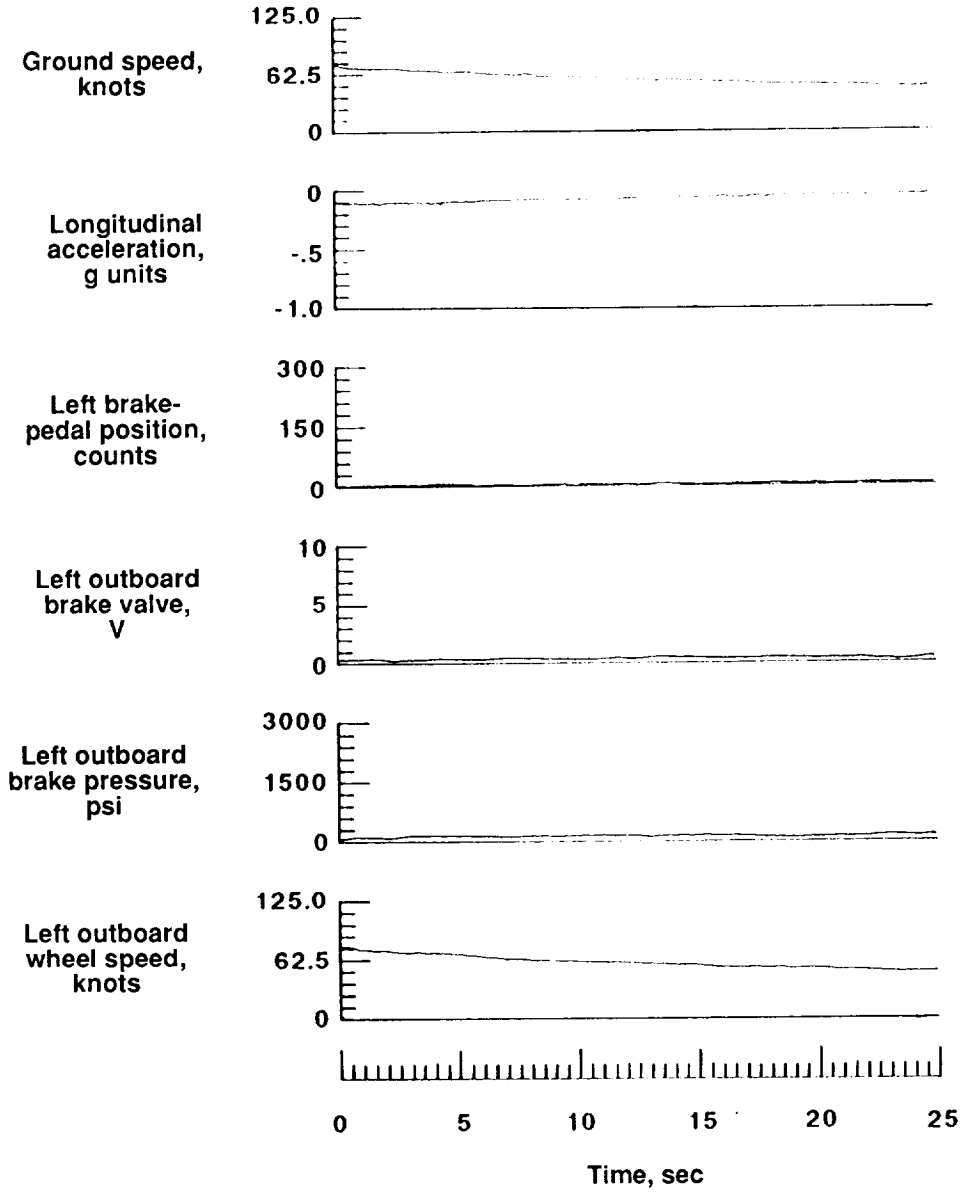

(a) Dry asphalt, nonbraking, flight 431, run 14T.

Figure 45. Examples of Boeing 737 parameter time histories and data plots obtained during test runs at BNAS.

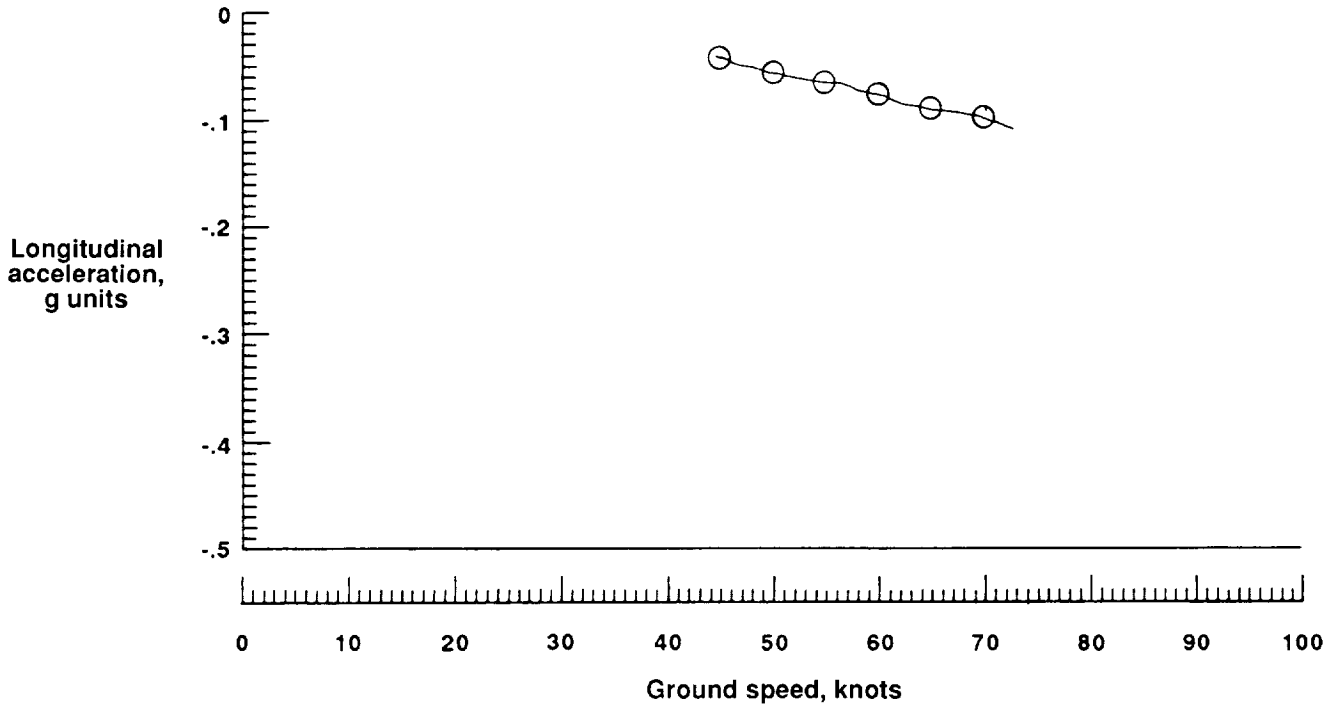

(b) Dry asphalt, nonbraking, flight 431, run 14T, longitudinal acceleration versus ground speed.

Figure 45. Continued.

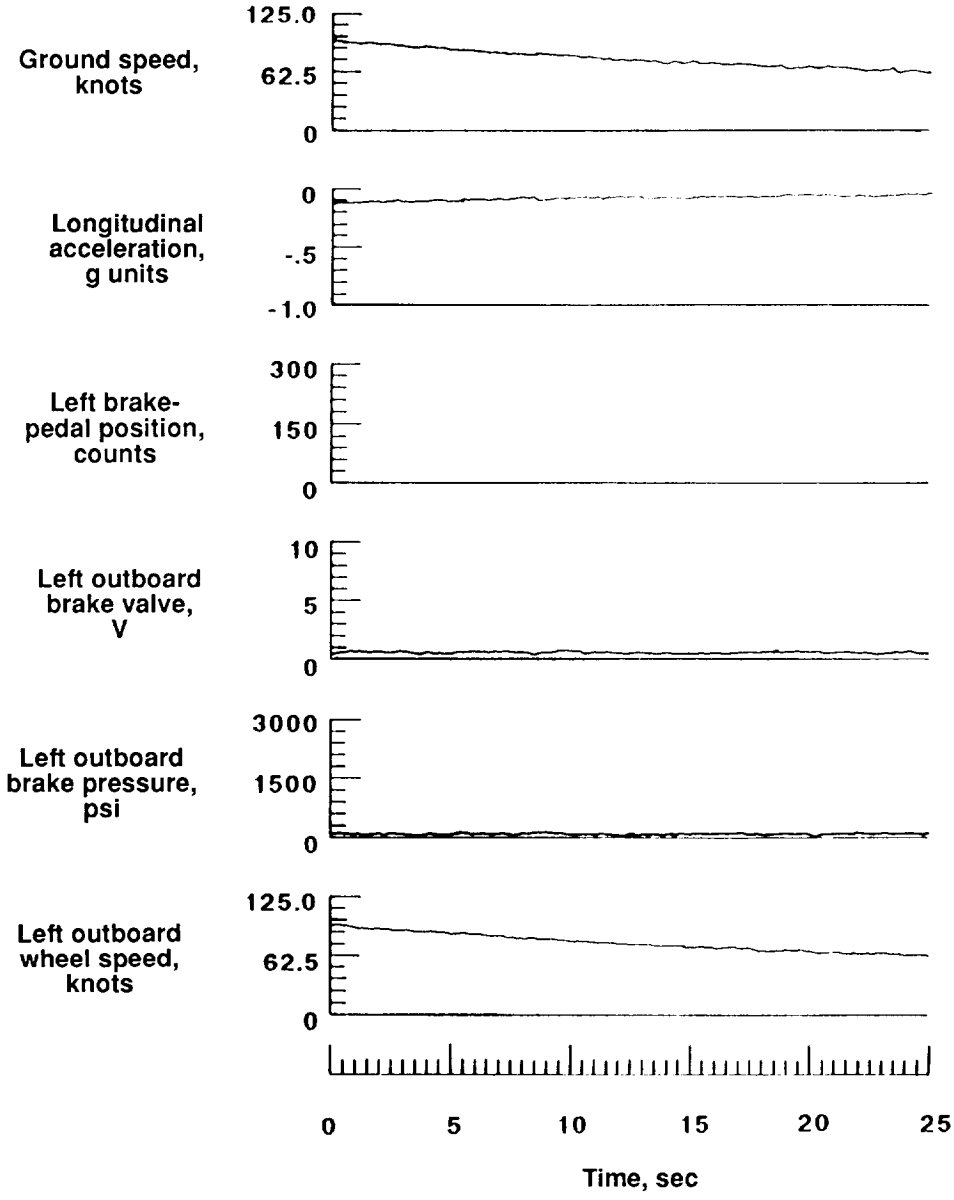

(c) Dry asphalt, nonbraking, flight 432, run 14R2.

Figure 45. Continued.

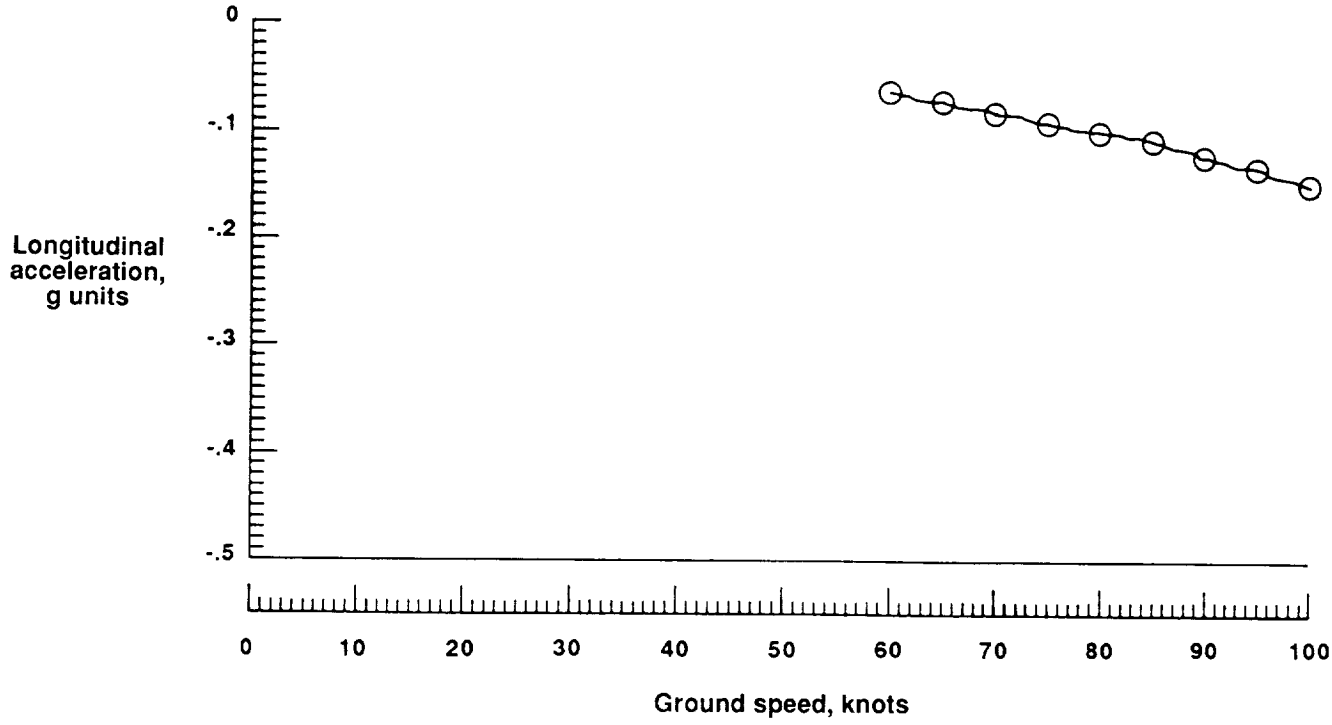

(d) Dry asphalt, nonbraking, flight 432, run 14R2, longitudinal acceleration versus ground speed.

Figure 45. Continued.

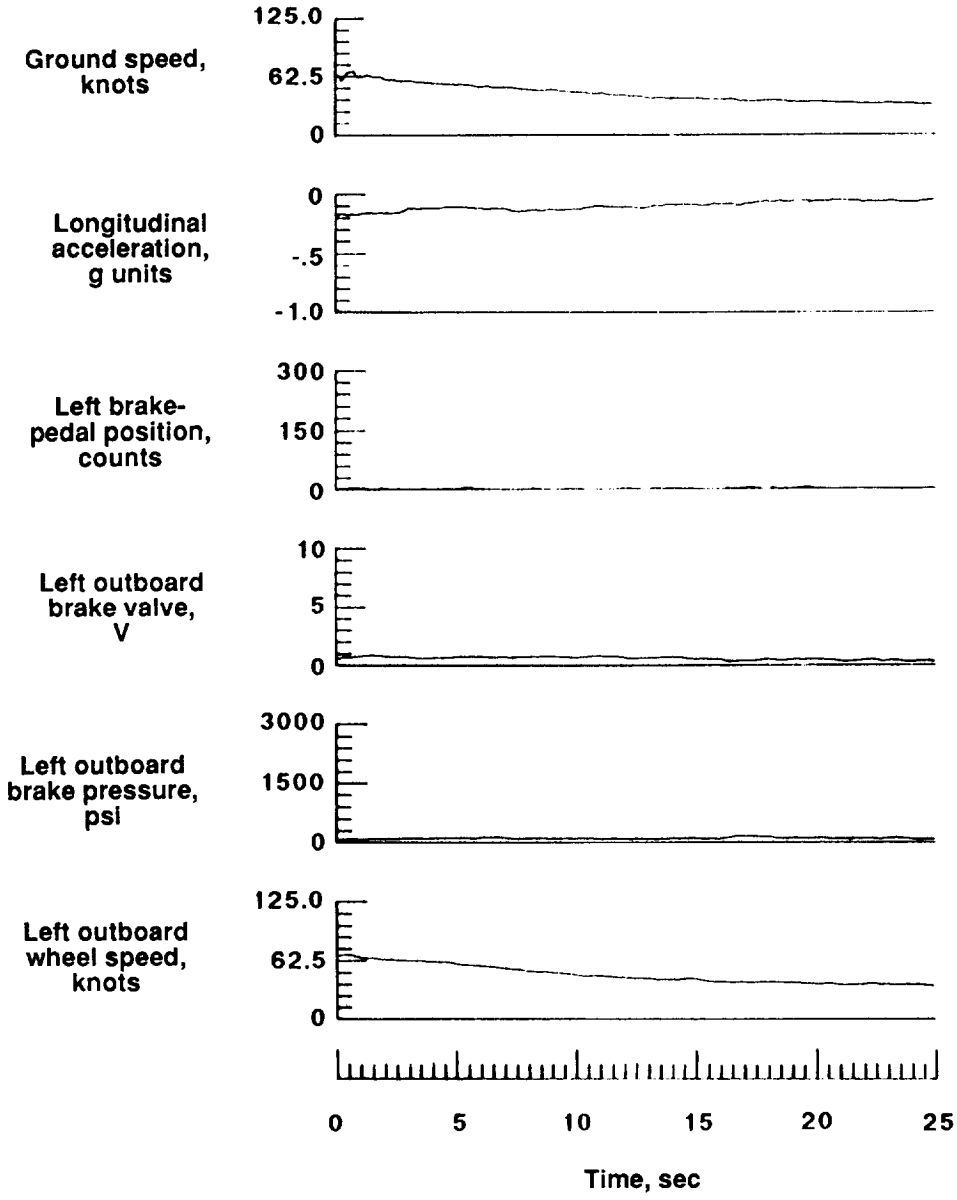

(e) 4-in. wet snow, nonbraking, flight 432, run 9.

Figure 45. Continued.

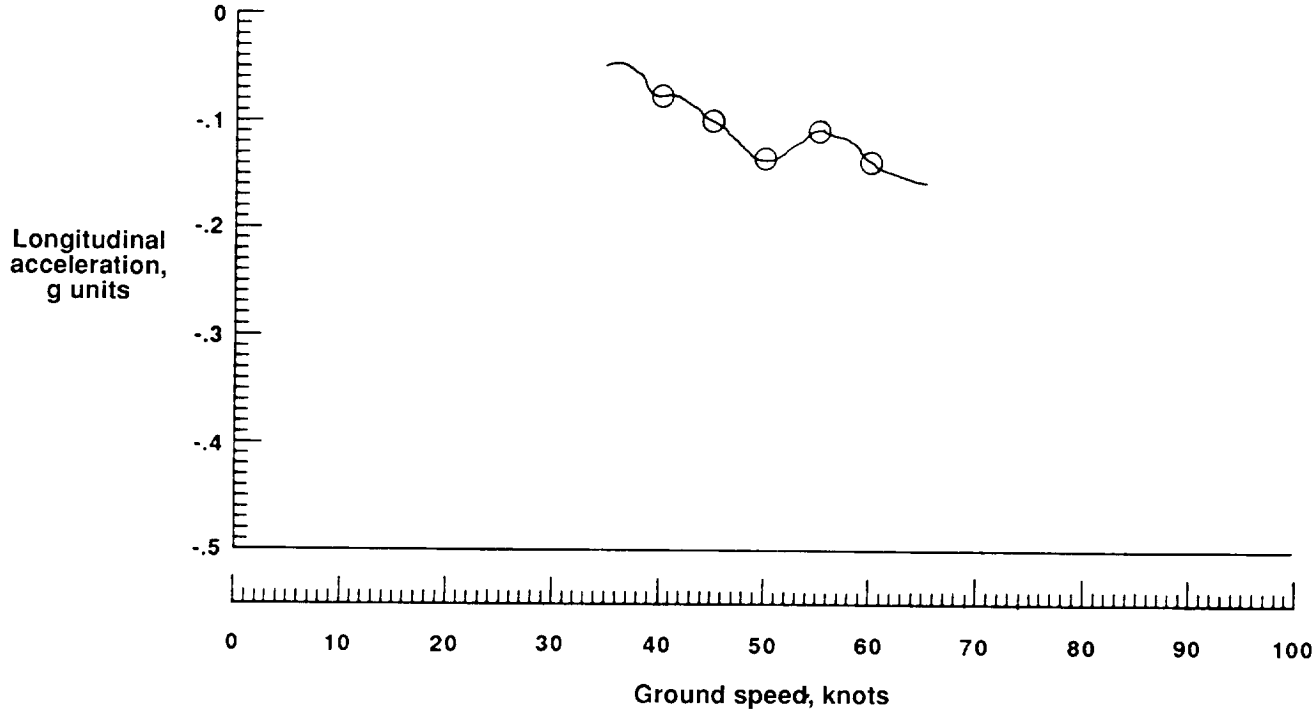

(f) 4-in. wet snow, nonbraking, flight 432, run 9, longitudinal acceleration versus ground speed.

Figure 45. Continued.

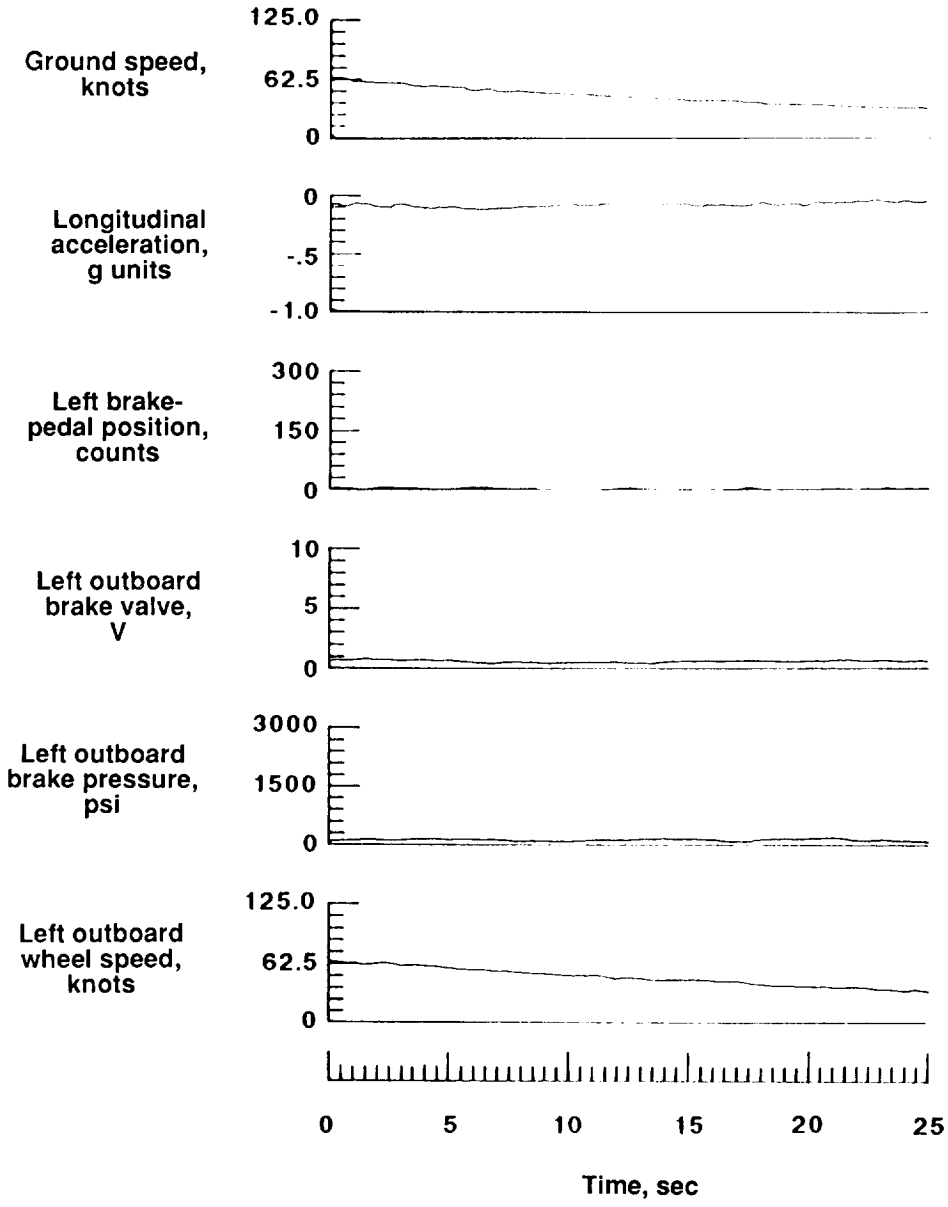

(g) 4-in. wet snow, nonbraking, flight 432, run 7.

Figure 45. Continued.

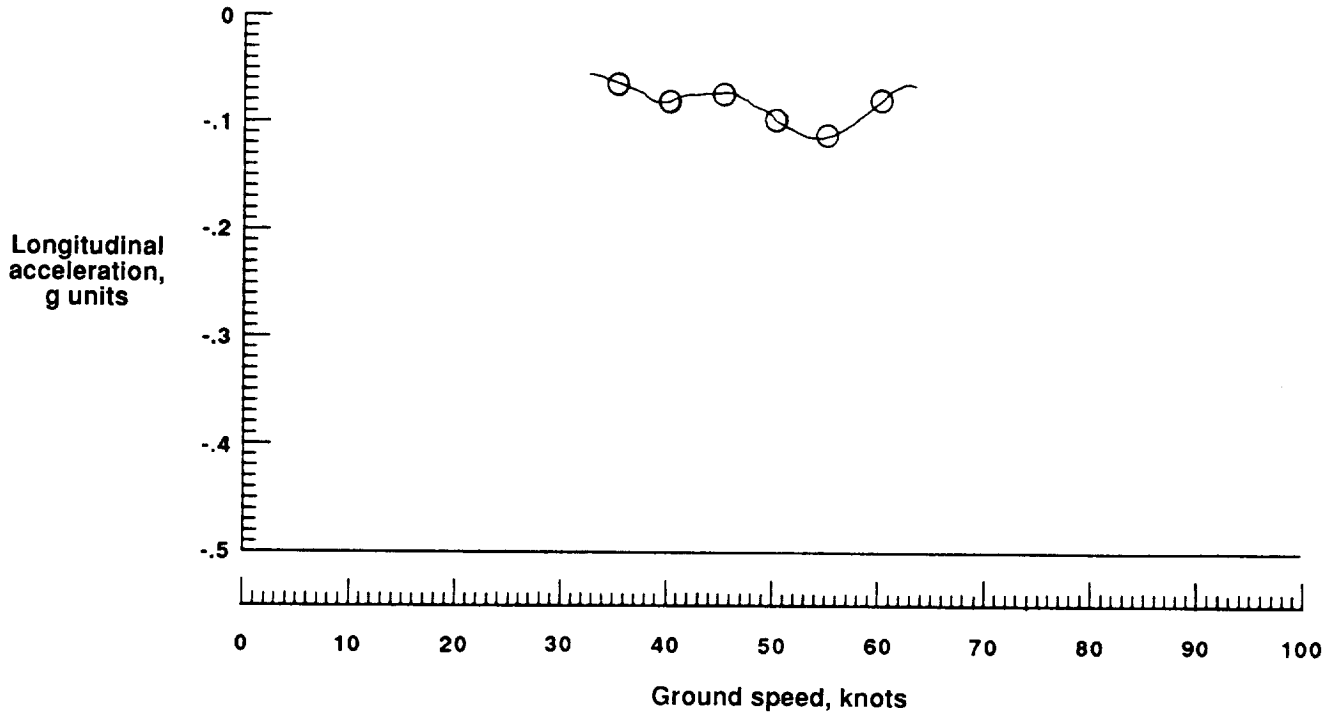

(h) 4-in. wet snow, nonbraking, flight 432, run 7, longitudinal acceleration versus ground speed.

Figure 45. Continued.

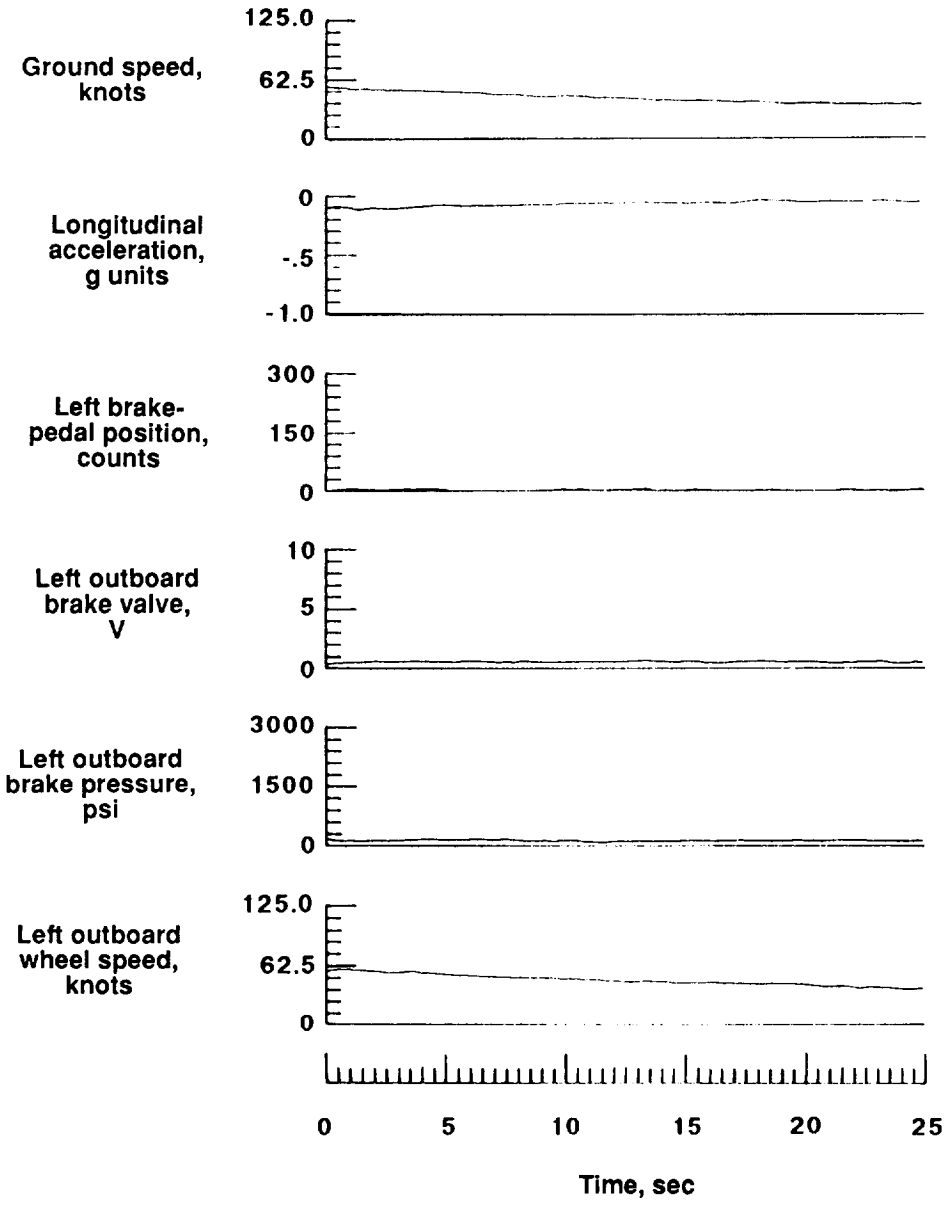

(i) 6-in. dry snow, nonbraking, flight 430, run 7.

Figure 45. Continued.

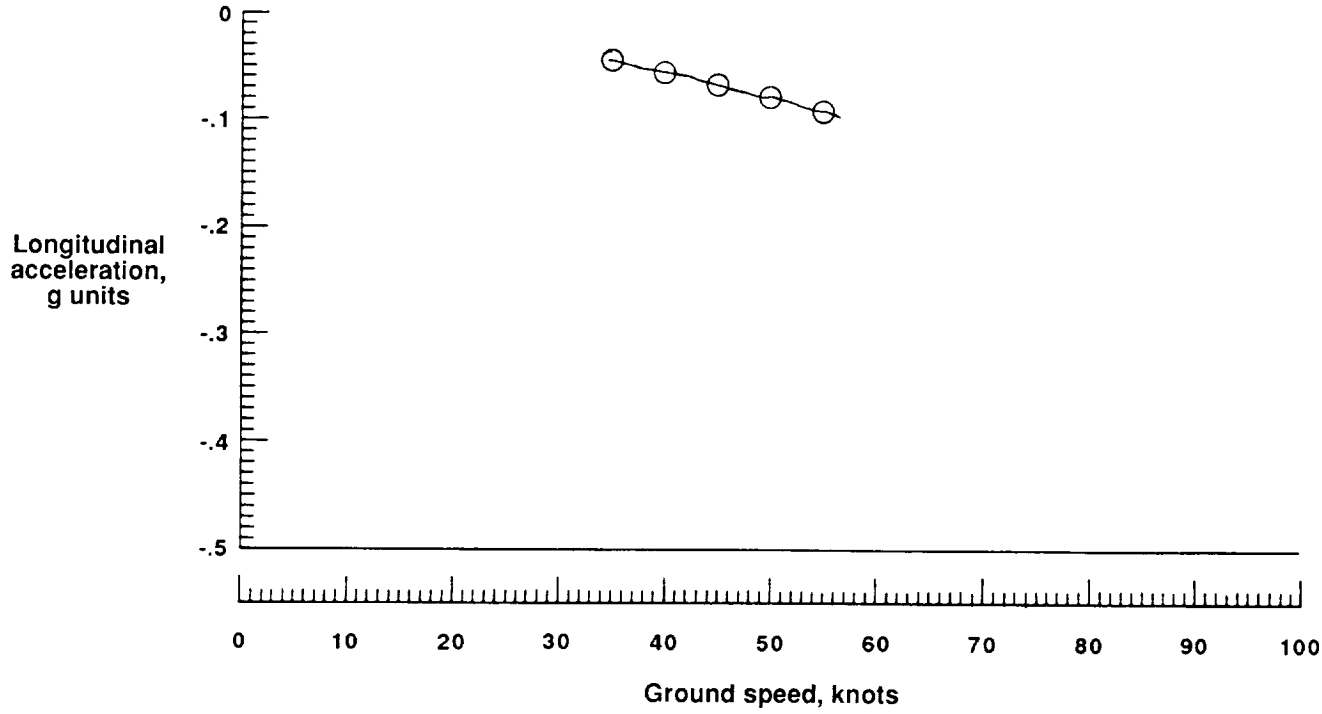

(j) 6-in. dry snow, nonbraking, flight 430, run 7, longitudinal acceleration versus ground speed.

Figure 45. Continued.

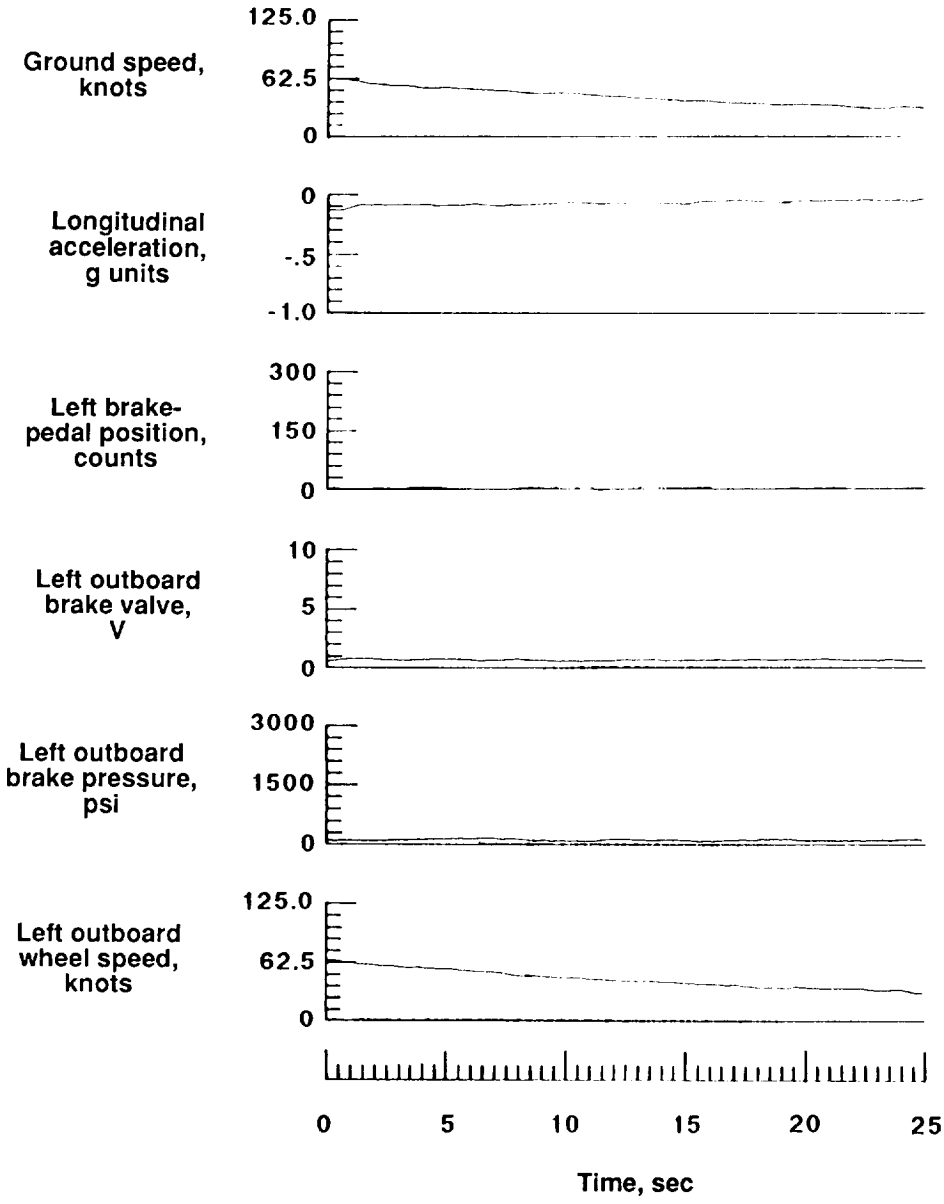

(k) 6-in. dry snow, nonbraking, flight 430, run 9.

Figure 45. Continued.

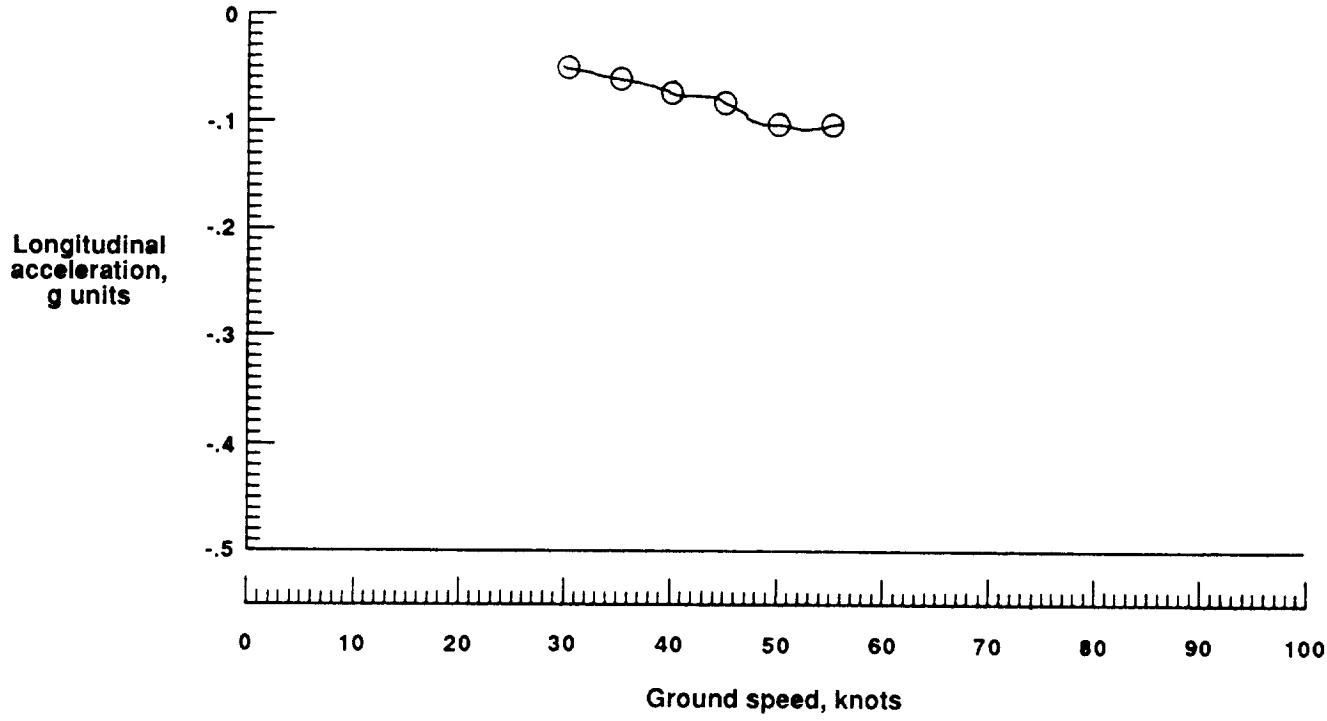

(l) 6-in. dry snow, nonbraking, flight 430, run 9, longitudinal acceleration versus ground speed.

Figure 45. Continued.

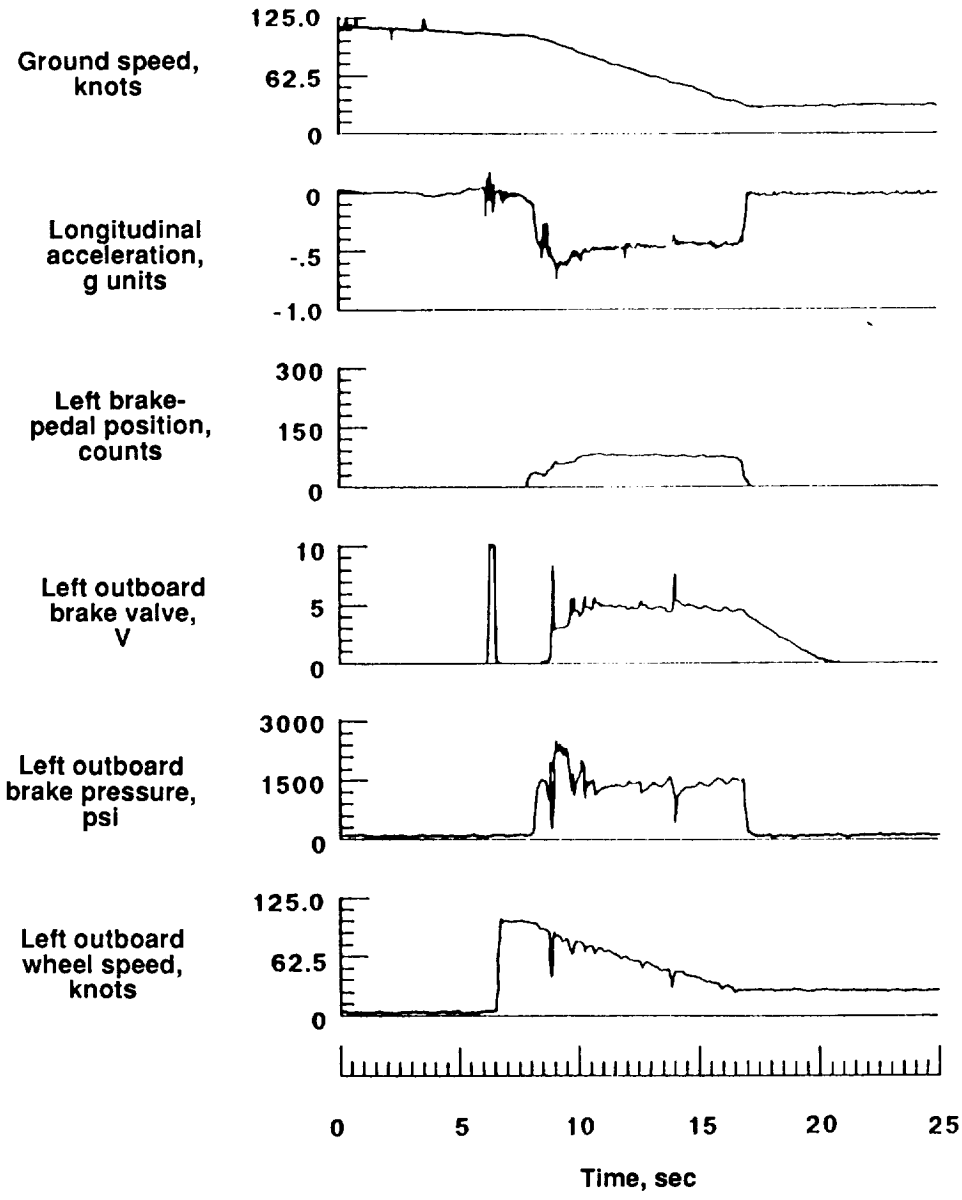

(m) Dry asphalt, maximum antiskid braking, flight 410, run 18.

Figure 45. Continued.

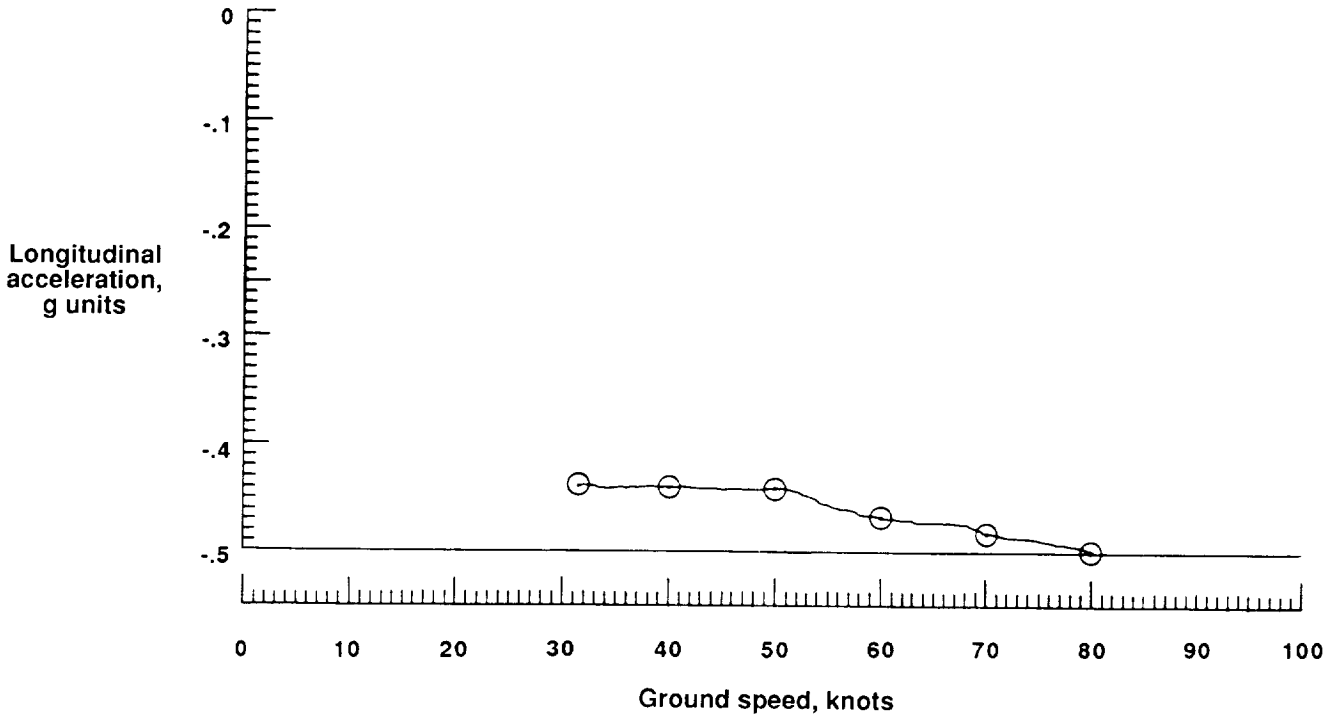

(n) Dry asphalt, maximum antiskid braking, flight 410, run 18, longitudinal acceleration versus ground speed.

Figure 45. Continued.

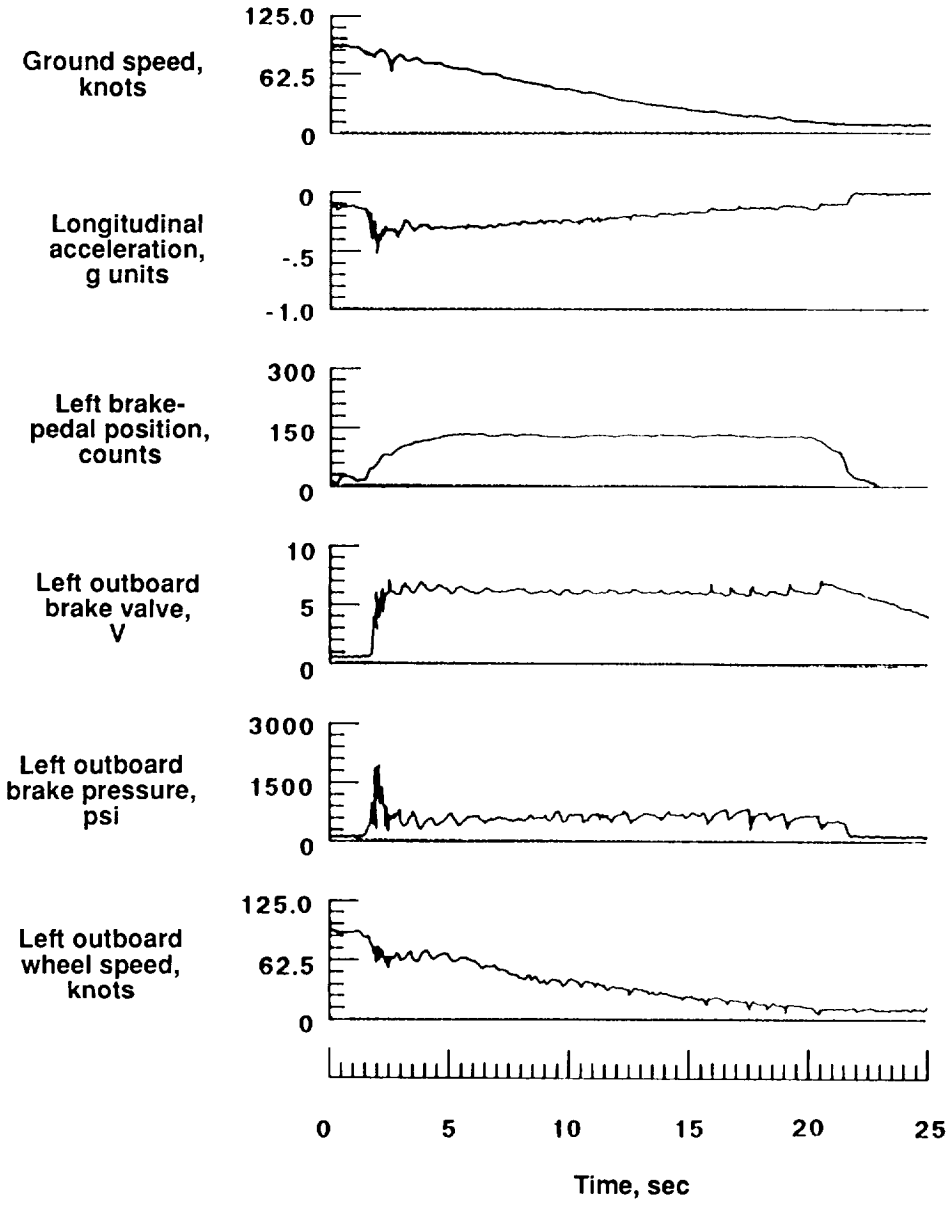

(o) 6-in. loose snow, maximum antiskid braking, flight 430, run 5.

Figure 45. Continued.

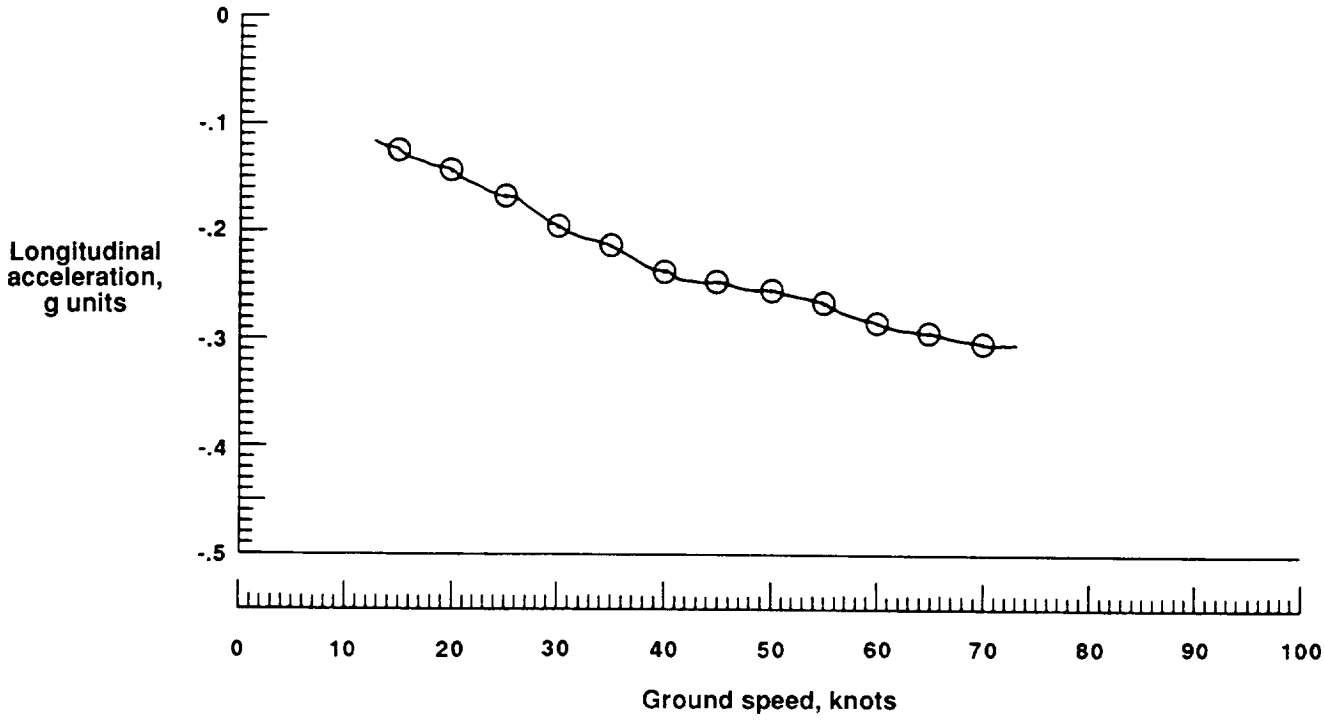

(p) 6-in. loose snow, maximum antiskid braking, flight 430, run 5, longitudinal acceleration versus ground speed.

Figure 45. Continued.

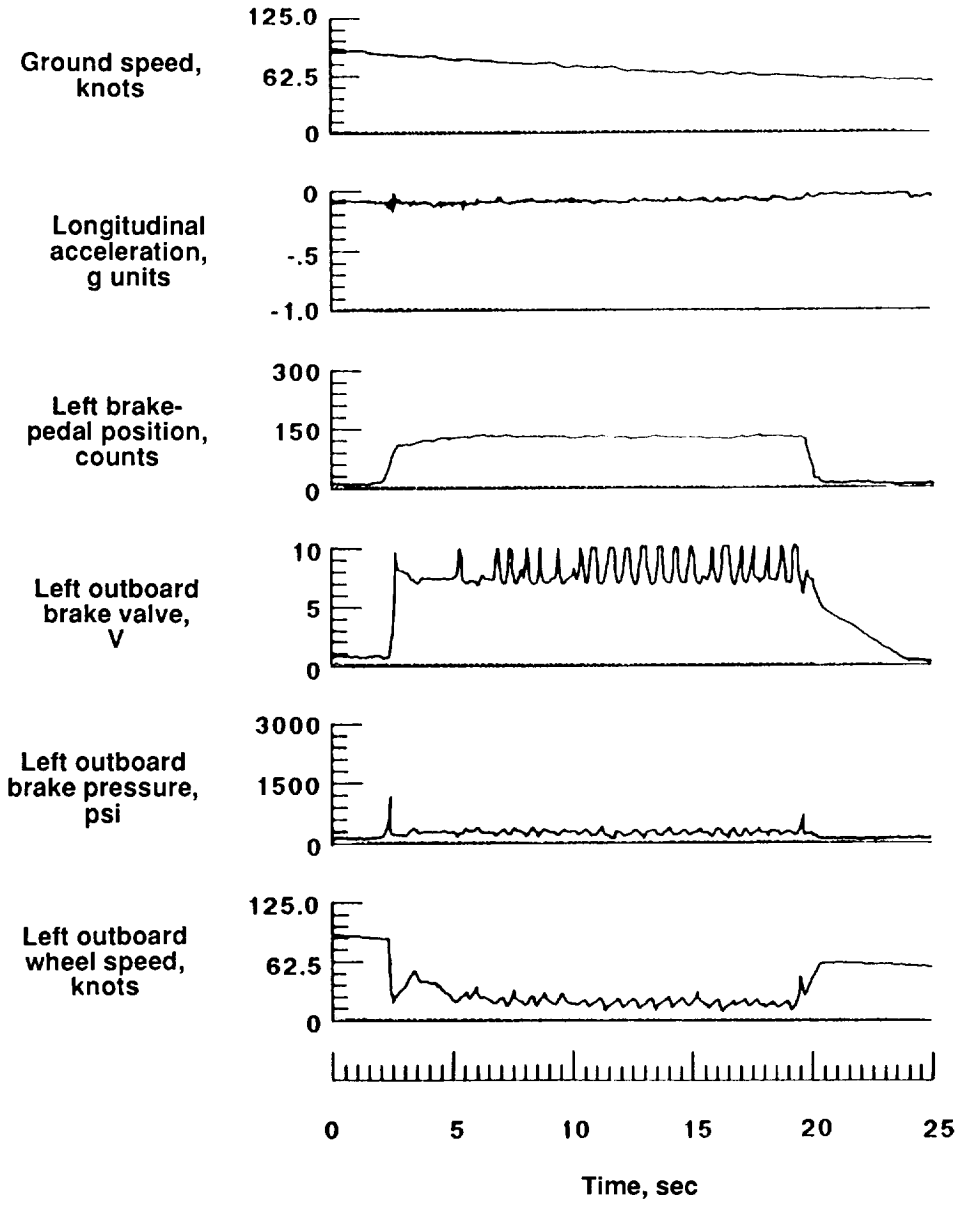

(q) Ice-covered asphalt, maximum antiskid braking, flight 433, run 5.

Figure 45. Continued.

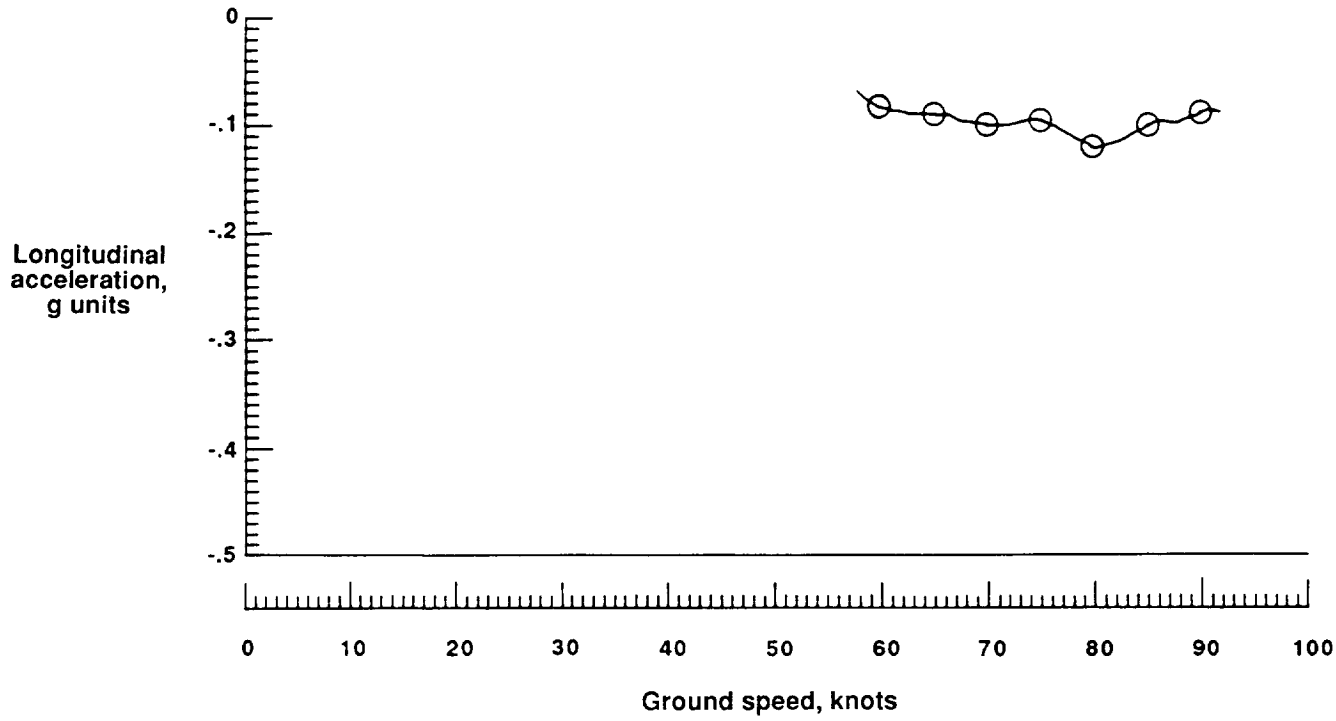

(r) Ice-covered asphalt, maximum antiskid braking, flight 433, run 5, longitudinal acceleration versus ground speed.

Figure 45. Concluded.

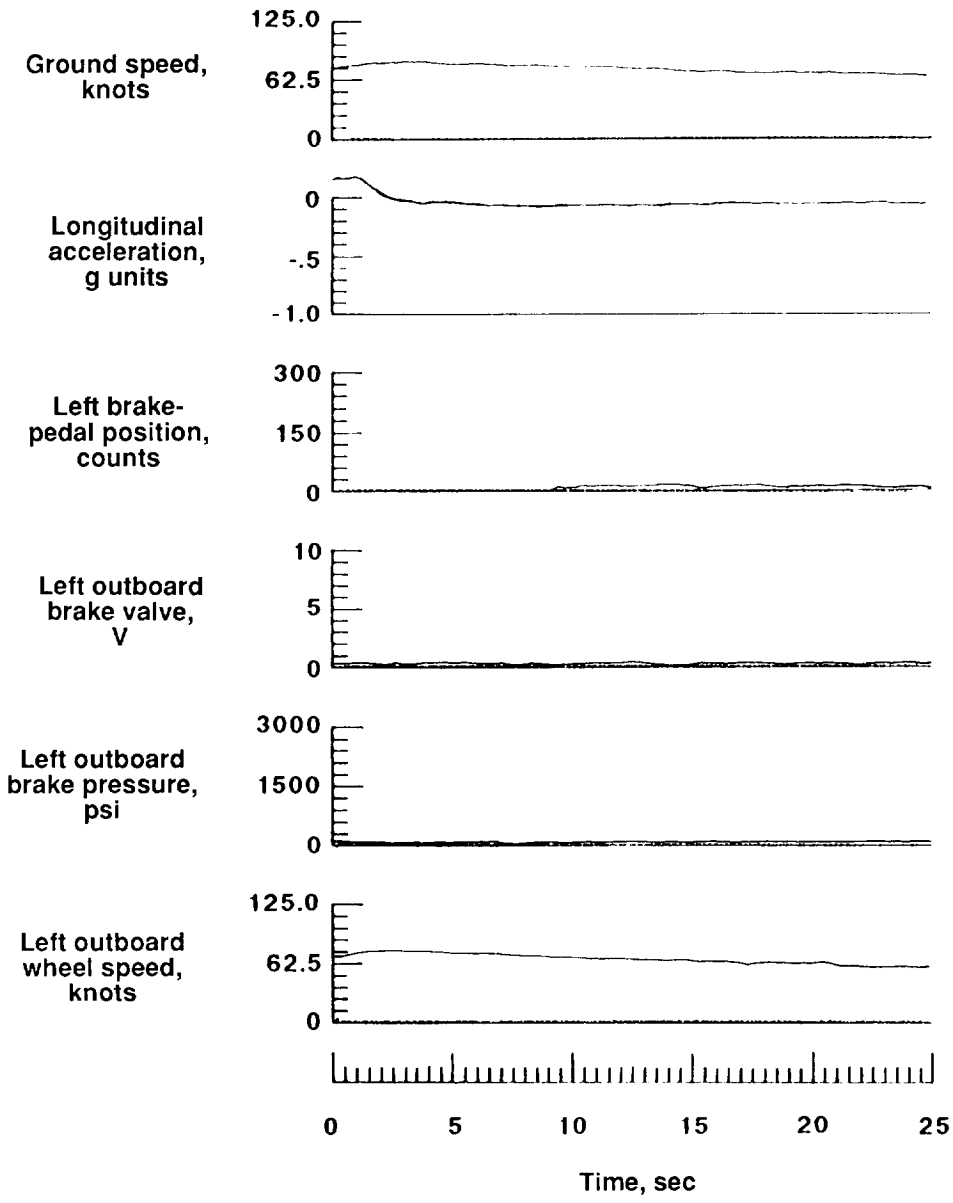

(a) Dry asphalt, nonbraking, flight 028, run CAL.

Figure 46. Examples of Boeing 727 parameter time histories and data plots obtained during test runs at BNAS.

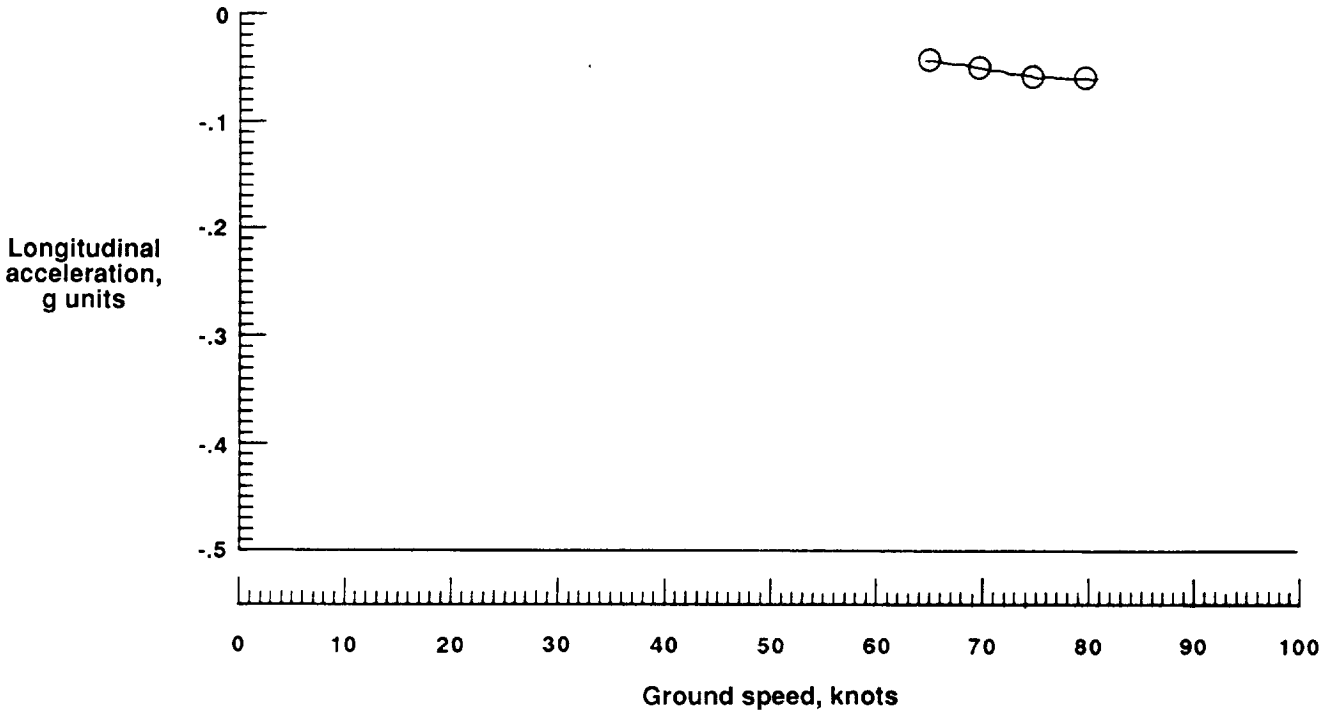

(b) Dry asphalt, nonbraking, flight 028, run CAL, longitudinal acceleration versus ground speed.

Figure 46. Continued.

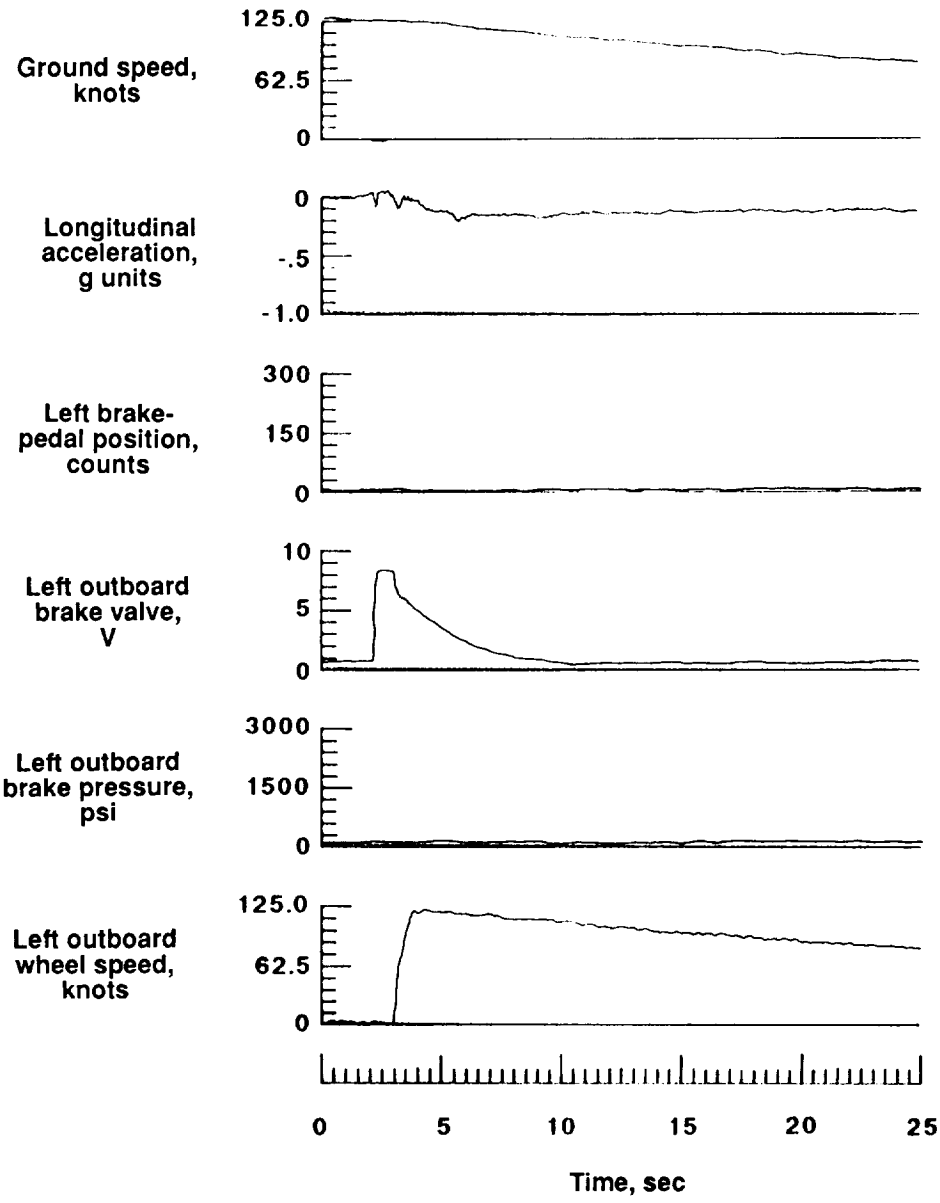

(c) Dry asphalt, nonbraking, flight 006, run 13.

Figure 46. Continued.

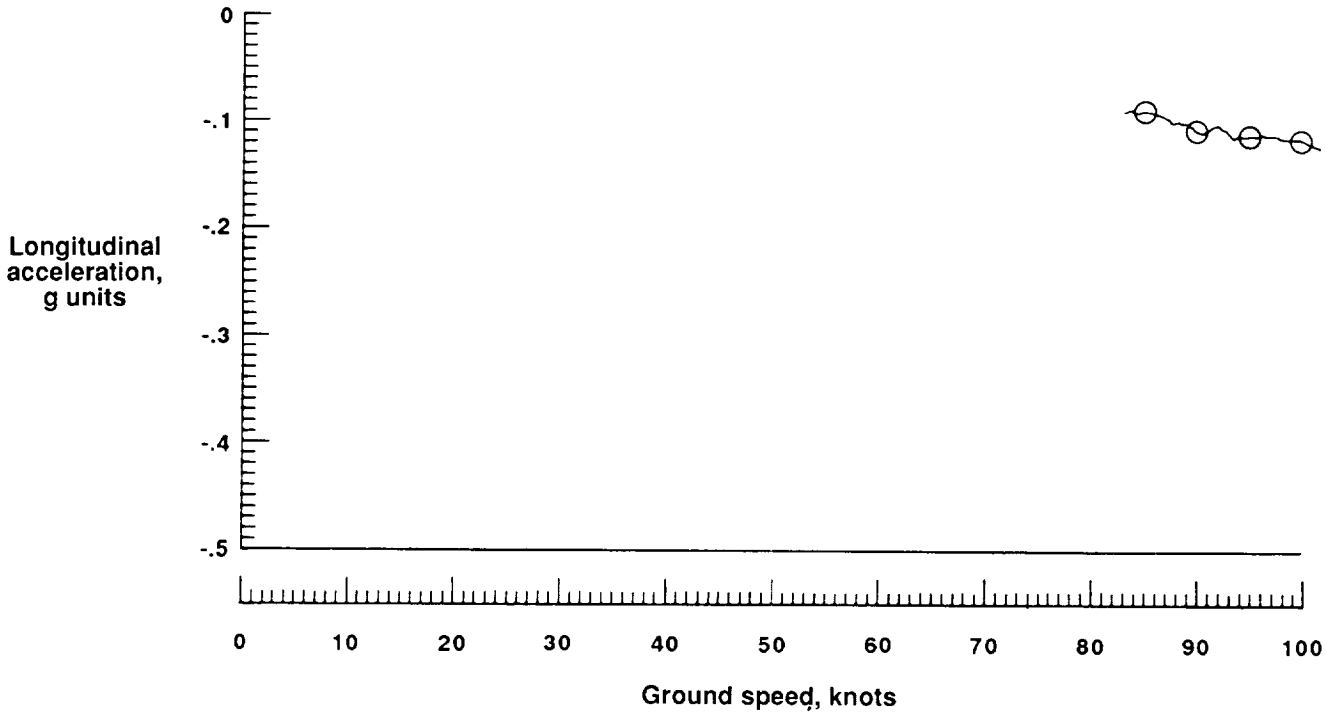

(d) Dry asphalt, nonbraking, flight 006, run 13, longitudinal acceleration versus ground speed.

Figure 46. Continued.

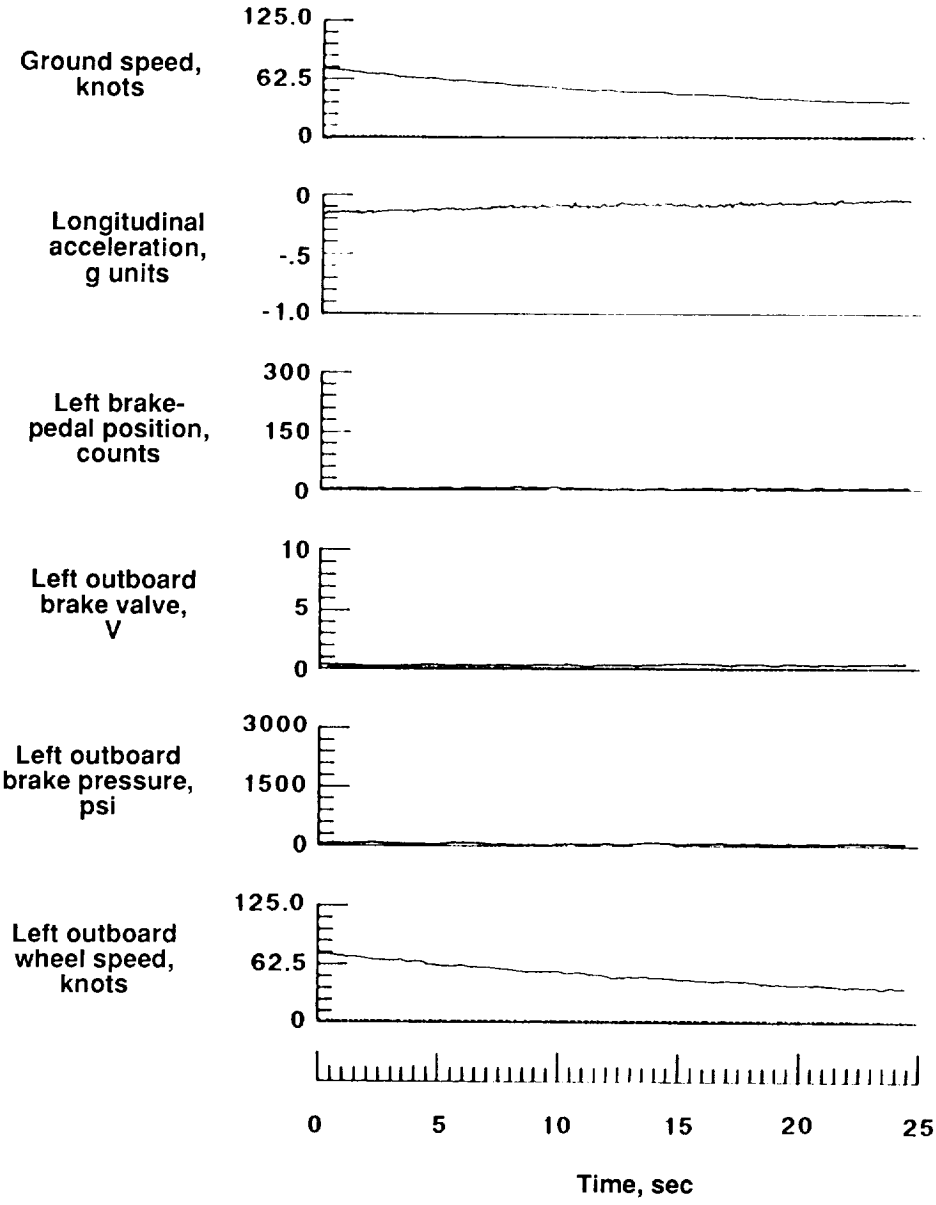

(e) 4.5-in. loose snow, nonbraking, flight 022, run 2.

Figure 46. Continued.

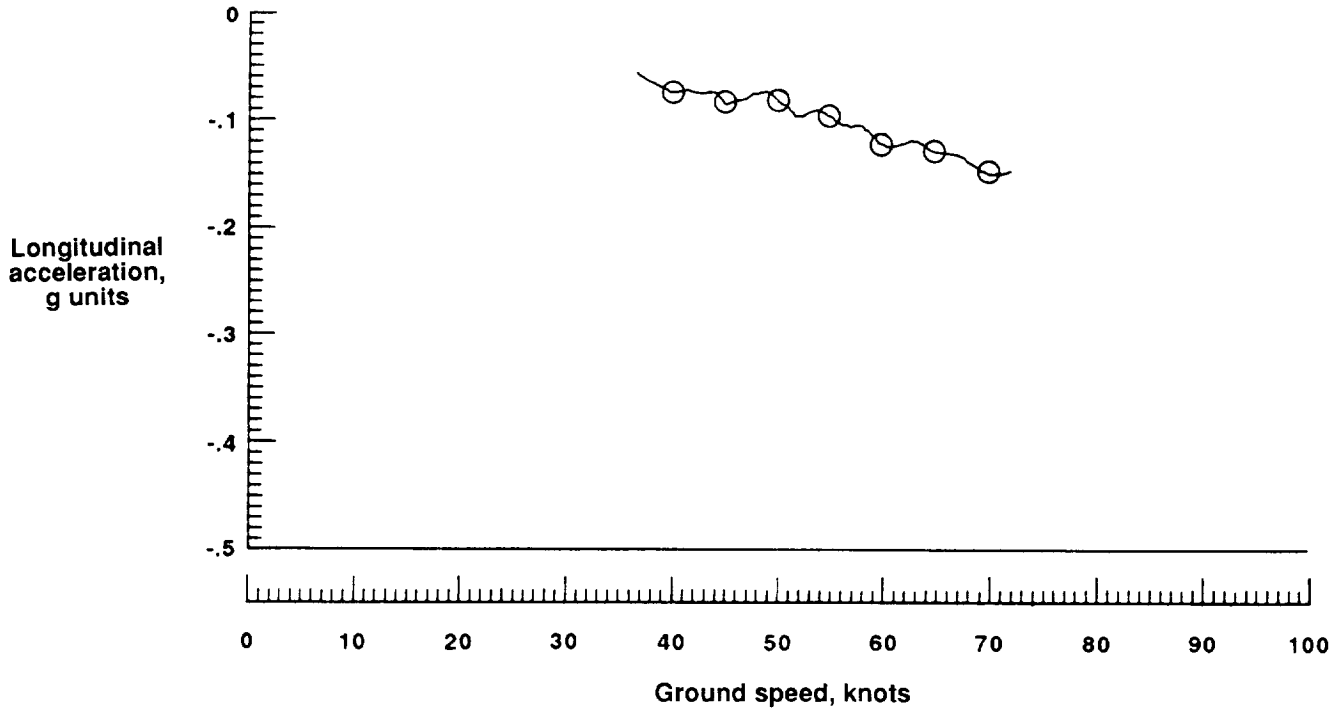

(f) 4.5-in. loose snow, nonbraking, flight 022, run 2, longitudinal acceleration versus ground speed.

Figure 46. Continued.

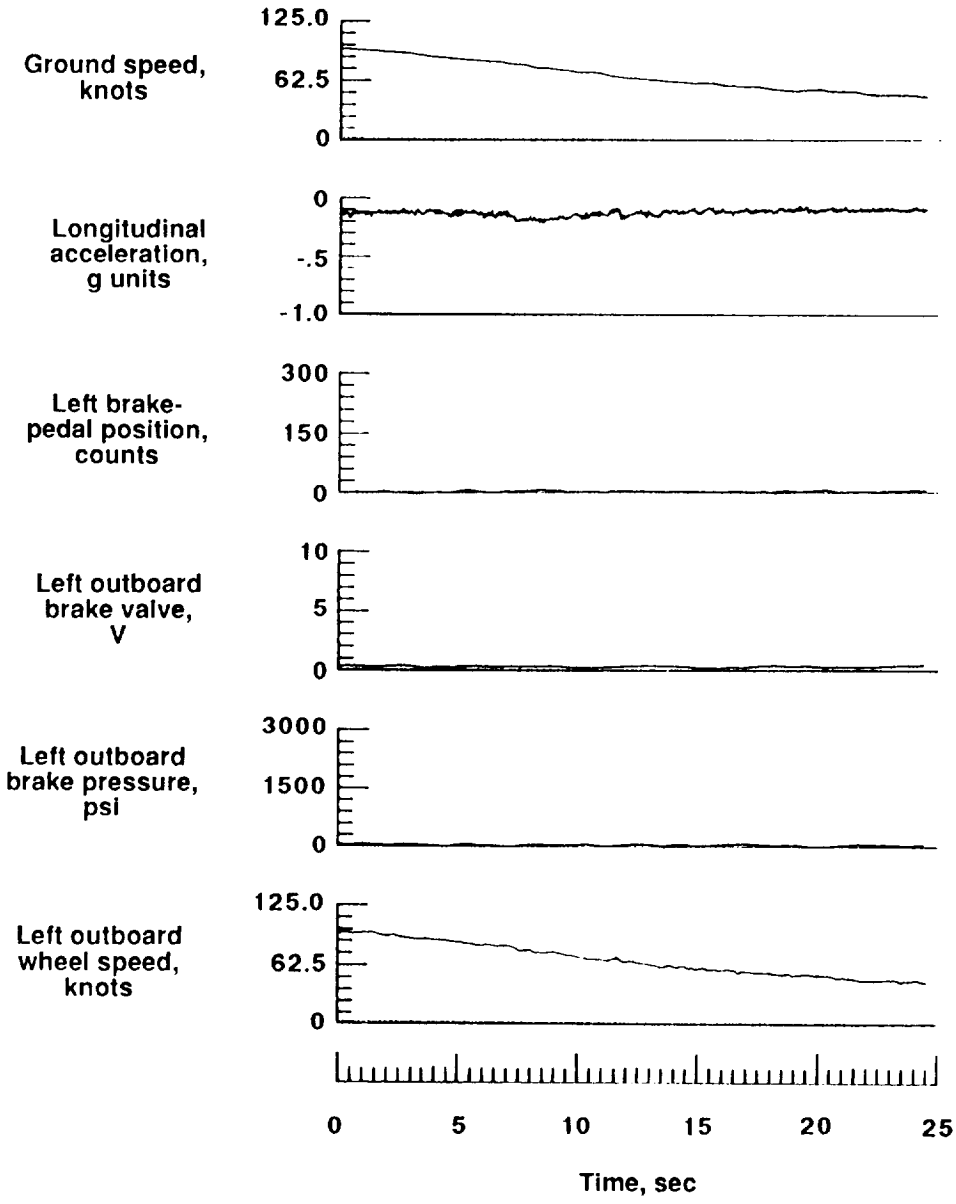

(g) 4.5-in. loose snow, nonbraking, flight 022, run 6.

Figure 46. Continued.

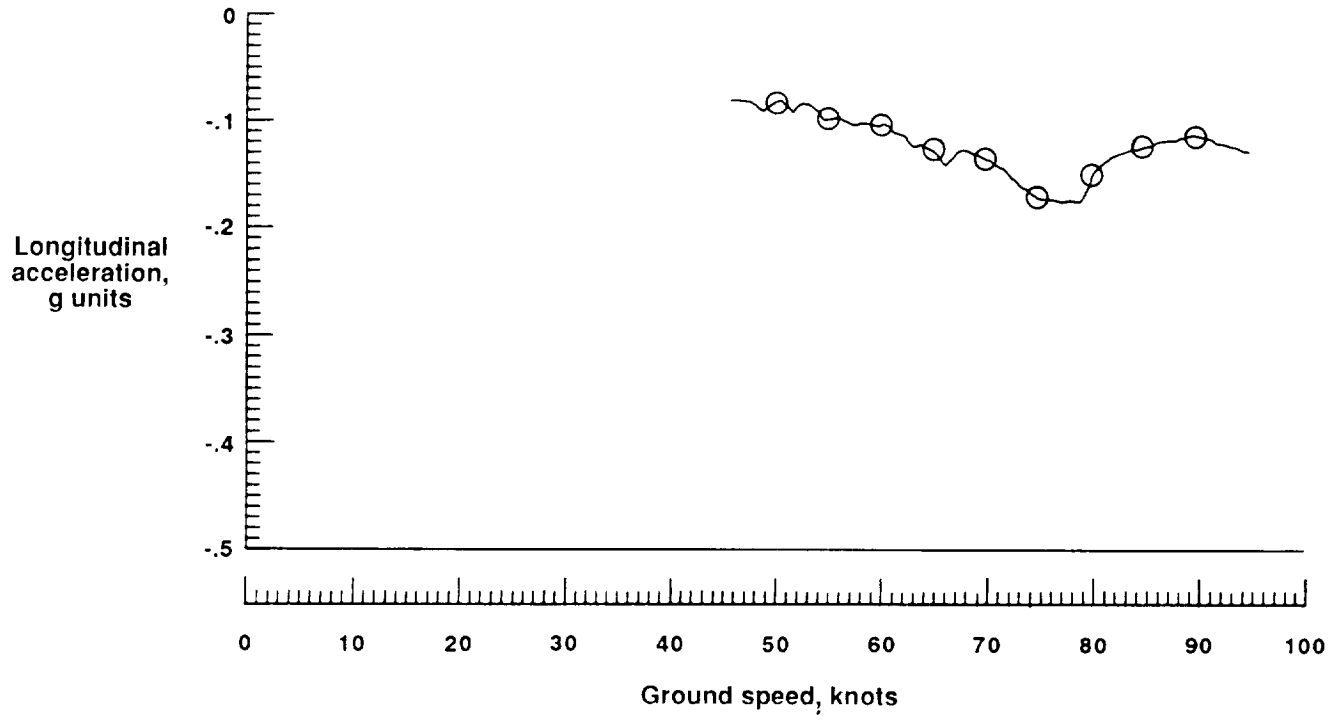

(h) 4.5-in. loose snow, nonbraking, flight 022, run 6, longitudinal acceleration versus ground speed.

Figure 46. Continued.

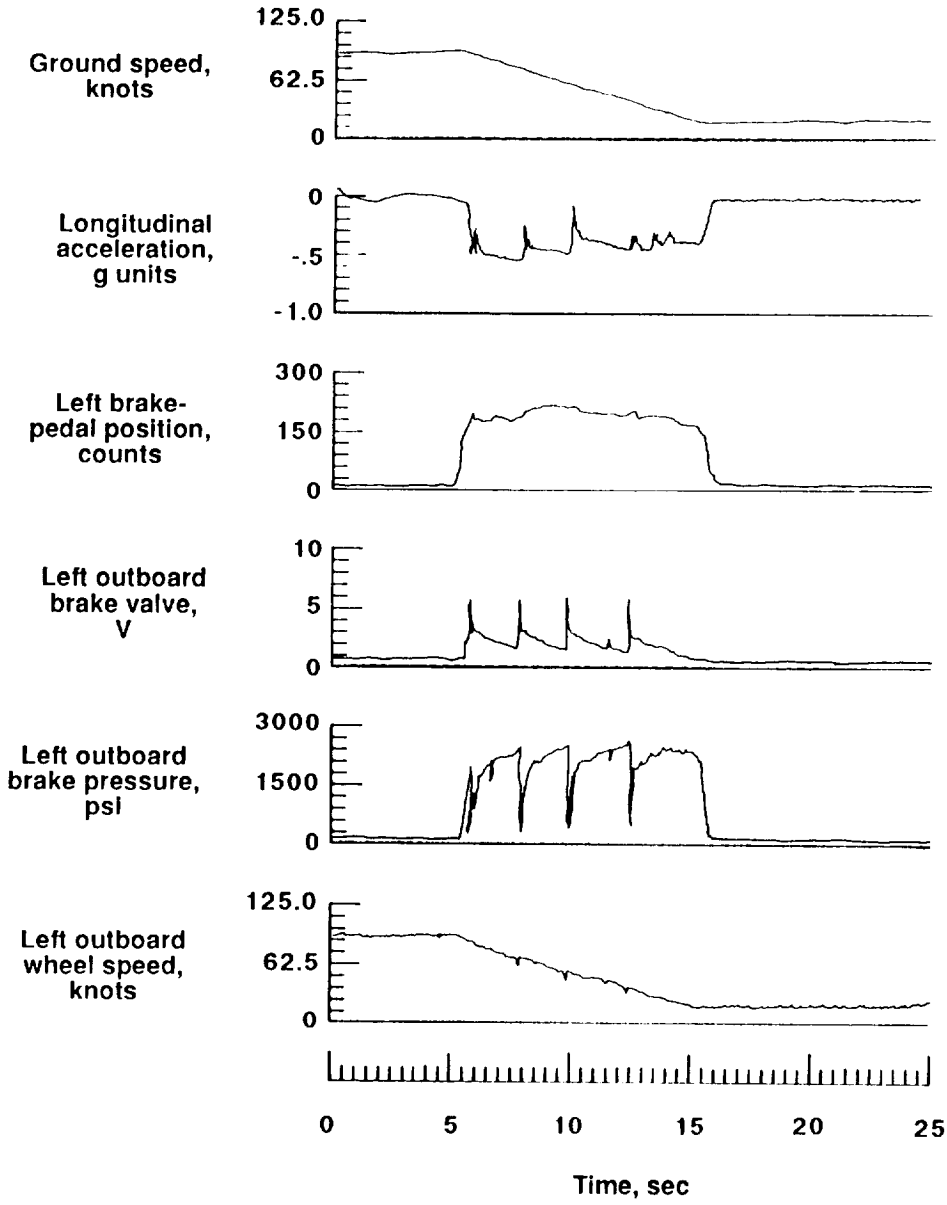

(i) Dry asphalt, maximum antiskid braking, flight 006, run 11.

Figure 46. Continued.

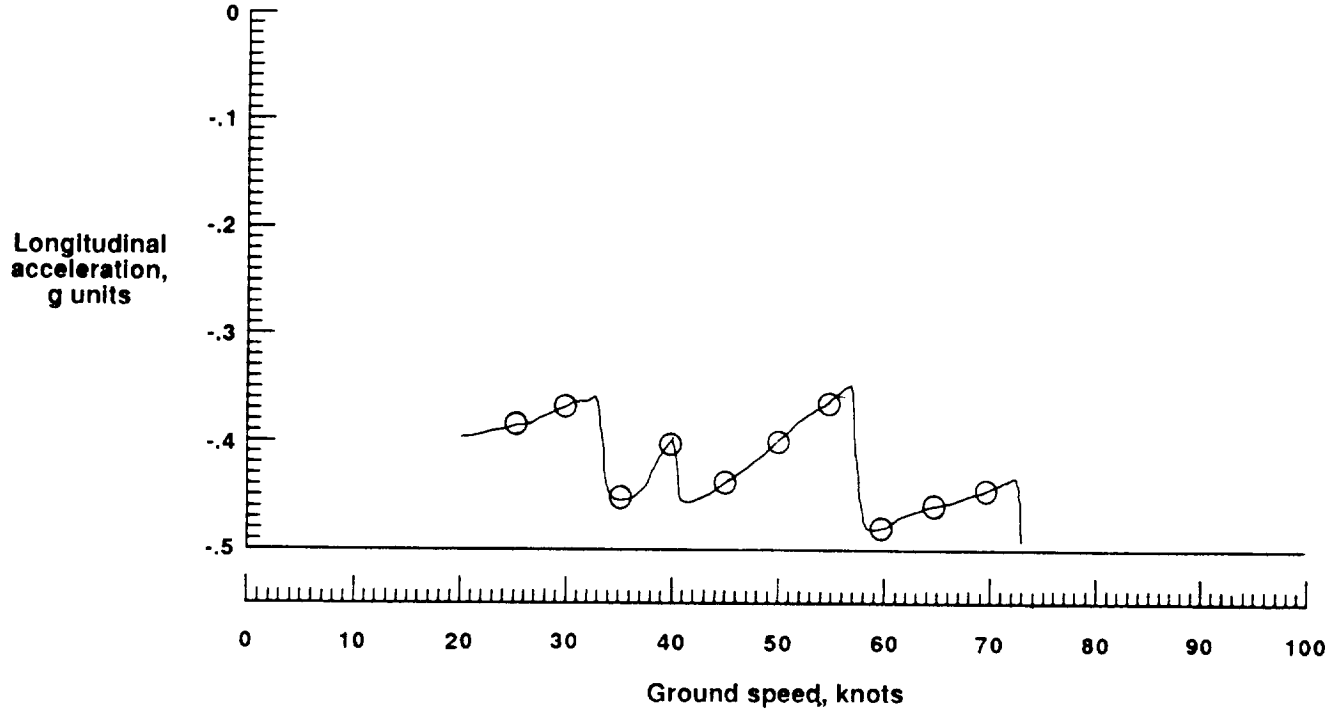

(j) Dry asphalt, maximum antiskid braking, flight 006, run 11, longitudinal acceleration versus ground speed.

Figure 46. Continued.

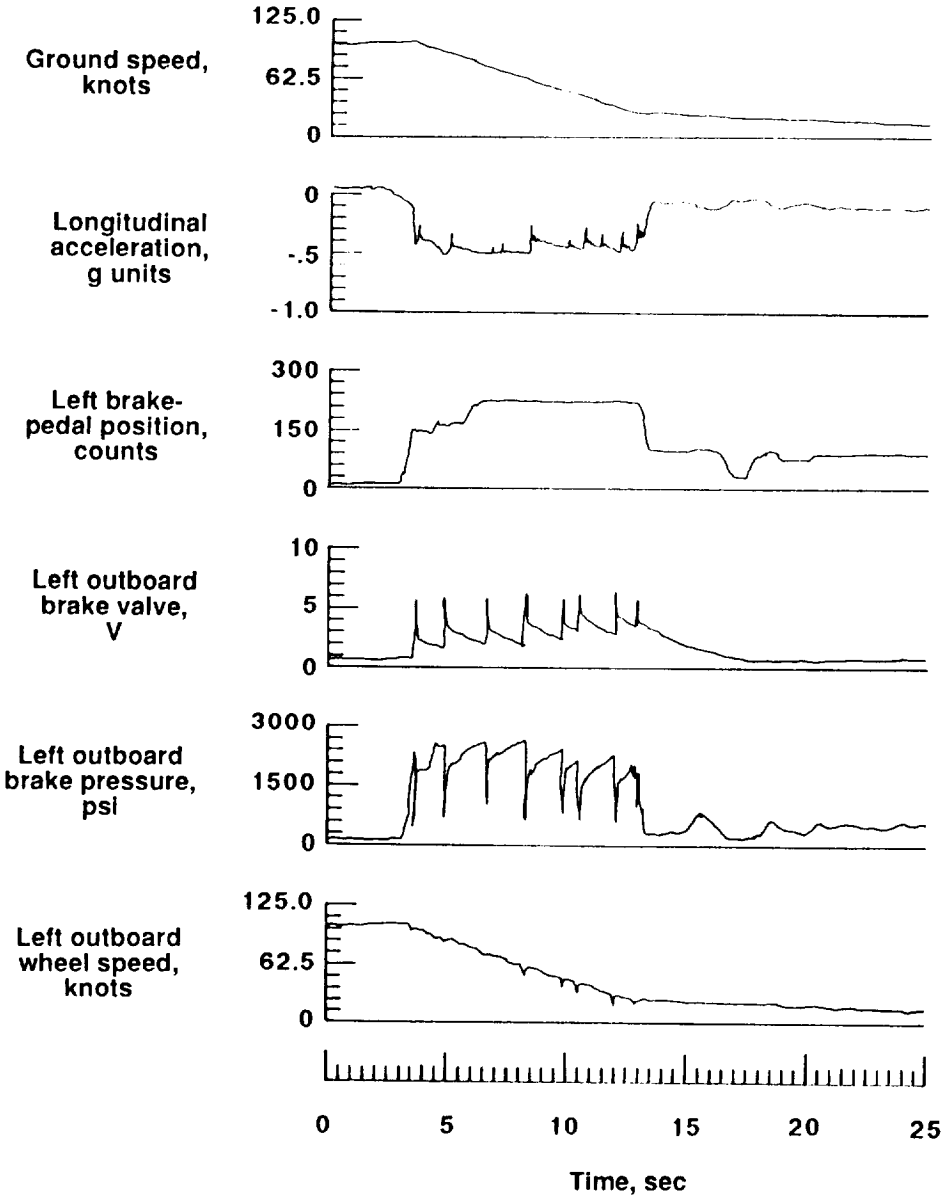

(k) Dry asphalt, maximum antiskid braking, flight 011, run 9.

Figure 46. Continued.

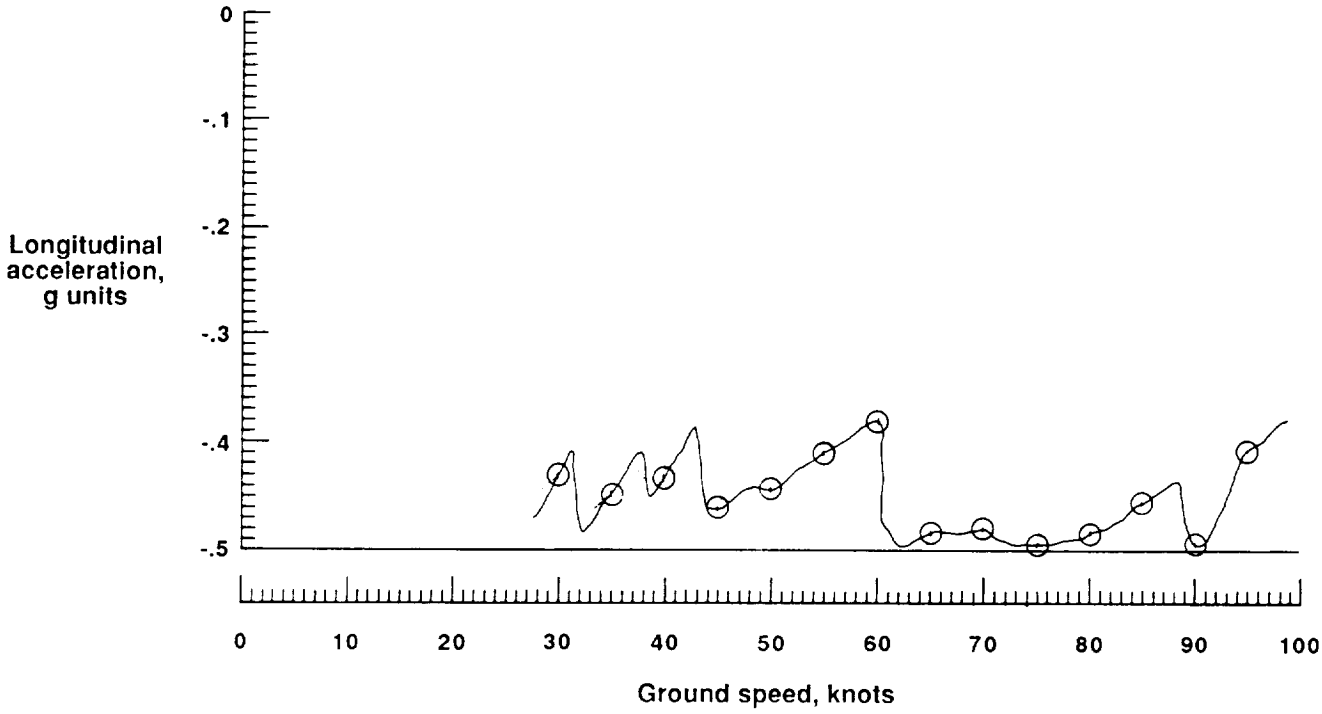

(l) Dry asphalt, maximum antiskid braking, flight 011, run 9, longitudinal acceleration versus ground speed.

Figure 46. Continued.

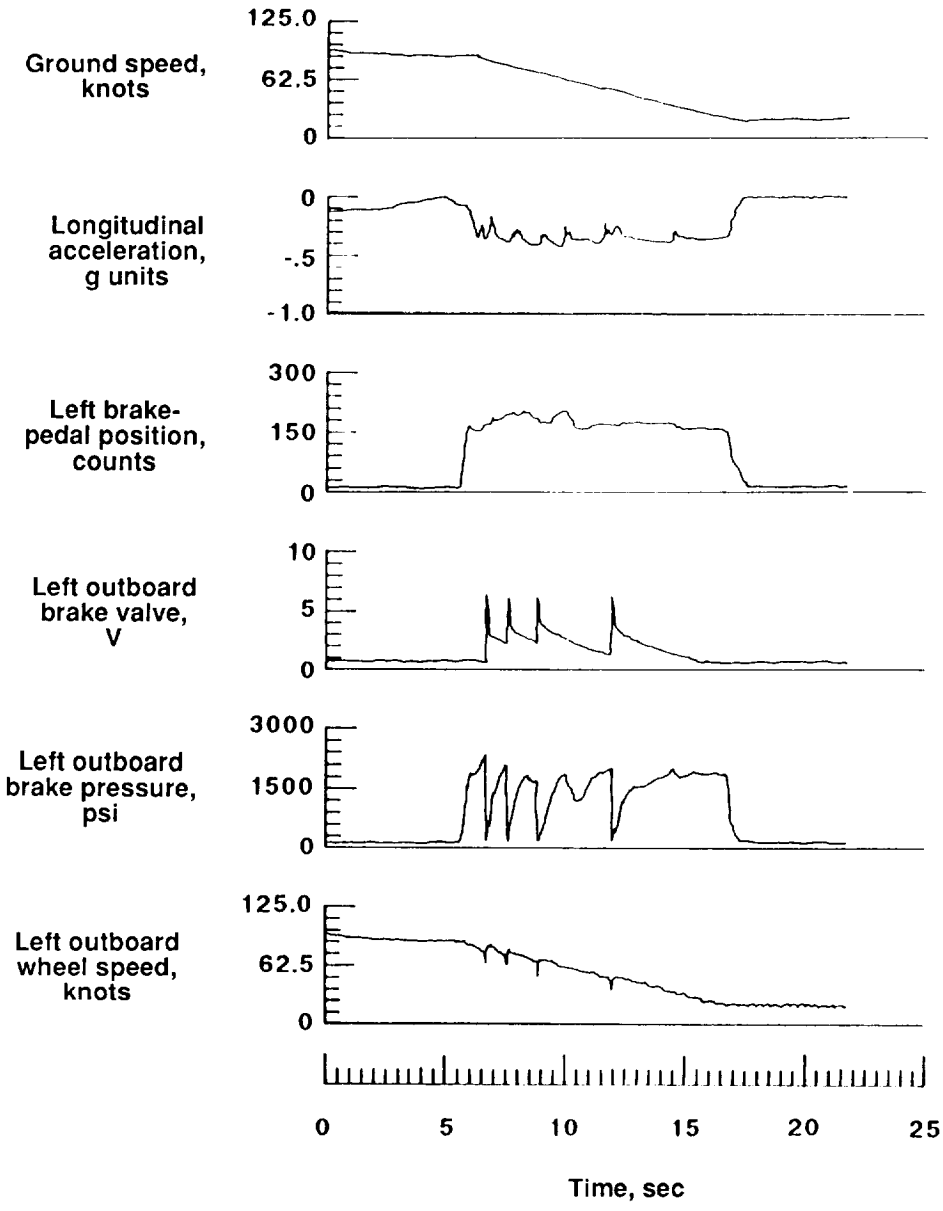

(m) Truck-wet asphalt, maximum antiskid braking, flight 005, run 8R1.

Figure 46. Continued.

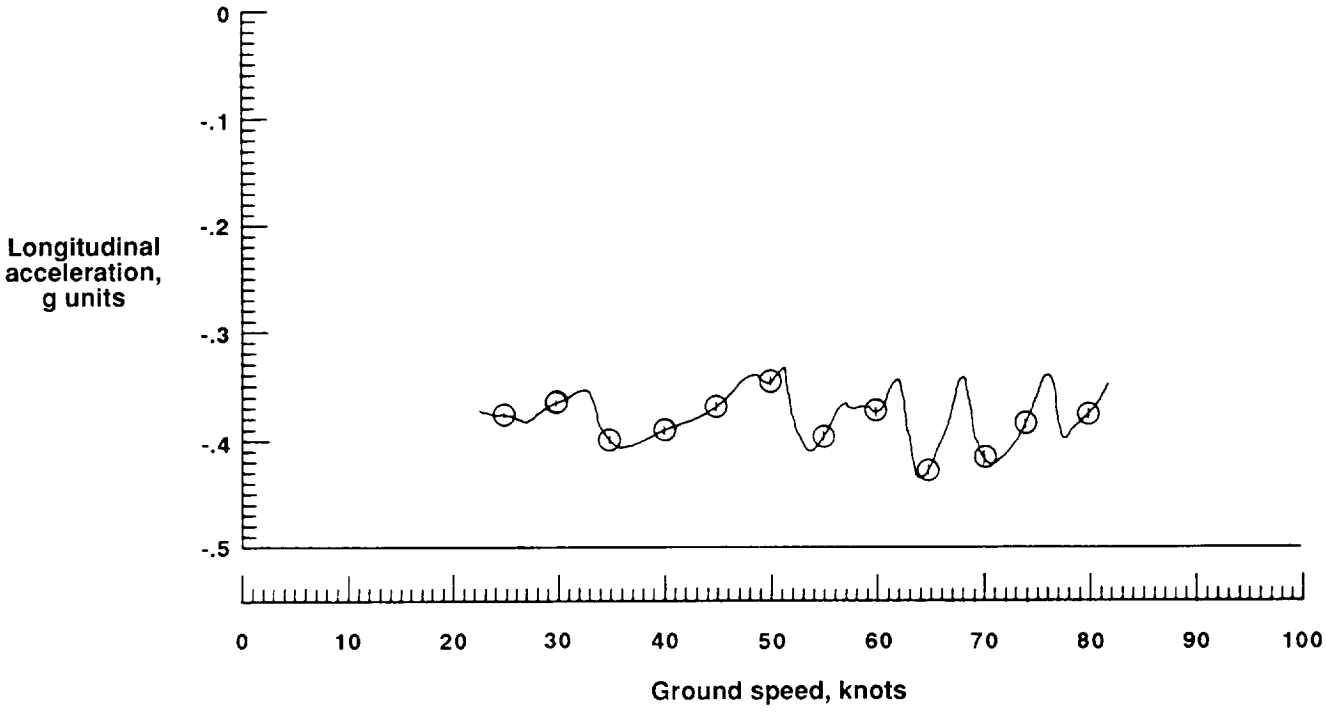

(n) Truck-wet asphalt, maximum antiskid braking, flight 005, run 8R1, longitudinal acceleration versus ground speed.

Figure 46. Continued.

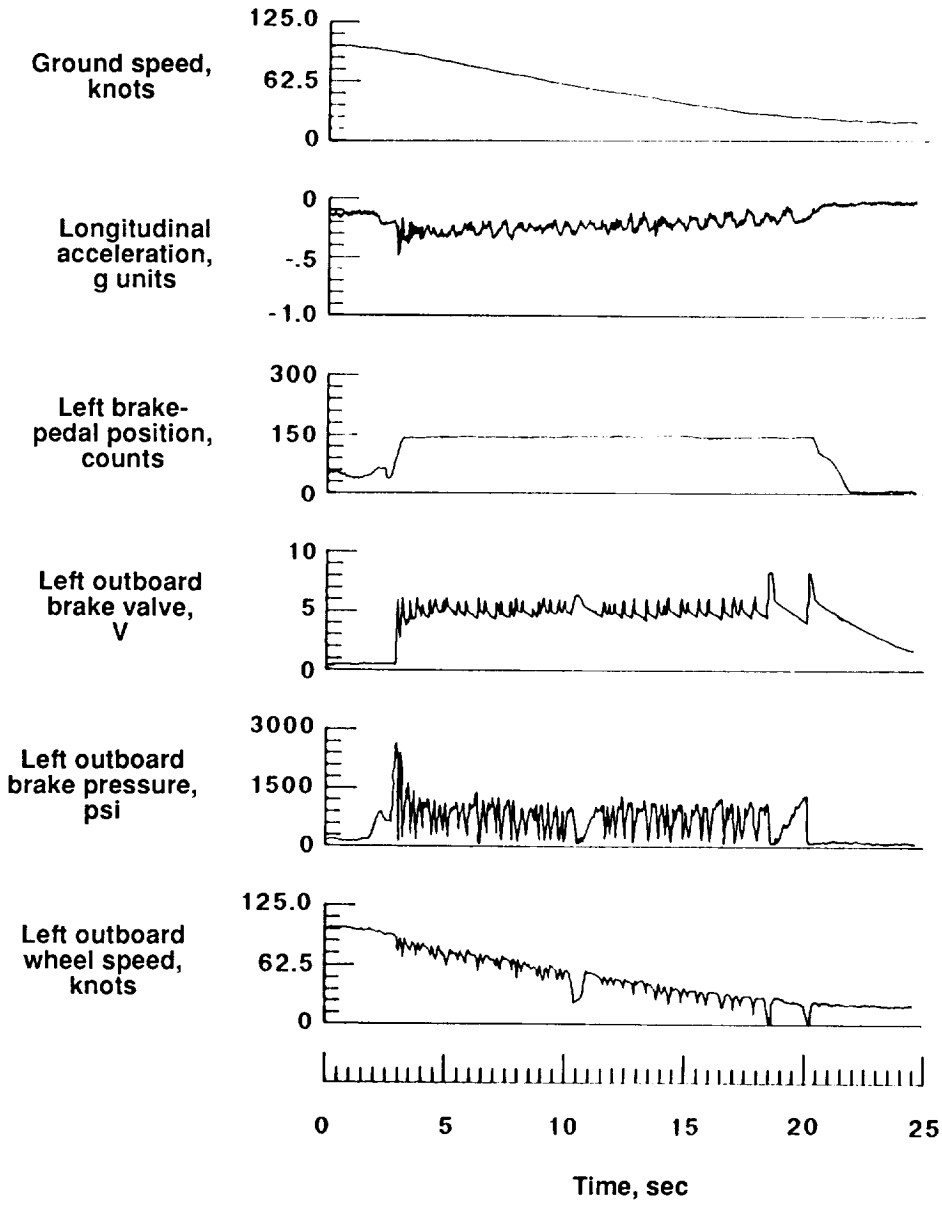

(o) 4.5-in. loose snow, maximum antiskid braking, flight 022, run 5.

Figure 46. Continued.

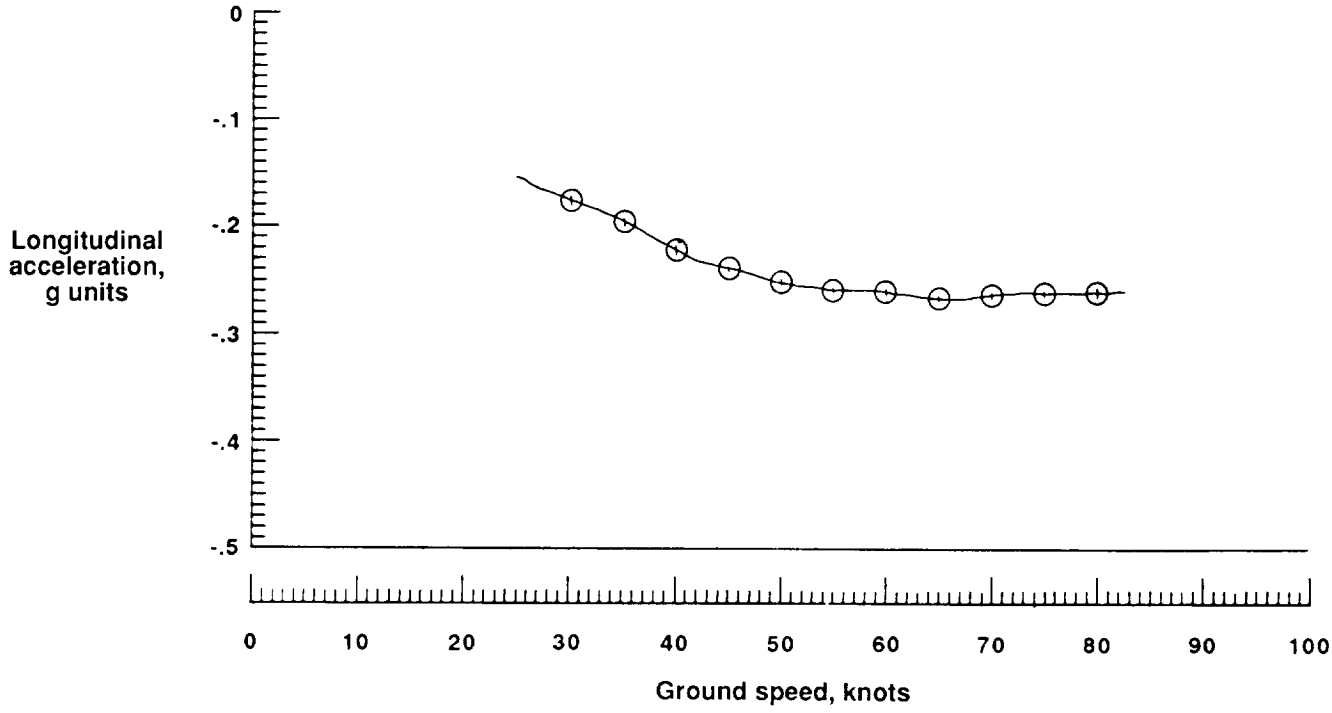

(p) 4.5-in. loose snow, maximum antiskid braking, flight 022, run 5, longitudinal acceleration versus ground speed.

Figure 46. Continued.

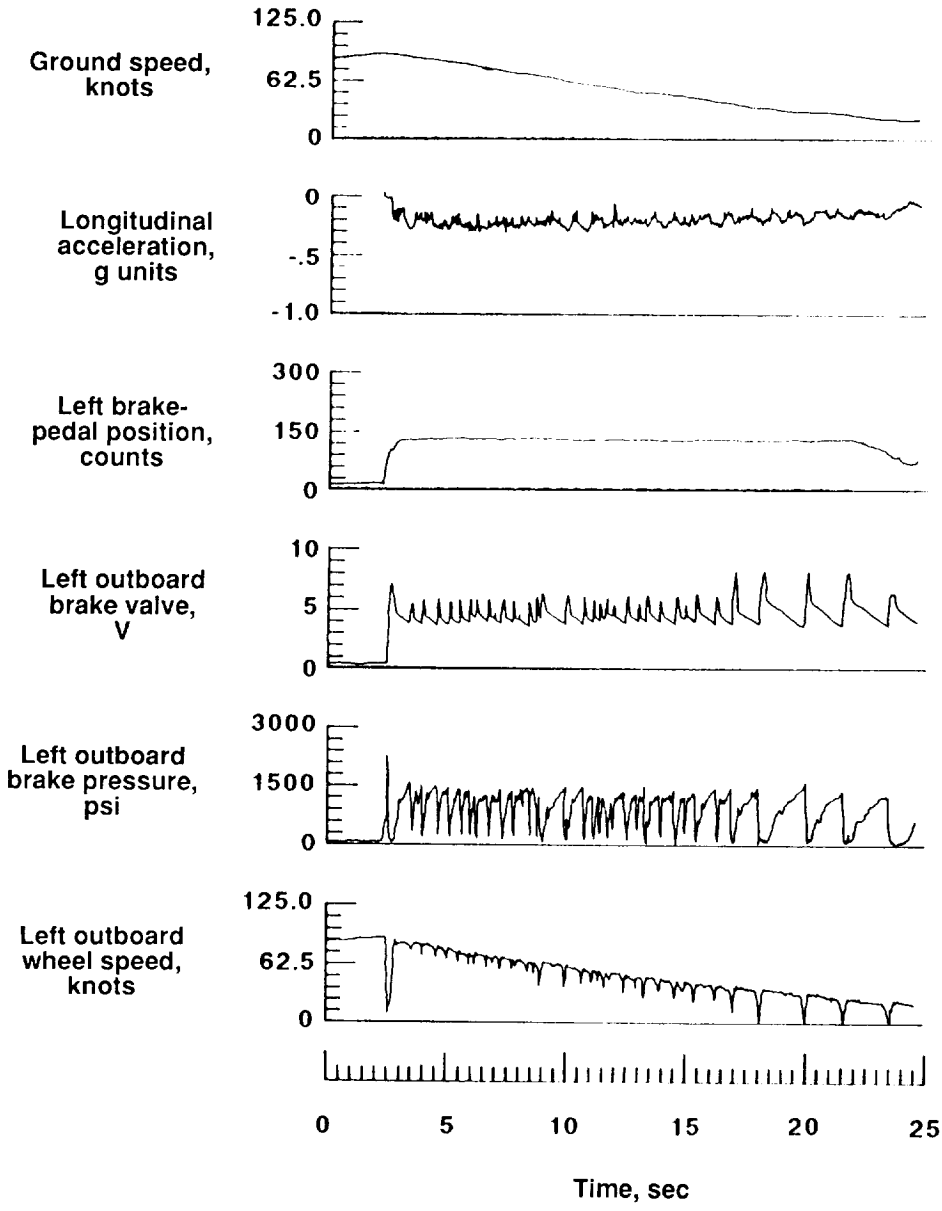

(q) UCAR on snow- and ice-covered asphalt, maximum antiskid braking, flight 025, run 5R1.

Figure 46. Continued.

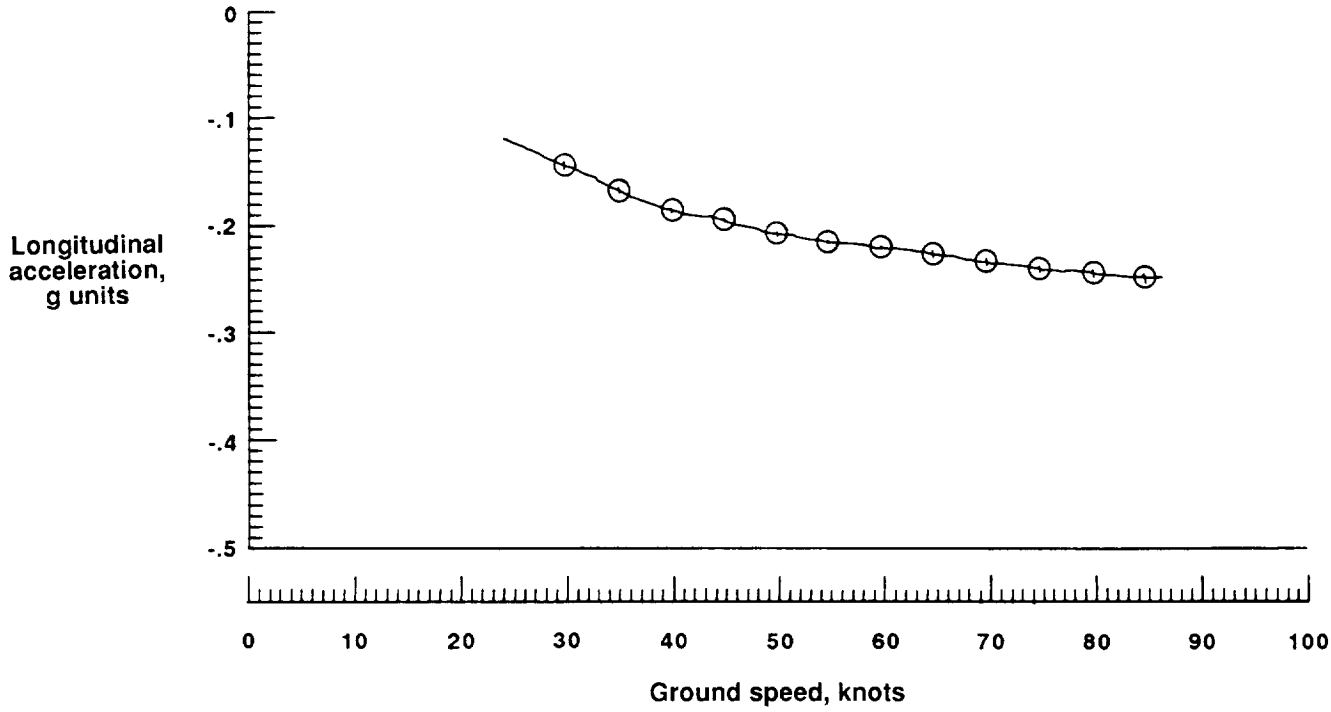

(r) UCAR on snow- and ice-covered asphalt, maximum antiskid braking, flight 025, run 5R1, longitudinal acceleration versus ground speed.

Figure 46. Concluded.

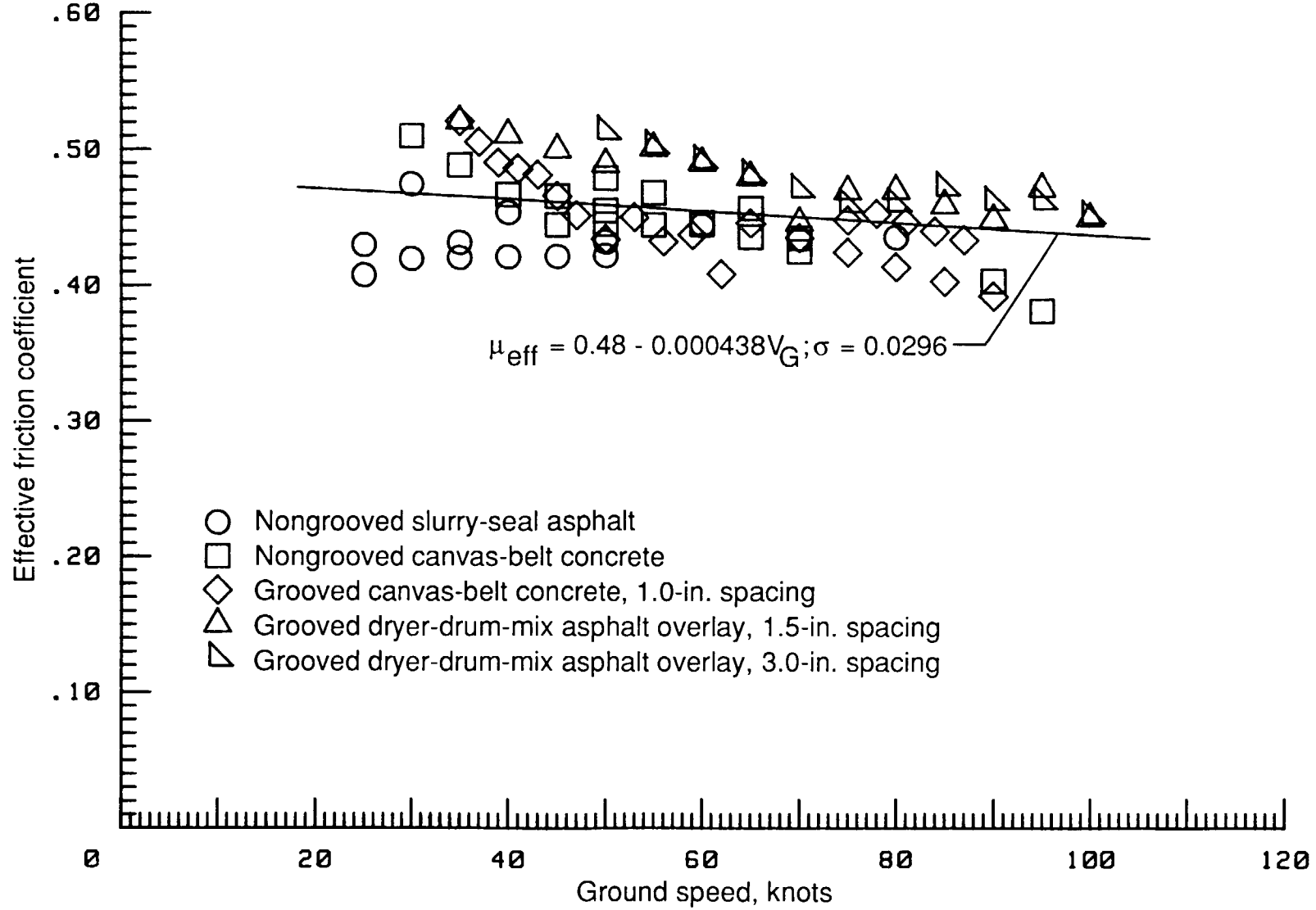

Figure 47. Variation of Boeing 737 effective friction coefficient with ground speed for dry-runway test conditions.

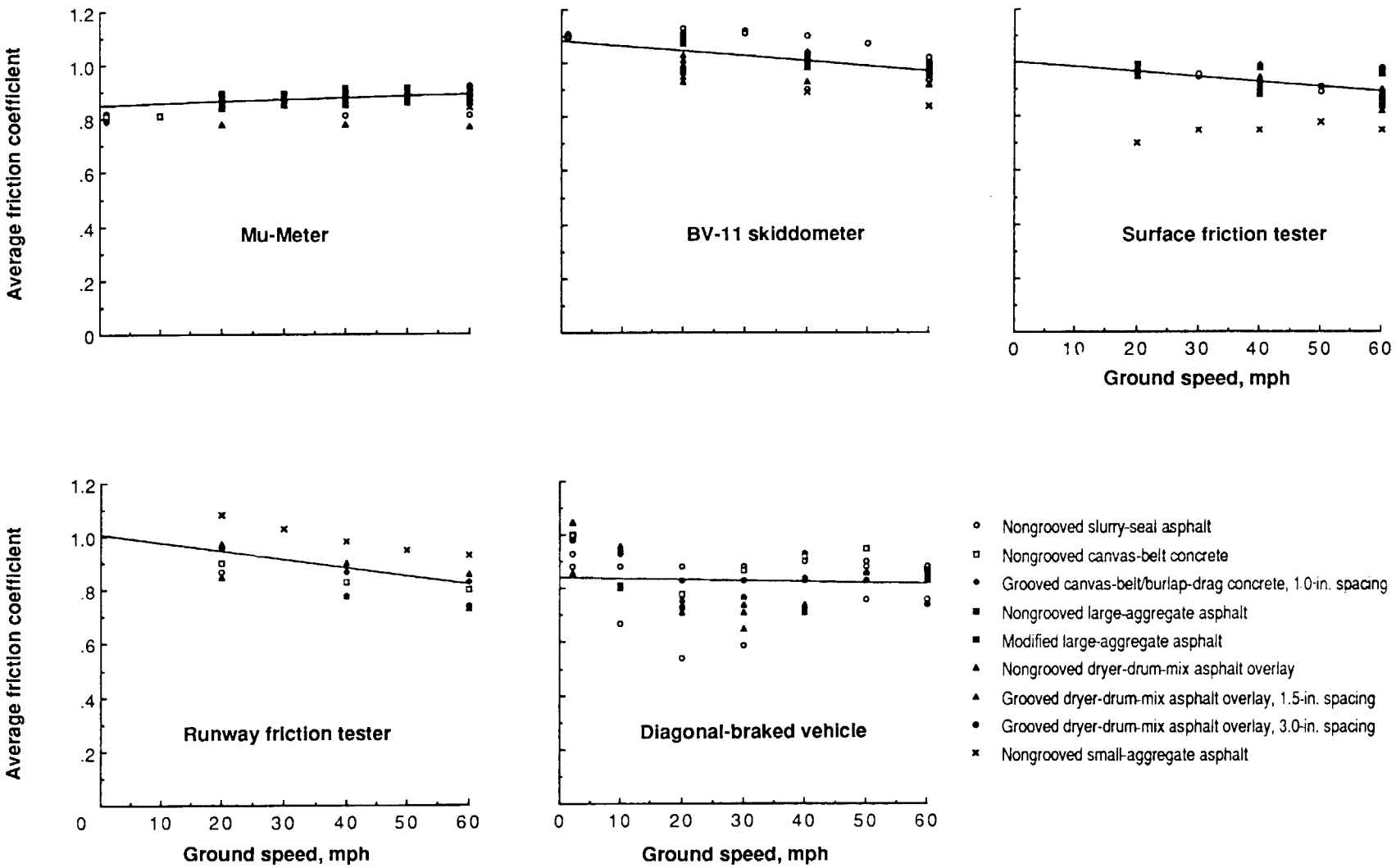

Figure 48. Ground-vehicle friction data obtained on different dry-runway test surfaces.

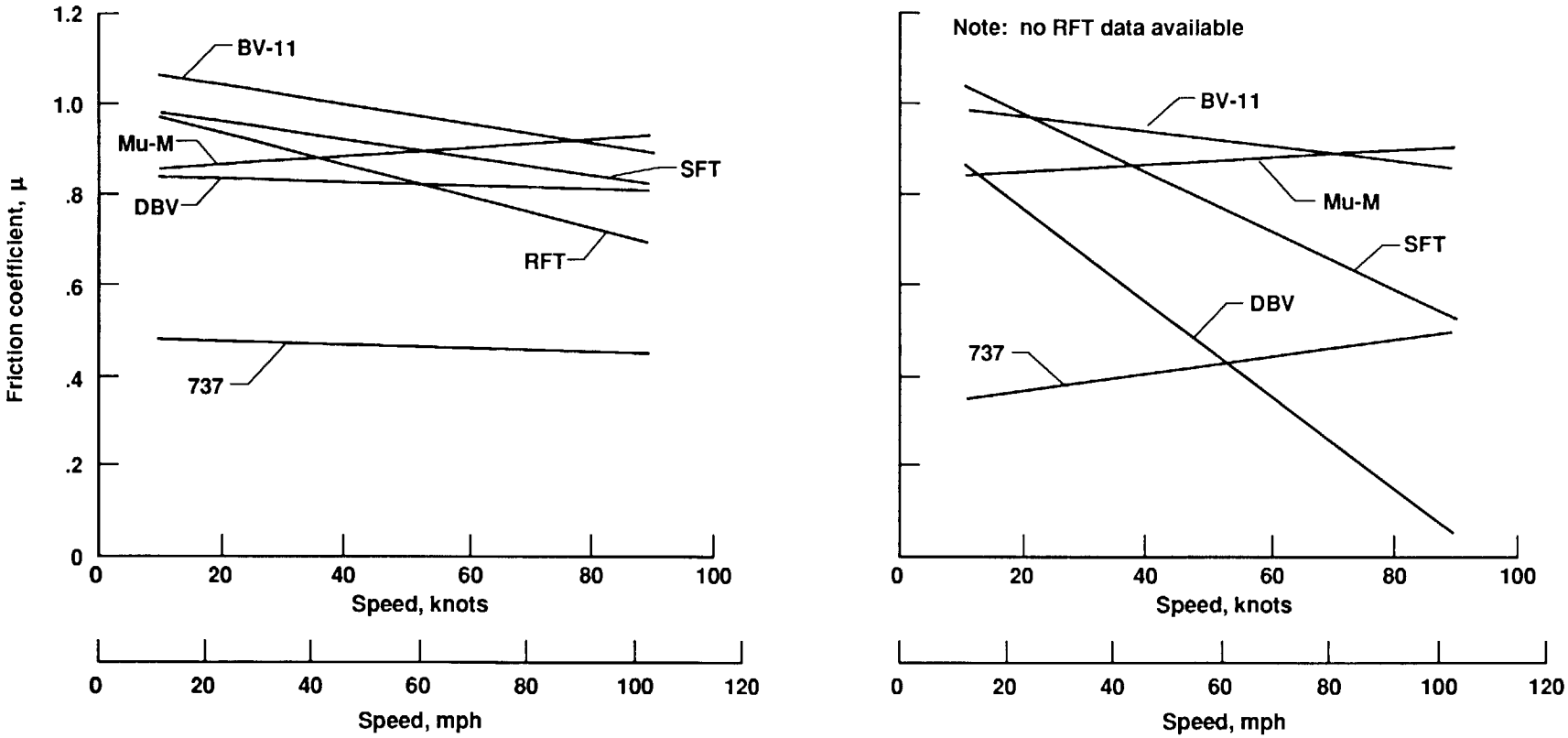

(a) Dry, all surfaces.

(b) Rain wet, SSA.

Figure 49. Range of Boeing 737 aircraft and ground-vehicle friction data for different runway test-surface conditions.

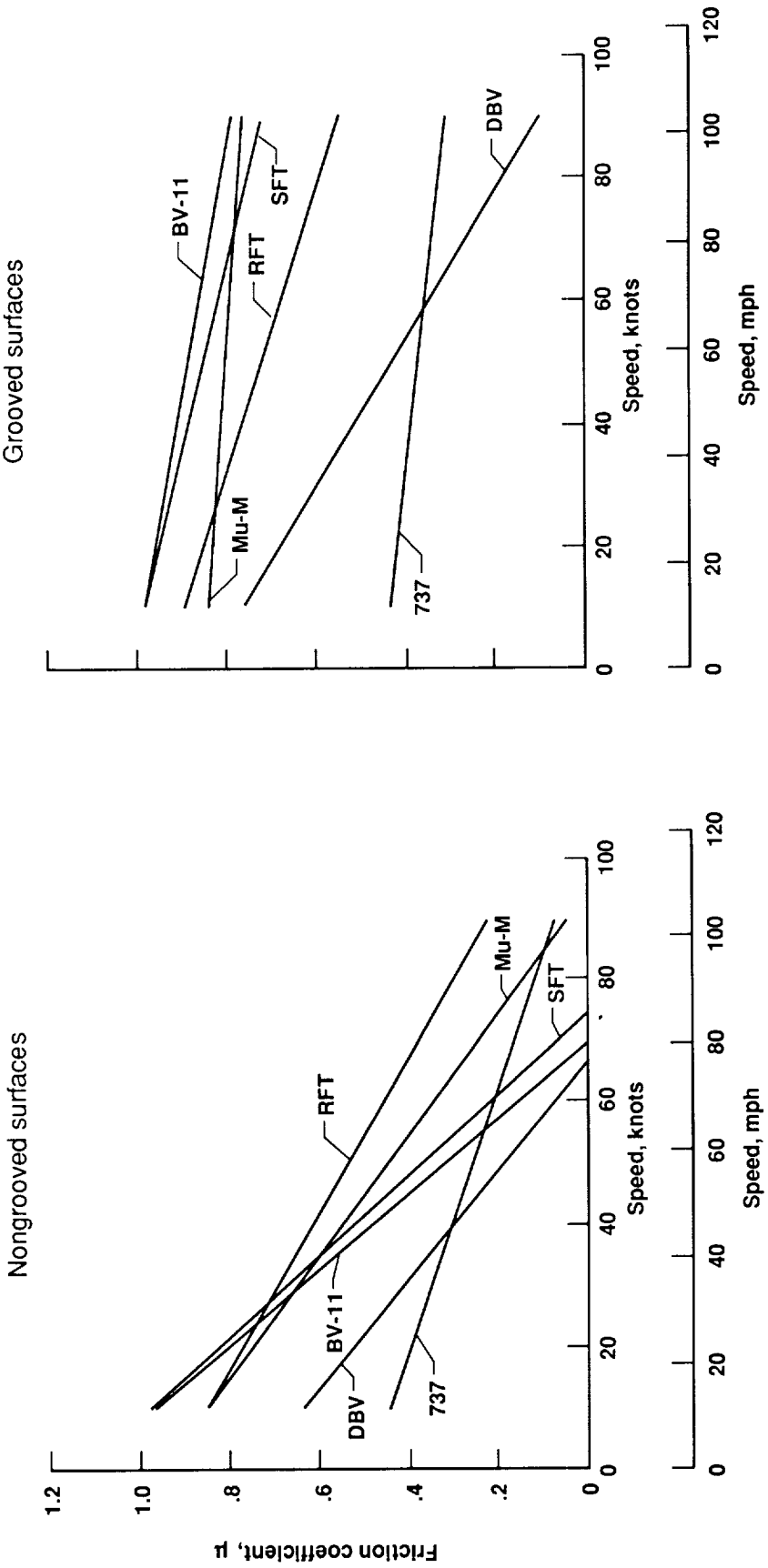

(c) Truck-wet surfaces.

Figure 49. Continued.

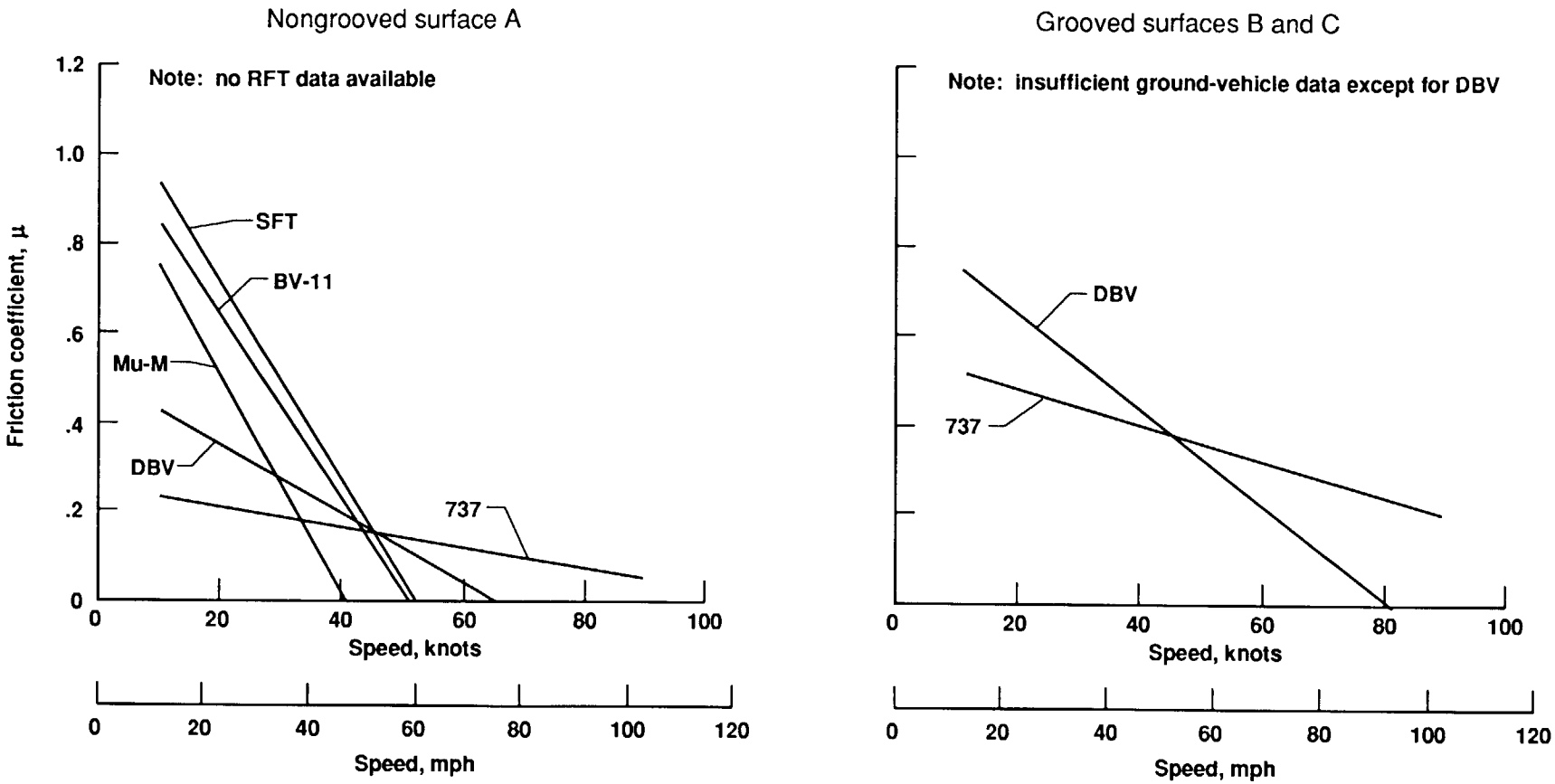

(d) Flooded concrete surfaces at Wallops Flight Facility.

Figure 49. Continued.

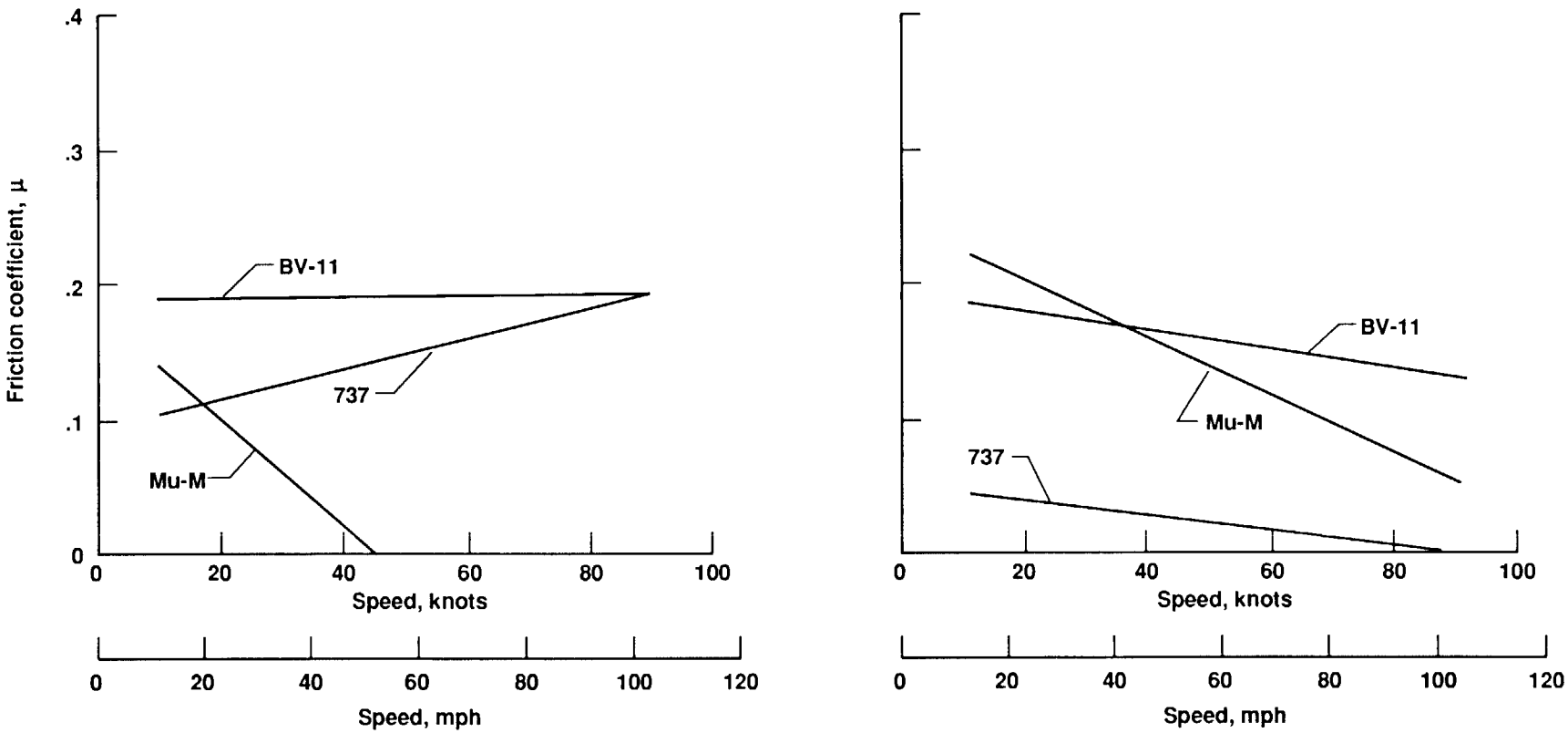

(e) 1.5-in. new wet snow.

(f) Glare ice.

Figure 49. Concluded.

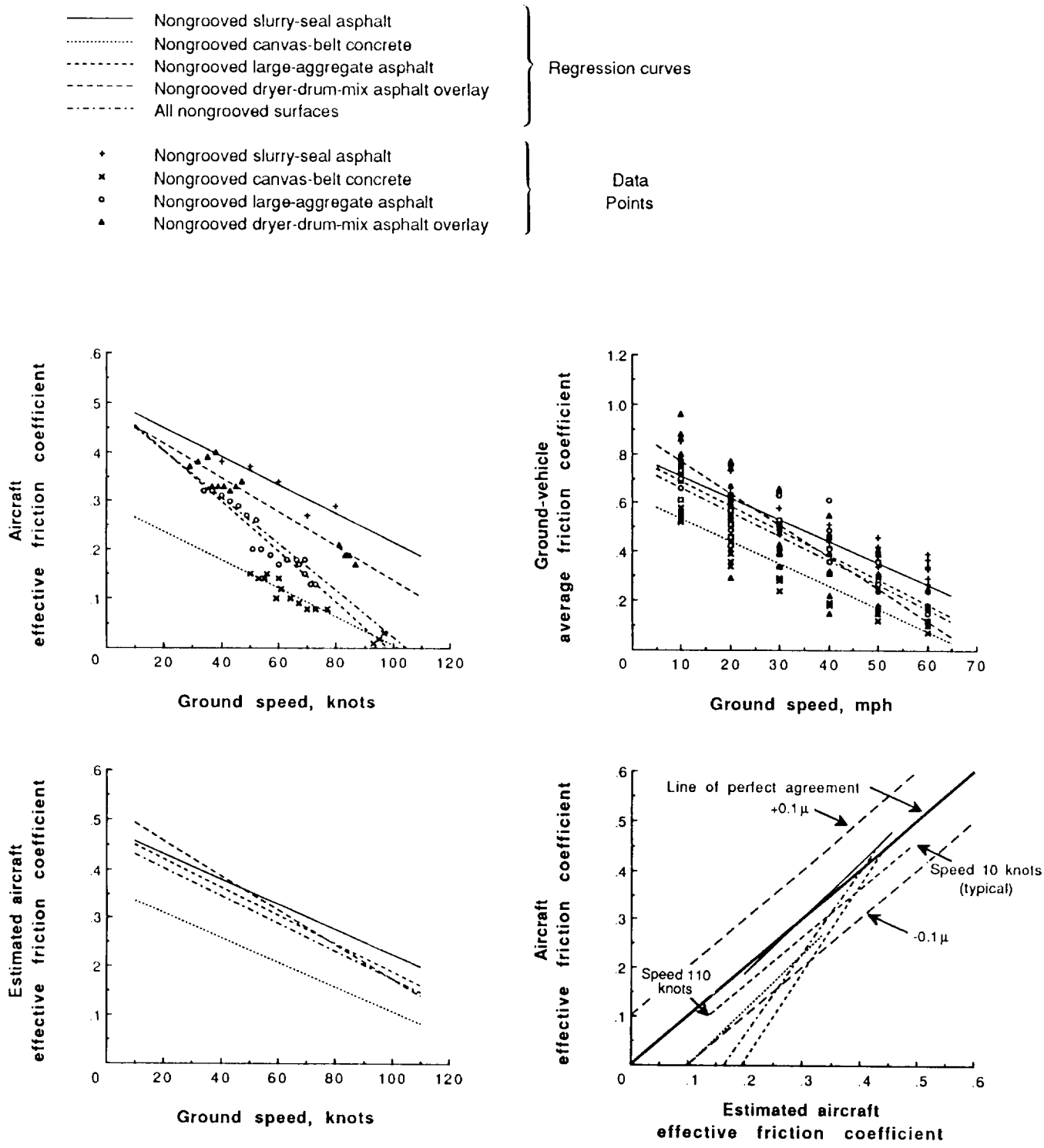

(a) DBV data.

Figure 50. Variation of Boeing 737 aircraft and ground-vehicle friction data with speed and variation of estimated aircraft braking performance with actual braking performance on truck-wet, nongrooved test surfaces.

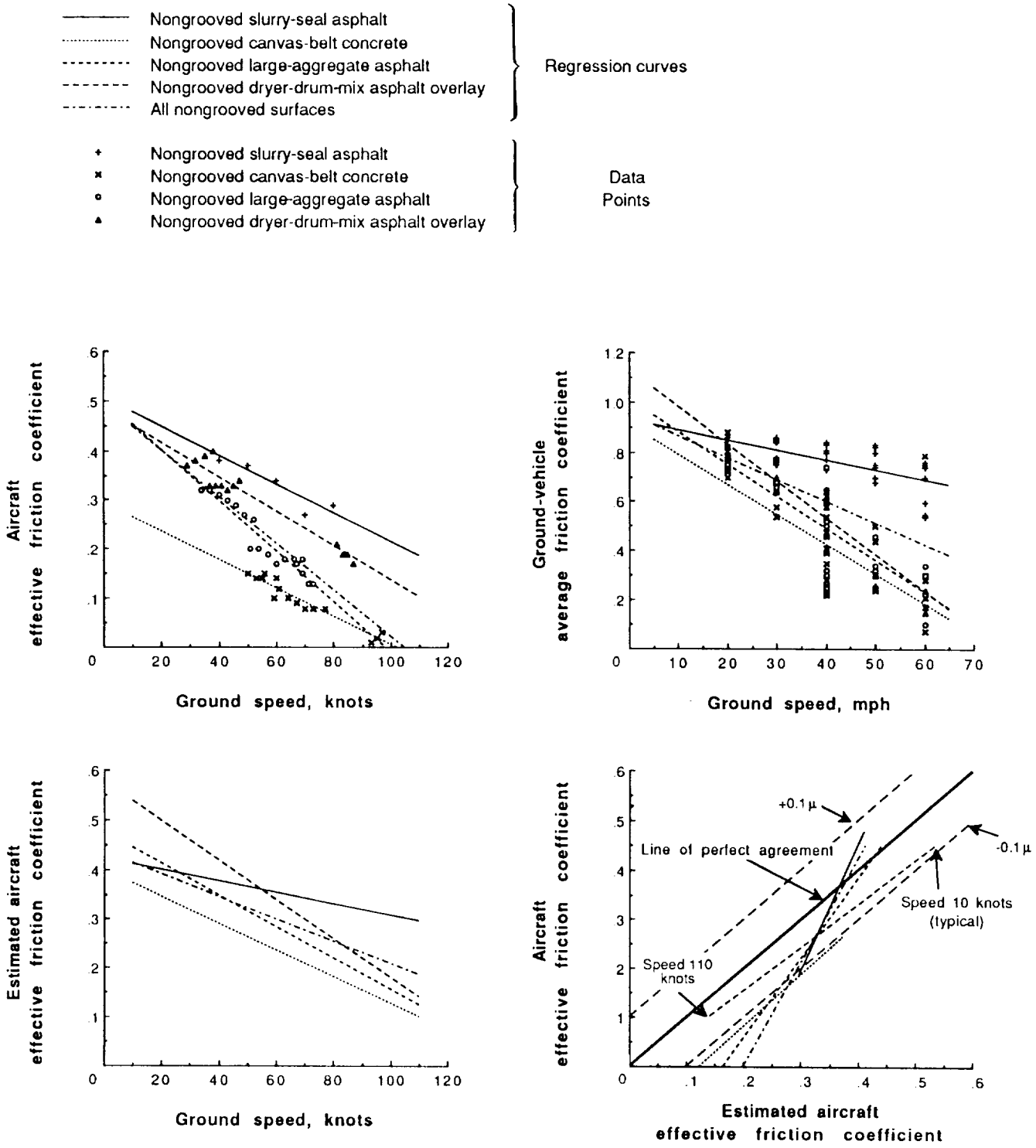

(b) Mu-Meter data.

Figure 50. Continued.

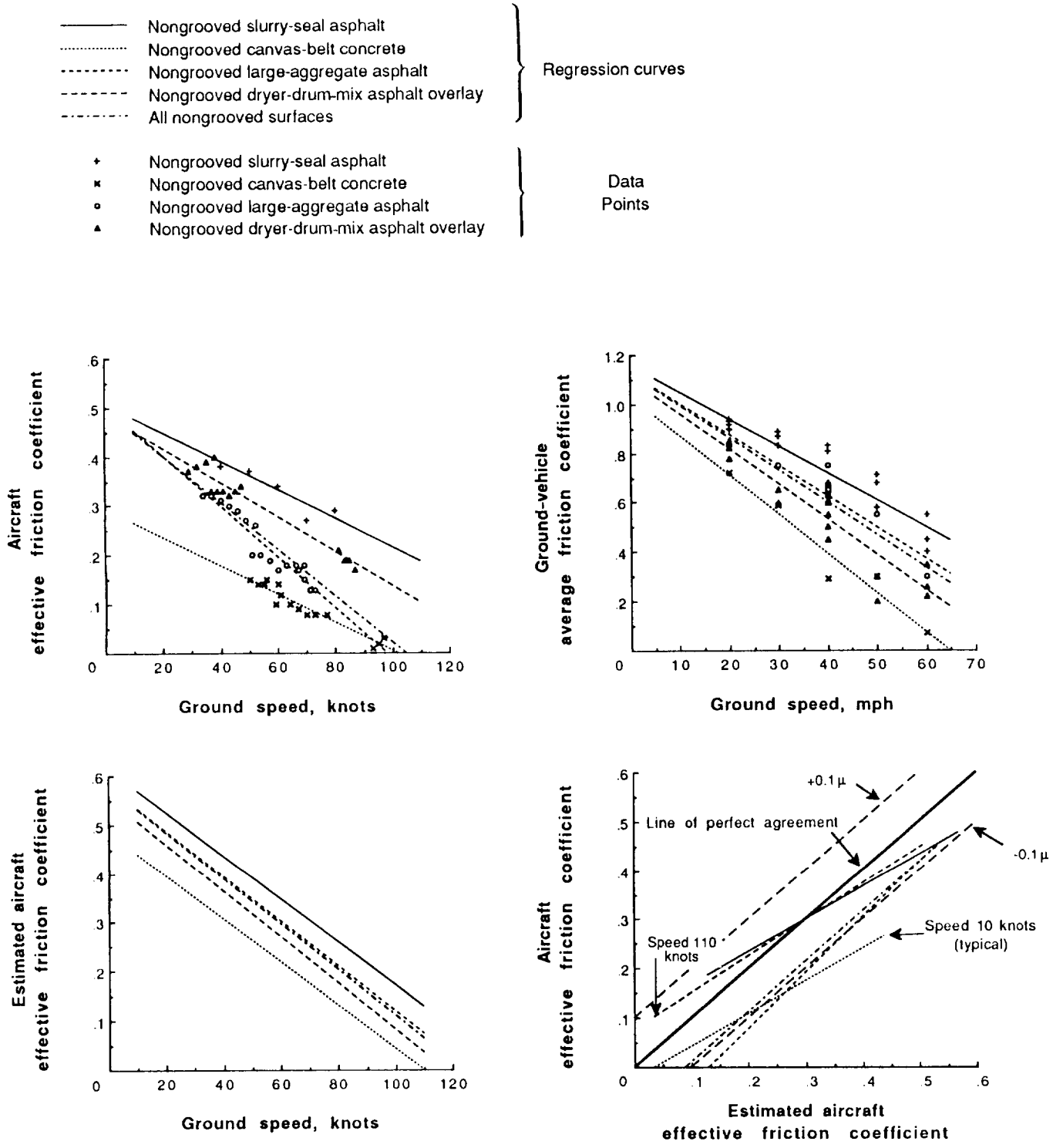

(c) SFT data.

Figure 50. Continued.

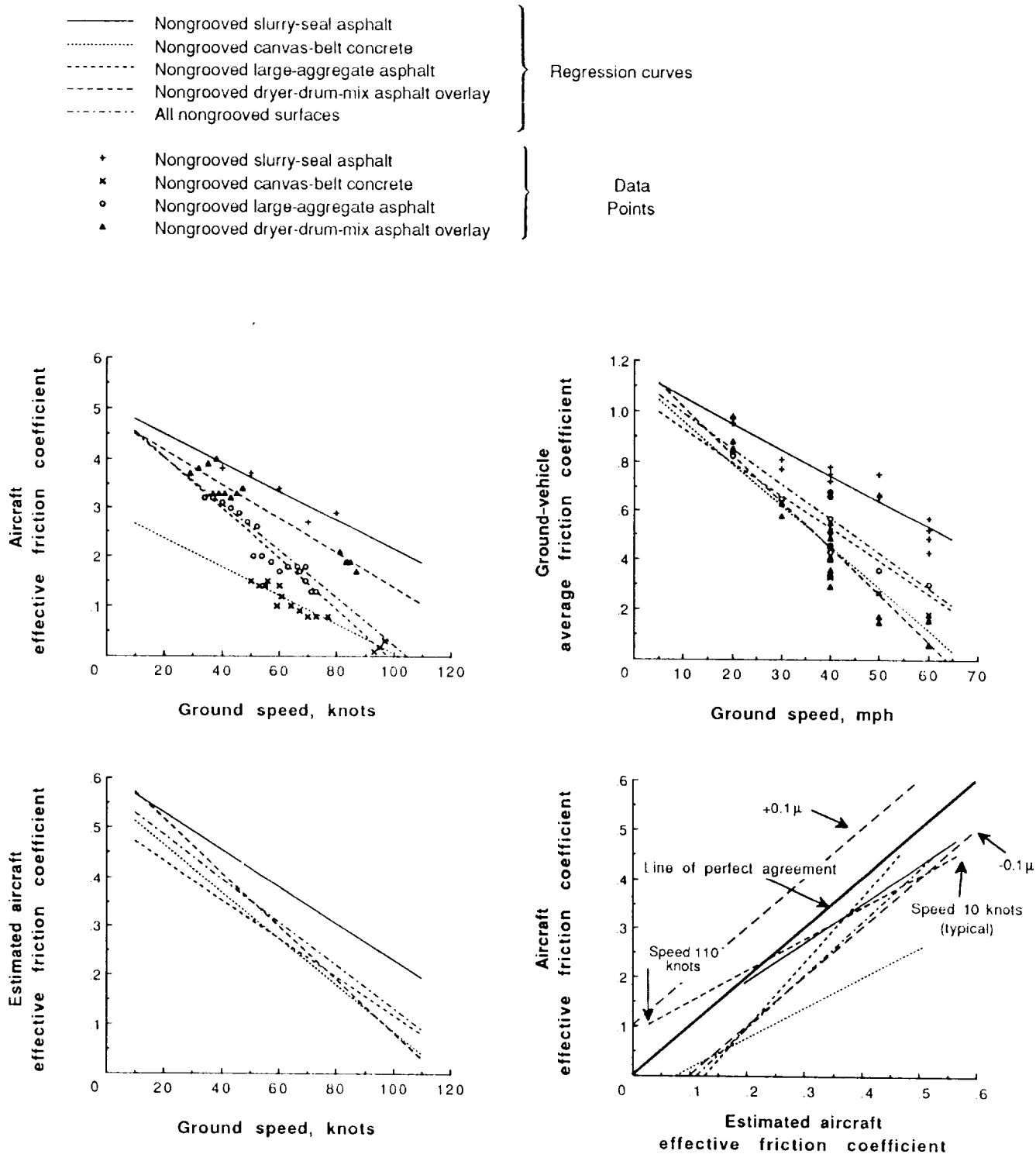

(d) BV-11 skiddometer data.

Figure 50. Concluded.

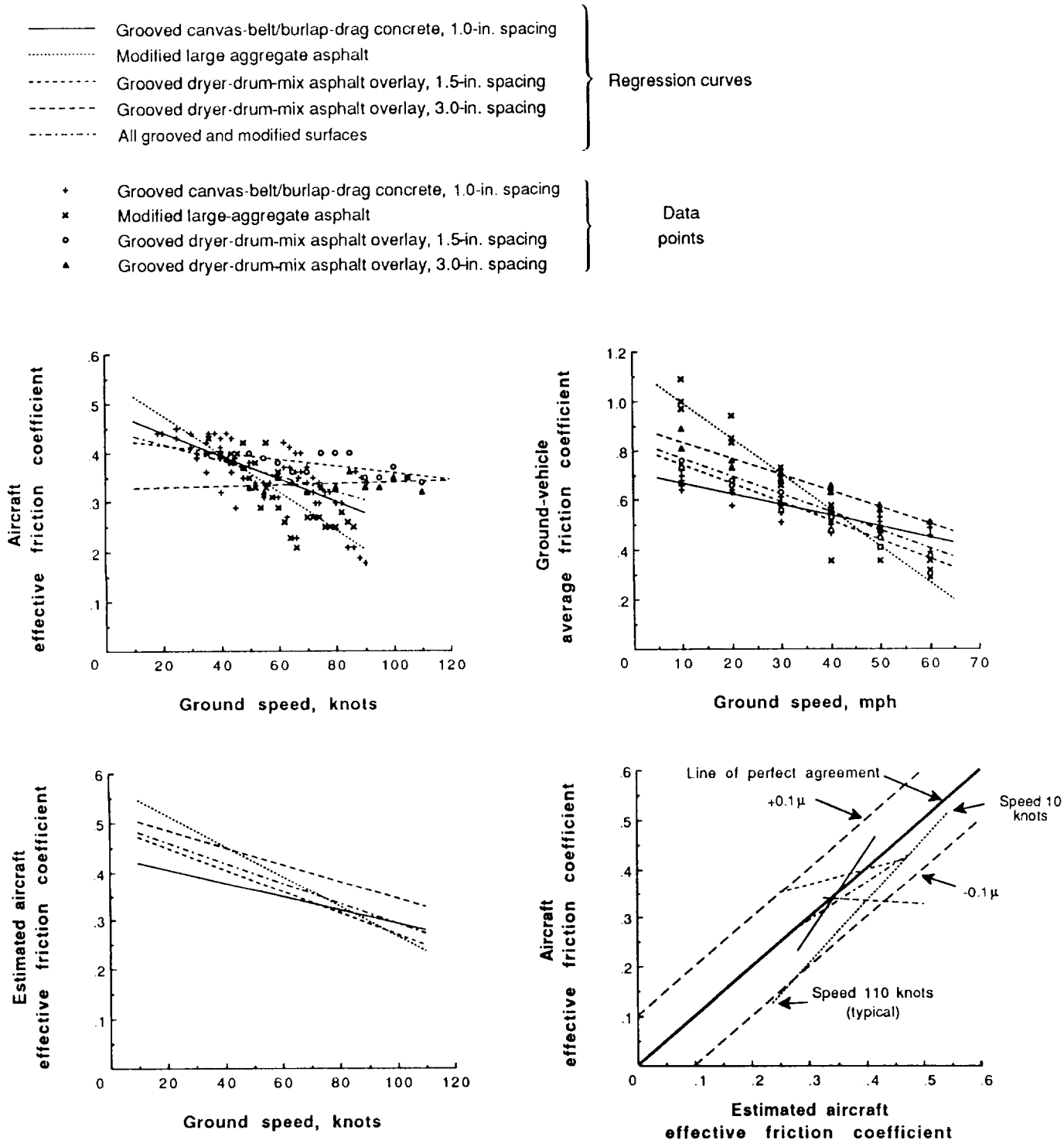

(a) DBV data.

Figure 51. Variation of Boeing 737 aircraft and ground-vehicle friction data with speed and variation of estimated aircraft braking performance with actual braking performance on truck-wet, grooved test surfaces.

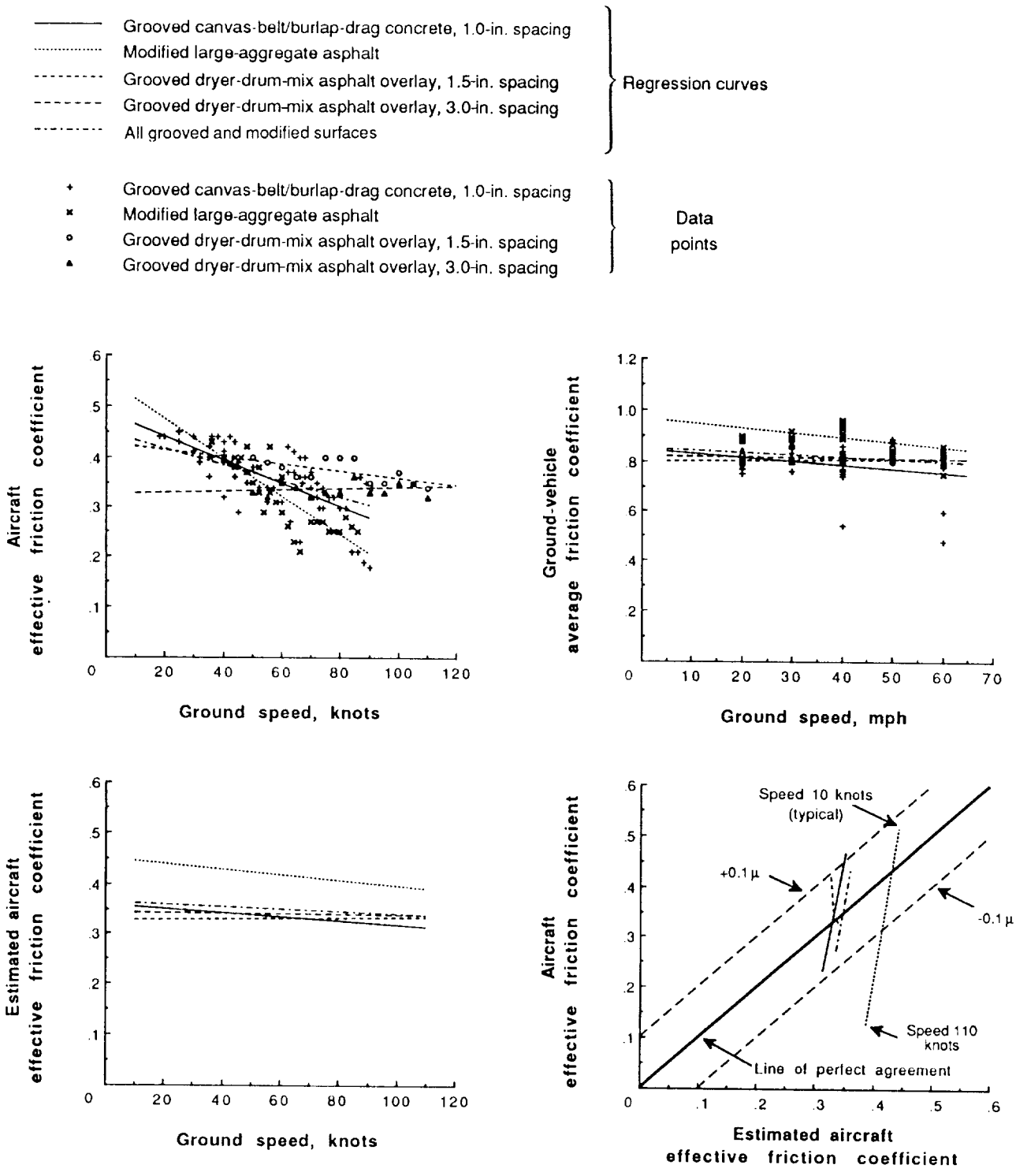

(b) Mu-Meter data.

Figure 51. Continued.

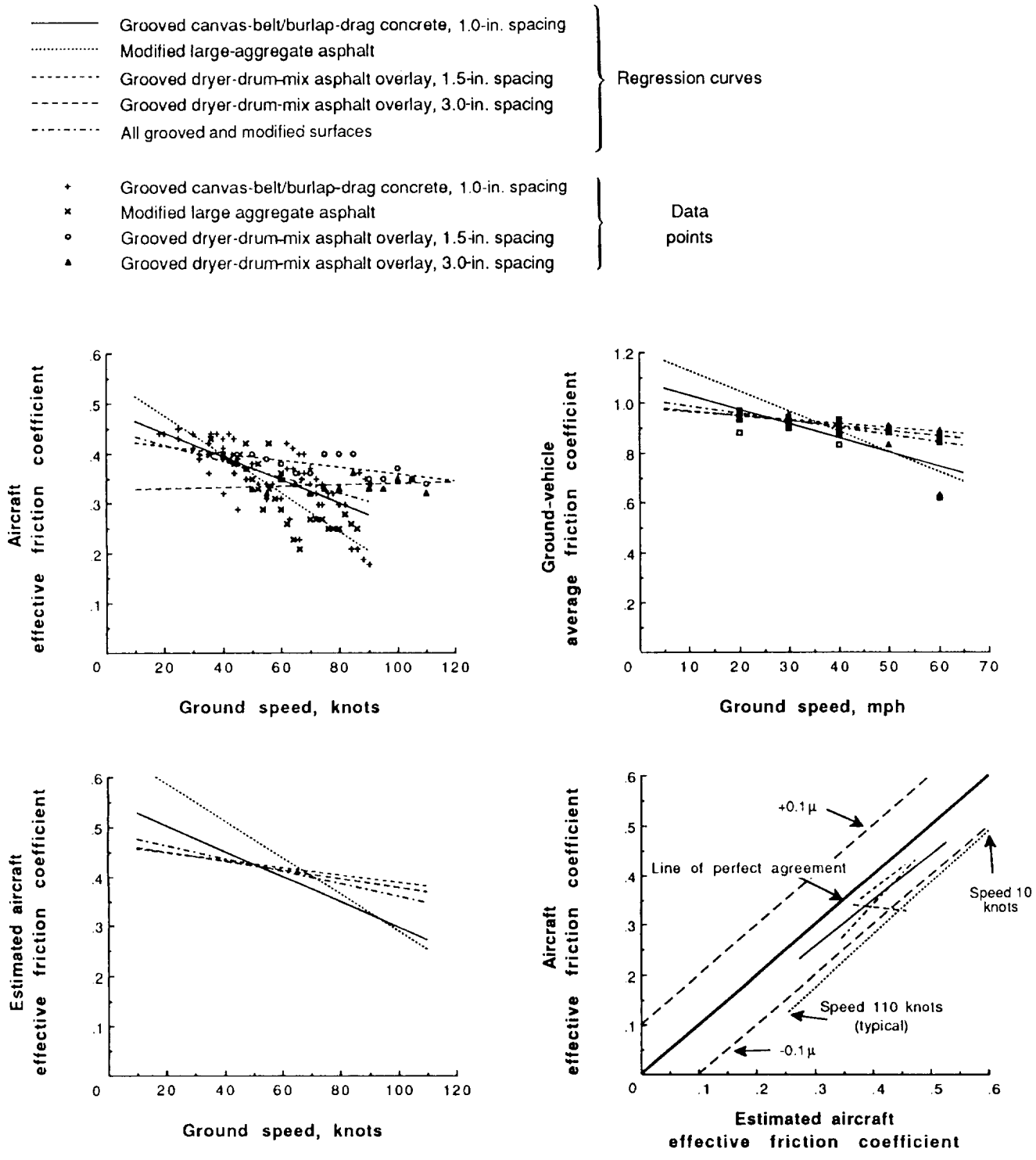

(c) SFT data.

Figure 51. Continued.

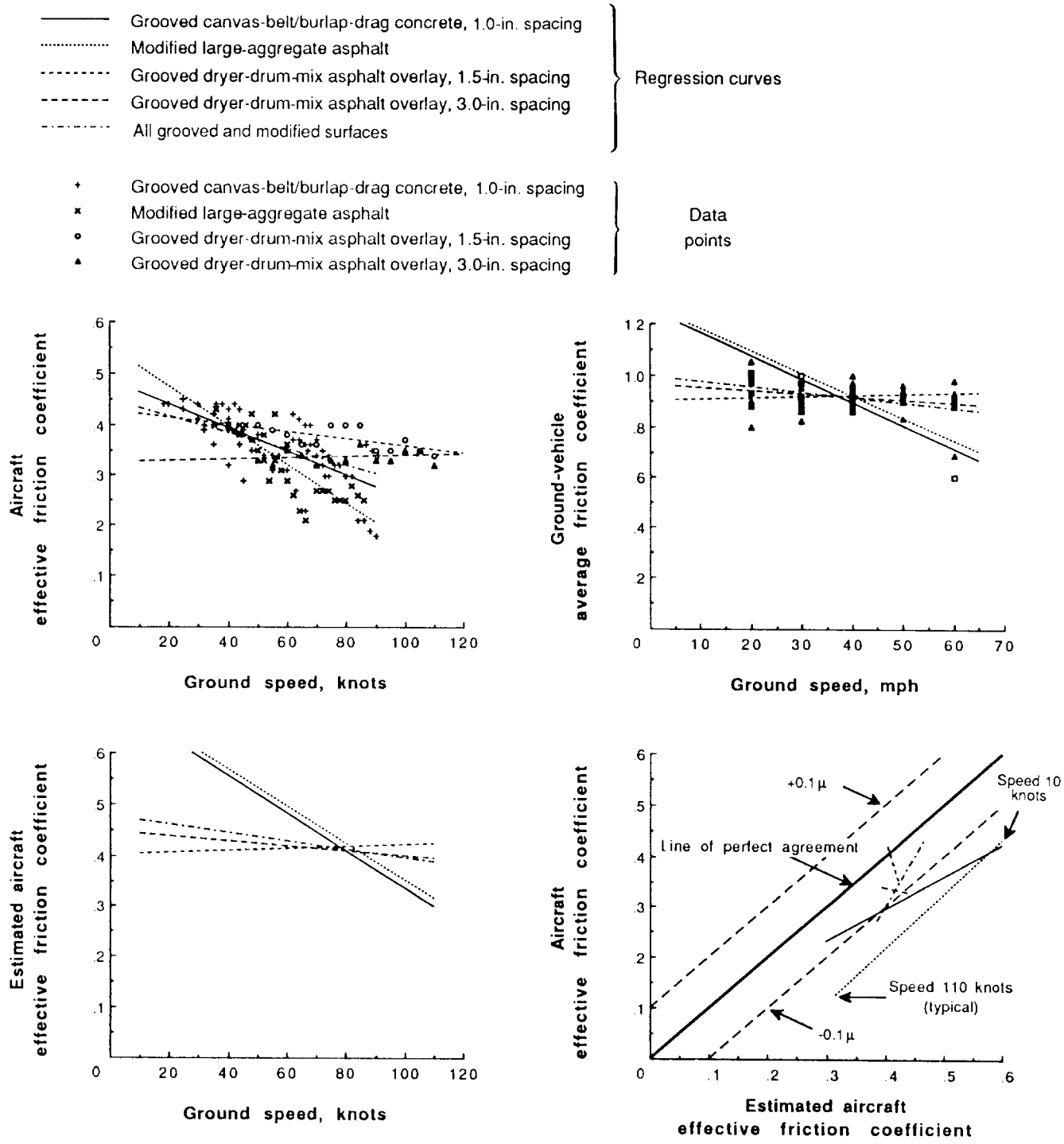

(d) BV-11 skiddometer data.

Figure 51. Concluded.

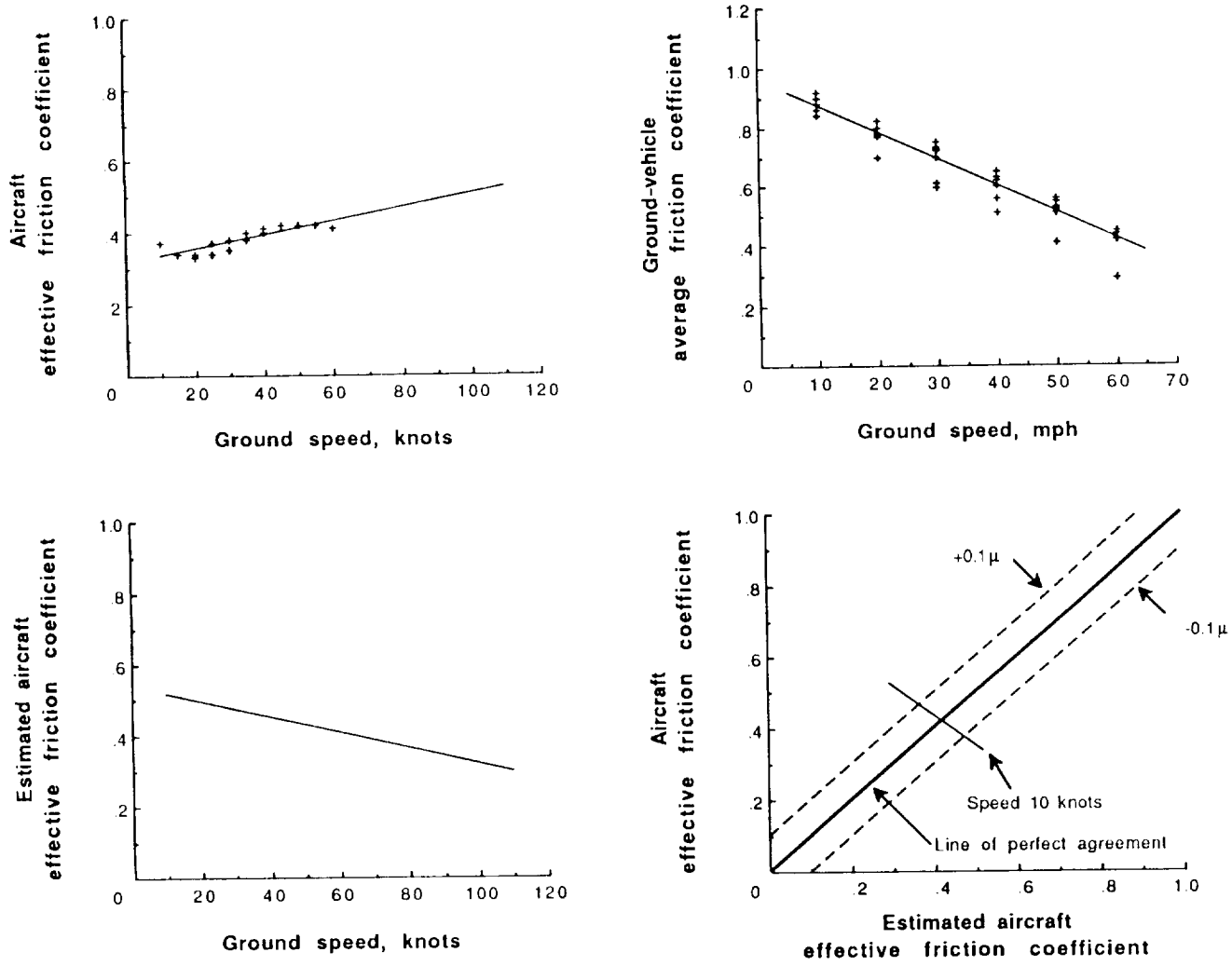

(a) DBV data.

Figure 52. Variation of Boeing 737 aircraft and ground-vehicle friction data with speed and variation of estimated aircraft braking performance with actual braking performance on rain-wet, nongrooved, slurry-seal asphalt test surfaces.

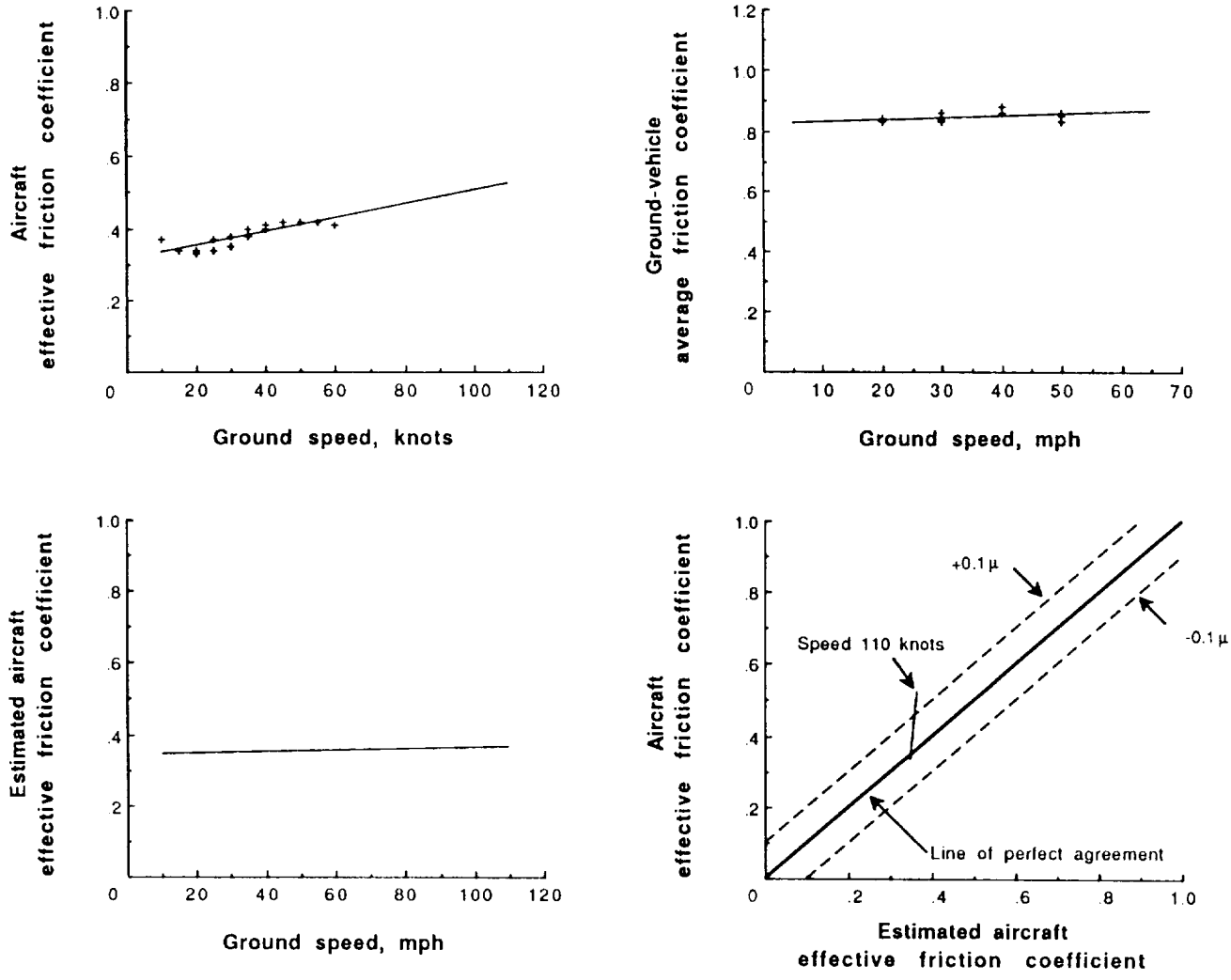

(b) Mu-Meter data.

Figure 52. Continued.

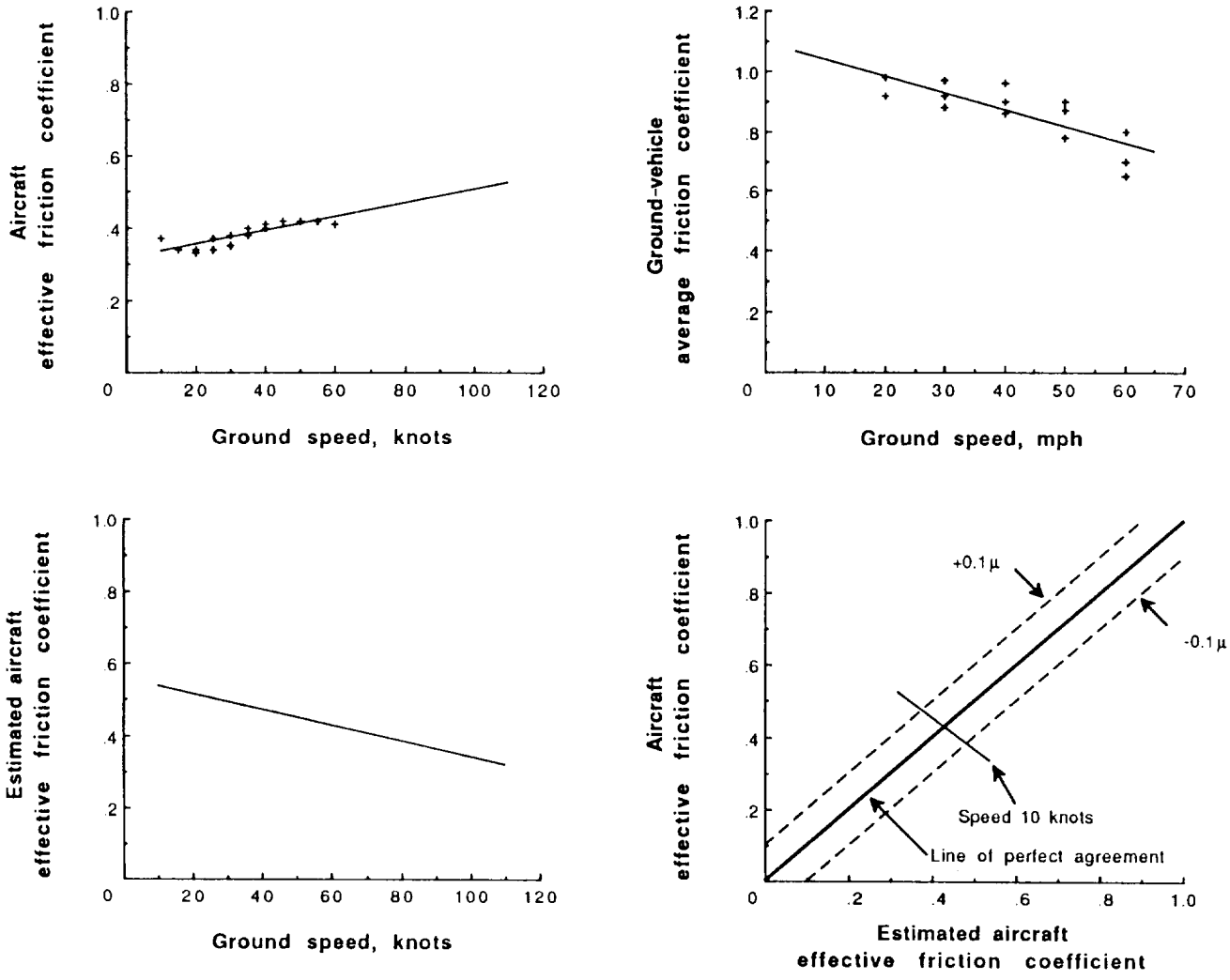

(c) SFT data.

Figure 52. Continued.

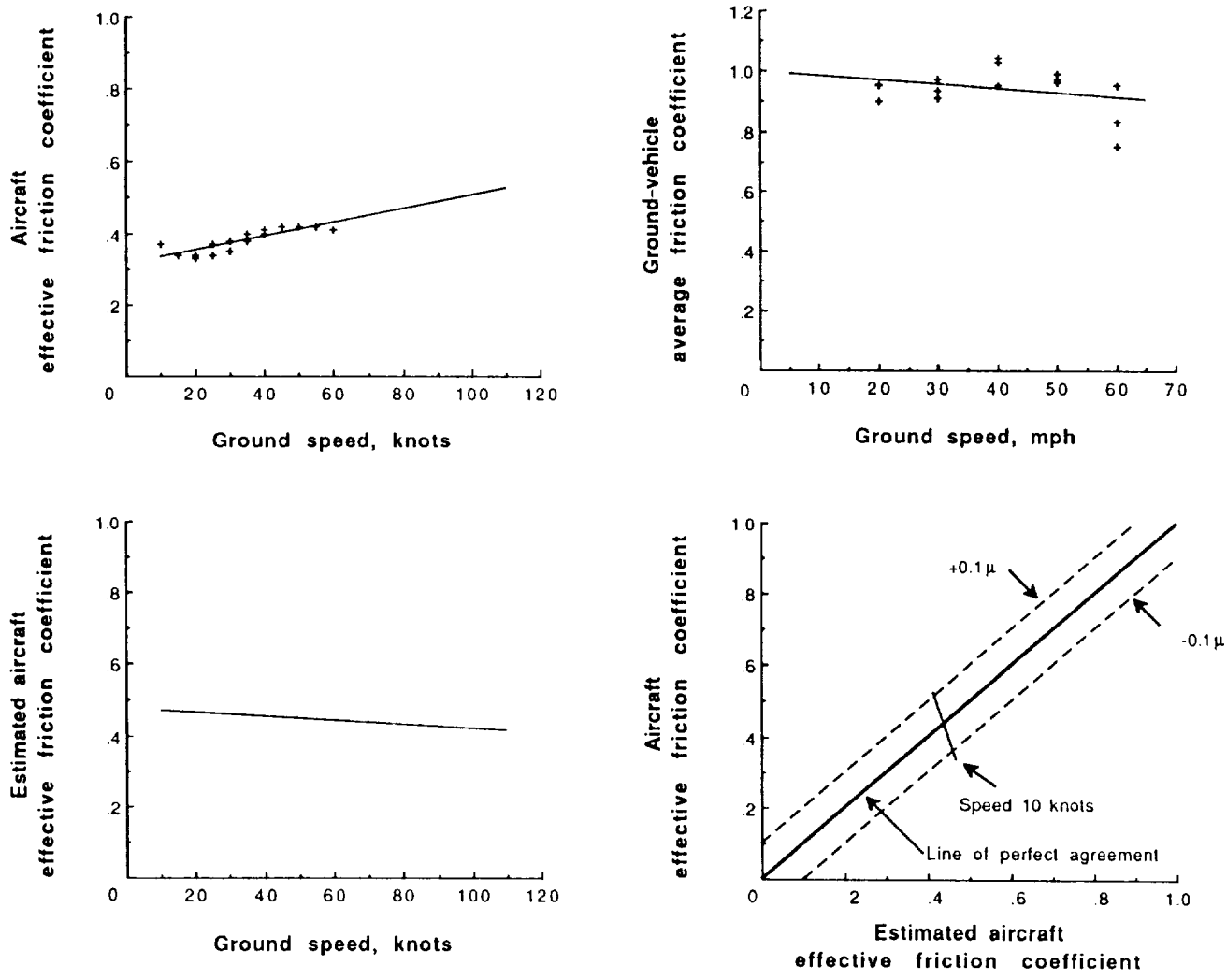

(d) BV-11 skiddometer data.

Figure 52. Concluded.

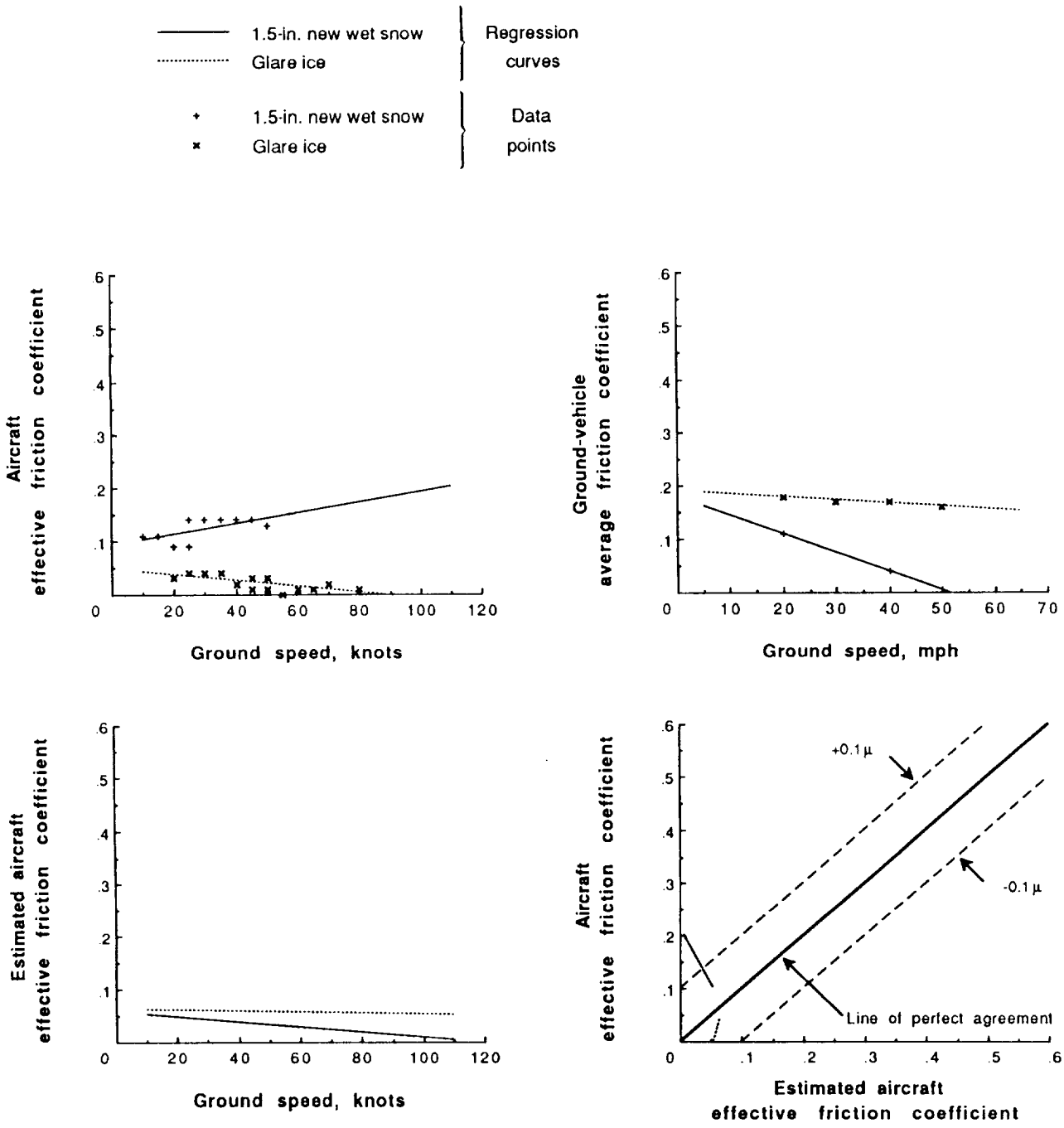

(a) Mu-Meter data.

Figure 53. Variation of Boeing 737 aircraft and ground-vehicle friction data with speed and variation of estimated aircraft braking performance with actual braking performance on snow- and ice-covered runways.

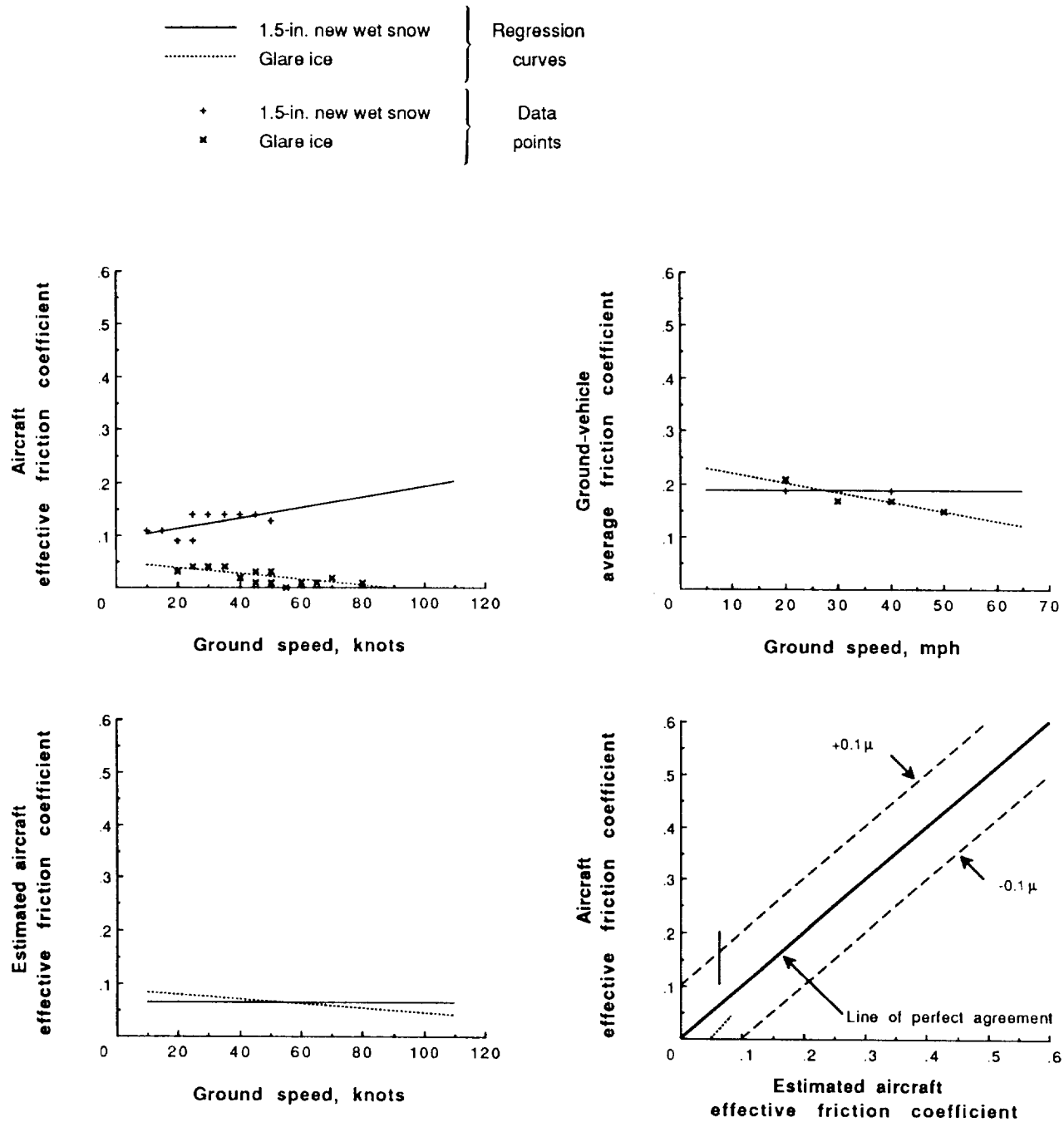

(b) BV-11 skiddometer data.

Figure 53. Concluded.

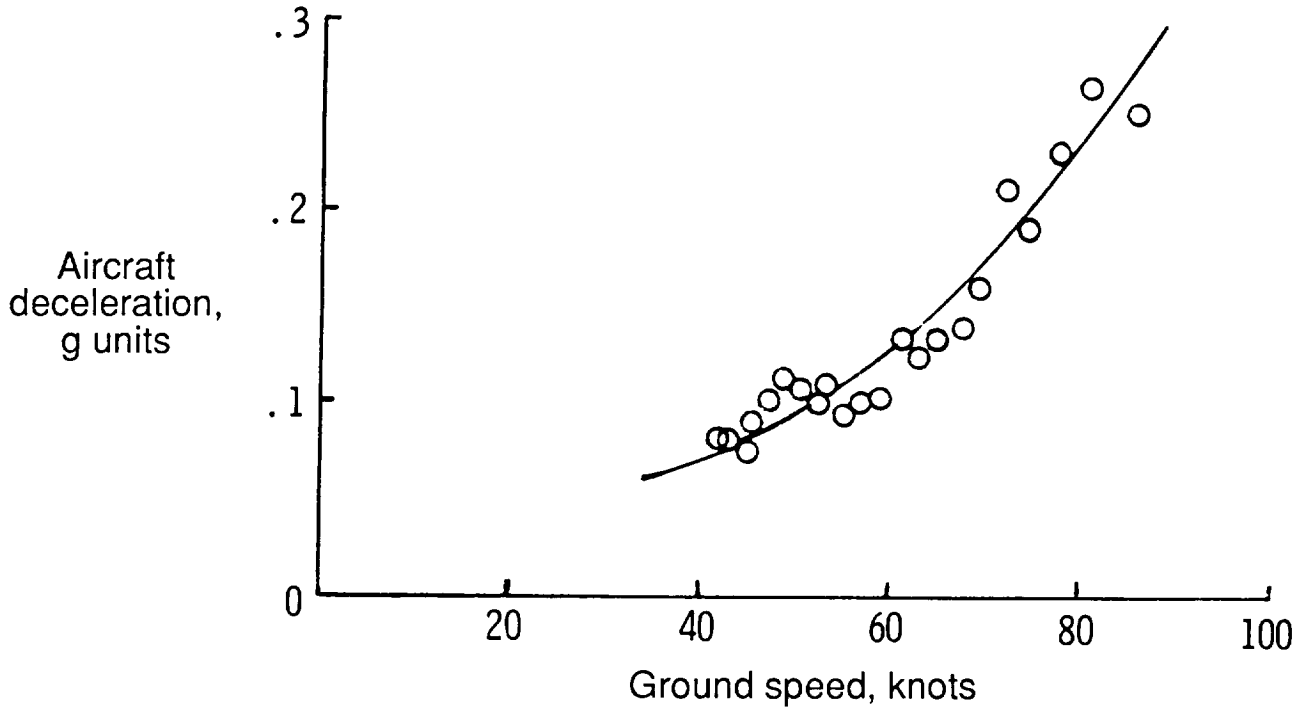

Figure 54. Boeing 737 deceleration in 6-in. loose snow. Landing flaps = 40°; spoilers extended; idle forward thrust; no wheel braking; Snow specific gravity = 0.32; Headwind component = 9.8 knots.

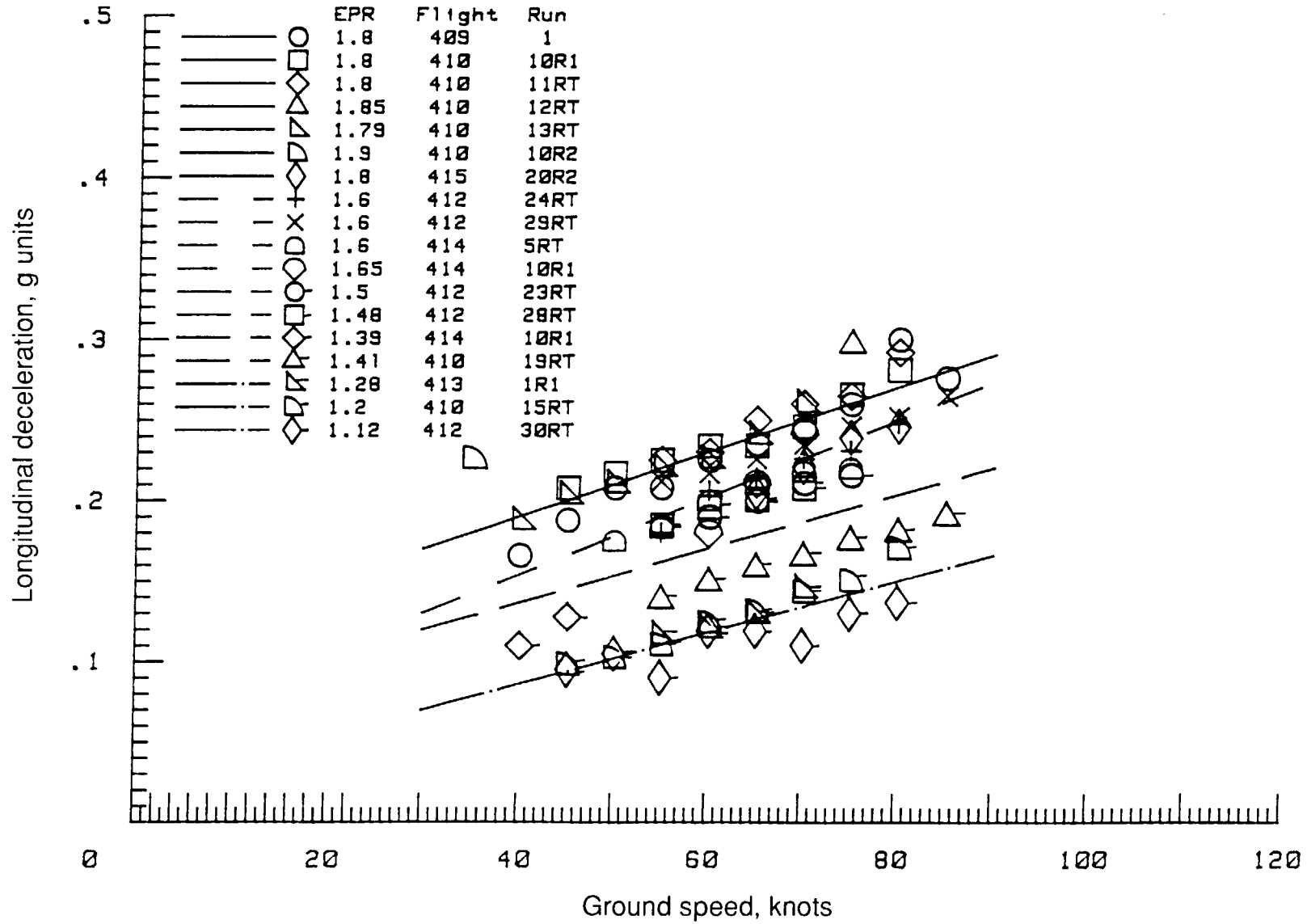

Figure 55. Reverse-thrust performance of Boeing 737 aircraft. (Data include aerodynamic drag and tire rolling resistance.)

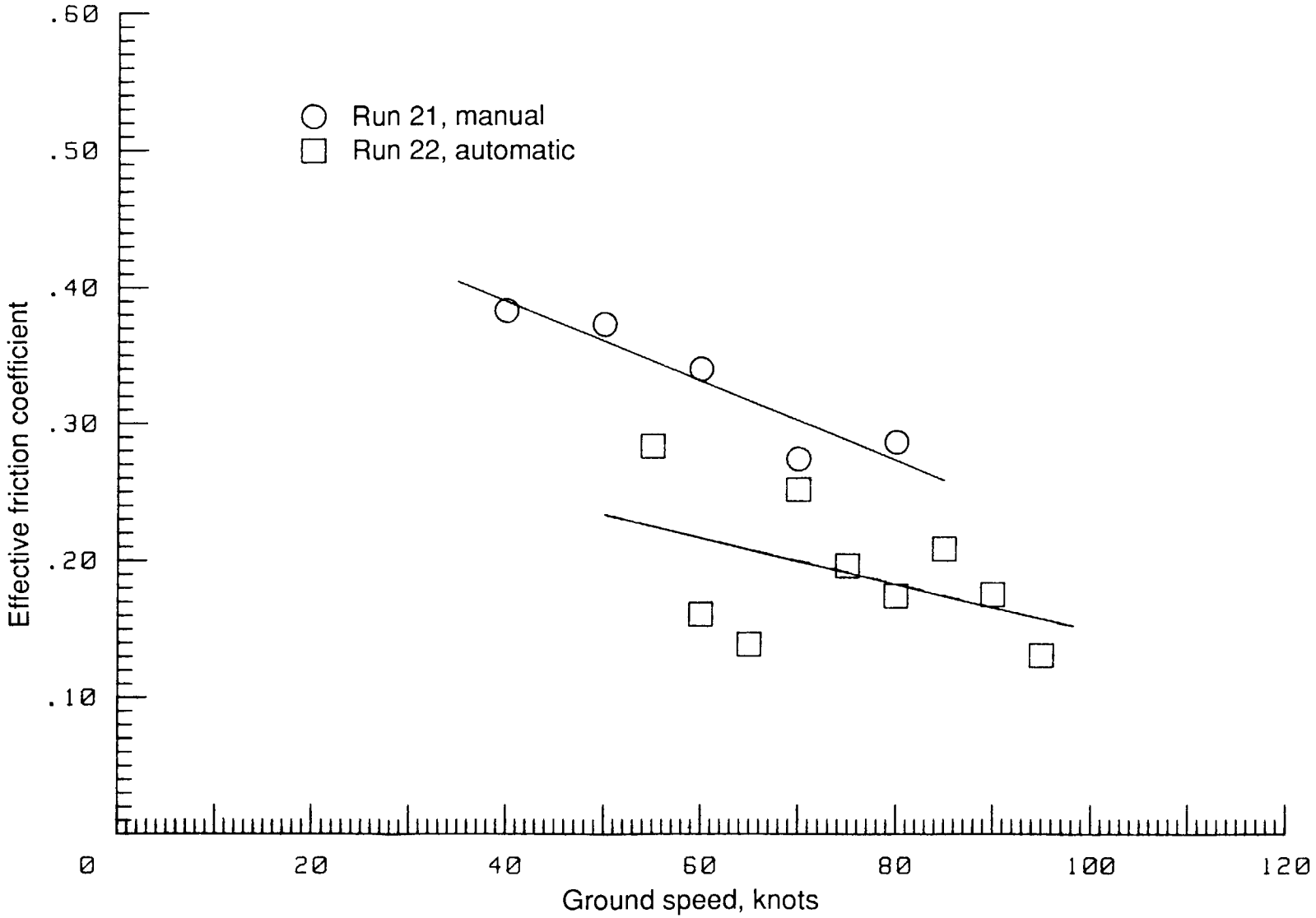

Figure 56. Comparison of Boeing 737 effective friction coefficient with ground speed for manual and automatic braking modes on truck-wet, slurry-seal asphalt, flight 412.

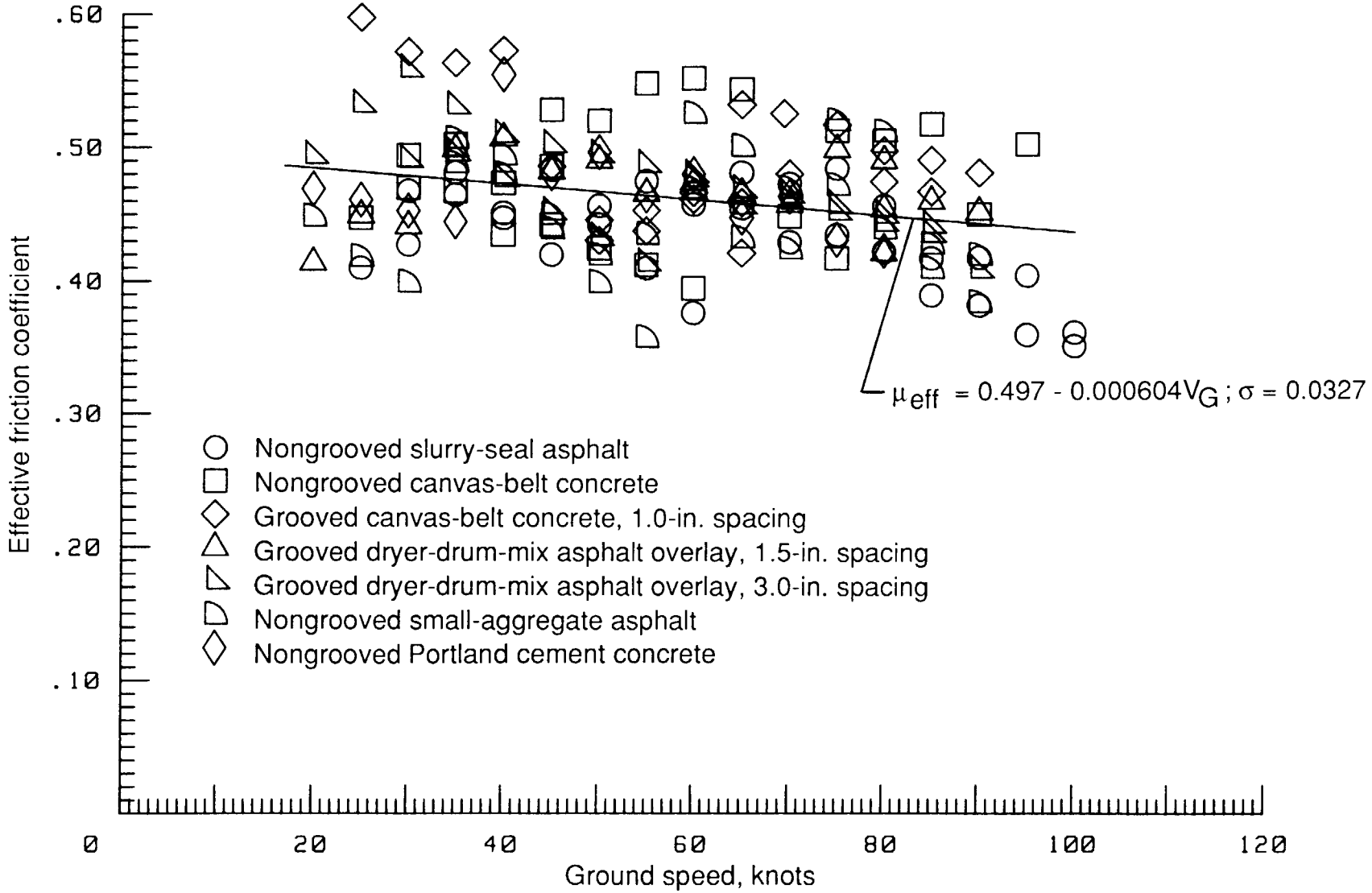

Figure 57. Comparison of Boeing 727 effective friction coefficient with ground speed for dry-runway test conditions.

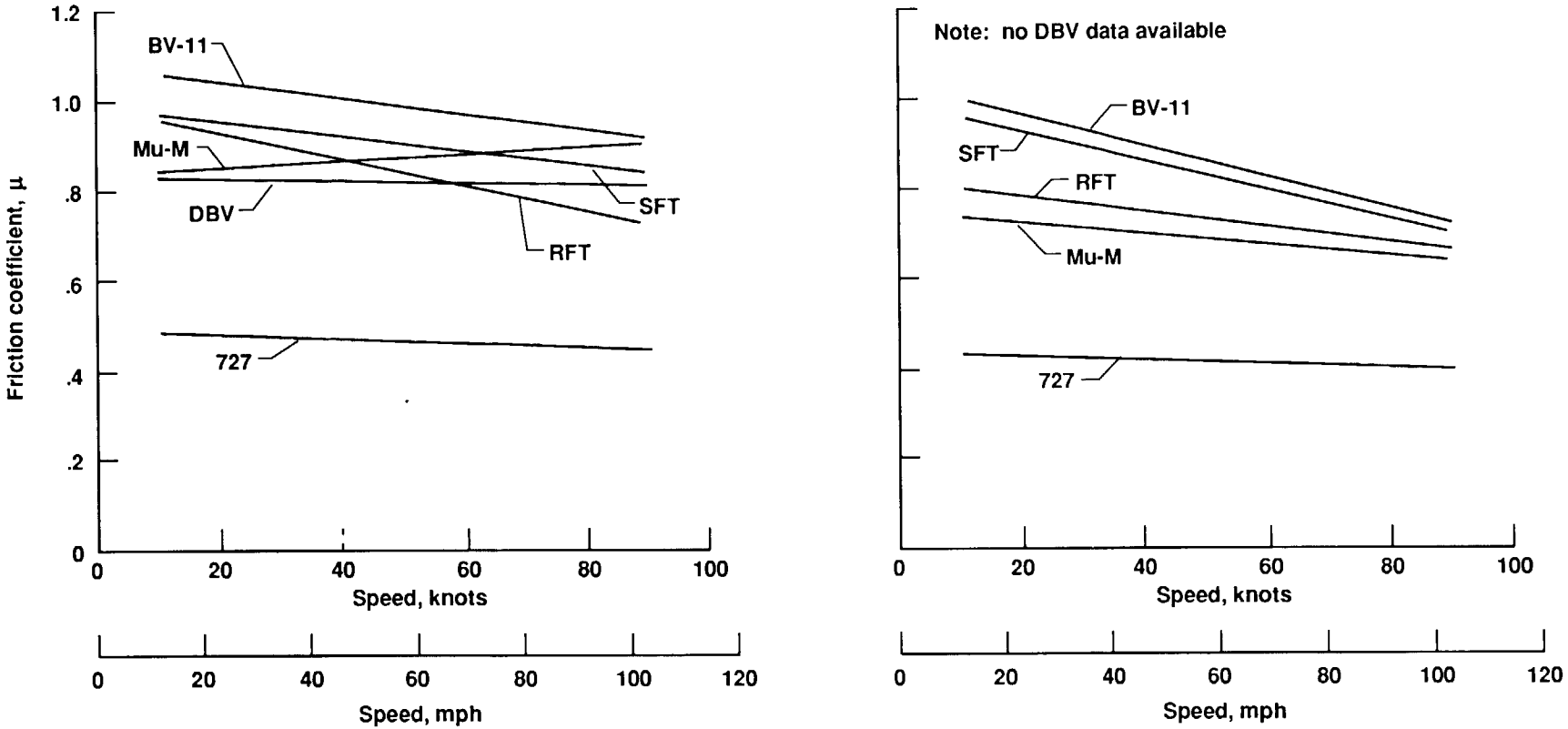

(a) Dry, all surfaces.

(b) Rain-damp, PFC surface at Pease AFB; Rain rate = 0.01 in/hr; Water depth < 0.01 in.

Figure 58. Range of Boeing 727 aircraft and ground-vehicle friction data for different runway test-surface conditions.

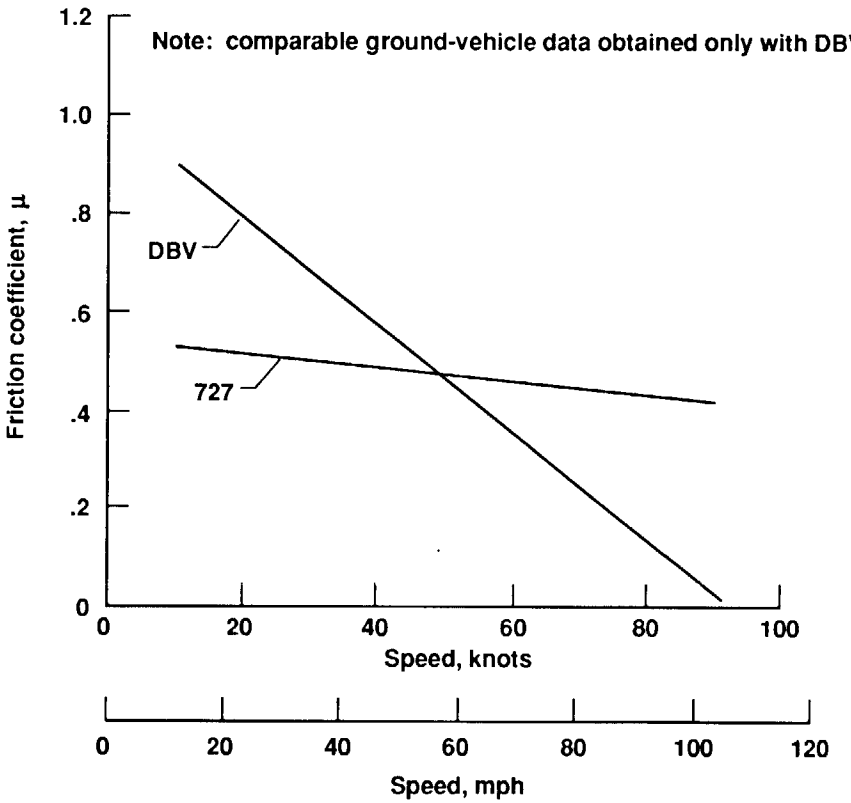

(c) Rain-damp, slurry-seal asphalt; Rain rate = 0.01 in/hr; Water depth < 0.01 in.

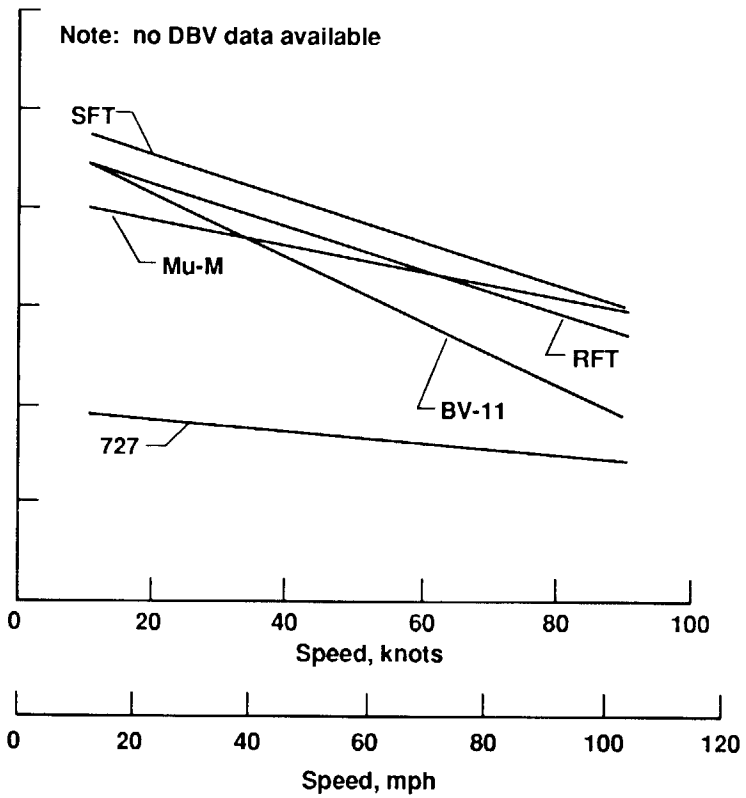

(d) Rain-wet, nongrooved, small-aggregate asphalt at BNAS; Rain rate = 0.16 in/hr; Water depth = 0.04 to 0.06 in.

Figure 58. Continued.

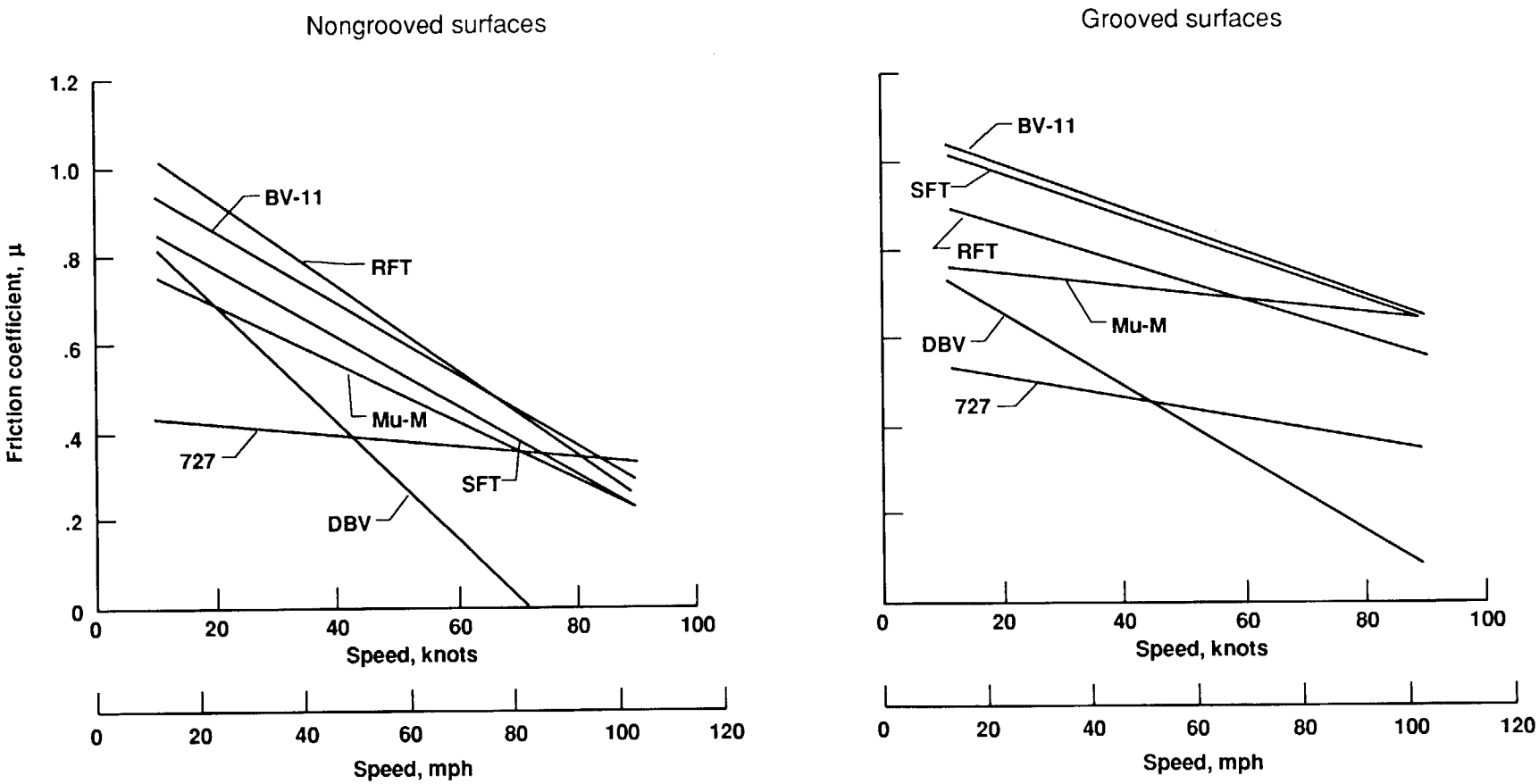

(e) Truck-wet surfaces.

Figure 58. Continued.

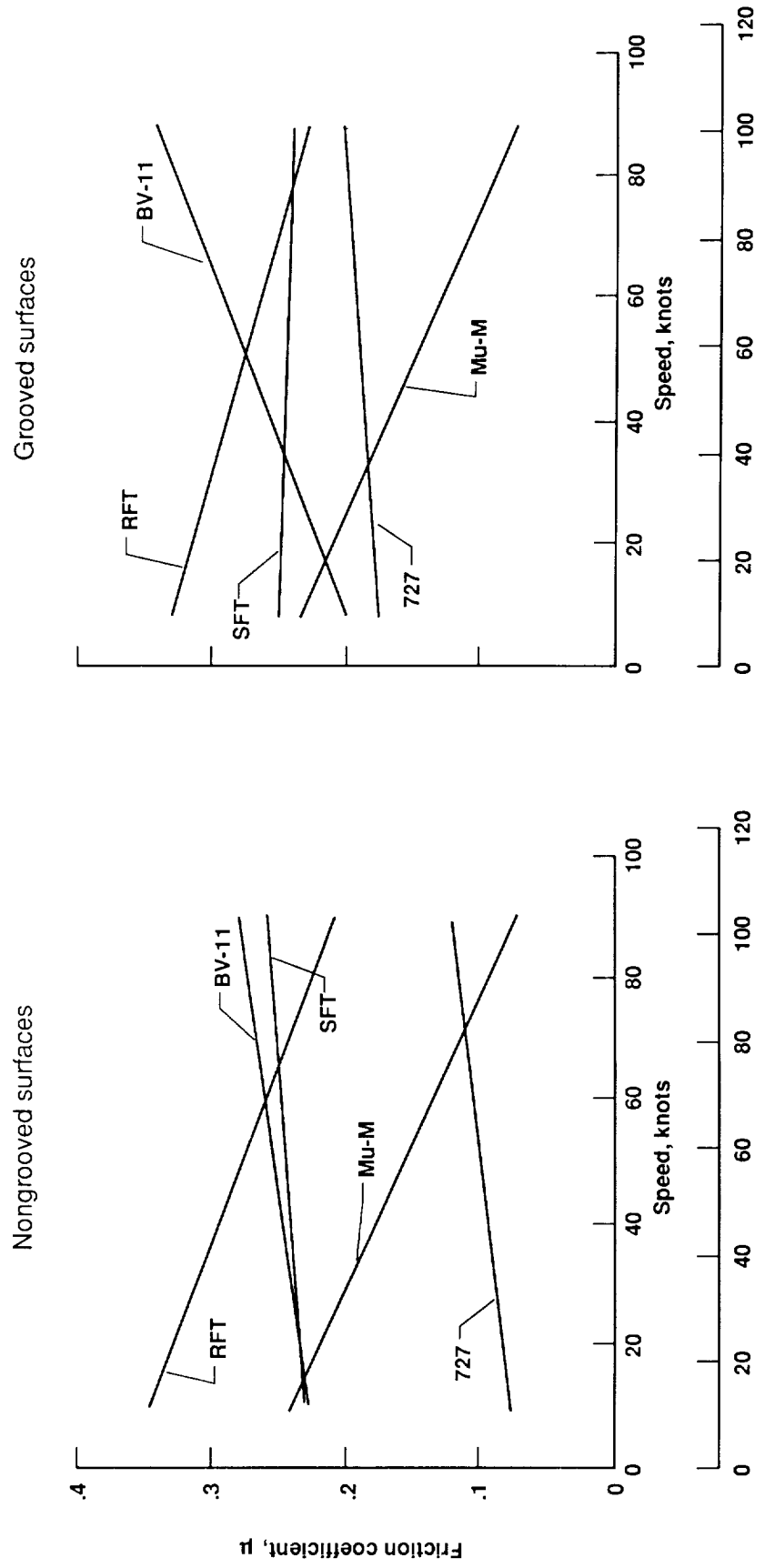

(f) 1.5-in. wet snow.

(g) Packed snow on ice.

Figure 58. Continued.

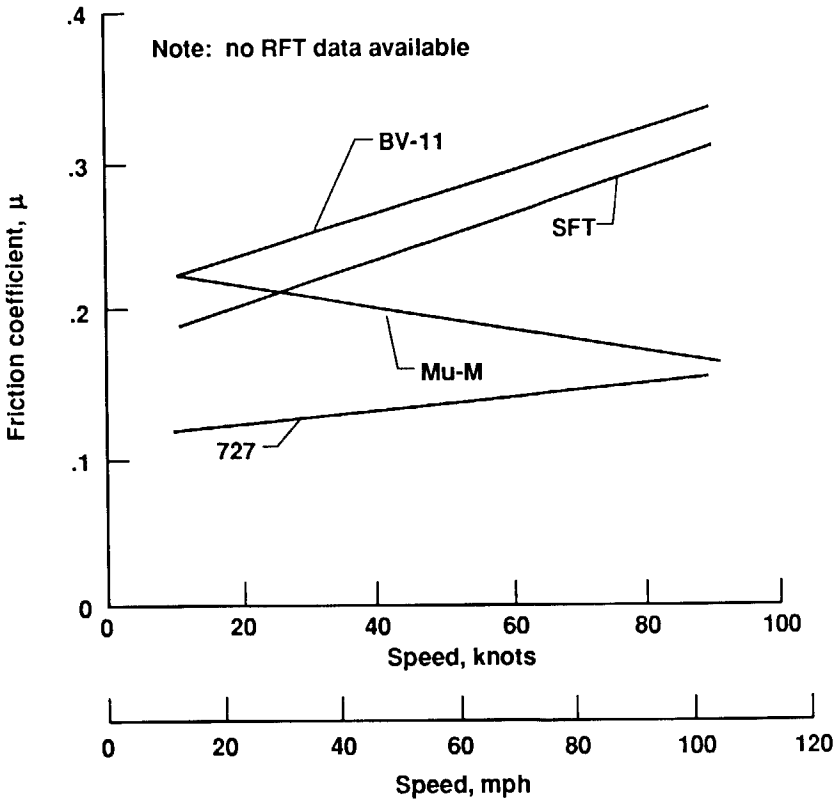

(h) Dry snow on ice.

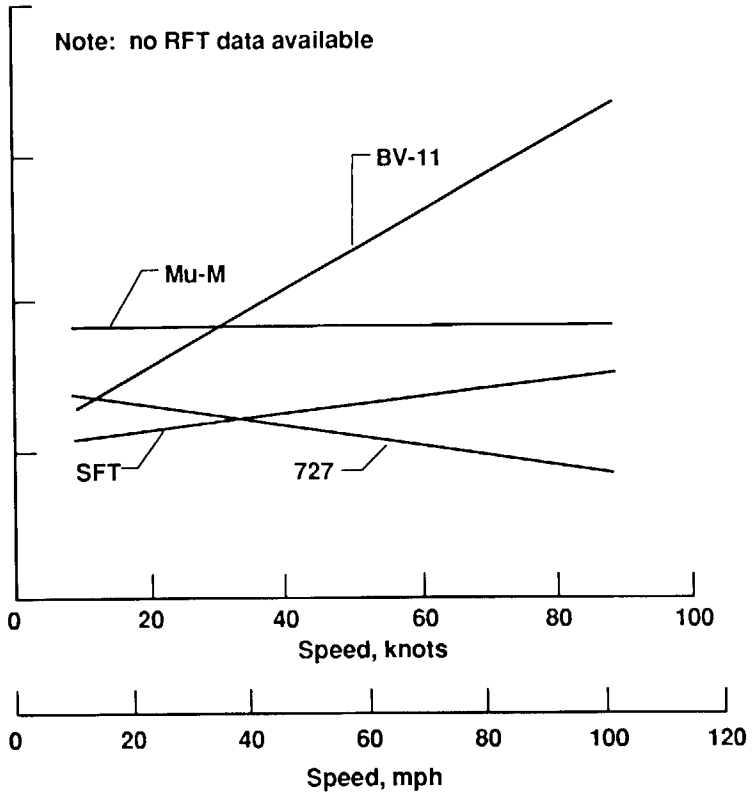

(i) Urea on ice.

Figure 58. Continued.

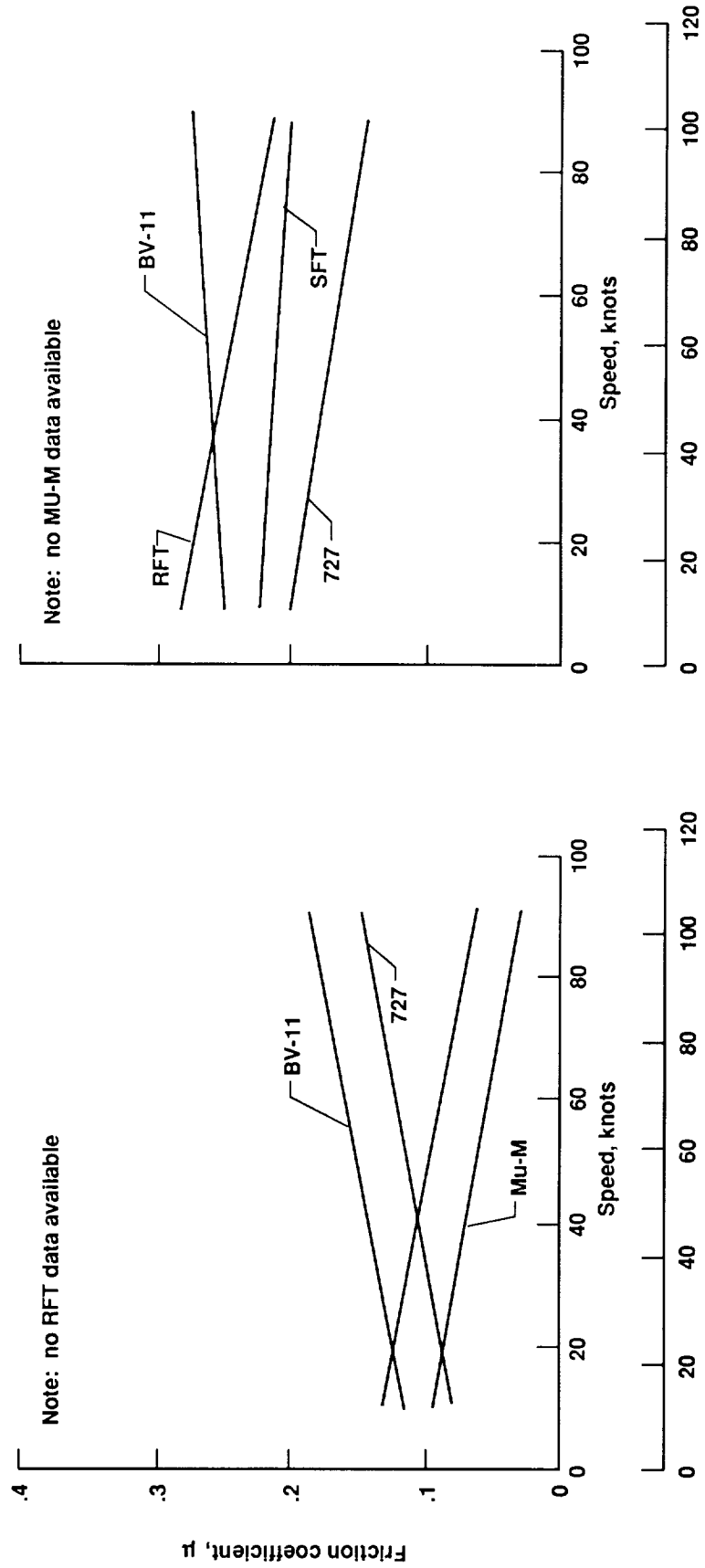

(j) Loose dry snow.

(k) UCAR on ice.

Figure 58. Continued.

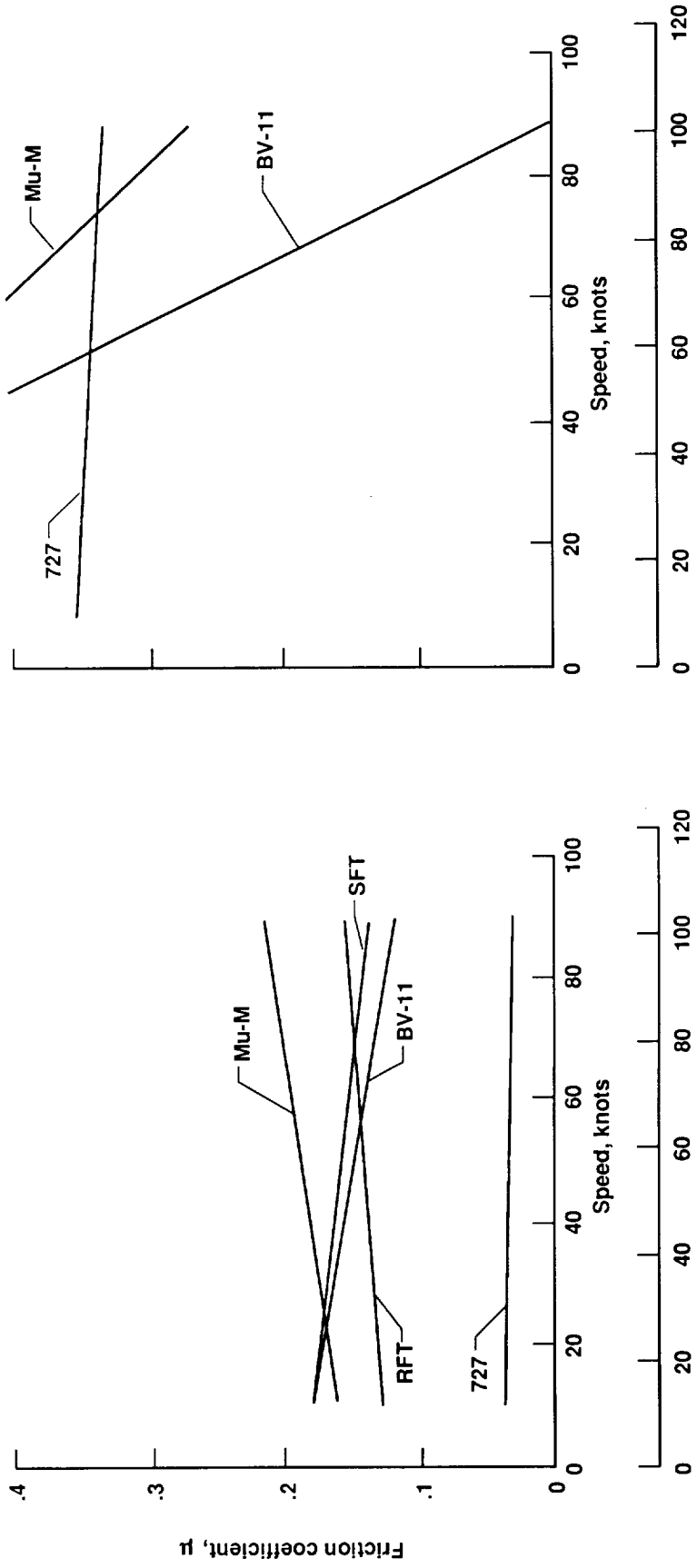

(l) Solid ice.

(m) 0.25-in. slush.

Figure 58. Concluded.

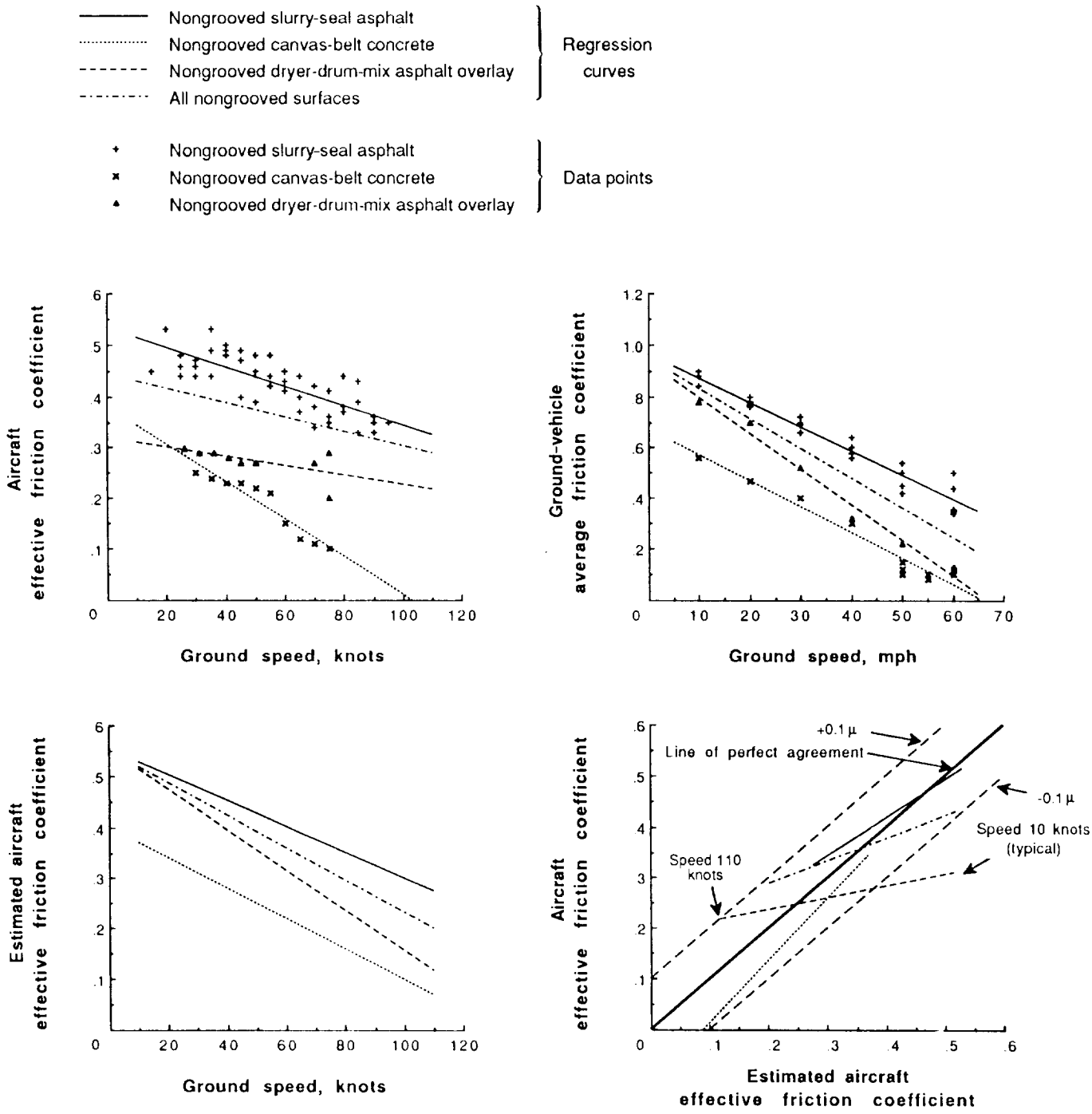

(a) DBV data.

Figure 59. Variation of Boeing 727 aircraft and ground-vehicle friction data with speed and variation of estimated aircraft braking performance with actual braking performance on truck-wet, nongrooved test surfaces.

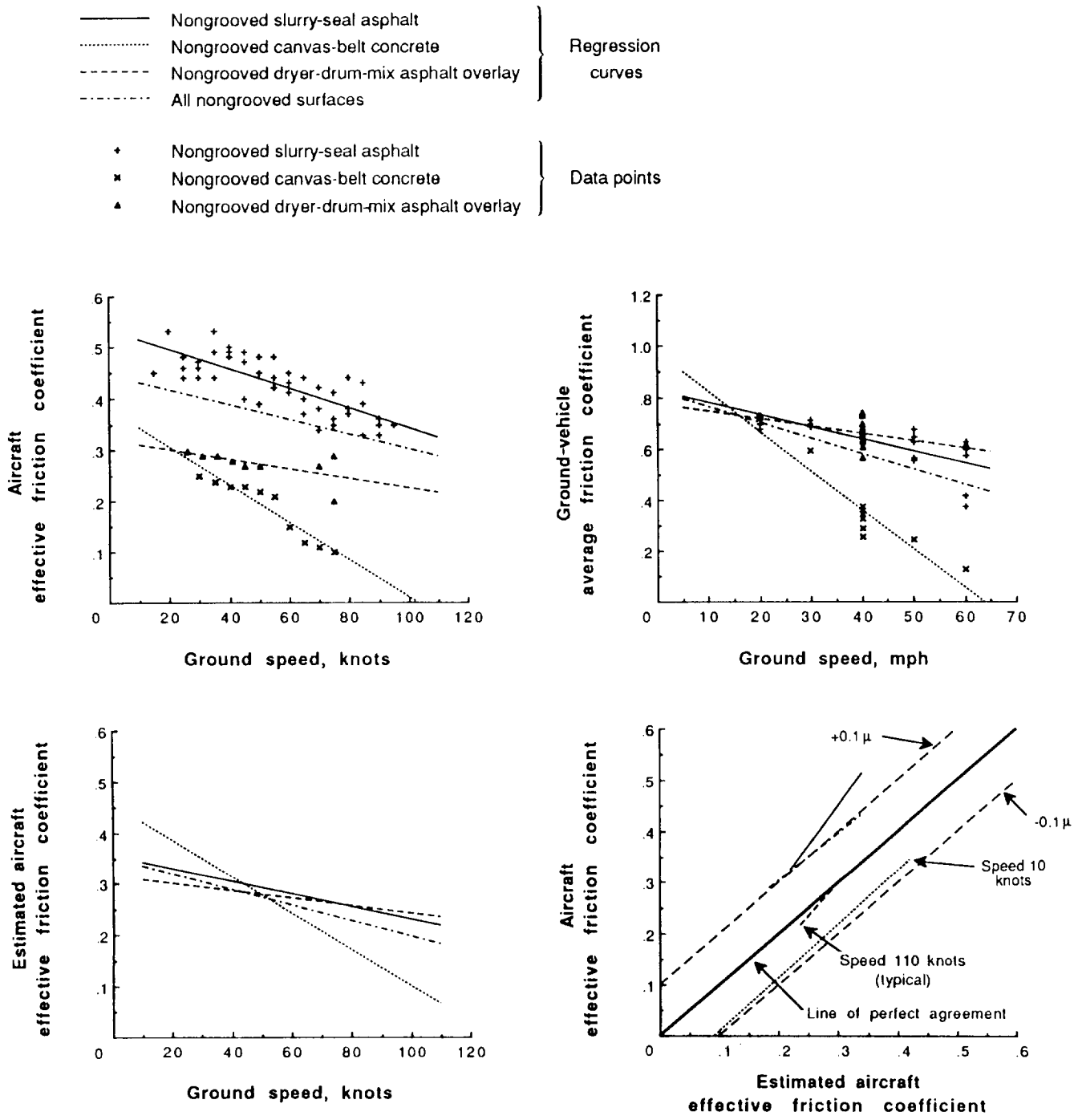

(b) Mu-Meter data.

Figure 59. Continued.

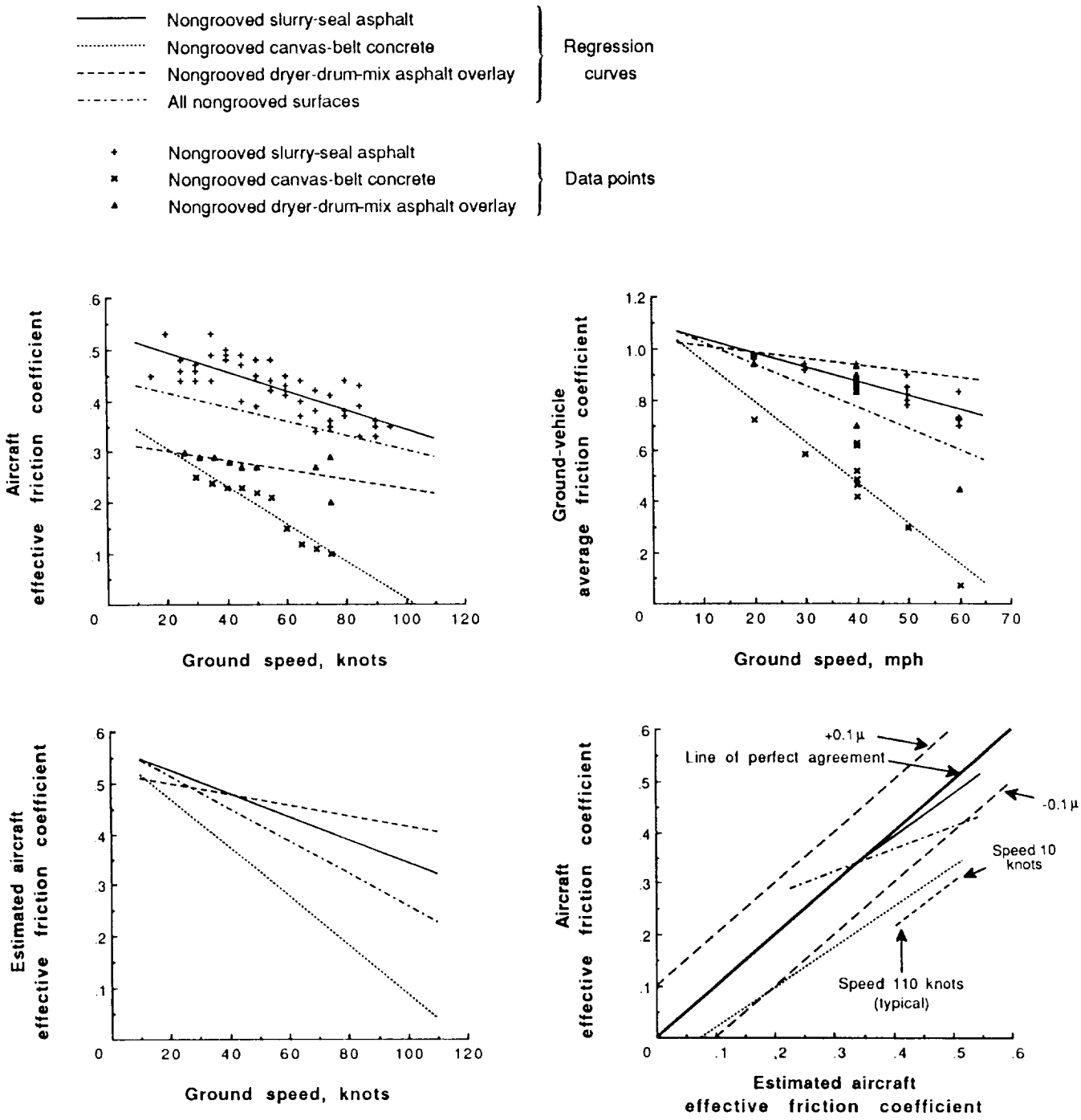

(c) SFT data.

Figure 59. Continued.

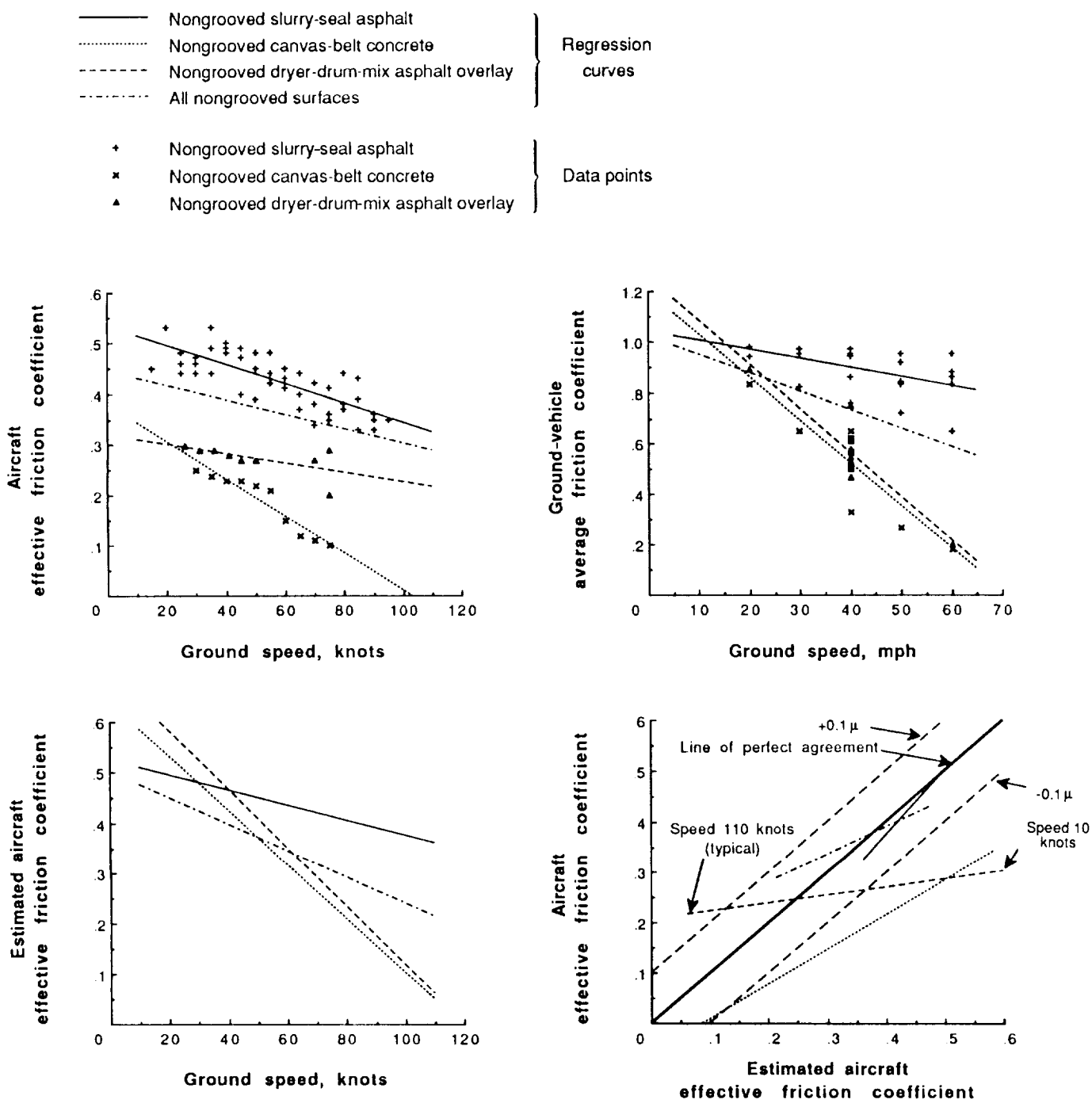

(d) BV-11 skiddometer data.

Figure 59. Continued.

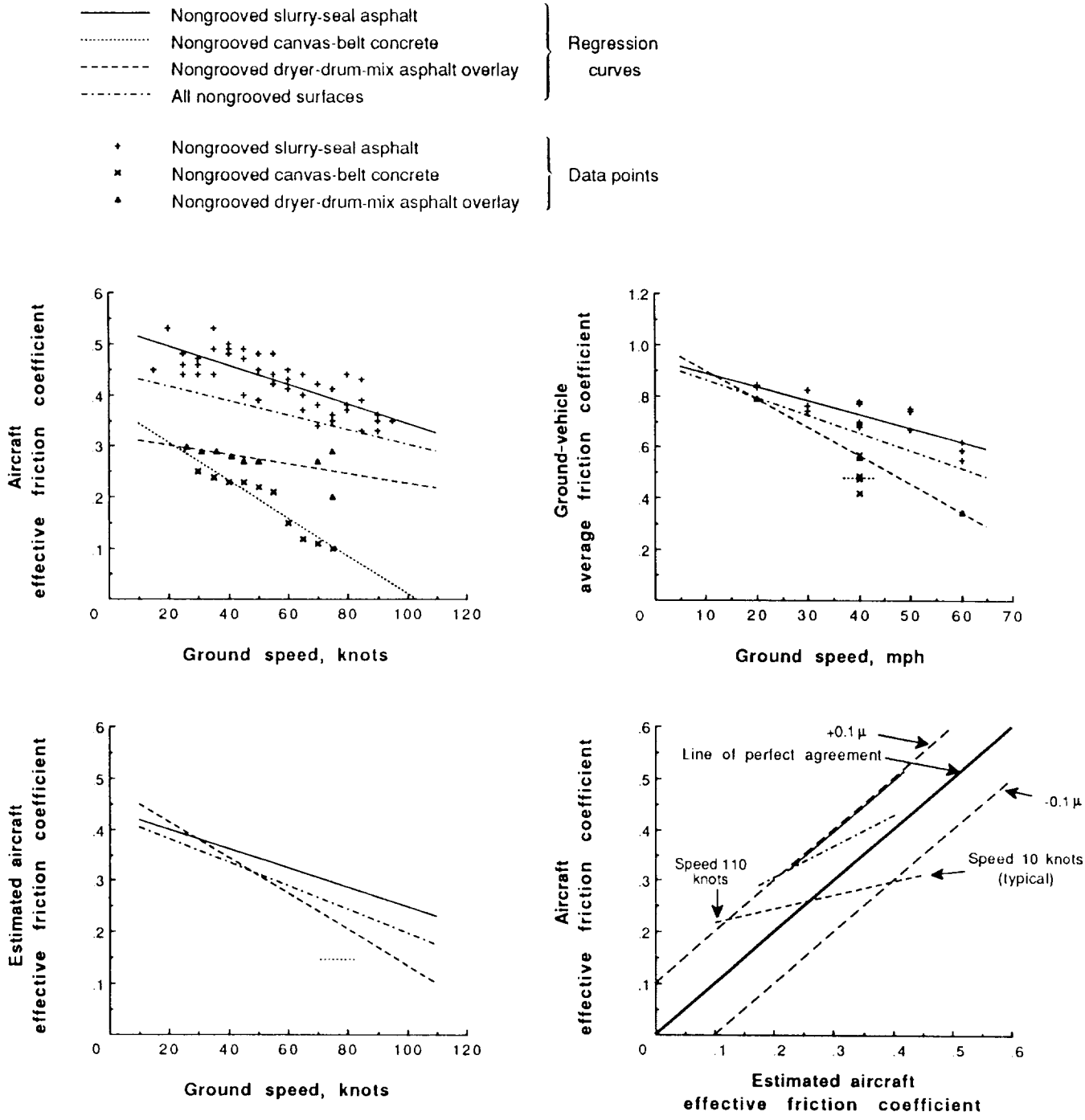

(e) RFT data.

Figure 59. Concluded.

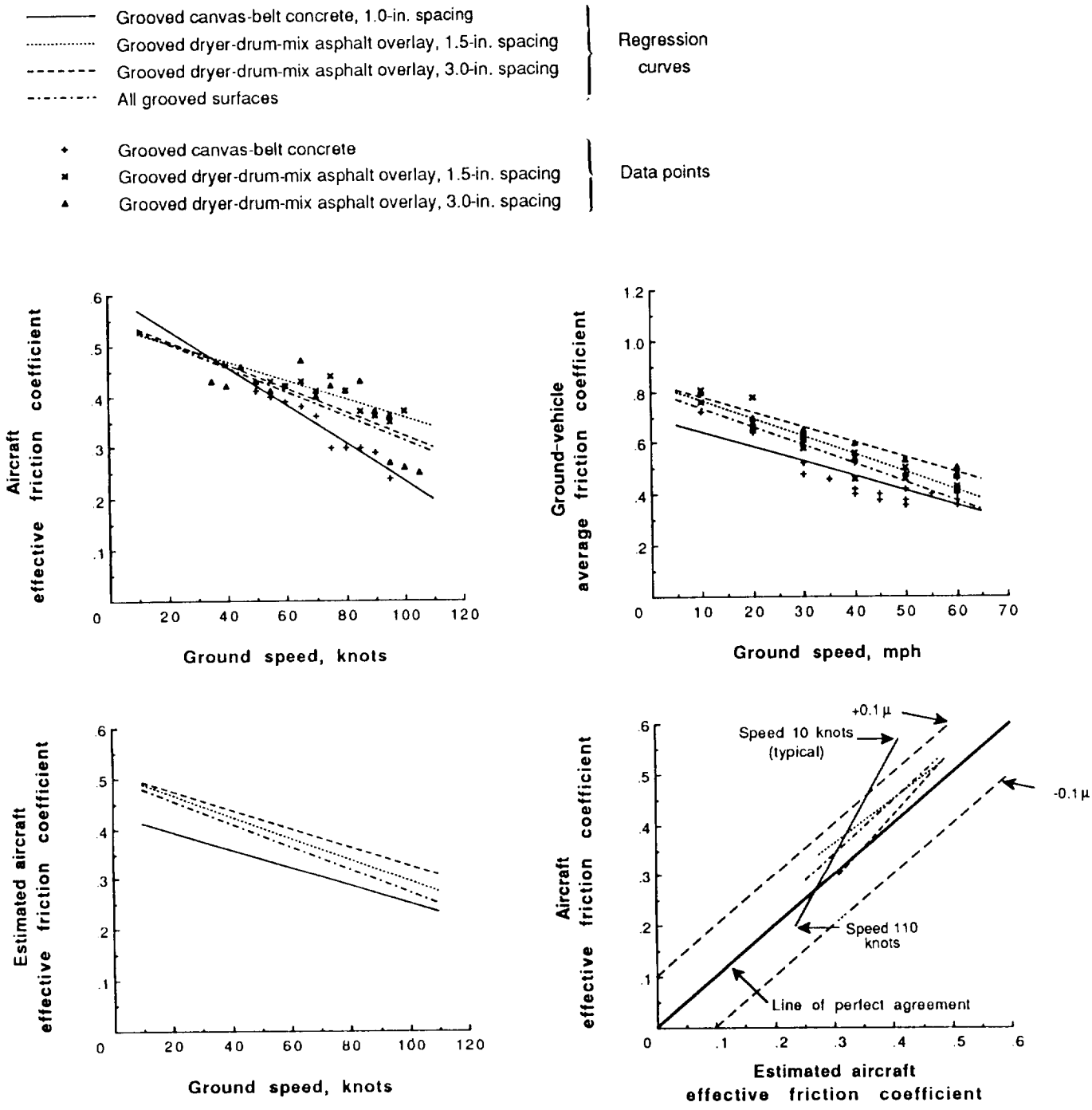

(a) DBV data.

Figure 60. Variation of Boeing 727 aircraft and ground-vehicle friction data with speed and variation of estimated aircraft braking performance with actual braking performance on truck-wet, grooved test surfaces.

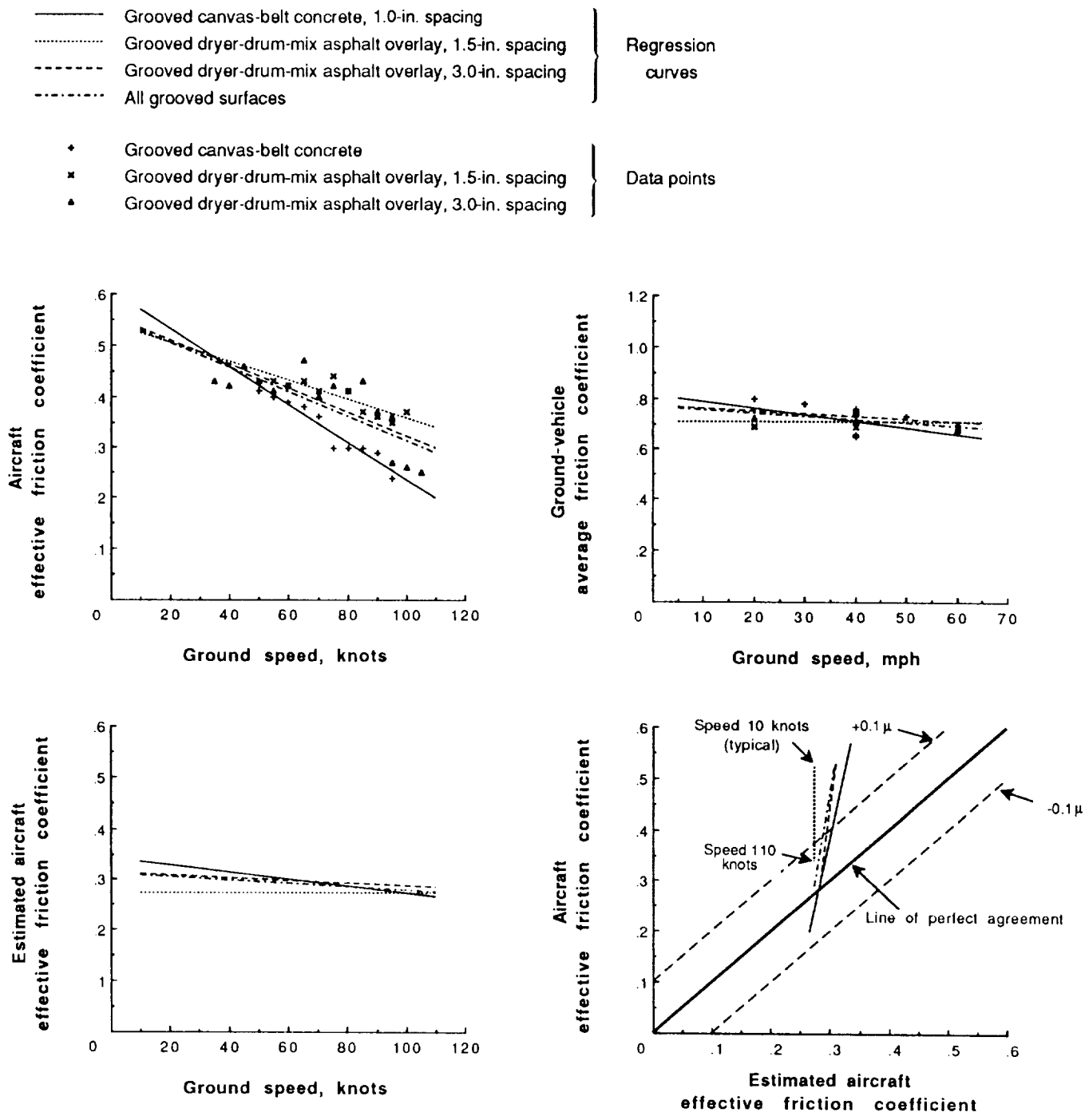

(b) Mu-Meter data.

Figure 60. Continued.

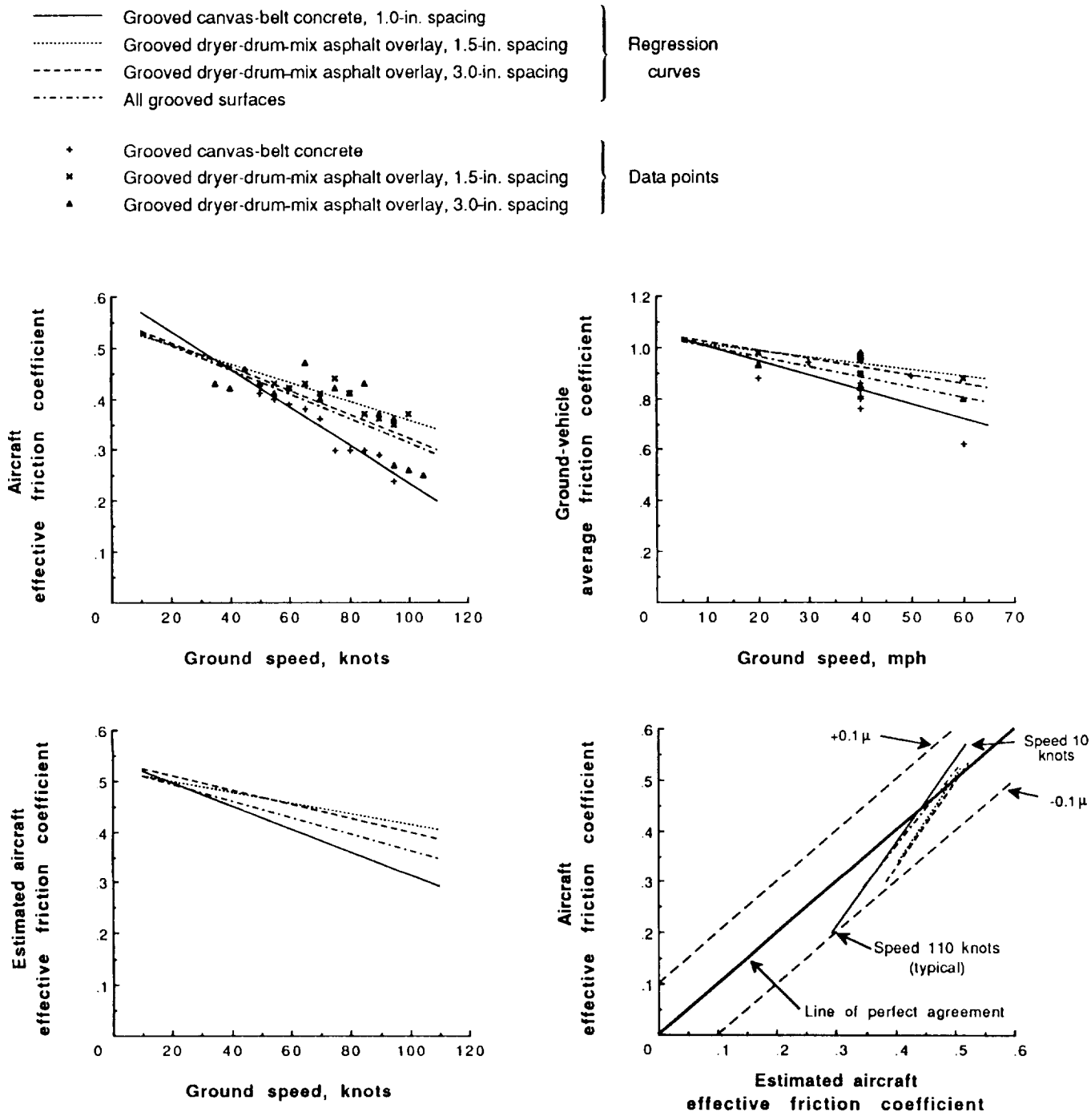

(c) SFT data.

Figure 60. Continued.

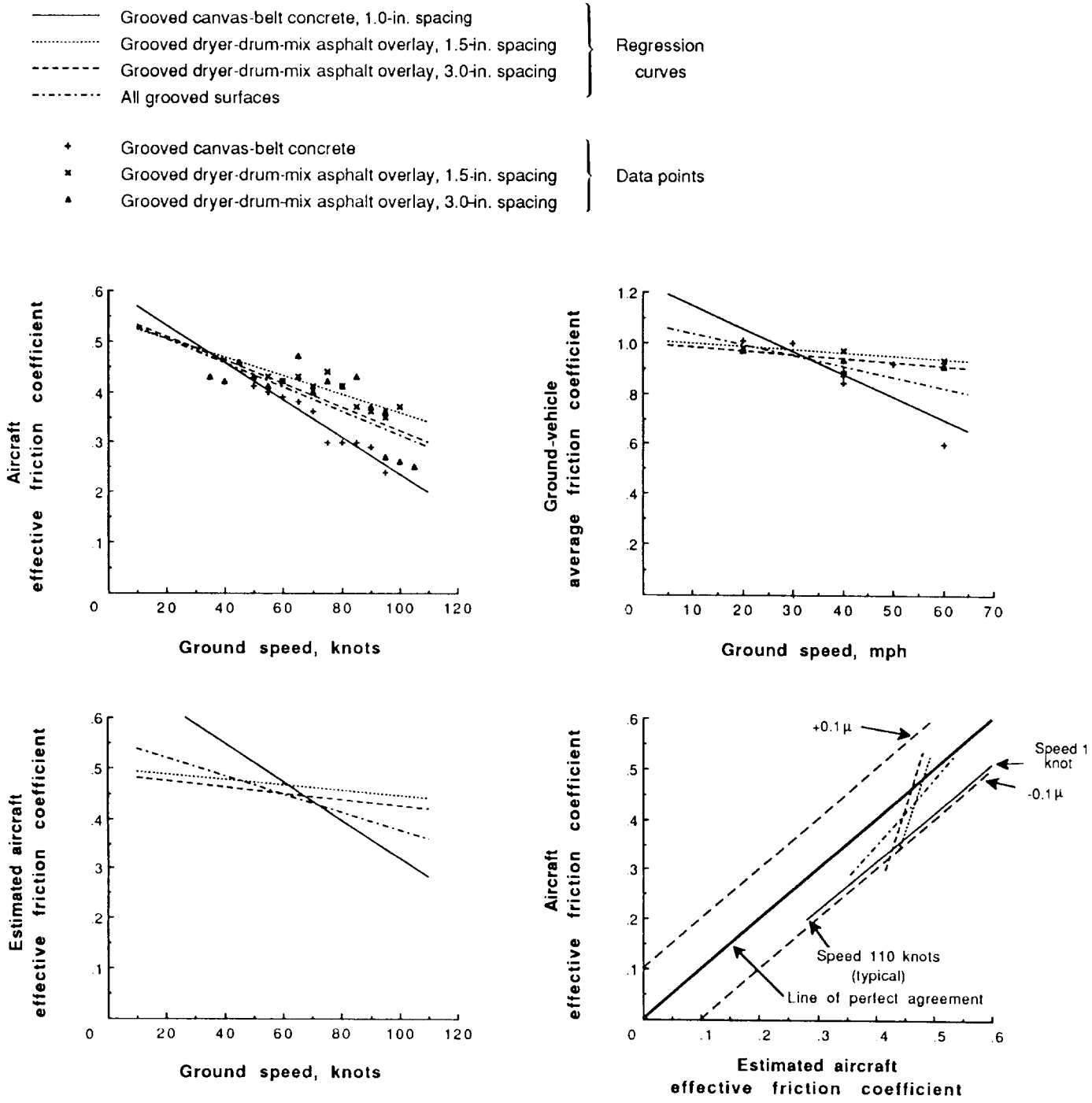

(d) BV-11 skiddometer data.

Figure 60. Continued.

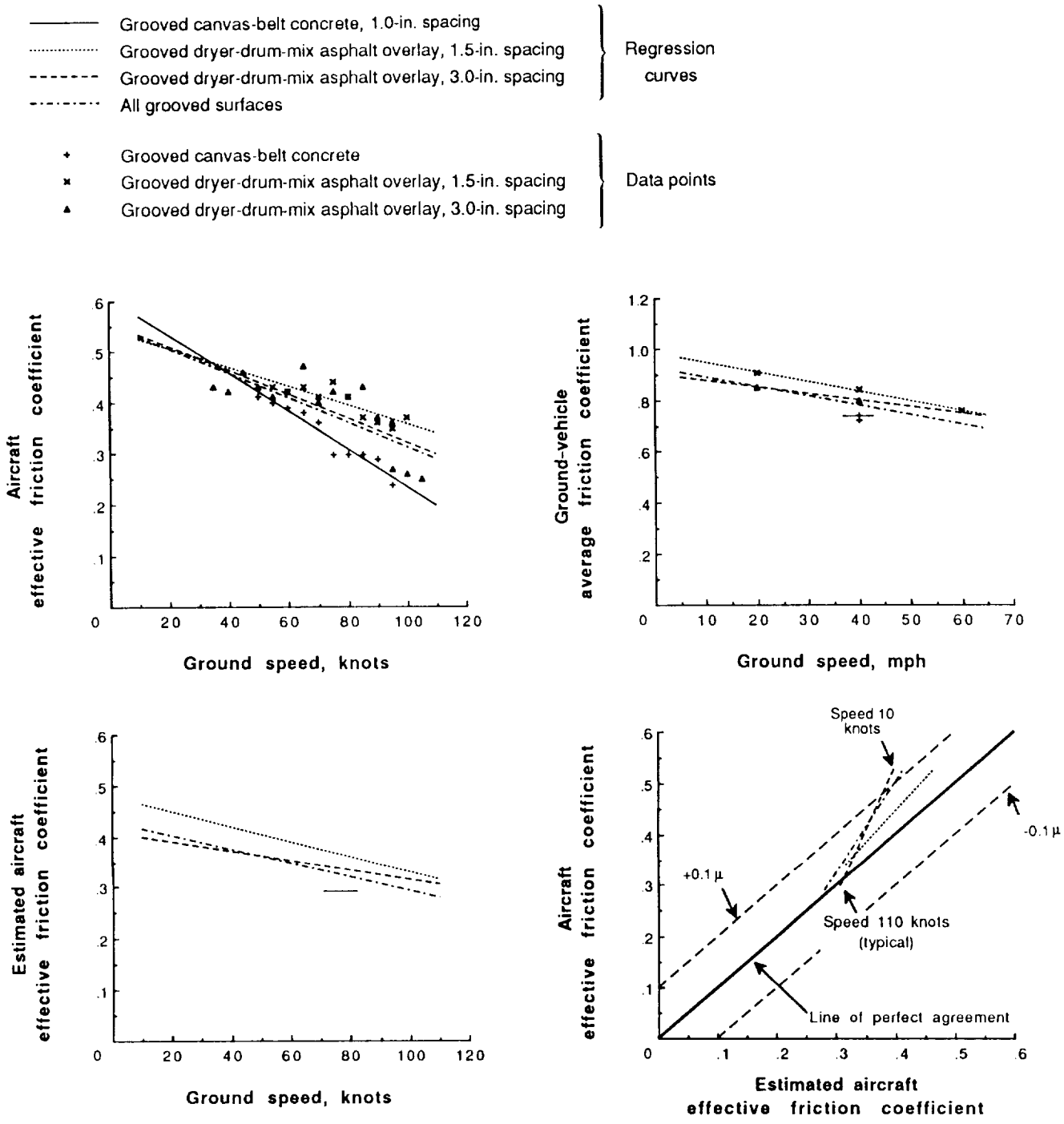

(e) RFT data.

Figure 60. Concluded.

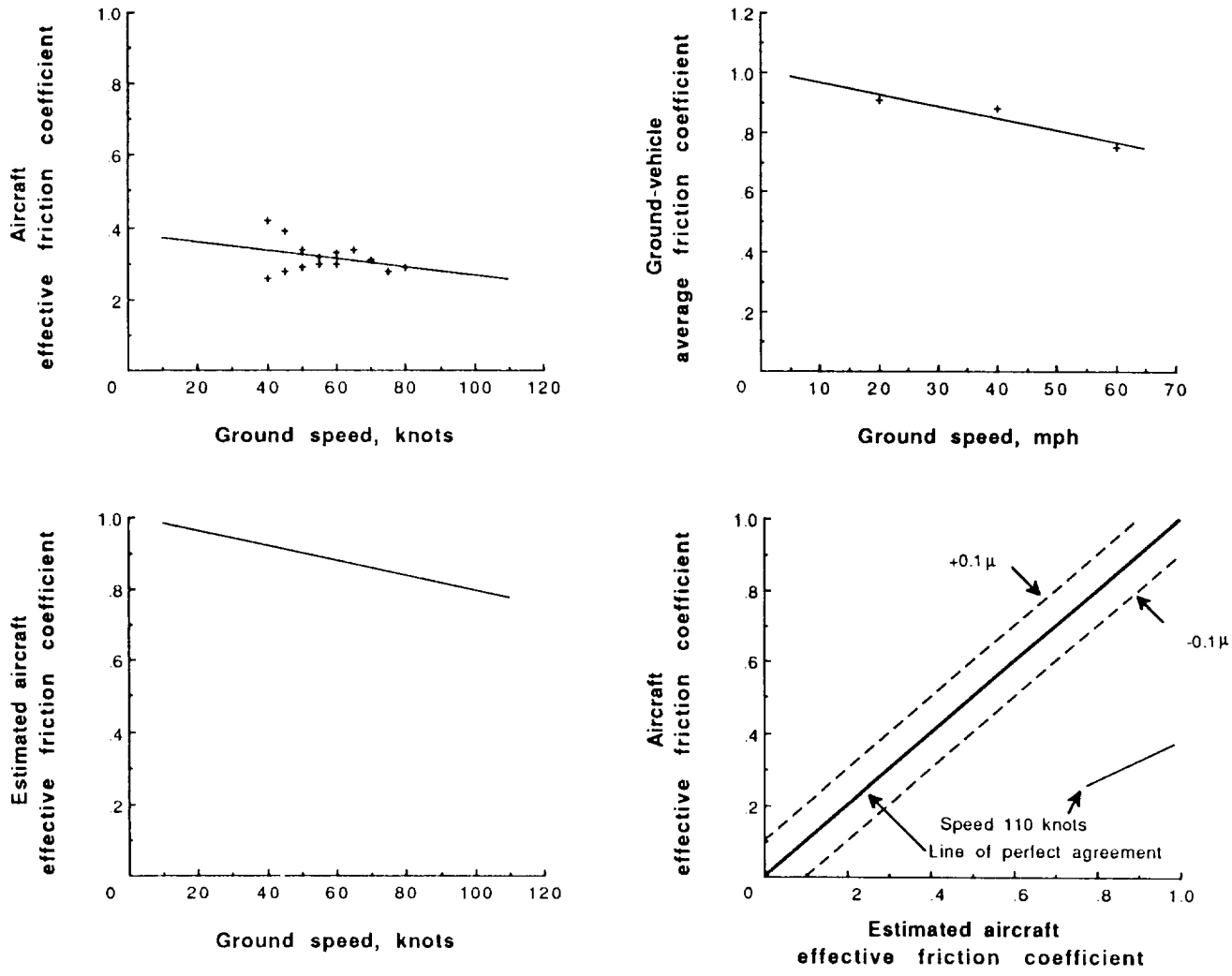

(a) SFT data.

Figure 61. Variation of Boeing 727 aircraft and ground-vehicle friction data with speed and variation of estimated aircraft braking performance with actual braking performance on rain-wet, nongrooved, small-aggregate asphalt surface.

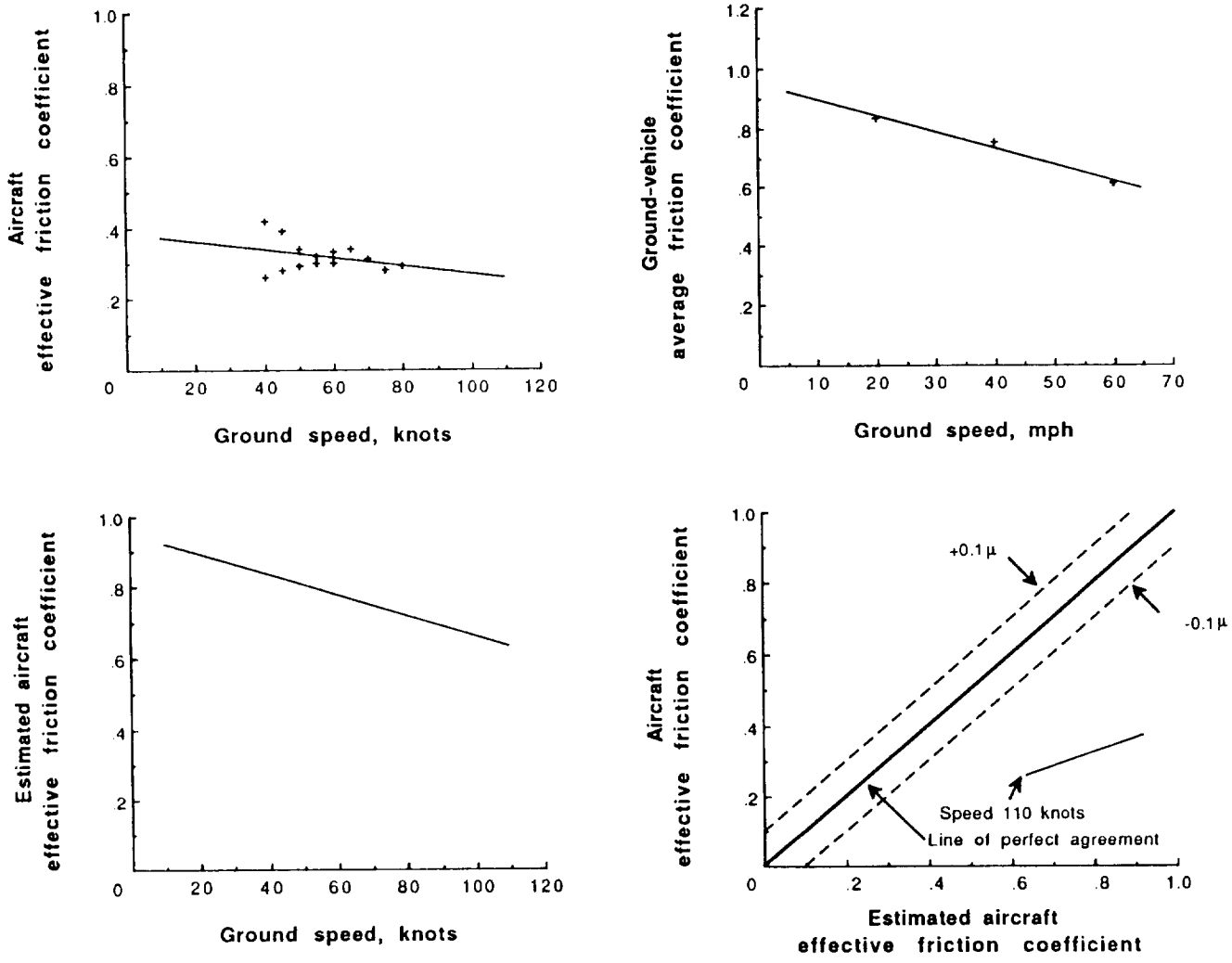

(b) BV-11 skiddometer data.

Figure 61. Continued.

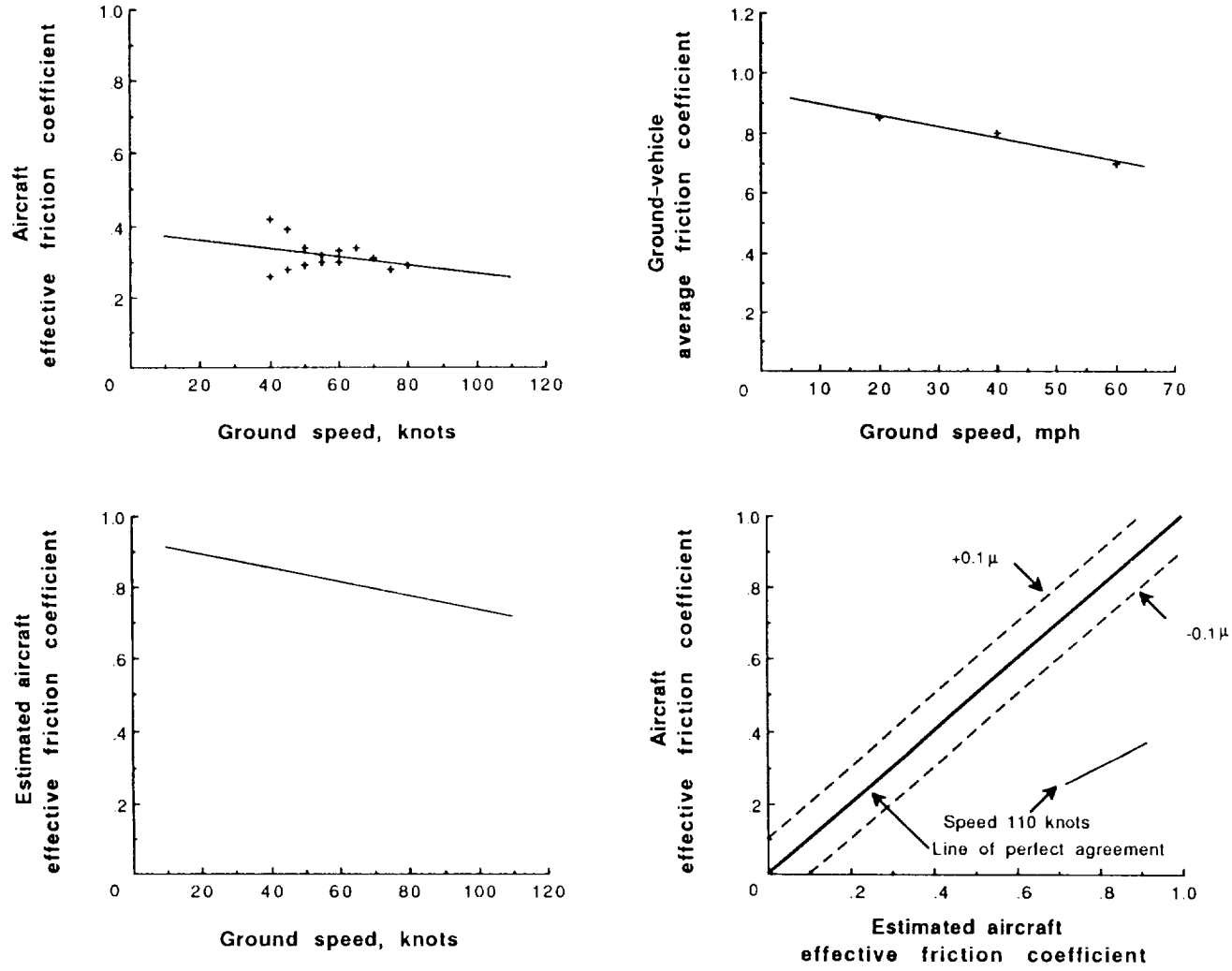

(c) RFT data.

Figure 61. Concluded.

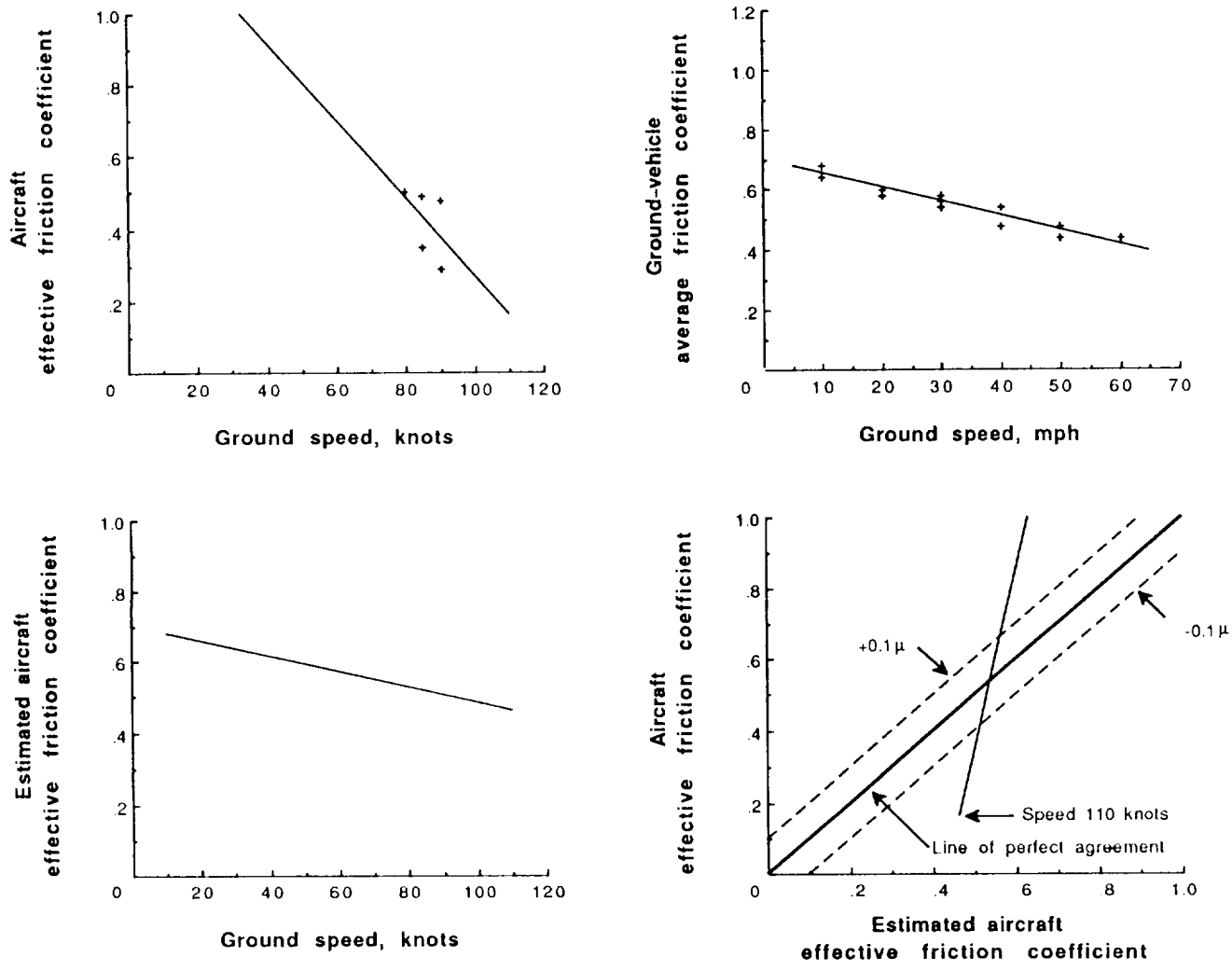

(a) DBV data.

Figure 62. Variation of Boeing 727 aircraft and ground-vehicle friction data with speed and variation of estimated aircraft braking performance with actual braking performance on rain-wet, grooved 1-in. spacing, canvas-belt, concrete surface.

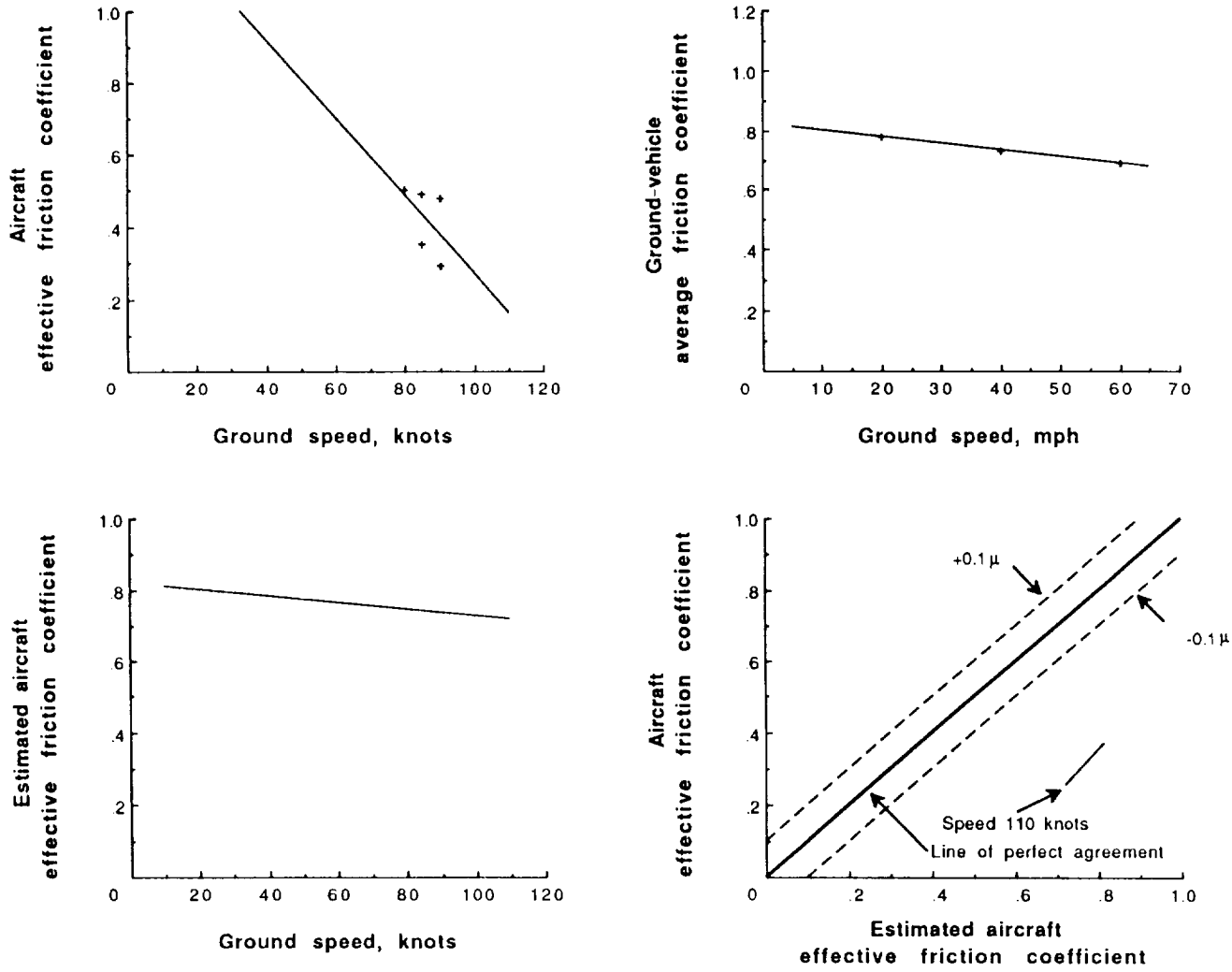

(b) Mu-Meter data.

Figure 62. Concluded.

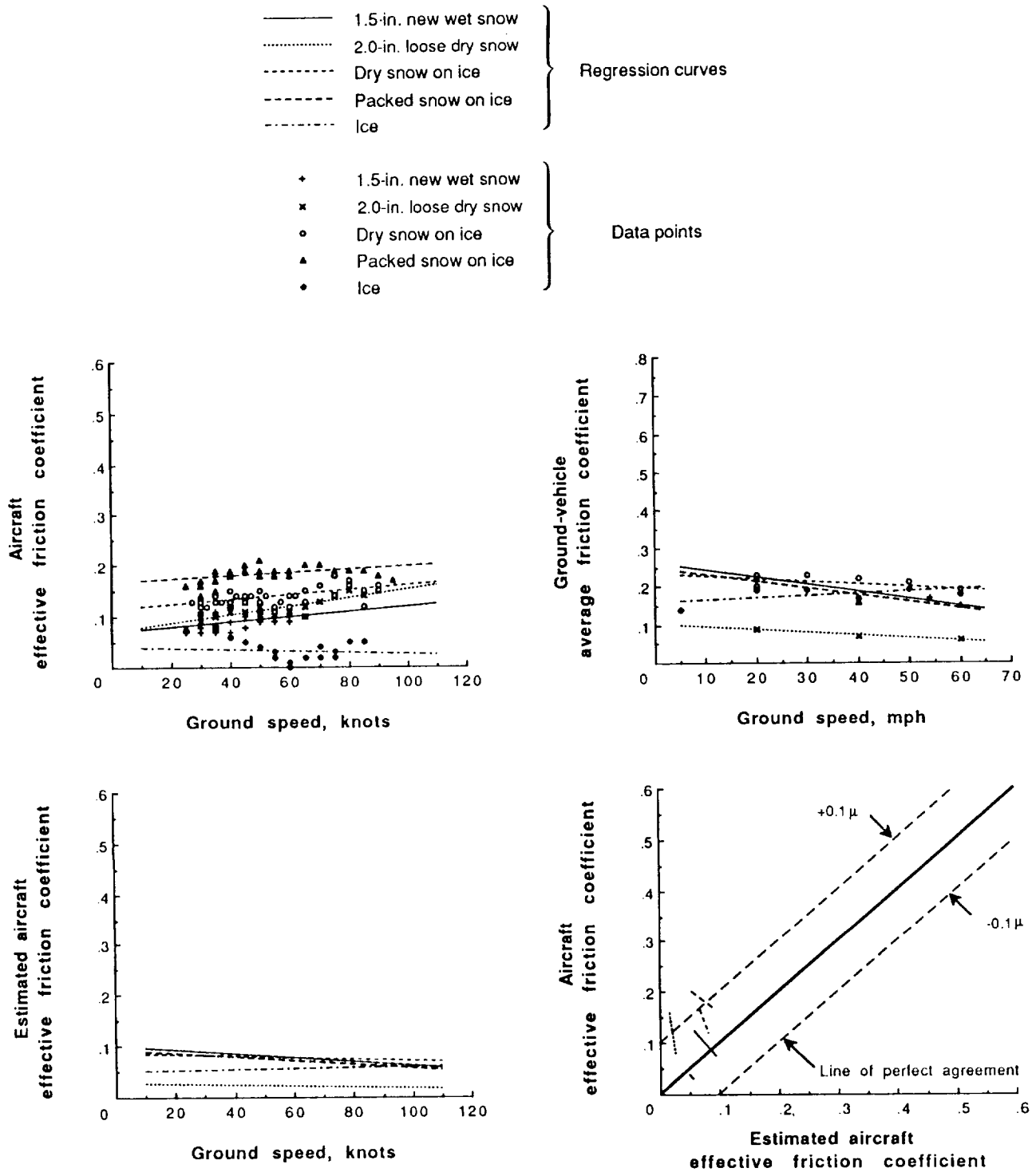

(a) Mu-Meter data.

Figure 63. Variation of Boeing 727 aircraft and ground-vehicle friction data with speed and variation of estimated aircraft braking performance with actual braking performance on snow- and ice-covered runways.

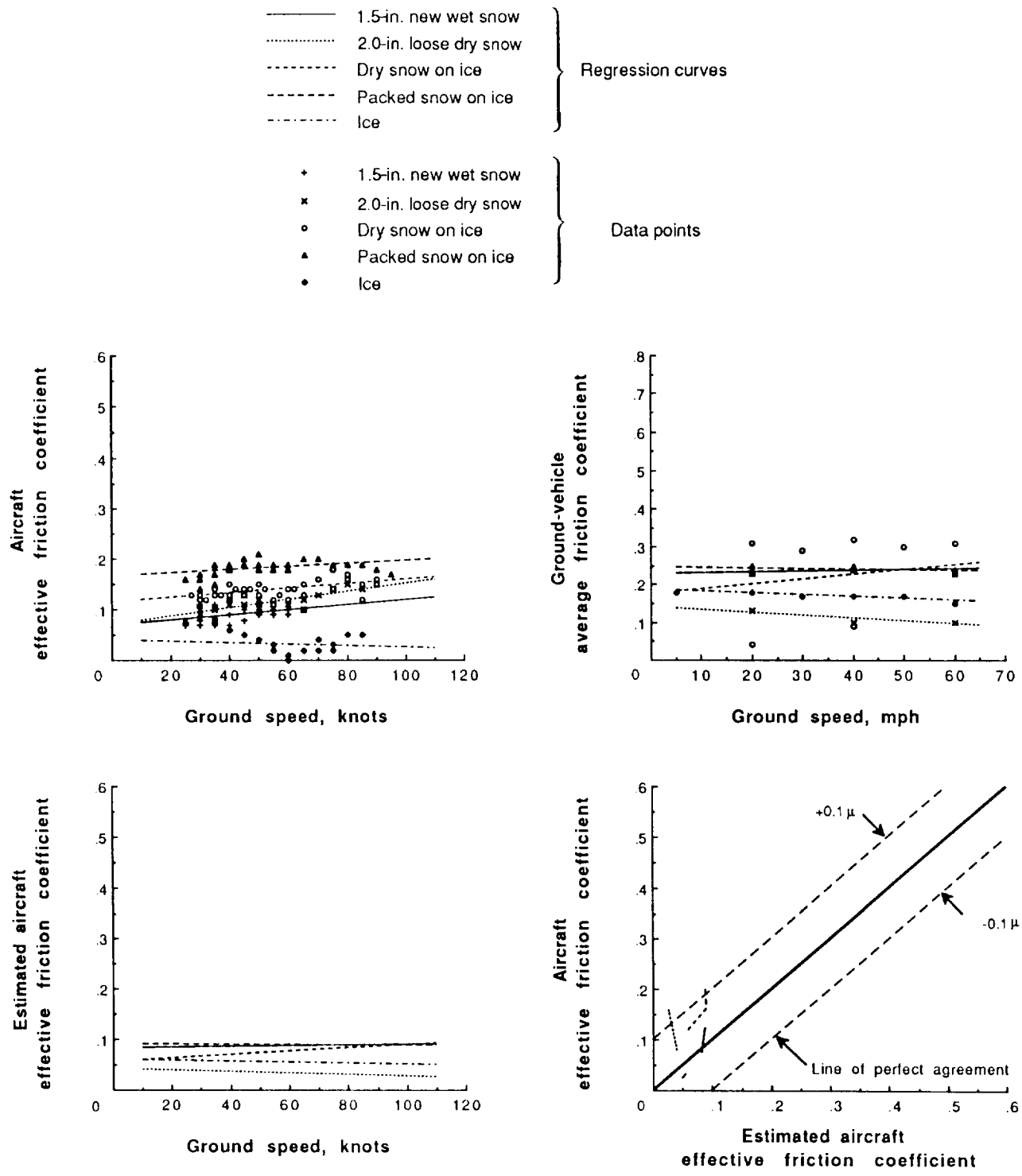

(b) SFT data.

Figure 63. Continued.

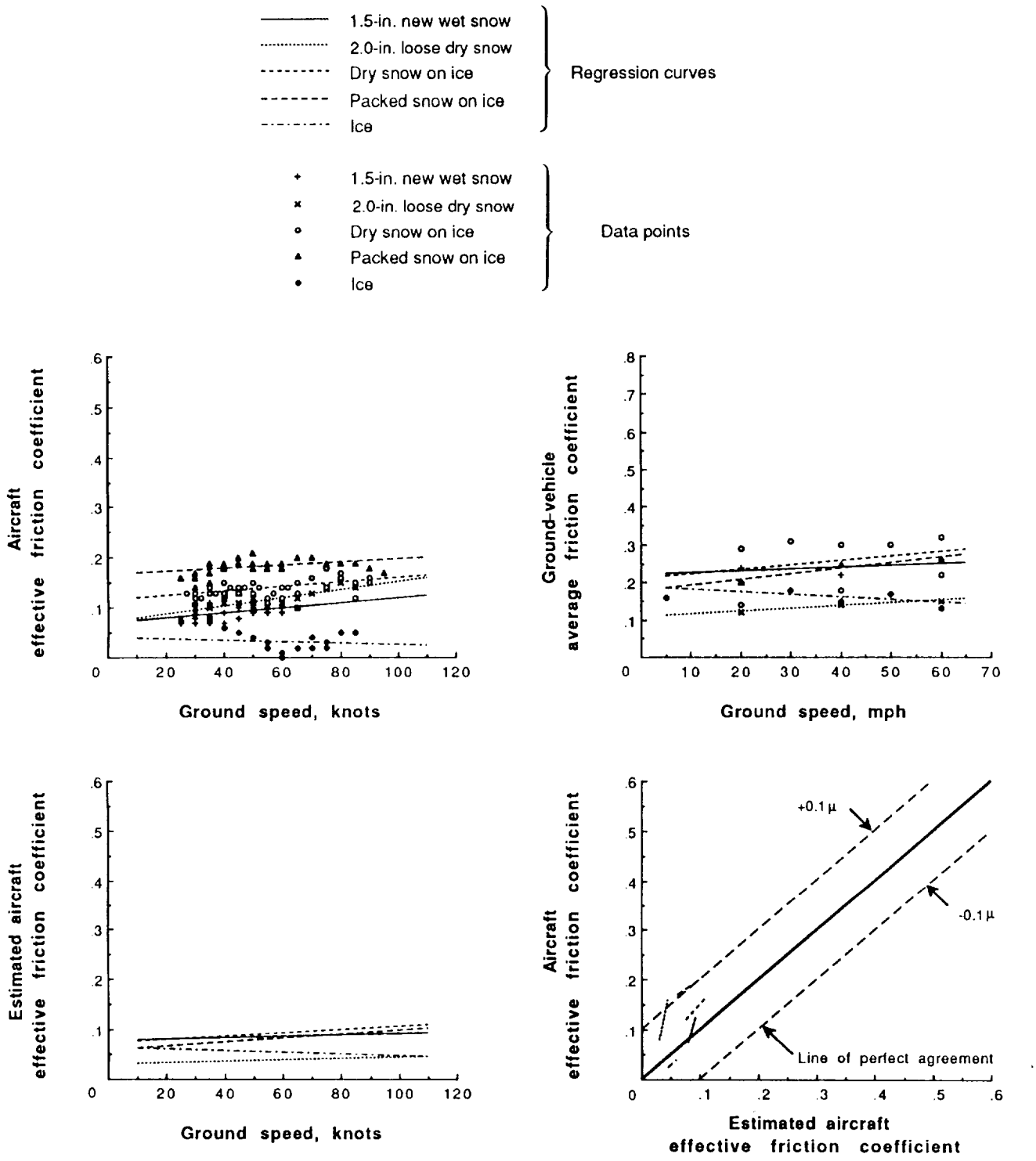

(c) BV-11 skiddometer data.

Figure 63. Continued.

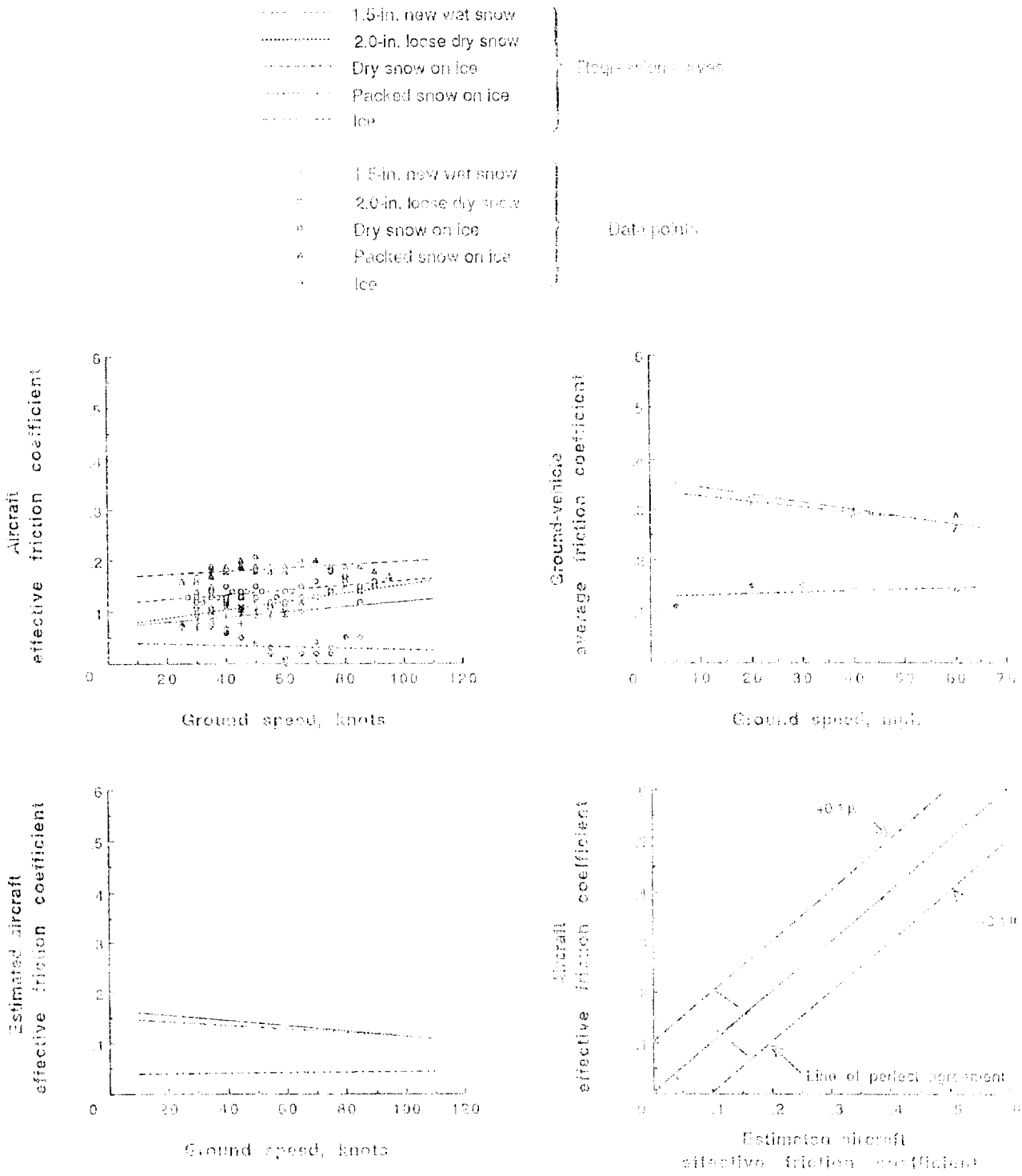

(d) RFT data.

Figure 63. Concluded.

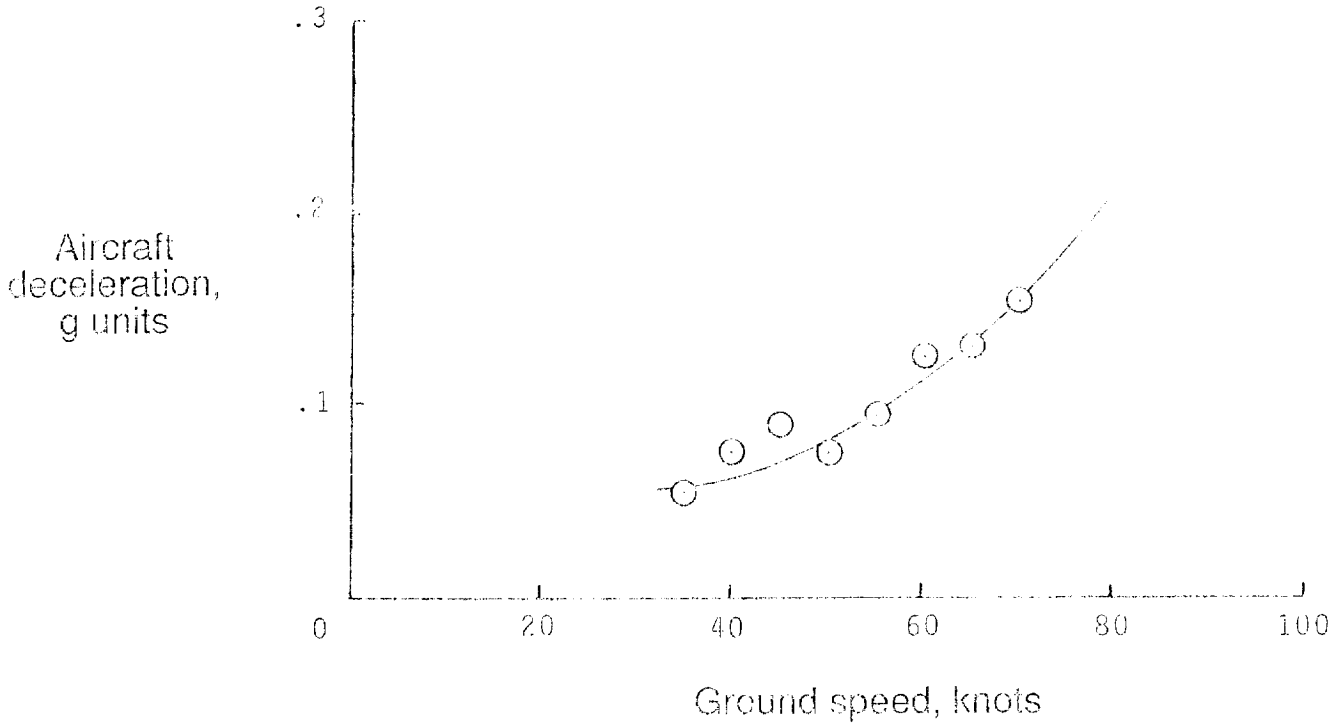

Figure 64. Boeing 727 deceleration in 4.5-in. loose snow. Landing flaps = 30°; spoilers extended; idle forward thrust; no wheel braking; Snow specific gravity = 0.27; Headwind component = 5.2 knots.

C-54

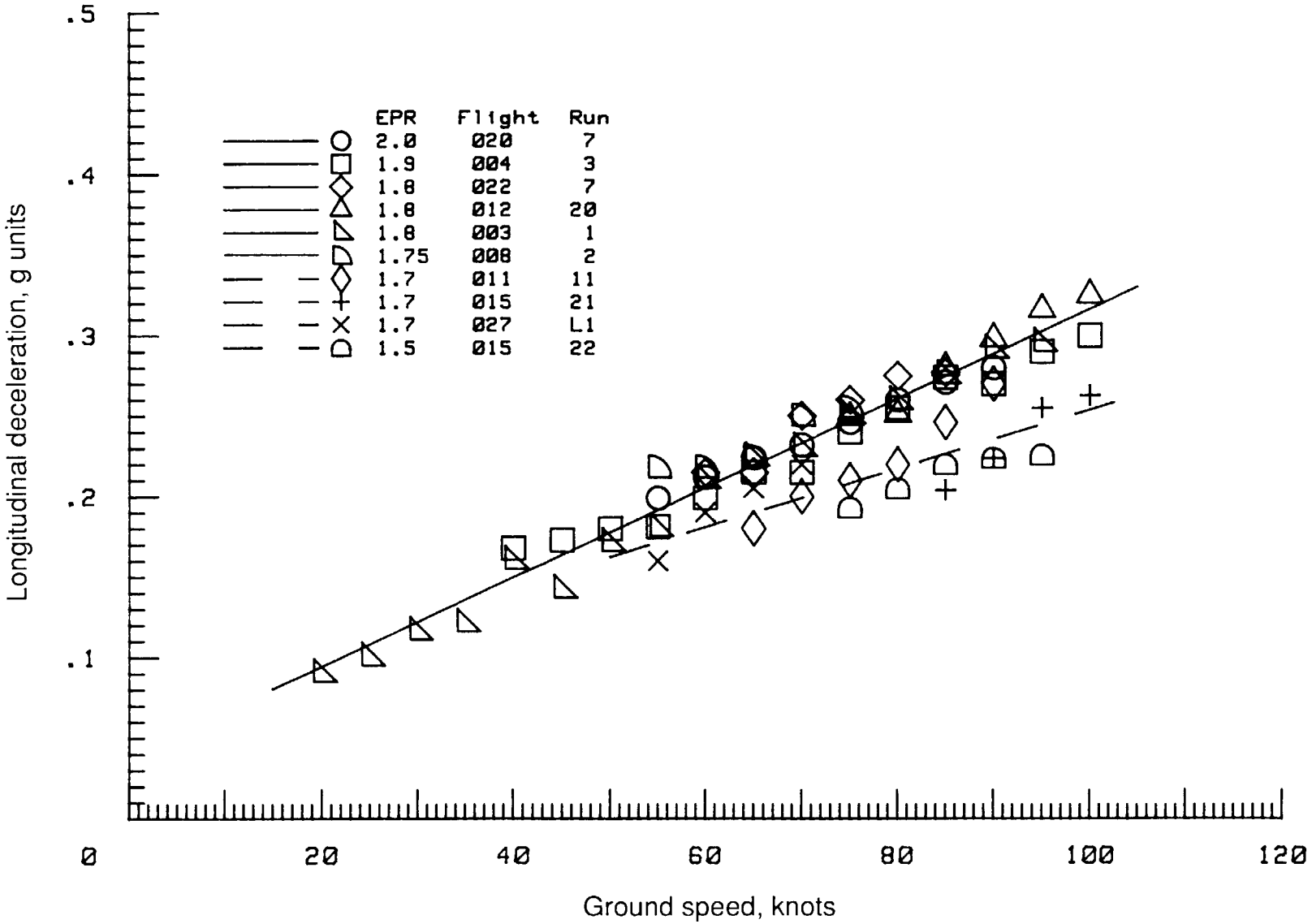

Figure 65. Reverse-thrust performance of Boeing 727 aircraft. (Aerodynamic drag and tire rolling resistance are included in the data.)

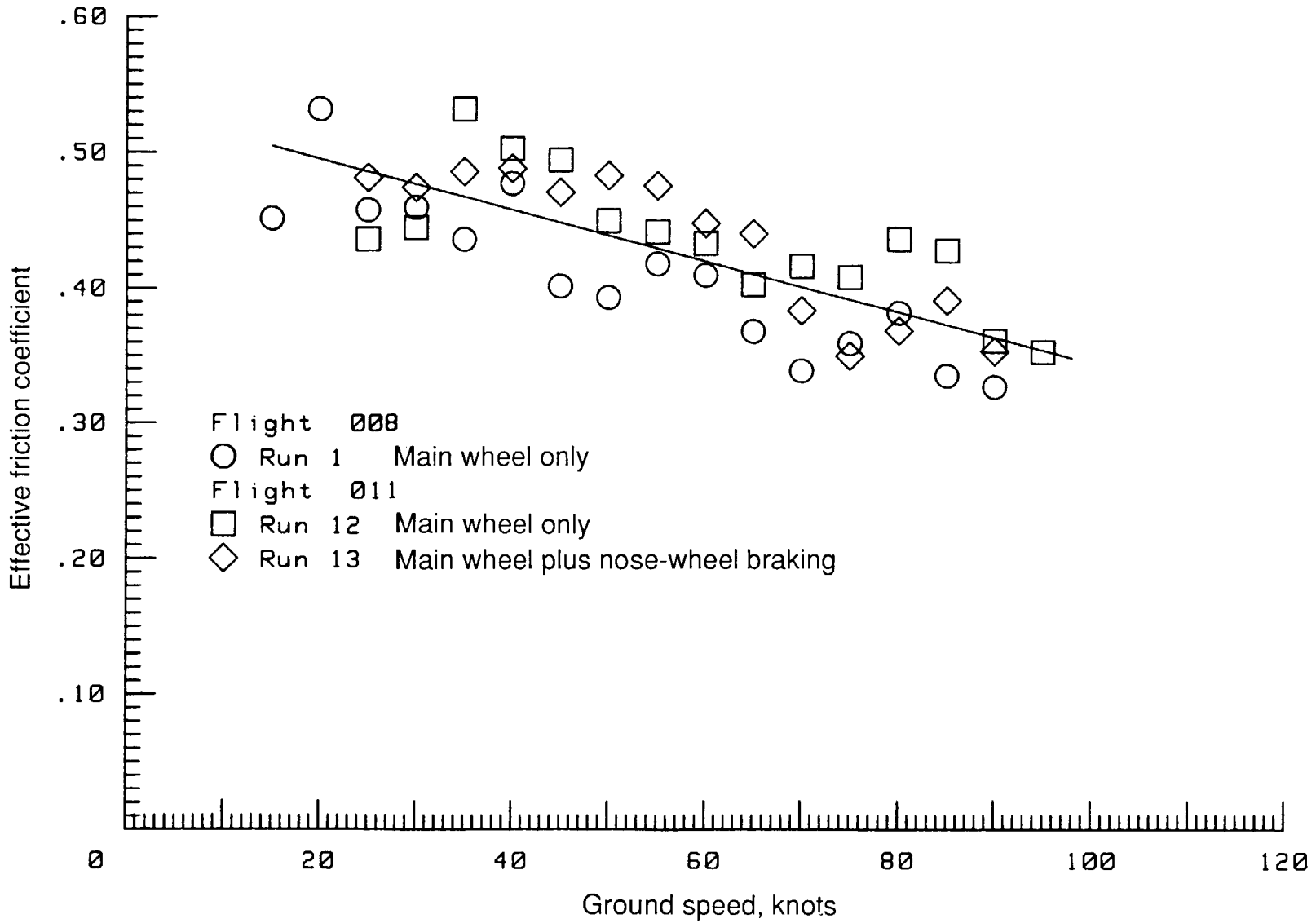

Figure 66. Comparison of Boeing 727 effective friction coefficient with speed for main wheel only and main wheel plus nose-wheel braking modes on truck-wet, slurry-seal asphalt.

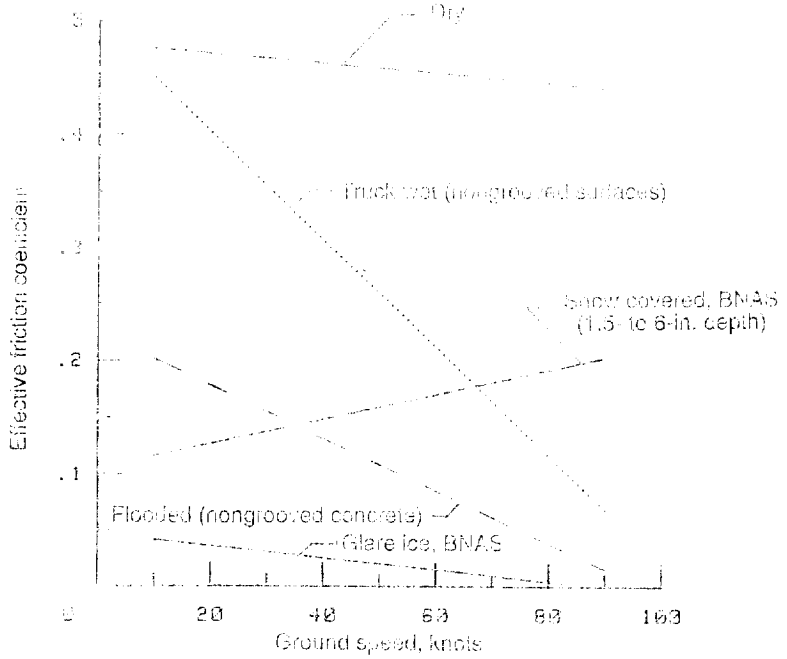

(c) Boeing 737 test aircraft. Landing flaps = 40°; spoilers extended; idle forward thrust; manual braking.

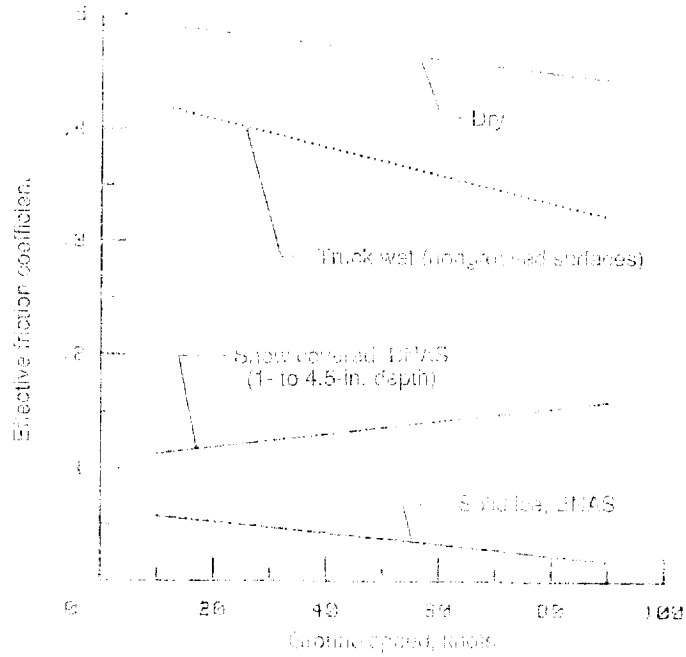

(d) Boeing 727 test aircraft. Landing flaps = 30°; spoilers extended; idle forward thrust; main wheel brakes only.

Figure 67. Comparison of aircraft braking friction performance on dry and wet runway surfaces and conditions.

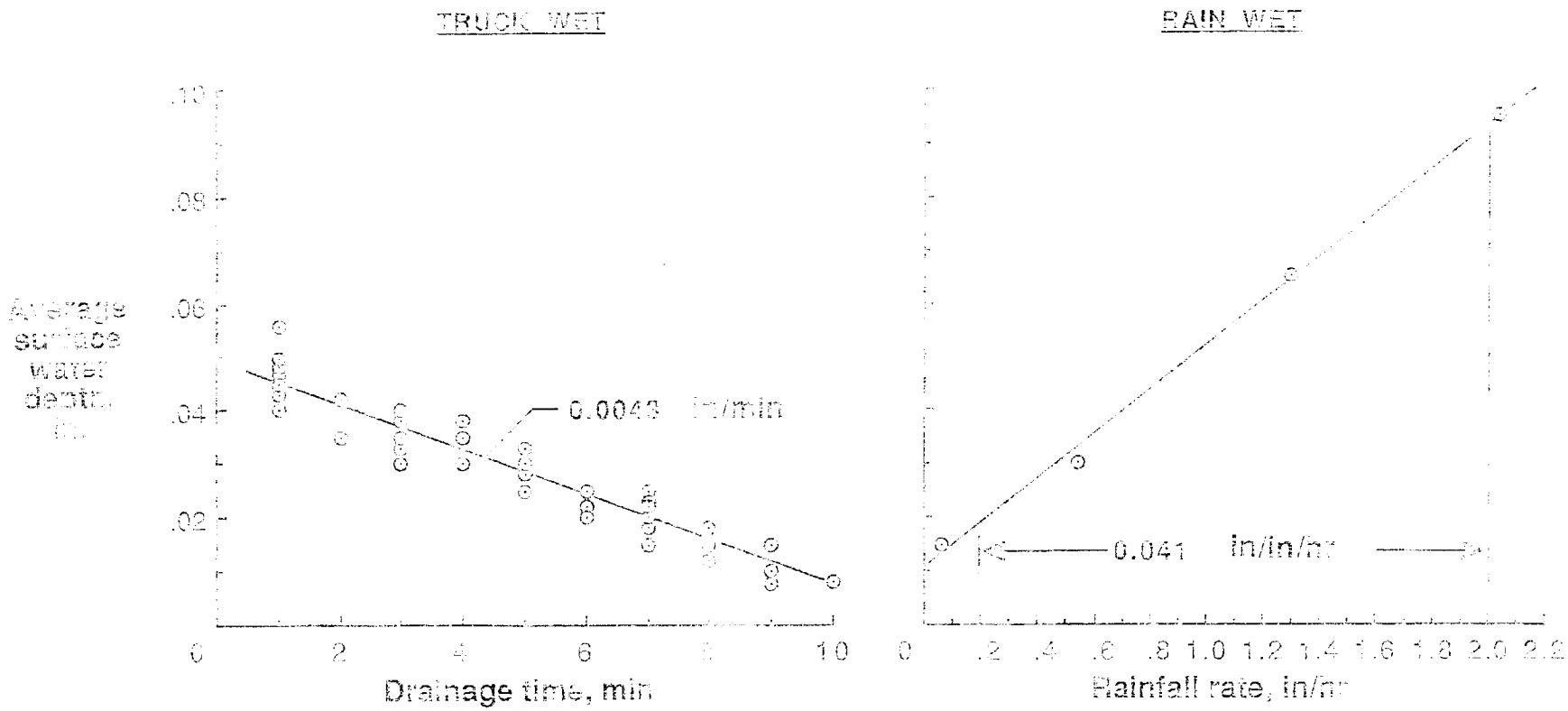

Figure 68. Surface water drainage and accumulation measurements. Nongrooved slurry-seal asphalt; calm winds; 1-percent crown; Average texture depth = 0.0263 in.

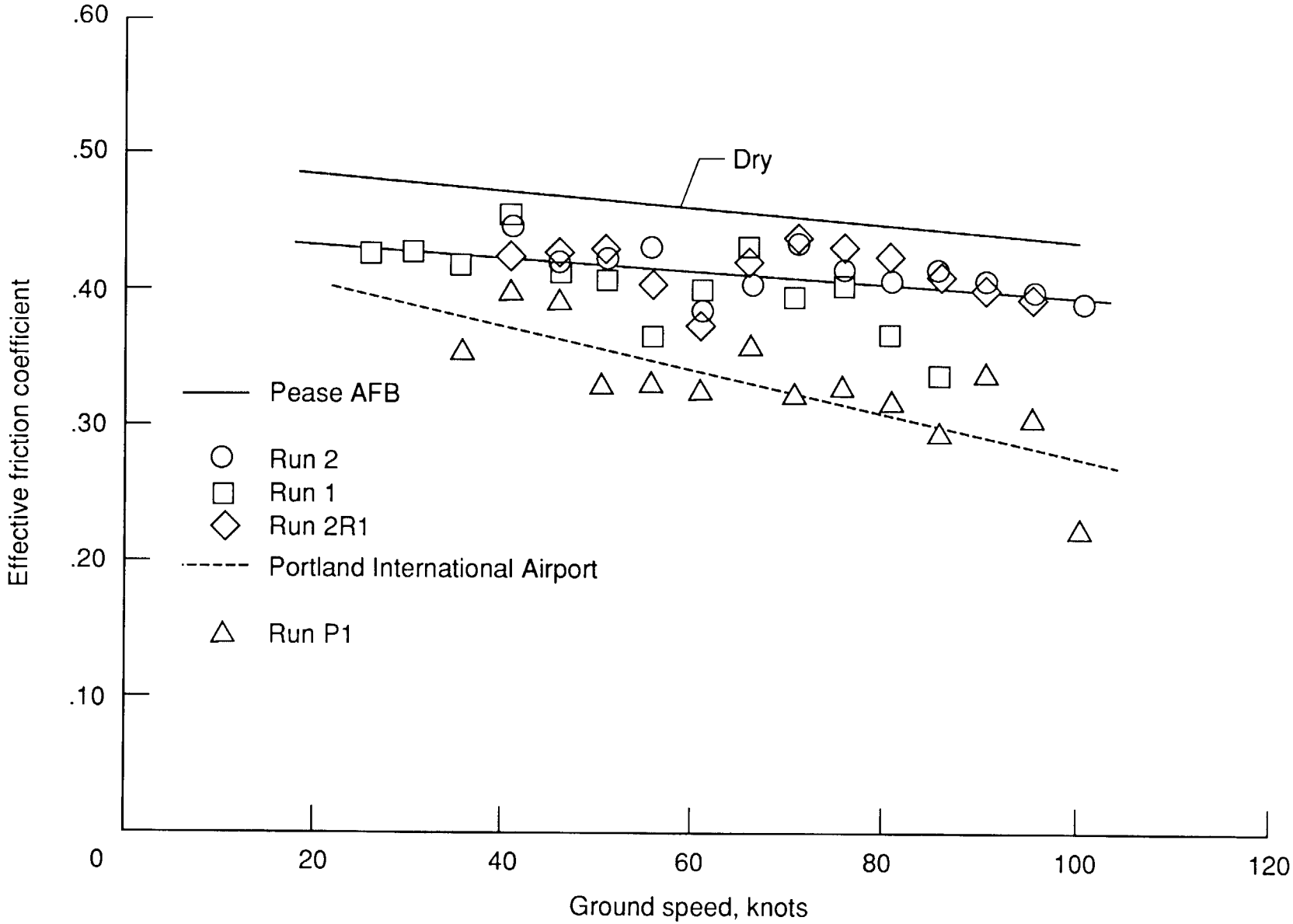

Figure 69. Boeing 727 aircraft braking friction performance obtained on rain-damp porous friction course runway surfaces.

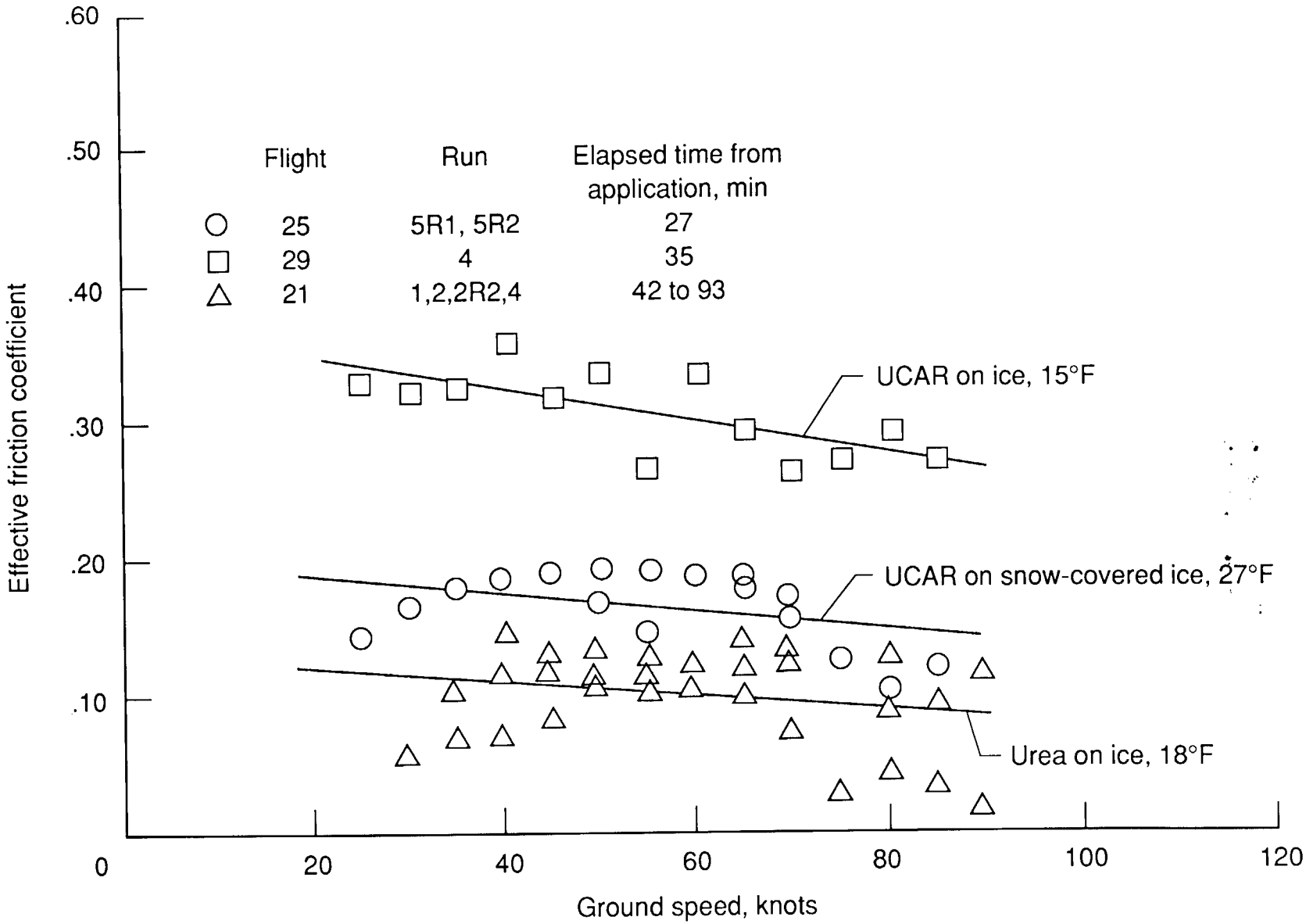

Figure 70. Effect of runway chemical treatment type and elapsed time on Boeing 727 tire friction performance on ice-covered runway at BNAS.

NASA National Aeronautics and Space Administration

Report Documentation Page

1. Report No.	2. Government Accession No.	3. Recipient's Catalog No.
NASA TP-2917		

4. Title and Subtitle
Evaluation of Two Transport Aircraft and Several Ground Test Vehicle Friction Measurements Obtained for Various Runway Surface Types and Conditions
A Summary of Test Results From Joint FAA/NASA Runway Friction Program

5. Report Date
February 1990

6. Performing Organization Code

7. Author(s)
Thomas J. Yager, William A. Vogler, and Paul Baldasare

8. Performing Organization Report No.
L-16536

10. Work Unit No.
505-63-41-02

9. Performing Organization Name and Address
NASA Langley Research Center
Hampton, VA 23665-5225

11. Contract or Grant No.

13. Type of Report and Period Covered
Technical Paper

12. Sponsoring Agency Name and Address
National Aeronautics and Space Administration
Washington, DC 20546-0001

14. Sponsoring Agency Code

15. Supplementary Notes
Thomas J. Yager and Paul Baldasare: Langley Research Center, Hampton, Virginia.
William A. Vogler: PRC Kentron, Inc., Aerospace Technologies Division, Hampton, Virginia.

16. Abstract

Tests with specially instrumented NASA Boeing 737 and 727 aircraft together with several different ground friction-measuring devices have been conducted for a variety of runway surface types and conditions. These tests are part of a Joint FAA/NASA Aircraft/Ground-Vehicle Runway Friction Program aimed at obtaining a better understanding of aircraft ground handling performance under adverse weather conditions and defining relationships between aircraft and ground-vehicle tire friction measurements. Aircraft braking performance for dry, wet, and snow- and ice-covered runway conditions is discussed as well as ground-vehicle friction data obtained under similar runway conditions. For a given contaminated runway surface condition, the correlation between ground vehicles and aircraft friction data is identified. The influence of major test parameters on friction measurements such as speed, test-tire characteristics, type and amount of surface contaminant, and ambient temperature is discussed. The effect of surface type on wet friction levels is also evaluated from comparative data collected on grooved and ungrooved concrete and asphalt surfaces.

17. Key Words (Suggested by Authors(s))	18. Distribution Statement
Tire friction Aircraft braking performance Ground friction measurement vehicles Contaminated runways	Unclassified—Unlimited Subject Category 05

19. Security Classif. (of this report)	20. Security Classif. (of this page)	21. No. of Pages	22. Price
Unclassified	Unclassified	30	A03

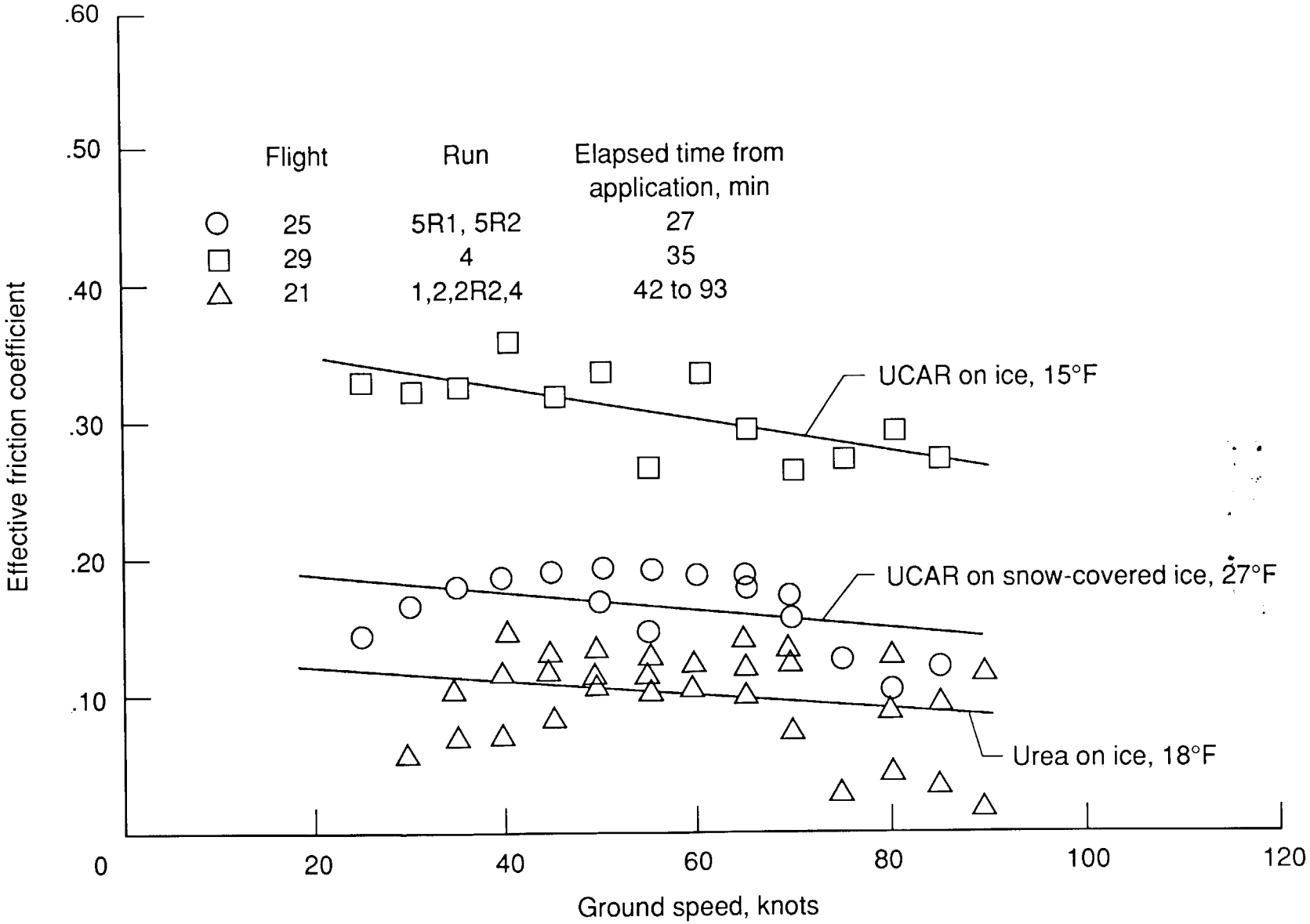

Figure 70. Effect of runway chemical treatment type and elapsed time on Boeing 727 tire friction performance on ice-covered runway at BNAS.

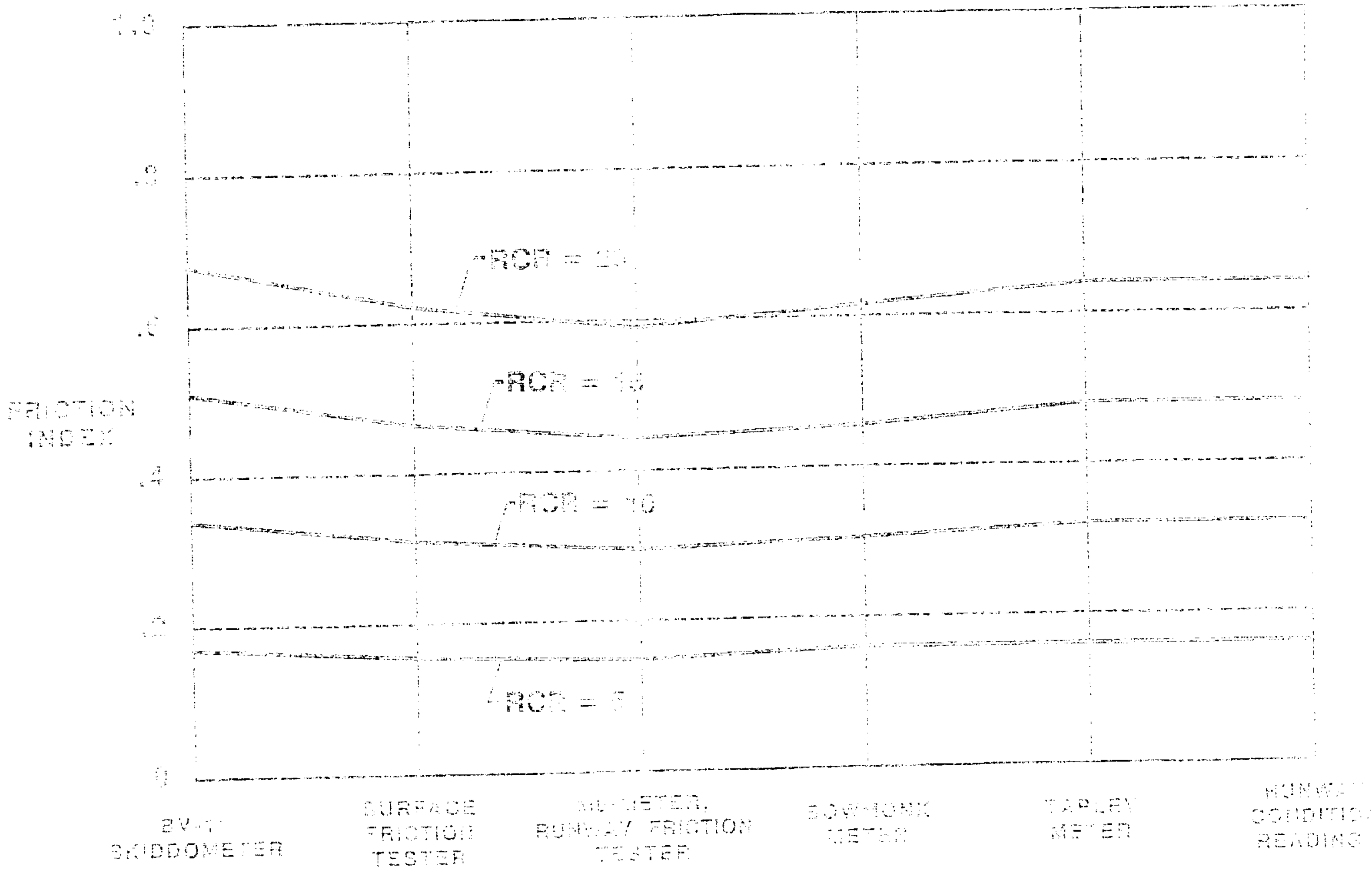

Figure 72. Ground-vehicle friction correlation to compacted snow and ice-covered runway conditions. (Maximum friction index value of 1.0 equals RCR of 32.)

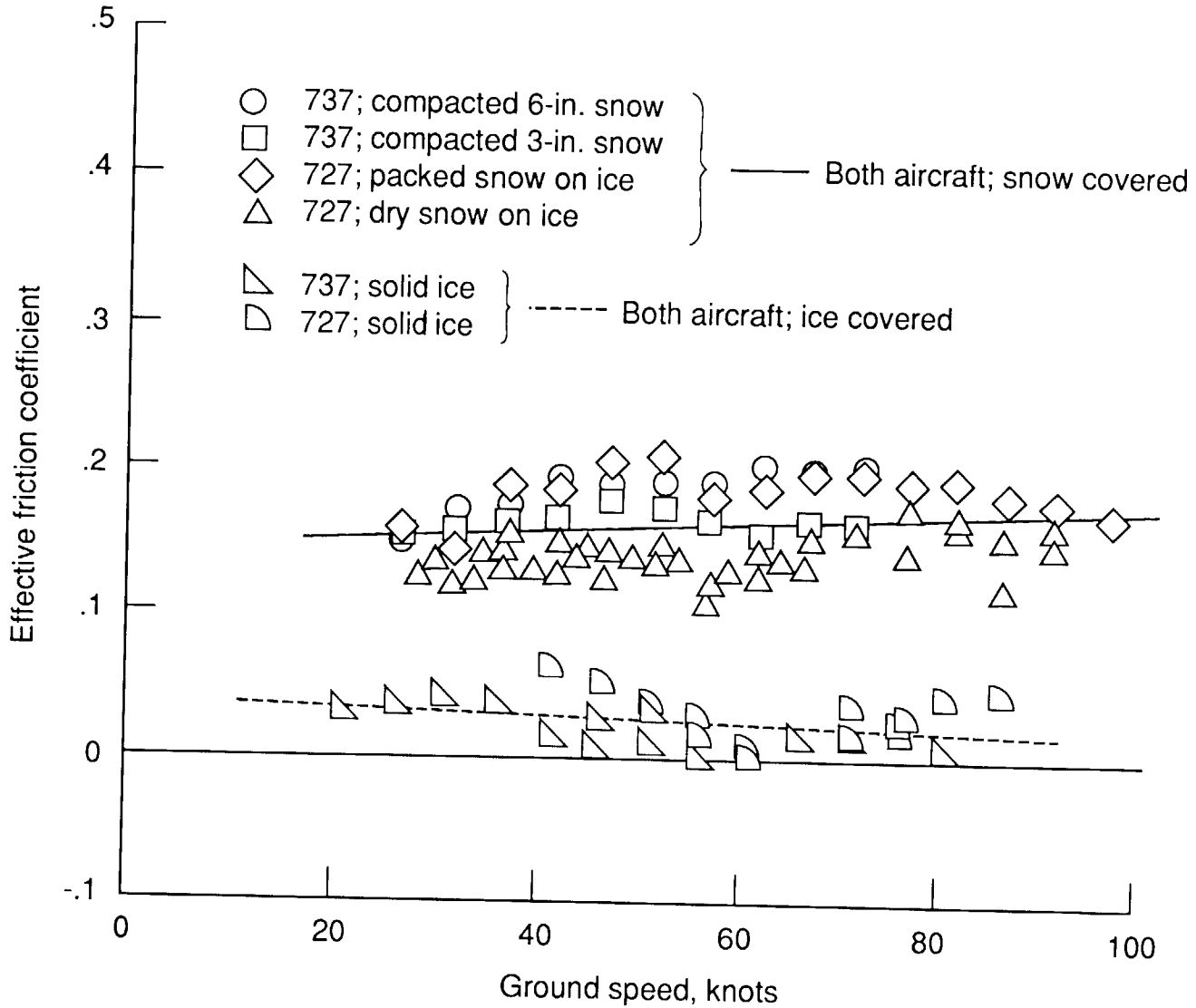

Figure 73. Comparison of Boeing 737 and 727 braking performances on compacted snow- and ice-covered runway surfaces at BNAS.

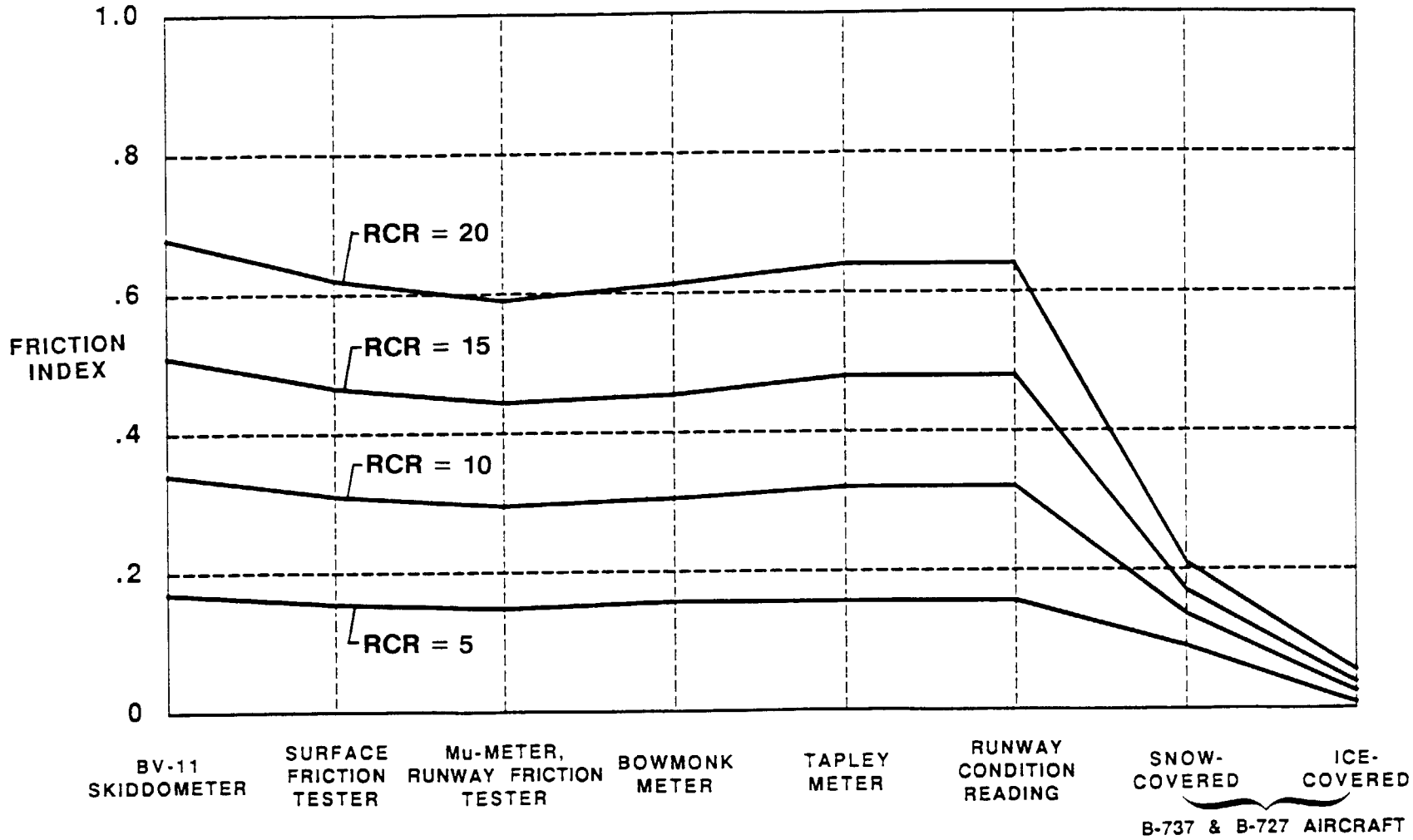

Figure 74. Aircraft and ground-vehicle correlation for compacted snow- and ice-covered runway conditions. (Maximum friction index value of 1 equals RCR of 32.)

NASA
National Aeronautics and Space Administration

Report Documentation Page

1. Report No.	2. Government Accession No.	3. Recipient's Catalog No.
NASA TP-2917		

4. Title and Subtitle
Evaluation of Two Transport Aircraft and Several Ground Test Vehicle Friction Measurements Obtained for Various Runway Surface Types and Conditions
A Summary of Test Results From Joint FAA/NASA Runway Friction Program

5. Report Date
February 1990

6. Performing Organization Code

7. Author(s)
Thomas J. Yager, William A. Vogler, and Paul Baldasare

8. Performing Organization Report No.
L-16536

10. Work Unit No.
505-63-41-02

9. Performing Organization Name and Address
NASA Langley Research Center
Hampton, VA 23665-5225

11. Contract or Grant No.

13. Type of Report and Period Covered
Technical Paper

12. Sponsoring Agency Name and Address
National Aeronautics and Space Administration
Washington, DC 20546-0001

14. Sponsoring Agency Code

15. Supplementary Notes
Thomas J. Yager and Paul Baldasare: Langley Research Center, Hampton, Virginia.
William A. Vogler: PRC Kentron, Inc., Aerospace Technologies Division, Hampton, Virginia.

16. Abstract

Tests with specially instrumented NASA Boeing 737 and 727 aircraft together with several different ground friction-measuring devices have been conducted for a variety of runway surface types and conditions. These tests are part of a Joint FAA/NASA Aircraft/Ground-Vehicle Runway Friction Program aimed at obtaining a better understanding of aircraft ground handling performance under adverse weather conditions and defining relationships between aircraft and ground-vehicle tire friction measurements. Aircraft braking performance for dry, wet, and snow- and ice-covered runway conditions is discussed as well as ground-vehicle friction data obtained under similar runway conditions. For a given contaminated runway surface condition, the correlation between ground vehicles and aircraft friction data is identified. The influence of major test parameters on friction measurements such as speed, test-tire characteristics, type and amount of surface contaminant, and ambient temperature is discussed. The effect of surface type on wet friction levels is also evaluated from comparative data collected on grooved and ungrooved concrete and asphalt surfaces.

17. Key Words (Suggested by Authors(s))	18. Distribution Statement
Tire friction Aircraft braking performance Ground friction measurement vehicles Contaminated runways	Unclassified—Unlimited Subject Category 05

19. Security Classif. (of this report)	20. Security Classif. (of this page)	21. No. of Pages	22. Price
Unclassified	Unclassified	300	A13

NASA FORM 1626 OCT 86
NASA-Langley, 1990
For sale by the National Technical Information Service, Springfield, Virginia 22161-2171